

Performance Test of a Steam-Assisted Elevated Flare With Passive FTIR



FINAL REPORT

May 2010

Marathon Petroleum Company, LLC
Texas Refining Division
502 10th Street South
Texas City, Texas 77590

Testing Conducted
September 15 - 24, 2009

Prepared by
Clean Air Engineering, Inc.
Project No: 10810



Table of Contents

| | | |
|------------|---|------------|
| 1.0 | <i>Background & Summary</i> | 1-1 |
| 2.0 | <i>Introduction</i> | 2-1 |
| 2.1 | Objectives of Test Program | 2-1 |
| 2.2 | Testing Organization | 2-1 |
| 2.3 | Flare System Components | 2-2 |
| 2.3.1 | Purpose..... | 2-2 |
| 2.3.2 | Flare Tip..... | 2-2 |
| | Table 2.3-1: Texas City Main Flare Summary of Description and Design Specifications | 2-2 |
| 2.3.3 | Flare Automatic Steam Control System..... | 2-3 |
| | Table 2.3-2: Automatic Steam Control System Components..... | 2-3 |
| 2.4 | Mikron IR Cameras | 2-4 |
| 2.4.1 | Background on IR Smoke Monitors..... | 2-4 |
| 2.4.2 | Use of IR Cameras during Marathon Texas City Test Project..... | 2-5 |
| 2.5 | Video Cameras | 2-6 |
| | Figure 2.5-1: Image from PFTIR Aiming Camera..... | 2-6 |
| | Figure 2.5-2: Image from FLIR A320 IR Camera | 2-7 |
| | Figure 2.5-3: Image from FLIR GasFind IR LW Camera..... | 2-7 |
| | Figure 2.5-4: Image from Axis Q1755 Camera..... | 2-8 |
| 2.6 | Passive FTIR | 2-8 |
| 2.7 | Flare Test Program | 2-9 |
| 2.7.1 | Steam Demand and API 521 | 2-9 |
| | Figure 2.7-1: API 521 Table 11 Suggested Steam Rates | 2-10 |
| 2.7.2 | Test Conditions | 2-12 |
| | Figure 2.7-3: S/VG vs. Condition | 2-13 |
| | Figure 2.7-4: S/HC vs. Condition..... | 2-13 |
| 3.0 | <i>Summary of Results</i> | 3-1 |
| 3.1 | Summary and Key Data Trends by Test Series | 3-1 |
| 3.1.1 | Combustion Efficiency with Increasing Steam Rates | 3-1 |
| 3.1.1.1 | Test Series A – Typical Base Load Conditions | 3-1 |
| | Figure 3.1-1: CE vs. S/VG for Base Load Conditions | 3-2 |
| | Figure 3.1-2: X-Axis Zoom of Base Conditions, CE vs. S/VG..... | 3-3 |
| | Figure 3.1-3: CE vs. S/S521 for Base Load Conditions..... | 3-4 |
| 3.1.1.2 | Test Series B – Refinery Fuel Gas | 3-6 |
| | Figure 3.1-4: Refinery Fuel Gas CE vs. S/VG | 3-6 |
| | Figure 3.1-5: Refinery Fuel Gas S/S521 with Combustion Efficiency | 3-7 |
| 3.1.1.3 | Test Series C – Propane | 3-8 |
| | Figure 3.1-6: Propane Test Series CE vs. S/VG..... | 3-8 |
| | Figure 3.1-7: Propane Test Series CE vs. S/S521 | 3-9 |
| 3.1.1.4 | Test Series D & E – Propylene/Butylene Olefins | 3-10 |
| | Figure 3.1-8: Olefin Test Series CE vs. S/VG..... | 3-10 |
| | Figure 3.1-9: Olefin Test Series CE vs. S/S521 | 3-11 |
| 3.1.2 | Observed Impacts of Hydrogen..... | 3-12 |
| 3.1.2.1 | Test Series F – Increasing Hydrogen Content | 3-13 |
| | Figure 3.1-10: Combustion Efficiency as Hydrogen Content Increases | 3-13 |
| 3.1.2.2 | Test Series G – Increasing Nitrogen Content..... | 3-14 |

Performance Test of a Steam-Assisted Elevated Flare
Marathon Petroleum Company, Texas City Main Flare

| | | |
|---------|--|------|
| | Figure 3.1-11: Combustion Efficiency with Decreasing NHV_{VG} | 3-14 |
| 3.2 | Summary and Key Data Trends of Whole Data Set | 3-15 |
| 3.2.1 | Composite of All Hydrocarbons Tested | 3-15 |
| | Figure 3.2-1: Combustion Efficiency vs. S/VG Composite of All Materials Tested | 3-15 |
| | Figure 3.2-2: Combustion Efficiency vs. S/S521 Composite of All Materials Tested.... | 3-16 |
| 3.2.2 | Combustion Zone Gas Net Heating Value | 3-17 |
| | Figure 3.2-3: CZG NHV vs. CE for All Materials Tested | 3-17 |
| 3.2.3 | Visible Emissions and Combustion Efficiency | 3-18 |
| | Table 3.2-1: Visual Flame Rating Descriptions | 3-18 |
| | Figure 3.2-4: Combustion Efficiency vs. Visible Emissions Ratings for All Materials Tested..... | 3-19 |
| 3.2.4 | Comparisons to API 521 Table 11 | 3-20 |
| | Figure 3.2-5: Incipient Smoke Point vs. API 521 Table 11 Predictions..... | 3-20 |
| | Figure 3.2-6: Incipient Smoke Point Varies with Mass Load | 3-21 |
| | Table 3.2-2: Runs with Visible Emissions Ratings 4.5 – 5.5 | 3-22 |
| 3.3 | Factors Influencing Test Results..... | 3-23 |
| 3.3.1 | Mechanical Damage of Flare Tip..... | 3-23 |
| | Figure 3.3-1: Steam Leak at Shaping Steam Ring | 3-23 |
| 3.3.2 | Wind Effects | 3-25 |
| | Figure 3.3-3: Example of Good Plume Alignment with PFTIR..... | 3-25 |
| | Figure 3.3-4: Example of Poor Plume Alignment with PFTIR | 3-26 |
| | Figure 3.3-5: Comparative View from PFTIR Aiming Camera..... | 3-26 |
| | Figure 3.3-6: Wind Flagging Algorithm | 3-27 |
| | Figure 3.3-7: Day by Day Wind Roses | 3-28 |
| 3.3.3 | PFTIR Aiming Issues..... | 3-29 |
| | Figure 3.3-8: Aiming Test: Video Stills from Each Test Point | 3-30 |
| | Figure 3.3-9: Aiming Test: Measured Components | 3-31 |
| | Figure 3.3-10: Aiming Test: Measured Components - Zoomed | 3-31 |
| | Figure 3.3-11: Aiming Test: CO_2/CO and CO_2/THC Ratios..... | 3-32 |
| | Figure 3.3-12: Aiming Test: Combustion Efficiency..... | 3-33 |
| | Figure 3.3-13: Aiming Test: Steam Ratios..... | 3-33 |
| | Figure 3.3-14: Aiming Test: Flow and CZG | 3-34 |
| | Figure 3.3-15: Aiming Test: VG Composition | 3-34 |
| 3.3.4 | Overall Test Variability..... | 3-35 |
| 3.3.4.1 | PFTIR Precision Assessment..... | 3-35 |
| | Figure 3.3-17: Long Term Stability Run by Run Variability | 3-37 |
| | Figure 3.3-18: Confidence Interval Determination from LTS Data | 3-38 |
| 3.3.4.2 | Dilution Assumption..... | 3-39 |
| | Figure 3.3-19: CO_2/CO Ratio Comparison on LTS Runs | 3-39 |
| 3.3.5 | PFTIR Calibration..... | 3-40 |
| 3.3.5.1 | Radiance Calibrations | 3-40 |
| | Figure 3.3-20: PFTIR Radiance Calibrations..... | 3-40 |
| 3.3.5.2 | Hot Cell Calibration..... | 3-41 |
| | Figure 3.3-21: PFTIR Hot Cell Calibration Curve – CO_2 | 3-41 |
| | Figure 3.3-22: PFTIR Hot Cell Calibration Curve - CO | 3-42 |
| | Figure 3.3-23: PFTIR Hot Cell Calibration Curve – Methane | 3-42 |
| 3.3.6 | Methane and Heavy Hydrocarbons | 3-43 |
| 3.3.7 | PFTIR Component Errors | 3-43 |
| 3.3.8 | Lack of Integrated Sampling | 3-44 |

Performance Test of a Steam-Assisted Elevated Flare
Marathon Petroleum Company, Texas City Main Flare

| | | |
|------------|---|-------------------|
| 3.4 | Conclusions | 3-45 |
| 3.5 | Recommendations for Further Study | 3-45 |
| 4.0 | <i>PFTIR Testing Method and Procedure.....</i> | <i>4-1</i> |
| 4.1 | Description and Principles of Passive FTIR | 4-1 |
| 4.2 | PFTIR Siting Configuration | 4-2 |
| | Figure 4.2-1: Location of PFTIR Camera, Flare, and Cameras | 4-2 |
| | Figure 4.2-2: View of Main Flare from PFTIR Location | 4-3 |
| | Figure 4.2-3: Marathon Texas City Plot Plan (Area shown in Figure 4.2-1 shown in red) | 4-4 |
| 4.3 | Background | 4-5 |
| 4.4 | PFTIR Operation | 4-5 |
| | Figure 4.4-1: PFTIR Trailer | 4-6 |
| | Figure 4.4-2: The PFTIR Instrument | 4-6 |
| | Figure 4.4-3: Schematic of PFTIR set-up | 4-7 |
| 4.5 | PFTIR Data Reduction | 4-9 |
| | Figure 4.5-1: Contributions to Total Radiance | 4-9 |
| | Figure 4.5-2: PFTIR Data Analysis Progression | 4-13 |
| 4.6 | Q-Branch Subtraction | 4-14 |
| 5.0 | <i>Data Tables.....</i> | <i>5-1</i> |
| 5.1 | Data Summary Tables | 5-1 |
| | Table 5.1-1: Condition A19 Test Result Summary | 5-3 |
| | Table 5.1-2: Condition A11 Test Result Summary | 5-3 |
| | Table 5.1-3: Condition A8 Test Result Summary | 5-3 |
| | Table 5.1-4: Condition B Test Result Summary | 5-4 |
| | Table 5.1-5: Condition C Test Result Summary | 5-4 |
| | Table 5.1-6: Condition D Test Result Summary | 5-4 |
| | Table 5.1-7: Condition E Test Result Summary | 5-5 |
| | Table 5.1-8: Condition F Test Result Summary | 5-5 |
| | Table 5.1-9: Condition G Test Result Summary | 5-5 |
| | Table 5.1-10: LTS Test Result Summary | 5-5 |
| 5.2 | Test Condition A19 | 5-6 |
| 5.2.1 | Process Conditions | 5-6 |
| | Figure 5.2-1: Condition A19 Flow and CZG Heat Content | 5-6 |
| | Figure 5.2-2: Condition A19 Vent Gas Composition | 5-6 |
| 5.2.2 | Steam Ratios | 5-7 |
| | Table 5.2-1: Condition A19 Steam Ratios | 5-7 |
| 5.2.3 | Wind Conditions | 5-7 |
| | Figure 5.2-3: Condition A19. Wind Speed and Direction during Test | 5-7 |
| 5.2.4 | Results | 5-8 |
| 5.3 | Test Condition A11 | 5-9 |
| 5.3.1 | Process Conditions | 5-9 |
| | Figure 5.3-1: Condition A11 Flow and CZG Heat Content | 5-9 |
| 5.3.2 | Steam Ratios | 5-10 |
| | Table 5.3-1: Condition A11 Steam Ratios | 5-10 |
| 5.3.3 | Wind Conditions | 5-10 |
| | Figure 5.3-3: Condition A11. Wind Speed and Direction during Test | 5-11 |
| 5.3.4 | Results | 5-12 |
| 5.4 | Test Condition A8 | 5-13 |

Performance Test of a Steam-Assisted Elevated Flare
Marathon Petroleum Company, Texas City Main Flare

| | | |
|-------|---|------|
| 5.4.1 | Process Conditions | 5-13 |
| | Figure 5.4-1: Condition A8 Flow and CZG Heat Content | 5-13 |
| | Figure 5.4-2: Condition A8 Vent Gas Composition..... | 5-13 |
| 5.4.2 | Steam Ratios | 5-14 |
| | Table 5.4-1: Condition A8 Steam Ratios | 5-14 |
| 5.4.3 | Wind Conditions | 5-14 |
| | Figure 5.4-3: Condition A8. Wind Speed and Direction During Test..... | 5-14 |
| 5.4.4 | Results | 5-15 |
| 5.5 | Test Condition B..... | 5-16 |
| 5.5.1 | Process Conditions | 5-16 |
| | Figure 5.5-1: Condition B Flow and CZG Heat Content | 5-16 |
| | Figure 5.5-2: Condition B Vent Gas Composition..... | 5-16 |
| 5.5.2 | Steam Ratios | 5-17 |
| | Table 5.5-1: Condition B Steam Ratios..... | 5-17 |
| 5.5.3 | Wind Conditions | 5-17 |
| | Figure 5.5-3: Condition B. Wind Speed and Direction During Test..... | 5-17 |
| 5.5.4 | Results | 5-18 |
| 5.6 | Test Condition C..... | 5-19 |
| 5.6.1 | Process Conditions | 5-19 |
| | Figure 5.6-1: Condition C Flow and CGZ Heat Content | 5-19 |
| | Figure 5.6-2: Condition C Vent Gas Composition | 5-19 |
| 5.6.2 | Steam Ratios | 5-20 |
| | Table 5.6-1: Condition C Steam Ratios..... | 5-20 |
| 5.6.3 | Wind Conditions | 5-20 |
| | Figure 5.6-3: Condition C. Wind Speed and Direction during Test..... | 5-20 |
| 5.6.4 | Results | 5-21 |
| 5.7 | Test Condition D | 5-22 |
| 5.7.1 | Process Conditions | 5-22 |
| | Figure 5.7-1: Condition D Flow and CZG Heat Content | 5-22 |
| | Figure 5.7-2: Condition D Vent Gas Composition..... | 5-22 |
| 5.7.2 | Steam Ratios | 5-23 |
| | Table 5.7-1: Condition D Steam Ratios | 5-23 |
| 5.7.3 | Wind Conditions | 5-23 |
| | Figure 5.7-3: Condition D. Wind Speed and Direction during Test..... | 5-23 |
| 5.7.4 | Results..... | 5-24 |
| 5.8 | Test Condition E..... | 5-25 |
| 5.8.1 | Process Conditions | 5-25 |
| | Figure 5.8-1: Condition E Flow and CZG Heat Content..... | 5-25 |
| | Figure 5.8-2: Condition E Vent Gas Composition | 5-25 |
| 5.8.2 | Steam Ratios | 5-26 |
| | Table 5.8-1: Condition E Steam Ratios..... | 5-26 |
| 5.8.3 | Wind Conditions | 5-26 |
| | Figure 5.8-3: Condition E. Wind Speed and Direction during Test..... | 5-26 |
| 5.8.4 | Results..... | 5-27 |
| 5.9 | Test Condition F..... | 5-28 |
| 5.9.1 | Process Conditions | 5-28 |
| | Figure 5.9-1: Condition F Flow and CZG Heat Content..... | 5-28 |
| | Figure 5.9-2: Condition F Vent Gas Composition | 5-29 |
| 5.9.2 | Steam Ratios | 5-29 |

Performance Test of a Steam-Assisted Elevated Flare
Marathon Petroleum Company, Texas City Main Flare

| | | |
|------------|--|------------|
| | Table 5.9-1: Condition F Steam Ratios | 5-29 |
| 5.9.3 | Wind Conditions | 5-30 |
| | Figure 5.9-3: Condition F. Wind Speed and Direction during Test | 5-30 |
| 5.9.4 | Results | 5-31 |
| 5.10 | Test Condition G | 5-32 |
| 5.10.1 | Process Conditions | 5-32 |
| | Figure 5.10-1: Condition G Flow and CZG Heat Content | 5-32 |
| | Figure 5.10-2: Condition G Vent Gas Composition | 5-33 |
| 5.10.2 | Steam Ratios | 5-33 |
| | Table 5.10-1: Condition G Steam Ratios | 5-33 |
| 5.10.3 | Wind Conditions | 5-34 |
| | Figure 5.10-3: Condition G. Wind Speed and Direction during Test | 5-34 |
| 5.10.4 | Results | 5-35 |
| 5.11 | Long Term Stability Test | 5-36 |
| 5.11.1 | Process Conditions | 5-36 |
| | Figure 5.11-1: Long Term Stability Flow and CZG Heat Content | 5-36 |
| | Figure 5.11-2: Long Term Stability Vent Gas Composition | 5-37 |
| 5.11.2 | Steam Ratios | 5-37 |
| | Table 5.11-1: Long Term Stability Steam Ratios | 5-37 |
| 5.11.3 | Wind Conditions | 5-38 |
| | Figure 5.11-3: Long Term Stability. Wind Speed and Direction during Test | 5-38 |
| 5.11.4 | Results | 5-39 |
| 6.0 | Appendix | 6-1 |
| A.1 | Calculations | 6-1 |
| A.2 | PFTIR Calibration and Operation | 6-1 |
| A.3 | VOC Emission Calculations | 6-1 |
| A.4 | Personnel Involved with Flare Performance Test | 6-1 |

Acknowledgements

The Primary Authors for this report were:

Ruth Cade – Marathon Petroleum Company

Scott Evans – Clean Air Engineering

This report would not have been possible without extensive input and feedback from others involved with this project. We wish to acknowledge the following people for their invaluable contributions to this project and this report.

Brian Wilt – Marathon Petroleum Company

Alejandro Acuna – Marathon Petroleum Company

Dr. Robert Spellicy – Industrial Monitor and Control Corporation

Dr. Jim Seebold – Chevron (Ret.)

Dr. Laura Kinner – Emission Monitoring

Jim Franklin – John Zink Company, LLC

Peter Kaufmann – Clean Air Engineering

Daniel Roesler – Clean Air Engineering

Nadia Lazzar – Clean Air Engineering

1.0 BACKGROUND & SUMMARY

As required by a Clean Air Act Section 114 request requiring testing of a refinery steam-assisted flare, Marathon Petroleum Company (“Marathon”) conducted performance testing of its main flare in Texas City, Texas. The main objective of the test was to better understand the impacts of steam on the overall emissions performance of the flare in terms of combustion efficiency (CE). Marathon has implemented an automatic steam control system for this flare designed to mitigate periods of flare over-steaming. The performance test was conducted using a Passive Fourier Transform Infrared (PFTIR) Spectroscopy instrument developed and operated by Industrial Monitor and Control Corporation (IMACC).

The purpose and major benefit of a steam injection system is to significantly reduce the amount of smoke that would otherwise be created by combustion. In a typical system, steam is injected into the flare combustion zone to deliver educted air as well as mixing energy. Over-steaming is a generic description of an undesirable operating condition possible in steam-assisted flare systems. In an over-steaming scenario, it is possible that the amount of steam and educted air introduced into the combustion reaction zone diminishes, rather than promotes, the efficiency of the combustion process if introduced in large enough quantities.



Figure 1-1. Texas City Main Flare

A flare’s operating envelope should be bounded by excess visible emissions (i.e. too little steam) and excess emissions of volatile organic compounds (“VOCs”) (i.e. too much steam). The efficiency of any particular steam injection system with respect to smoke suppression is easily measured by monitoring steam rates and visually observing smoking performance. However, the ability to measure or even identify excess emissions caused by over-steaming is a more difficult task. Standard emission estimation techniques have generally assumed a 98% combustion efficiency or higher when calculating VOC emissions from flares.

Performance Test of a Steam-Assisted Elevated Flare Marathon Petroleum Company, Texas City Main Flare

Regulatory requirements for flares are contained in 40 CFR §60.18 and §63.11. These requirements were developed from a series of flare emissions tests led by the United States Environmental Protection Agency (US EPA) from 1983 – 1986.¹ The requirements include maintaining a flare pilot, operating with a minimum net heating value of 300 BTU/scf in the vent gas, operating at exit velocities of less than 60 ft/s (or 400 ft/s depending upon the vent gas net heating value) and operating with a limited amount of visible emissions. However, a flare can be operated in compliance with these requirements and still be over-steamed.

Previous tests of flare performance, including the US EPA tests in the mid-1980s, have been conducted on pilot-scale test flares at moderate to high vent gas loads. However, a flare typically operates at low vent gas loads (i.e., high turndown) under normal conditions until a process upset or other operating condition requires the operator to flare waste gas. Thus, the flare normally operates at high turndown for the majority of the operating year, a condition for which there is little to no available performance data.

In the past, measuring the combustion products from a flare was difficult and dangerous. Recent technological advances, however, have produced remote sensing instruments capable of indicating the presence of combustion products such as carbon dioxide, carbon monoxide and select hydrocarbons without the safety hazards introduced by physically sampling a flare plume. One such instrument is the PFTIR, which characterizes a plume's chemical make-up (carbon dioxide, carbon monoxide, and total hydrocarbons) in units of concentration x pathlength. The absolute concentration cannot be determined, but the product (concentration x pathlength) measured in ppmv x meters, can be used in the combustion efficiency calculations. The PFTIR instrument is a new tool that has not yet been blind validated against extractive sampling results. The Texas Commission of Environmental Quality (TCEQ) evaluated the PFTIR against extractive FTIR in 2004². Marathon's Texas City main flare performance test was the first time the PFTIR was used on an operating industrial flare.

¹ EVALUATION OF THE EFFICIENCY OF INDUSTRIAL FLARES: TEST RESULTS, United States Environmental Protection Agency, Office of Air Quality Planning and Standards, EPA-600/2-84-095, May 1984

EVALUATION OF THE EFFICIENCY OF INDUSTRIAL FLARES: FLARE HEAD DESIGN AND GAS COMPOSITION,, United States Environmental Protection Agency, Office of Air Quality Planning and Standards, EPA-600/2-85-106, September 1985

EVALUATION OF THE EFFICIENCY OF INDUSTRIAL FLARES: H₂S GAS MIXTURES AND PILOT ASSISTED FLARES, United States Environmental Protection Agency, Office of Air Quality Planning and Standards, EPA-600/2-86-080, September 1986

² PASSIVE FTIR PHASE 1 TESTING OF SIMULATED AND CONTROLLED FLARE SYSTEMS, Texas Commission on Environmental Quality, June 2004

Performance Test of a Steam-Assisted Elevated Flare Marathon Petroleum Company, Texas City Main Flare

The PFTIR performance test conducted on Marathon's Texas City refinery's main flare produced valuable insights into the flare's efficiency performance under a variety of conditions. Tests were conducted while flaring gases containing saturates, olefins, nitrogen and hydrogen mixtures. For each Test Series, steam was increased from the manufacturer's recommended minimum cooling steam rate to the point of snuffing the flare. For the majority of tests conducted, combustion efficiency declined with increasing steam at constant vent gas mass loading and constant composition. High combustion efficiencies could be achieved at minimum cooling steam rates on the Texas City main flare.

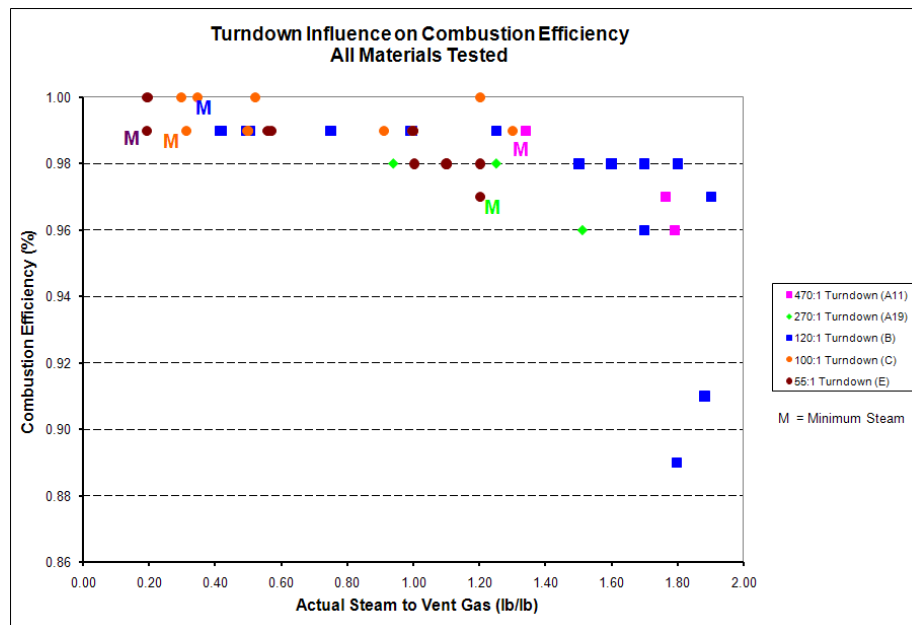


Figure 1-2. Combustion Efficiency vs. S/VG: Composite of All Materials Tested

This data demonstrates that this flare can likely achieve 98% combustion efficiency during turndown operation with proper steam delivery system design.

The performance test data also yielded insights into variables that could potentially be used as parametric monitoring points to ensure high efficiency during stand-by operation. One variable is a calculated term representing the net heating value (NHV) of the combustion zone gas (CZG). The combustion zone for an elevated steam-assisted flare is directly above the flare's tip, and is the point in which all materials combine for combustion. The net heating value (NHV) of the combustion zone gas is therefore the resulting heat content of the mixture that is created by the vent gas from the flare header, the pilot gas, and the total steam, in this case including center, lower, and upper steam. The CZG NHV showed strong correlations to combustion efficiency regardless of vent gas composition, with efficiency declining between 200 – 250 BTU/scf. See Figure 1-3 below.

Performance Test of a Steam-Assisted Elevated Flare Marathon Petroleum Company, Texas City Main Flare

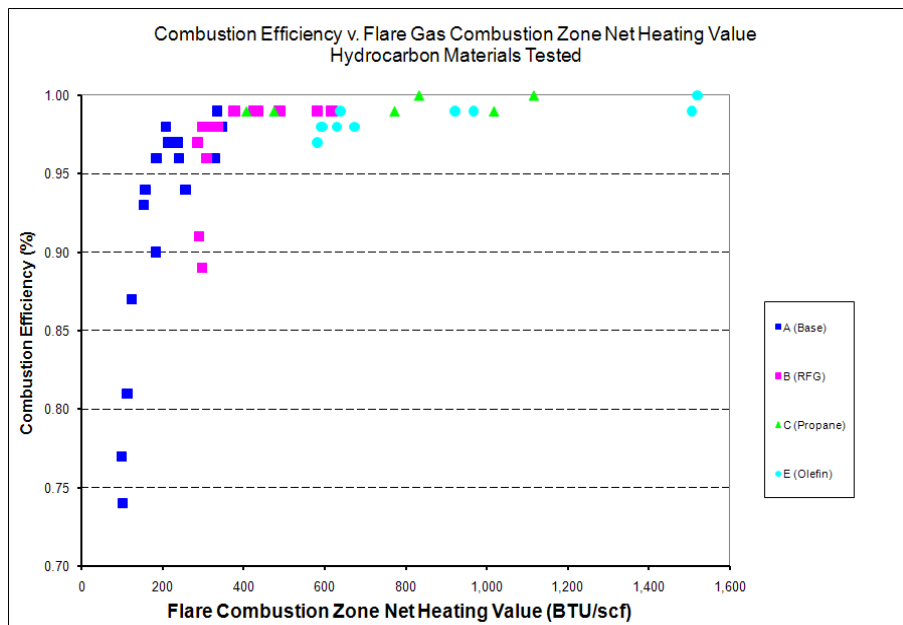


Figure 1-3. Combustion Zone Gas NHV vs. CE for All Materials Tested

The test data also showed that a visible flame has higher combustion efficiency than a steam-induced transparent flame. Combustion efficiency becomes erratic and declines rapidly when enough steam is added to turn a visible yellow flame invisible. High combustion efficiencies were also observed while the main flare experienced unacceptable levels of visible emissions.

While not yet blind validated against extractive analysis techniques, the PFTIR instrument appears to be a good tool to identify general flare performance trends. Additional research is needed to characterize the instrument's overall precision and bias. The combustion reaction products measured by the PFTIR appeared to show variability and scatter in terms of the carbon dioxide component, but less so in terms of combustion efficiency. There are many factors that could influence the efficiency performance of a flare, including those associated with the flare operation and design. Other factors contributing to component variability could also include atmospheric conditions, flame movement/plume tracking, instrument specific factors such as the specific detector used or the spectral wavelength used for plume component quantification as well as variability introduced by the measurement technique itself. Another potential cause of the observed data variability could be flare plume inhomogeneity -- pockets of differing compositions exist within the plume resulting in a plume cross-section with varying composition. The PFTIR's field of view is small relative to the plume size, which could enhance rather than normalize these variations in plume composition. A single source of data variability was not determined as part of this test.

2.0 INTRODUCTION

2.1 Objectives of Test Program

The overall objectives of the test program were as follows:

1. Implement a performance test program that demonstrates compliance with 98% combustion efficiency requirements as determined by the PFTIR remote sensing analyzer, over a range of vent gas compositions and steam to vent gas (“S/VG”) ratios at turndown operating scenarios.
2. Evaluate key variables such as Combustion Zone Gas Heat Content (“CZG”), actual steam to vent gas ratio (“S/VG”), and a comparison of S/VG ratios predicted by API 521 to actual ratios (“API 521 Multiplier (S/S521)”) as key performance indicators that may assist in maintaining flare operation at high efficiency conditions.
3. Evaluate the viability and reliability of utilizing an infrared smoke detector to maintain flare operation at the “incipient smoke point”, a point that has been demonstrated through third-party pilot-scale test programs to be the highest point of combustion efficiency.
4. Conduct a flare performance test without incurring upsets or other malfunctions on refinery process equipment, which would generate additional sources of emissions.

2.2 Testing Organization

The test was conducted with the assistance of both Clean Air Engineering and Industrial Monitoring and Controls Corporation (IMACC).

Clean Air Engineering

500 W. Wood St.
Palatine, Illinois 60067

IMACC

800 Paloma, Suite 100
Round Rock, Texas 78645

Because the test required personnel from Marathon’s operations, maintenance, engineering, and environmental staff, a cross-functional team was formed between IMACC, Clean Air Engineering and Marathon in order to staff, monitor and record test results. A list of personnel present during the test is included in Appendix A.4.

2.3 Flare System Components

2.3.1 Purpose

A flare is one of the most important safety devices in use at a refinery. Its purpose is to safely combust gases generated by emergency or upset conditions within a process unit. As a result, a flare must operate over a large and variable range of operating scenarios. These vary from typical stand-by operation at minimum flow conditions to efficiently combusting gases generated from a full power outage or other process safety relief scenario.

Marathon's flare test focused on the stand-by (i.e. high turndown) operating range. Not only does this range encompass the majority of a flare's operating time, but it is also the range where performance test data are scarce.

2.3.2 Flare Tip

The Marathon Texas City main flare is an elevated steam-assisted flare. The flare tip is manufactured by Callidus Technologies and was installed in December, 2000. The tip has three points of steam addition: center steam, a lower steam ring, and an upper steam ring. The lower steam ring manifold piping has a connection to a small sweep gas ring used for shaping at the tip exit.

A description of the Main Flare and key design specification are listed in Table 2.3-1 below.

Table 2.3-1: Texas City Main Flare Summary of Description and Design Specifications

| Texas City Main Flare | | |
|--|---|----------------|
| Flare Tip Details | | |
| Flare Tip Manufacturer | Callidus Technologies | |
| Flare Tip Installation Date | December 2000 | |
| Flare Tip Size | 24 in. diameter, 23.25 in. effective diameter | |
| Flare Tip Model Number | BTZ-IS ³ /US-24-C | |
| Summary of Flare Design Information | | |
| <i>Parameter</i> | <i>Value</i> | <i>Units</i> |
| Design Purge Rate | 108 | scfh |
| Pilot Rate | 12 | lb/hr |
| Minimum Total Steam | 1250 | lb/hr |
| Maximum Hydraulic Capacity (i.e. Max Vent Gas Rate) | 500,000 | lb/hr |
| Maximum Smokeless Capacity | 165,000 | lb/hr |
| Height of Flare Tip | 159 | ft above grade |

Performance Test of a Steam-Assisted Elevated Flare
Marathon Petroleum Company, Texas City Main Flare

The main flare serves as relief protection for nine process units. Typical flare operation is in stand-by mode at approximately 1100 to 2000 lb/hr of base load flow or less than 0.5% of the hydraulic capacity -- a 250:1 turndown factor. Base load includes flare header sweep gas, seal purges from rotating equipment, sample stations, and various process vents from refinery equipment.

2.3.3 Flare Automatic Steam Control System

Marathon implemented an automatic steam control system prior to the performance test. This system consists of flow instruments for both the total steam rate and vent gas rate, as well as a smaller trim steam control valve for the lower steam ring. An instrument that detects visible emissions (i.e. smoke) using an infrared signal was also installed and tested for viability (see Section 2.4 for details). The existing flare header gas chromatograph installed pursuant to Texas HRVOC rules (30 TAC Chapter 115 Subchapter H, Division 1) was used to characterize vent gas composition.

Specific components of the steam control system are summarized in Table 2.3-2 with details below.

Table 2.3-2: Automatic Steam Control System Components

| Parameter | Technique | Vendor | Model |
|--|------------------------------|--|-------------------|
| Flare Gas Volumetric/ Mass Flow | Ultrasonic Time of Flight | GE Panametrics | DigitalFlow GM868 |
| Steam Mass Flow | Ultrasonic Time of Flight | GE Panametrics | DigitalFlow GS868 |
| Flare Gas Composition and Net Heating Value | Gas Chromatography | Siemens | Maxum II |
| Flare Gas Molecular Weight | Ultrasonic Time of Flight | GE Panametrics (same unit as above) | DigitalFlow GM868 |
| Incipient Smoke Point | Infrared Camera Qty 2 | Mikron / E ² Technology | Zoom™ 8100SM |

Flare Gas Flow Rate, Temperature, and Molecular Weight

A GE Panametrics ultrasonic flow meter measures flare gas flow rate, temperature and molecular weight. It is important to note that this instrument cannot distinguish between components of like molecular weight. For instance, it cannot distinguish propane from carbon dioxide (both having a molecular weight of 44 lb/lbmole). Since the steam control

Performance Test of a Steam-Assisted Elevated Flare Marathon Petroleum Company, Texas City Main Flare

requirements would be very different for the two compounds, the molecular weight measurement was not used independently in the control logic.

Note that the ultrasonic meter is spanned for the full flow range of the flare system. Manufacturer's specifications indicate reasonable accuracy at low flow conditions. Prior to testing, the ultrasonic flow meter was field calibrated by manufacturer representatives.

Flare Gas Composition

A Siemens Maxum II Gas Chromatograph monitors the flare gas compositions and heat content (BTU/scf). This analyzer provides an analytical data point approximately once every ten minutes.

Steam Flow Parameters

Steam flow is measured by a GE Panametrics ultrasonic flow meter. Prior to testing, steam control valve positioners were calibrated and checked for proper operation.

Incipient Smoke Point

The Zoom™ infrared smoke detectors were supplied by John Zink Company, but manufactured by Mikron/E² Technology. The Zoom™ is an IR sensor that monitors the flare flame to detect the presence of soot precursors. Two units were installed at approximately perpendicular points of view to accommodate atmospheric effects at the facility. Both detectors were calibrated and adjusted prior to testing.

2.4 Mikron IR Cameras

Two Mikron IR Cameras were installed for this test. The cameras, which are typically used for smoke detection, were tested for their ability to detect over-steaming in addition to smoke. This section discusses some of the background of using IR cameras for smoke detection as well as the details of the performance of the cameras during this test program. It should be noted that these "cameras" do not provide a visual image but data only. The IR cameras were included as part of this test program to evaluate its potential to be used as a trim control instrument to maintain flare operation near the incipient smoke point automatically, and not based upon empirical or parametric variables. As discussed below, the IR cameras were determined to not be technically feasible to protect the flare from over-steaming as part of an automatic control scheme.

2.4.1 Background on IR Smoke Monitors

Infrared smoke monitors have been used for many years to assist in smoke control for flares. Infrared energy from the flare flame is collected by means of a focusing optical lens that concentrates the energy on a sensitive infrared detector. The design tested uses two filters at separate wavelengths to allow the electronics to selectively amplify the infrared energy in the range of interest. These filters are on a continuously rotating "chopper wheel" which creates a pulsating "on/off" signal as each filter crosses the view path between the optical lens and

the detector. The electronic circuitry is synchronized with the chopper to provide the desired output based on the infrared energy levels passing through the two different filters.

A key parameter in the success of this technology is not only the circuitry and detector, but also the selection of the filters. The filters must be able to detect infrared energy in the range of interest while filtering out background, weather conditions, and other potentially interfering infrared energy. Interferences include the sun, so the detectors must be oriented so the sun is not in the line of view at any time of the year. The actual filters chosen are proprietary to the manufacturer. The intent is to select filters that will produce an increased level of infrared energy as the flame begins to smoke, a reduced level when the flame is not smoking, and an even lower or zero level when the flame is clear.

As smoke control was the primary driver for the development of these monitors, successful operation was achieved if smoking was eliminated or at least significantly reduced. The effects of over-steaming were not a major consideration in the use of smoke monitors. This is particularly true when smoke monitors were first used many years ago when flares typically operated at higher flow rates on a continuous basis. Flares operating at higher flow rates are harder to over-steam than flares operating at high turndown rates.

Testing is not known to have been conducted to demonstrate if infrared smoke monitors had the accuracy and range of detection to not only prevent smoke but also prevent over-steaming. It is an even greater challenge to accomplish this task from a range from very high turndown (low flow) flare flow rates up to higher flow (low turndown) flare flow rates. If an infrared smoke monitor could provide this range of operation with a high level of accuracy, it was hoped that it could be tuned to assist in keeping the steam at the incipient smoke point, as this point is believed to produce the highest combustion efficiency for flare operation.

2.4.2 Use of IR Cameras during Marathon Texas City Test Project

For this test, two Mikron / E²T M8100 Flare Smoke Monitors were installed so at least one monitor would have a good view of the flame regardless of wind direction. Both were located so the sun would not directly interfere with the infrared energy received by the detector.

The monitors were calibrated per the manufacturer's instructions to obtain a midrange control signal when the flame was somewhat luminous, but not smoking. During these calibrations, the flare was operating in relatively low flow, high turndown conditions. These were the main areas of interest for testing. Under these low flow conditions, the gain adjustment on both monitors had to be at almost full span to get the desired signal. However, high gain settings were found to produce erratic signals from the monitors.

In some cases, the high gains resulted in “false” signals when the flame was clear. Under these conditions, the monitor would have been incorrectly calling for more steam instead of less steam. When the gain was adjusted to stop the erratic signals, the output control could not produce enough signal strength to be used for flare control. The calibrations were adjusted several times during the testing and no calibration settings were found that could meet the requirements.

The conclusion is that the IR monitors cannot be used to keep a flare near the incipient smoke point at low flow rates and, in fact, could increase the chance of over-steaming. The monitors were not evaluated for performance at higher flow rates as all test were conducted at low flow conditions.

2.5 Video Cameras

During this test program, a total of six video cameras recorded flare activity from various locations. Three of these were IR cameras and three were visible light cameras. The purpose and location of each camera are described below. The location of all cameras can be seen on the plot plan shown in Figure 4.2-3.

PFTIR Aiming Camera

The PFTIR Aiming Camera is an IR camera mounted on the PFTIR telescope. The image from this camera is used by the PFTIR operator to aim the instrument. An examination of this video stream gives an indication of PFTIR aiming accuracy. An image from this camera is shown in Figure 2.5-1. The red square (added for this report) shows the area analyzed by the PFTIR. This red area completely fills the field of view of the PFTIR telescope during testing and indicates the area of the plume being sampled.



Figure 2.5-1: Image from PFTIR Aiming Camera

Performance Test of a Steam-Assisted Elevated Flare Marathon Petroleum Company, Texas City Main Flare

FLIR A320 Camera

The FLIR A320 camera was used to obtain a general view of flare operation in the IR. It has a broad spectral range from 7.5 to 13 microns (1333 to 769 wavenumbers). The temperature scale on the camera was not calibrated for this test and any temperature readings shown should be considered as relative indicators only. The camera was located approximately ninety degrees from the PFTIR siting location. An image from this camera is shown in Figure 2.5-2 below.

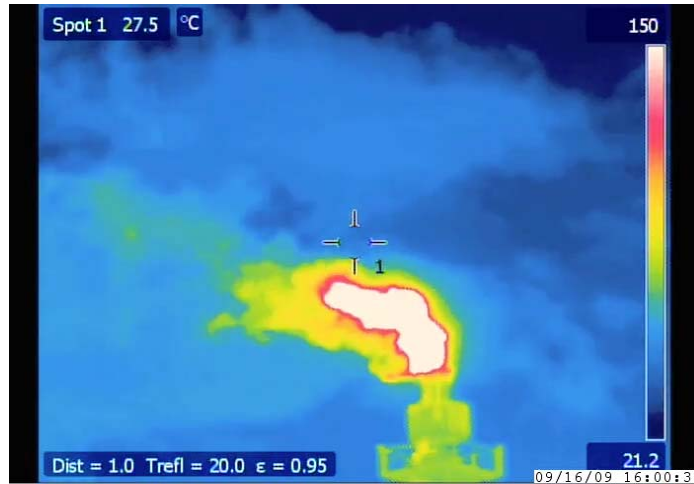


Figure 2.5-2: Image from FLIR A320 IR Camera

FLIR GasFind IR LW Camera

The FLIR GasFind IR LW camera was used to obtain a narrower spectral view of flare operation than that provided by the FLIR A320 camera. The GasFind LW camera operates in a spectral range of 10 to 11 microns (1000 to 909 wavenumbers). The camera was located approximately ninety degrees from the PFTIR siting location for the test program. An image from this camera is shown in Figure 2.5-3 below.



Figure 2.5-3: Image from FLIR GasFind IR LW Camera

Axis Q1755 Cameras

The Axis Q1755 cameras were used at each of the three visible camera locations. These HD cameras provide a detailed visible light image of flare operation. One camera was co-located with the two FLIR IR cameras. The other two were located near the Mikron IR cameras at their installed locations. The purpose of these two cameras was to provide a visual image to correspond to the data produced by the Mikron cameras. An image from the Axis camera located ninety degrees from the PFTIR site location is shown in Figure 2.5-4.



Figure 2.5-4: Image from Axis Q1755 Camera

2.6 Passive FTIR

The instrument used to determine the gas composition of the flare plume is the PFTIR analyzer. A detailed description of the instrument and the testing procedure are found in Section 4 with further detail in Appendix A.2.

The PFTIR operates on the principle of spectral analysis of thermal radiation emitted by hot gases. Passive means that no “active” infrared light source is used. Instead, the hot gases of the flare are the infrared source. The spectrometer is a receiver only. This approach is possible because the infrared emission spectra of hot gases have the same patterns or “fingerprints” as their absorption spectra. Consequently, observing a flare with an infrared instrument allows for identification and quantification of species through emission spectroscopy just as in absorption spectroscopy.

For this test program, the PFTIR operation and data analysis was overseen by Dr. Robert Spellicy of Industrial Monitor and Control Corporation (IMACC). The instrument and the analytical software were both developed by IMACC.

2.7 Flare Test Program

2.7.1 Steam Demand and API 521

Marathon's test program was designed to evaluate over-steaming under a variety of flaring conditions due to the wide operating range of the flare. Steam demand at a flare can vary for any number of reasons including:

- Compositional changes in vent gas – Saturated hydrocarbons such as methane and ethane require less steam for smokeless combustion than olefinic hydrocarbons like propylene or butene. Non-hydrocarbons or inerts like hydrogen and nitrogen require little to no steam for smokeless combustion; however, the amounts present may influence a flare's combustion efficiency performance.
- Mixing – Well-mixed combustion reactants require less steam for smokeless performance.
- Steam Pressure at Tip Nozzles – Subsonic steam flow conditions, typical during standby operation, require more steam to produce the same smokeless capacity at given conditions.

API 521 "Pressure-relieving and Depressuring Systems" is a design recommended practice issued by the American Petroleum Institute. API 521 suggests that a certain amount of steam is required for smokeless (Ringlemann 0) performance based upon the chemical composition of the hydrocarbons in the vent gas. However, the API 521 steam ratios are not related to combustion efficiency, but are utilized as a guide for the design of steam delivery systems for smoke suppression under worst-case design release scenarios. Proprietary commercial steam injection systems are of widely varying designs and may have differing degrees of effectiveness in smoke suppression than what is suggested by API 521.

One of the objectives of the Marathon Texas City test program was to determine if API 521 Table 11 (included below as Figure 2.7-1) could also serve as an operational guide or target, which may provide adequate steam and smokeless operation. As the intent of API 521 Table 11 was to serve as a design guide under relief loads, it was unknown if the same ratios would hold true for low flow operation as for high flow operation. If so, then the amount of steam recommended by API 521 could serve as a "minimum" target, and represent the amount of steam necessary to provide smokeless flare operation under all operating ranges. A multiple above the minimum API 521 ratio could then be utilized to establish an upper bound preventing over-steaming. The mathematical representation of this concept is known as the "S/S521" Ratio, which represents the amount of actual steam applied in excess of the minimum recommended by API 521 Table 11.

Performance Test of a Steam-Assisted Elevated Flare
Marathon Petroleum Company, Texas City Main Flare

Table 11 — Suggested injection steam rates

| Gases being flared | Steam required ^a |
|--------------------|---|
| | kg (lb) of steam per kg (lb) of hydrocarbon gas |
| Paraffins | |
| Ethane | 0,10 to 0,15 |
| Propane | 0,25 to 0,30 |
| Butane | 0,30 to 0,35 |
| Pentane plus | 0,40 to 0,45 |
| Olefins | |
| Ethylene | 0,40 to 0,50 |
| Propylene | 0,50 to 0,60 |
| Butene | 0,60 to 0,70 |
| Diolefins | |
| Propadiene | 0,70 to 0,80 |
| Butadiene | 0,90 to 1,00 |
| Pentadiene | 1,10 to 1,20 |
| Acetylenes | |
| Acetylene | 0,50 to 0,60 |
| Aromatics | |
| Benzene | 0,80 to 0,90 |
| Toluene | 0,85 to 0,95 |
| Xylene | 0,90 to 1,00 |

^a The suggested amount of steam that should be injected into the gases being flared in order to promote smokeless burning (Ringlemann 0) can be determined from this table. The given values provide a general guideline for the quantity of steam required. Consult the flare vendor for detailed steam requirements.

Figure 2.7-1: API 521 Table 11 Suggested Steam Rates

Performance Test of a Steam-Assisted Elevated Flare Marathon Petroleum Company, Texas City Main Flare

By plotting the API 521 predicted steam demand for saturates, olefins/aromatics, and diolefins based upon their molecular weight, a linear relationship emerged. Marathon's test program uses the linear relationship of the olefin/aromatic curve as the basis representing the amount of minimum steam API 521 Table 11 would require to achieve smokeless combustion. This is represented mathematically as:

$$S_{521}/VG = 0.0067 (MW) + 0.275$$

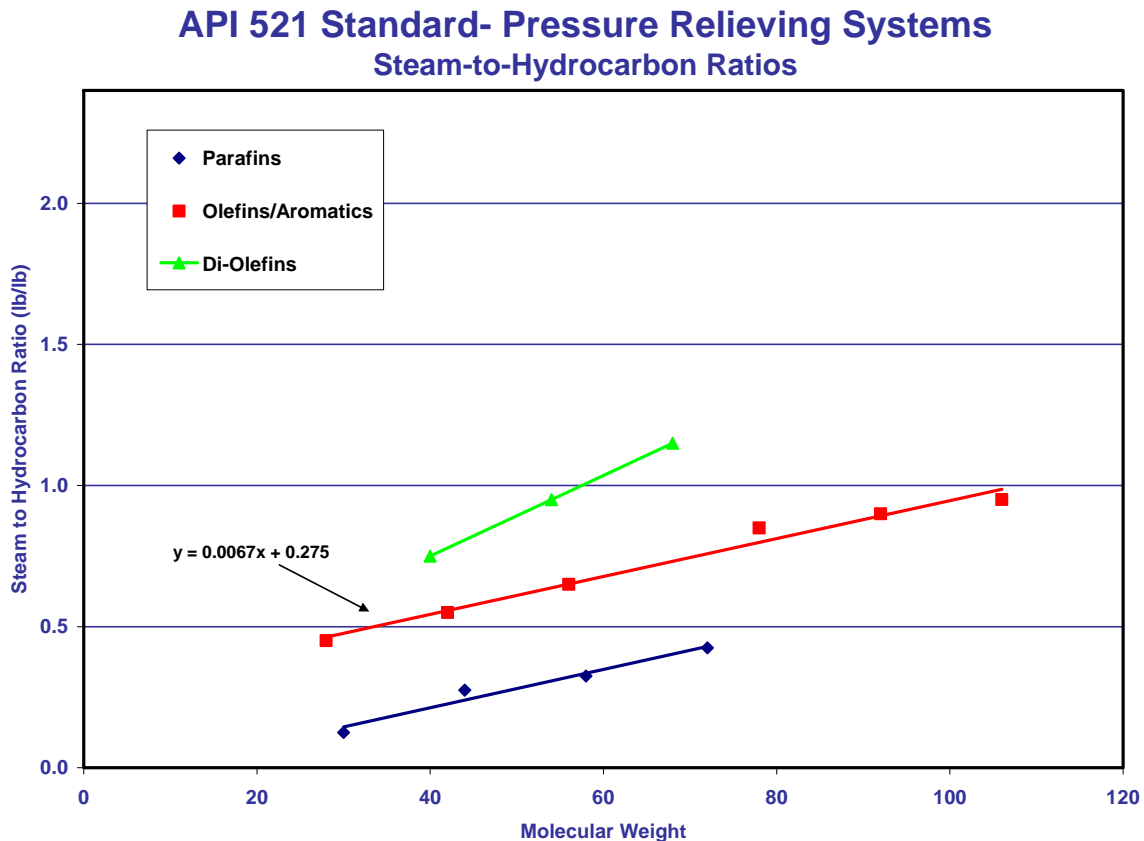


Figure 2.7-2: API 521 Steam-to-Hydrocarbon Ratios

Another key parameter used in evaluating over-steaming is the net heating value of the combustion zone gas abbreviated as CZG in this report. The CZG is the Lower Heating Value, expressed in Btu per standard cubic foot (Btu/scf), of the mixture of gases introduced into the combustion zone of the flare (i.e. at the flare tip). This value represents the resulting heat balance utilizing the inputs of vent gas, pilot gas, and steam. The CZG net heating value is a key parameter operators may use to optimize flare performance. The CZG is discussed further in Section 3.2.2.

2.7.2 Test Conditions

The following test series (A through G) was conducted with a different test gas composition or flow rate. Within each test, the steam flow was varied to achieve a range of S/VG ratios. The rationale for each test series is as follows:

- Test A To simulate plant normal base load -- this is the typical flow condition for the flare and represents day-to-day operation. Actual testing for this condition was conducted at three vent gas mass flow rates: 1,900 lb/hr, 1,100 lb/hr and 800 lb/hr. These flow rates are analyzed separately in this report and are designated as A19, A11 and A8 respectively. A19 and A11 are typical historic vent gas flow rates as measured by the vent gas flow meter. A8 was achieved by minimizing normal refinery fuel gas sweep for the sole purpose of achieving low heating value conditions suitable for Test G. Test A8 conditions are not representative of normal operating conditions of the Texas City main flare.
- Test B To evaluate flare performance with a higher flow rate of hydrocarbons by adding gas (refinery fuel gas) that has a low S/VG ratio for smokeless operation.
- Test C To evaluate flare performance at flow rates similar to Test B with addition of a saturated gas (propane) that would require a higher S/VG ratio for smokeless operation than the gas added in Test B. Propane is also one of the materials most frequently used in independent-pilot scale test studies.
- Test D Similar to Test C but add unsaturates (olefins) to evaluate performance at an even higher S/VG ratio needed for smokeless operation than added in Test C.
- Test E Same as Test D but with a higher flow rate (and thus higher unsaturate mass flow) to see the performance at higher flows for the unsaturate condition.
- Test F To evaluate performance when operating at higher levels of hydrogen than typically found in the base load. Hydrogen has been shown have exceptional combustion characteristics, but by nature has a low volumetric heat content (275 BTU/scf). Note that the base load may contain nominal amounts of hydrogen from 10 to 30% mole weight. Note that for the first part of this test, hydrogen was increased with the S/VG ratio held constant. For the last part of this test, a higher S/VG was used.
- Test G To evaluate performance with additional inerts (i.e. nitrogen) combined with hydrogen in the base load seeking an overall BTU/scf less than 300 (if possible) in vent gas or less than 200 in the combustion zone. In addition to the inert testing, this test provides a data point demonstrating the effect of the hydrogen benefit on a low BTU gas.

With exception of Tests F and G, at each of the conditions listed above several tests were performed at increasing steam rates. Steam was increased up to the point of flame outage for each run. Once the flame was verified as extinguished, the test condition was halted. For

Performance Test of a Steam-Assisted Elevated Flare Marathon Petroleum Company, Texas City Main Flare

each case, these are noted as “attempts” and are considered having zero combustion efficiency. Figures 2.7-3 and 2.7-4 below show the range of S/VG and S/HC ratios tested for each condition.

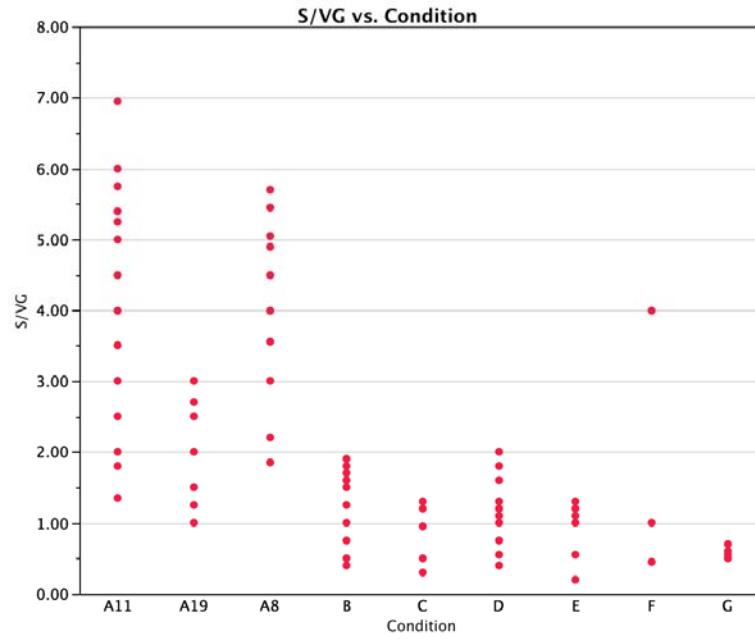


Figure 2.7-3: S/VG vs. Condition

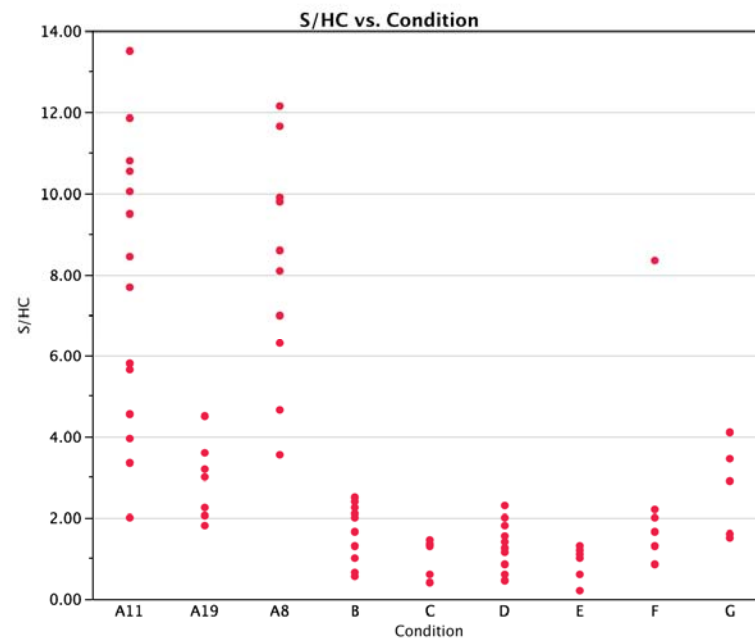


Figure 2.7-4: S/HC vs. Condition

3.0 SUMMARY OF RESULTS

3.1 Summary and Key Data Trends by Test Series

Tests A through E were analyzed individually and as a group to study the effect of steam on the combustion efficiency of a flare with hydrocarbon vent gases. Tests F and G were separately analyzed because they were primarily performed to study the effect of hydrogen and inerts on the combustion efficiency of the flare.

3.1.1 *Combustion Efficiency with Increasing Steam Rates*

For each test series presented below, relationships between combustion efficiency and at least two independent variables are presented: steam to vent gas ratio (S/VG) and actual steam to API 521 minimum (S/S521).

Condition A8 is not discussed since the sole purpose of this condition was to prepare for Test Condition G. Condition A8 is not representative of normal flare operation for the Texas City main flare. Furthermore, the PFTIR data for Condition A8 is compromised due to adverse wind conditions on the day of testing and is not considered valid data.

3.1.1.1 **Test Series A – Typical Base Load Conditions**

Test Series A represents typical base load conditions at the Texas City main flare. Both vent gas flow rates of 1,100 lb/hr (designated A11) and 1,900 lb/hr (designated A19) are grouped together on the figure below as they are representative of typical range of daily operation. The main flare header is partially swept with nitrogen as a sweep gas; therefore, this test series is a good comparator for increasing amounts of inerts in vent gas as well as operating at a higher turndown factor. Detailed data tables for Test Series A19 are found in Section 5.2, and for Test Series A11 in Section 5.3. Aiming accuracy was greater for Test Series A11 than for A19. Five out of twelve data points in A19 were impacted by wind direction with respect to PFTIR view angle, whereas none of the seventeen data points of A11 were impacted.

The point at which the flare was extinguished was much different from A Series to B Series conditions in terms of actual steam to vent gas ratios, but similar in terms of total steam flow rate. For the A Series, the flare extinguished to a zero (0%) combustion efficiency at S/VG ratios ranging from 3.5 to 7.5, or between 4,000 to 8,500 lb/hr total steam rate. The B Test

Performance Test of a Steam-Assisted Elevated Flare Marathon Petroleum Company, Texas City Main Flare

Series flame extinguished at ratios of 1.5 to 2, or between 5,700 to 8,300 lb/hr total steam rate. It is believed that a failed shaping ring on the flare tip, responsible for keeping the hot ball of gases together to facilitate combustion, contributed to early outages under certain wind directions.

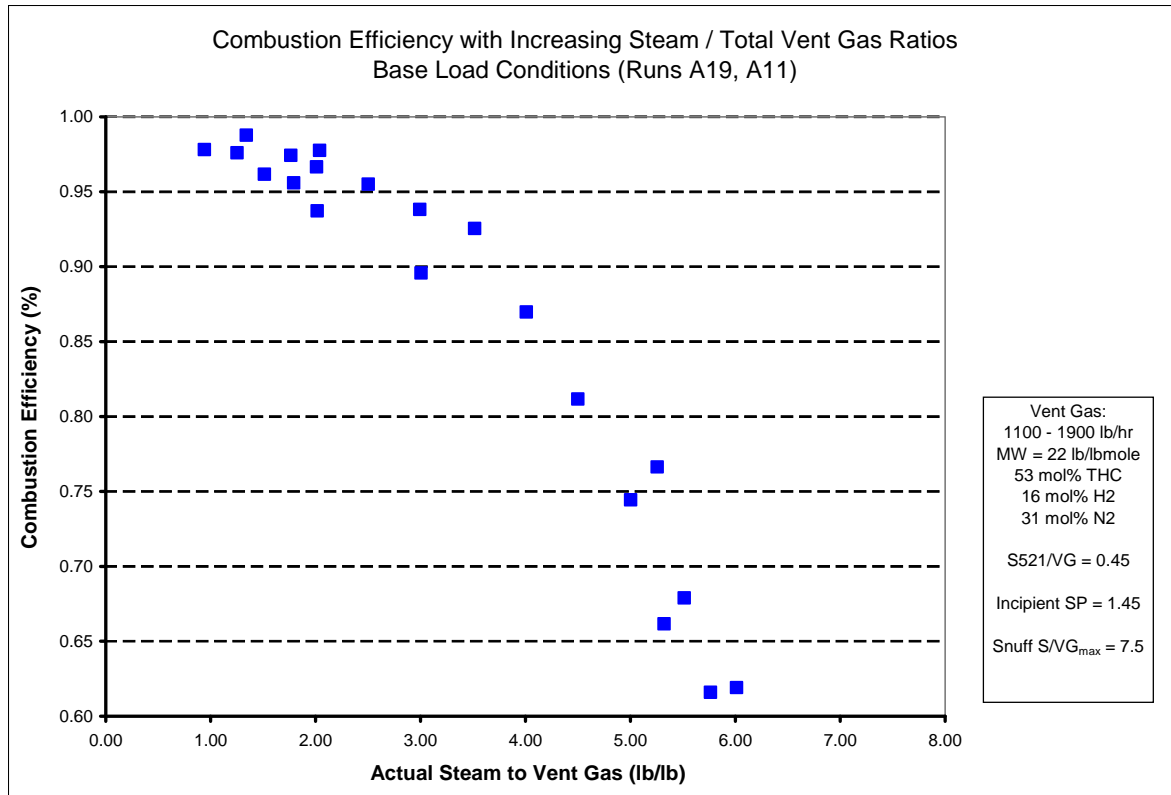


Figure 3.1-1: CE vs. S/VG for Base Load Conditions

The A11 Test series reached the highest S/VG ratios before extinguishment of any other test series conducted. Zooming in to a smaller X-axis scale below in Figure 3.1-2, it is seen that the combustion efficiency declines around a S/VG ratio of 2.

Performance Test of a Steam-Assisted Elevated Flare
Marathon Petroleum Company, Texas City Main Flare

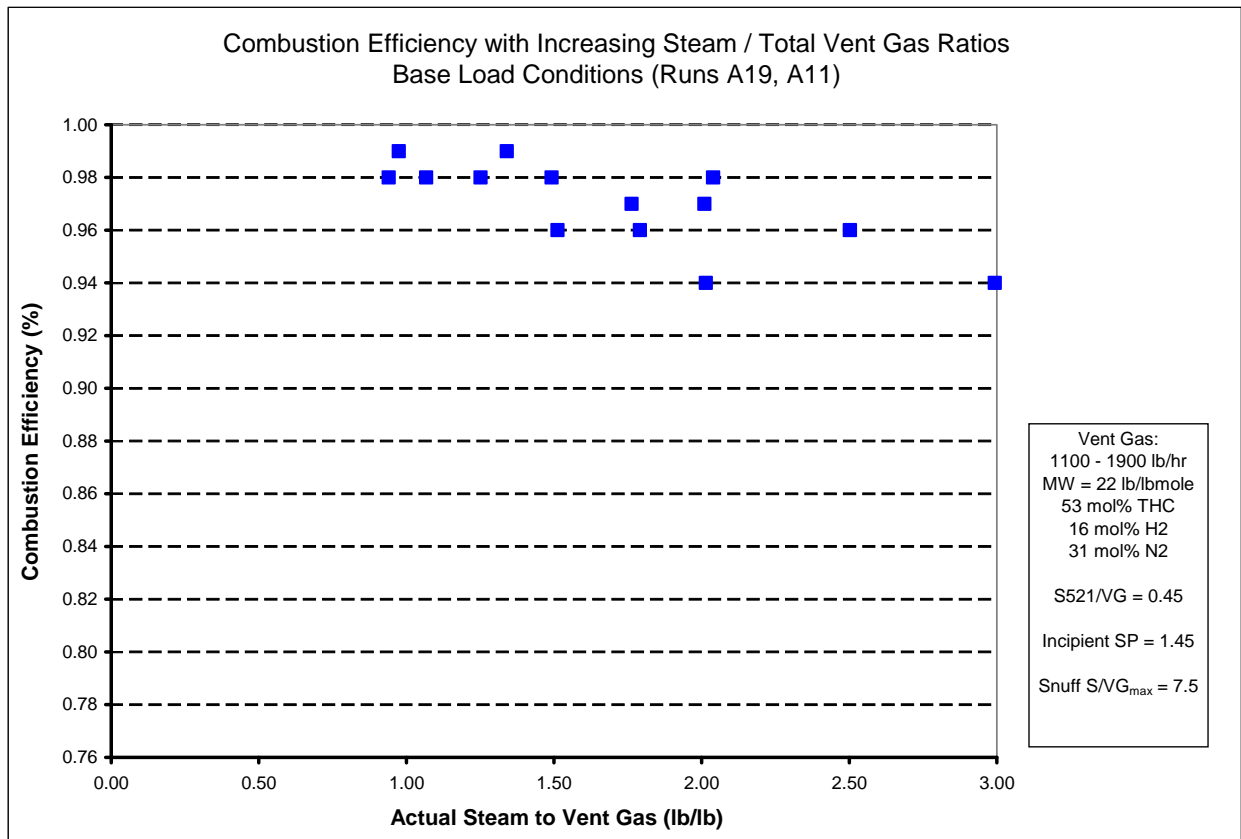


Figure 3.1-2: X-Axis Zoom of Base Conditions, CE vs. S/VG

Visible emissions were observed during Test Series A from 0.9 – 1.5 S/VG, or in terms of S/S521 at ratios of 2.2 – 3.2. As noted in Figure 3.1-3, the A Series Test runs have the tightest operating envelope between visible emissions and over-steaming. An S/S521 operating envelope of 3.5 lb/lb to 4.6 lb/lb is required to keep the flare between smoking and combustion efficiencies between 96% - 99%.

Performance Test of a Steam-Assisted Elevated Flare
Marathon Petroleum Company, Texas City Main Flare

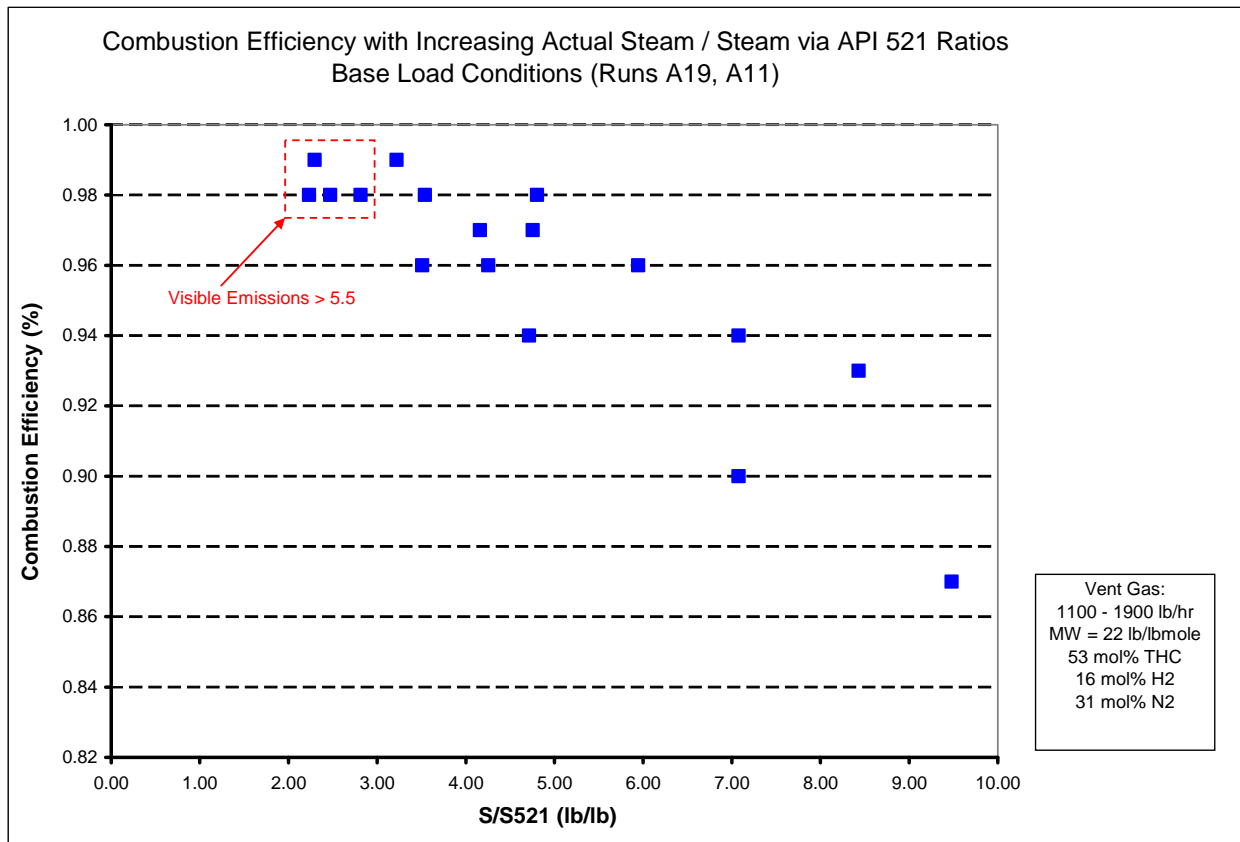


Figure 3.1-3: CE vs. S/S521 for Base Load Conditions

Variability in the combustion efficiency data is more pronounced in the A Series data than with other test conditions. This may be due to several factors:

1. Less stability of flare header composition – Since the test was conducted on an operating flare rather than a pilot test, the ability to maintain steady conditions was challenging throughout the test. The A Series runs are normal base load conditions, which have some natural variation that is more pronounced at low total flow rates. Nitrogen content varied from 16 to 41 mol%, total hydrocarbon content varied from 42 to 66 mol%, while molecular weight stayed relatively stable at 21 to 22 lb/lb-mole.
2. Higher concentration of inerts – Due to the low gas flow rates, the nitrogen content was more pronounced in this series. Of all the hydrocarbon test series, the A Series had the smallest amount of total hydrocarbons in the vent gas flow.
3. PFTIR signal strength – Achievement of a strong, steady signal on the PFTIR was more difficult at low vent gas flow rates.

4. PFTIR aiming accuracy – Several test conditions were severely impacted by wind direction and ability of the PFTIR to view a representative cross-section of the flare plume. This external influence is discussed in more detail in Section 3.2.2 below.
5. Turndown factor – The A series had the lowest total waste gas flow rate and was, therefore, more affected by wind and other external influences.
6. Inadequate mixing - Visually, it was apparent that the vent gas and steam was not well-mixed, as sections of the flare tip cross-section consisted of steam only rather than a mixture of vent gas and steam.

3.1.1.2 Test Series B – Refinery Fuel Gas

Test Series B was the most stable test series with the least degree of external influences to the test results. In this series, refinery fuel gas was added to the flare header to approximately double normal base load flow conditions. Vent gas composition was held to a very constant level throughout this test series. Aiming accuracy of the PFTIR instrument was also consistently high, with very few conditions where PFTIR view angle was compromised by wind direction. Detailed data tables for this test series are found in Section 5.5.

As can be seen in Figure 3.1-4 below, combustion efficiency remains relatively flat and then begins to decline rapidly around 1.75 S/VG ratio. The flame became transparent at S/VG ratios above 1.9.

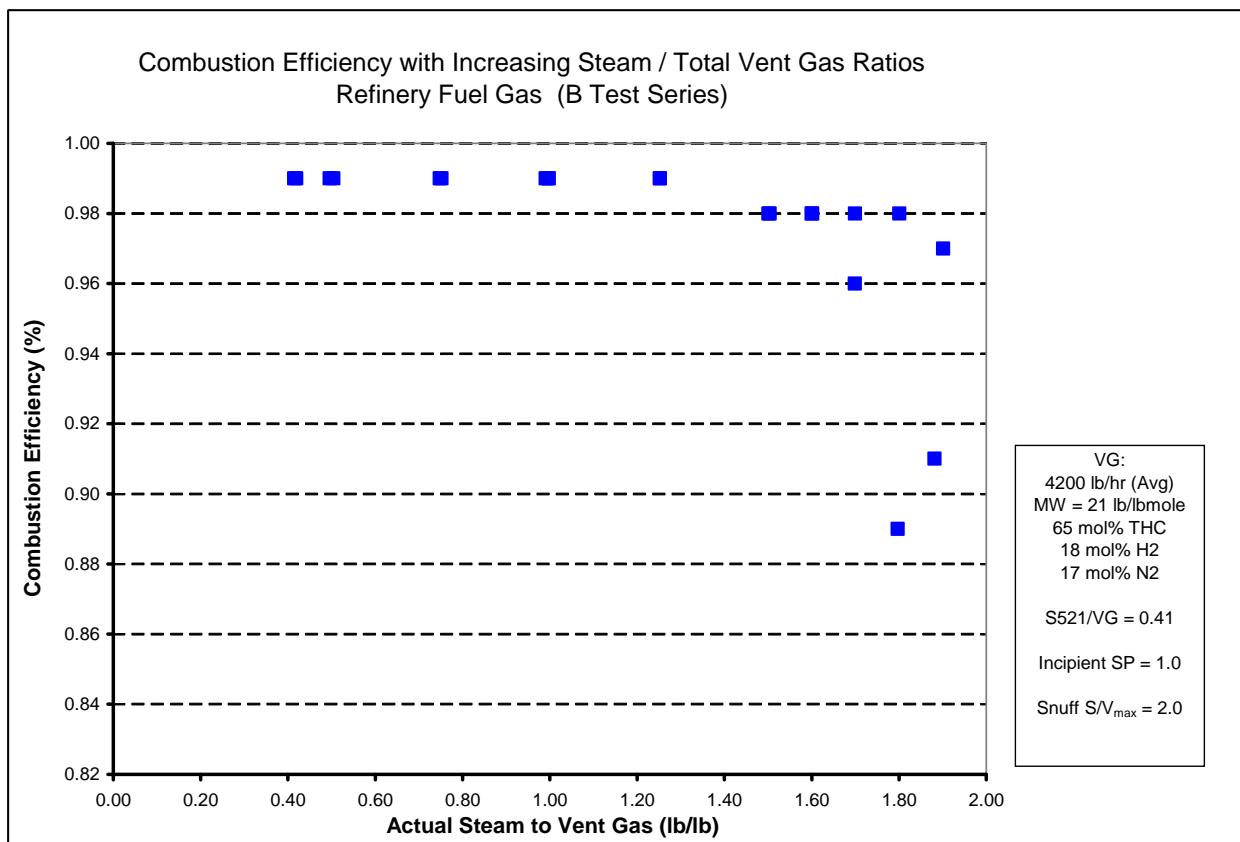


Figure 3.1-4: Refinery Fuel Gas CE vs. S/VG

Performance Test of a Steam-Assisted Elevated Flare Marathon Petroleum Company, Texas City Main Flare

Visible emissions were observed during Test Series B from 0.9 – 1.5 S/VG, or in terms of S/S521 at ratios of 2.2 – 3.2. As noted in Figure 3.1-5, the B Series Test runs have an operating envelope between visible emissions and over-steaming in terms of S/S521 of 1.9 lb/lb to 4.3 lb/lb to keep the flare between smoking and combustion efficiencies between 96% - 99%.

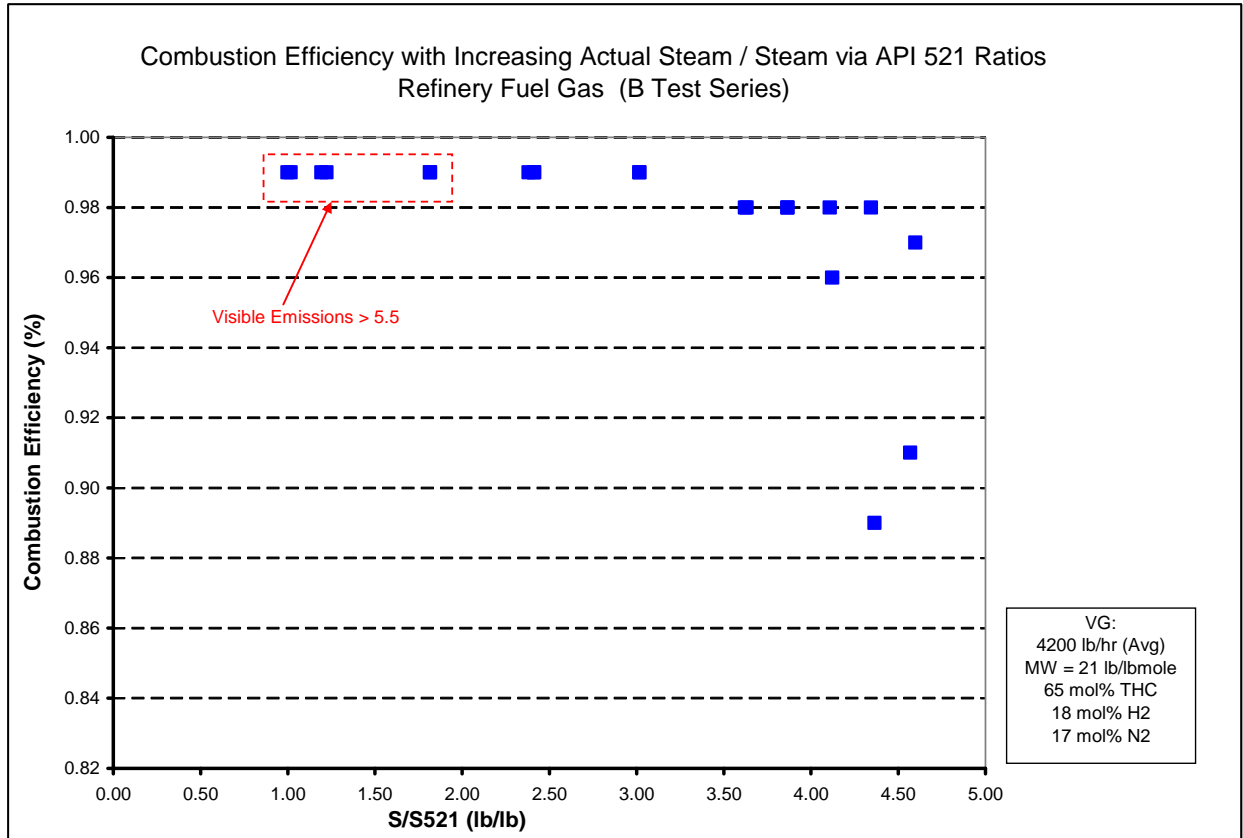


Figure 3.1-5: Refinery Fuel Gas S/S521 with Combustion Efficiency

3.1.1.3 Test Series C – Propane

Propane was one of the primary materials of choice used during previous pilot-scale extractive sampling performance tests of flares. Propane is readily available on the market in pure liquefied petroleum gas (LPG) form, and therefore used routinely as the hydrocarbon species to benchmark flare performance against. Detailed data tables for this test series are found in Section 5.6.

Flare combustion efficiency results remained flat until flame extinguishment for the propane test series. The combustion efficiency did not decline with increasing steam rates as seen in the other test materials. The incipient smoke point occurred at a 1.0 S/VG ratio and the flame was extinguished at 1.2 to 1.7 S/VG ratio with a total steam flow ranging from 7,000 to 10,000 lb/hr.

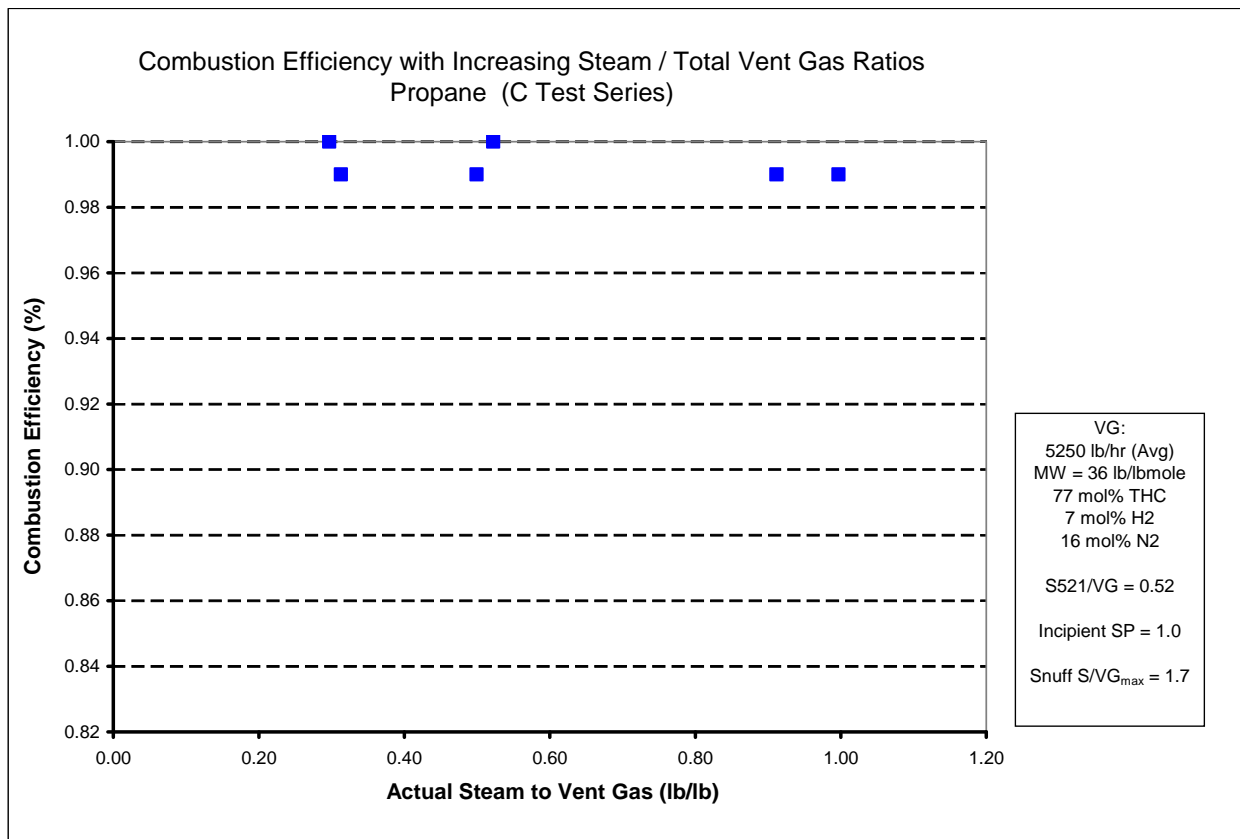


Figure 3.1-6: Propane Test Series CE vs. S/VG

Performance Test of a Steam-Assisted Elevated Flare Marathon Petroleum Company, Texas City Main Flare

Visible emissions were observed during Test Series C from 0.3 – 0.5 S/VG, or in terms of S/S521 at ratios of 0.6 – 0.96 lb/lb. As noted in Figure 3.1-7, the C Series Test runs have an operating envelope between visible emissions and over-steaming in terms of S/S521 of 1.0 lb/lb to 2.5 lb/lb is required to keep the flare between smoking and combustion efficiencies above 98%.

It is believed that the flare tip shaping ring damage caused premature extinguishments of the flare within this Test Series. When wind direction pushed the flame toward the area of the shaping steam line leak, the flare would shear off and go out.

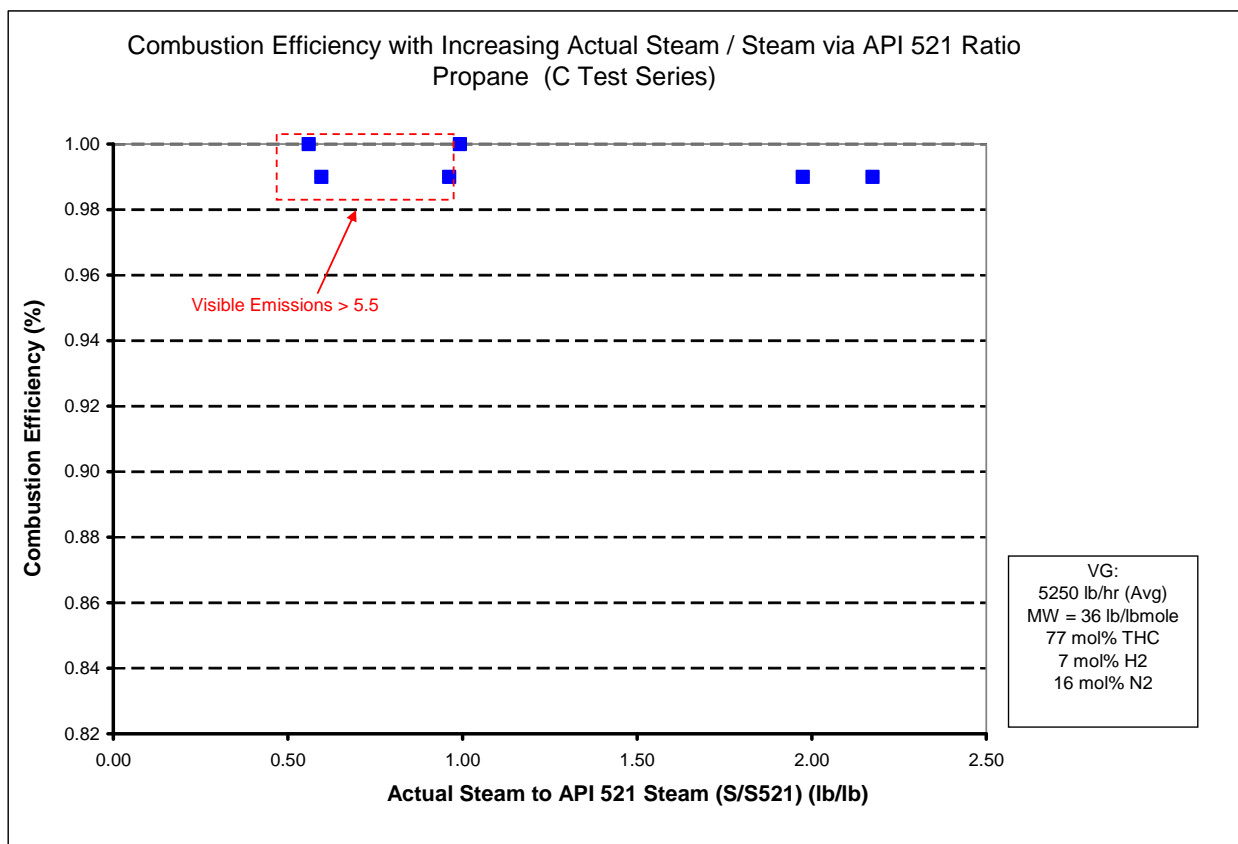


Figure 3.1-7: Propane Test Series CE vs. S/S521

It should also be noted that for generally all Test C runs, the amount of carbon dioxide detected by the PFTIR (in units of concentration x pathlength) was unusually high, and exceeded predictions of expected carbon dioxide present based upon a gross heat and material balance. As the quantity of carbon dioxide drives the combustion efficiency result, it is expected that this may have had an influence on the flat nature of the propane performance test curve.

3.1.1.4 Test Series D & E – Propylene/Butylene Olefins

Olefins require more steam for smokeless combustion due to unsaturated hydrocarbons. The primary purpose of Test Series D and E was to evaluate the incipient smoke point at turndown in comparison to the 0.55 lb steam per lb hydrocarbon predicted by API 521 Table 11. In addition, the 1983 CMA study trend that is primarily referenced when discussing flare over-steaming was conducted on propylene. It predicted a decline in flare combustion efficiency at steam to hydrocarbon ratios above 3.5 lb/lb. As noted below, the lower values achieved in the Marathon Texas City flare test could possibly be due to testing under a lower flow condition, or testing with a remote sensing technology versus extractive sampling of the composite flare plume.

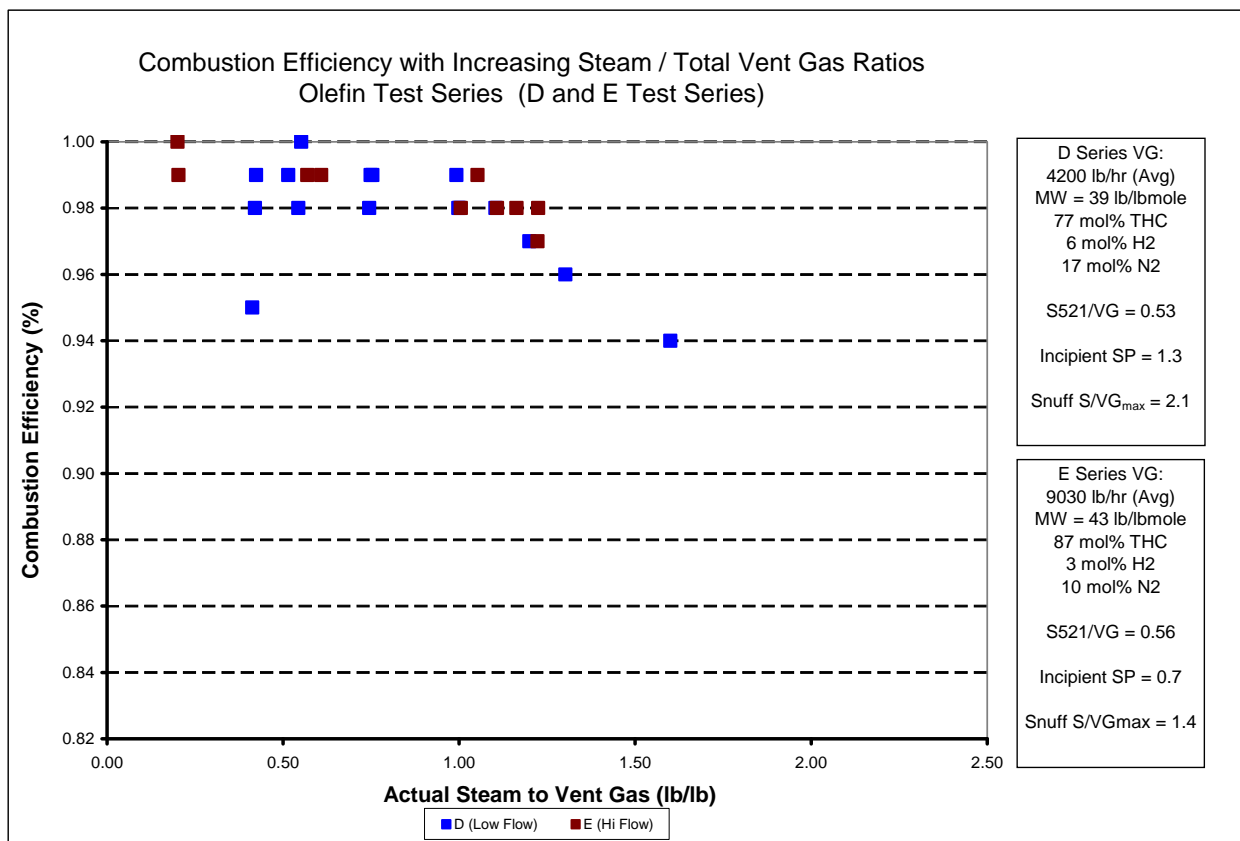


Figure 3.1-8: Olefin Test Series CE vs. S/VG

Performance Test of a Steam-Assisted Elevated Flare Marathon Petroleum Company, Texas City Main Flare

Visible emissions were observed during Test Series D & E from 0.4 – 0.9 S/VG. Test Series D was tested at a lower mass loading (approximately 4200 lb/hr vent gas flow rate), and resulted in an S/S521 operating envelope between visible emissions and over-steaming between 1.0 lb/lb to 2.1 lb/lb to keep the flare between smoking and combustion efficiencies above 98% as noted in Figure 3.1-9 below. Test Series E, tested at approximately 9030 lb/hr vent gas flow rate, resulted in an S/S521 operating envelope between 1.1 and 2.1 lb/lb.

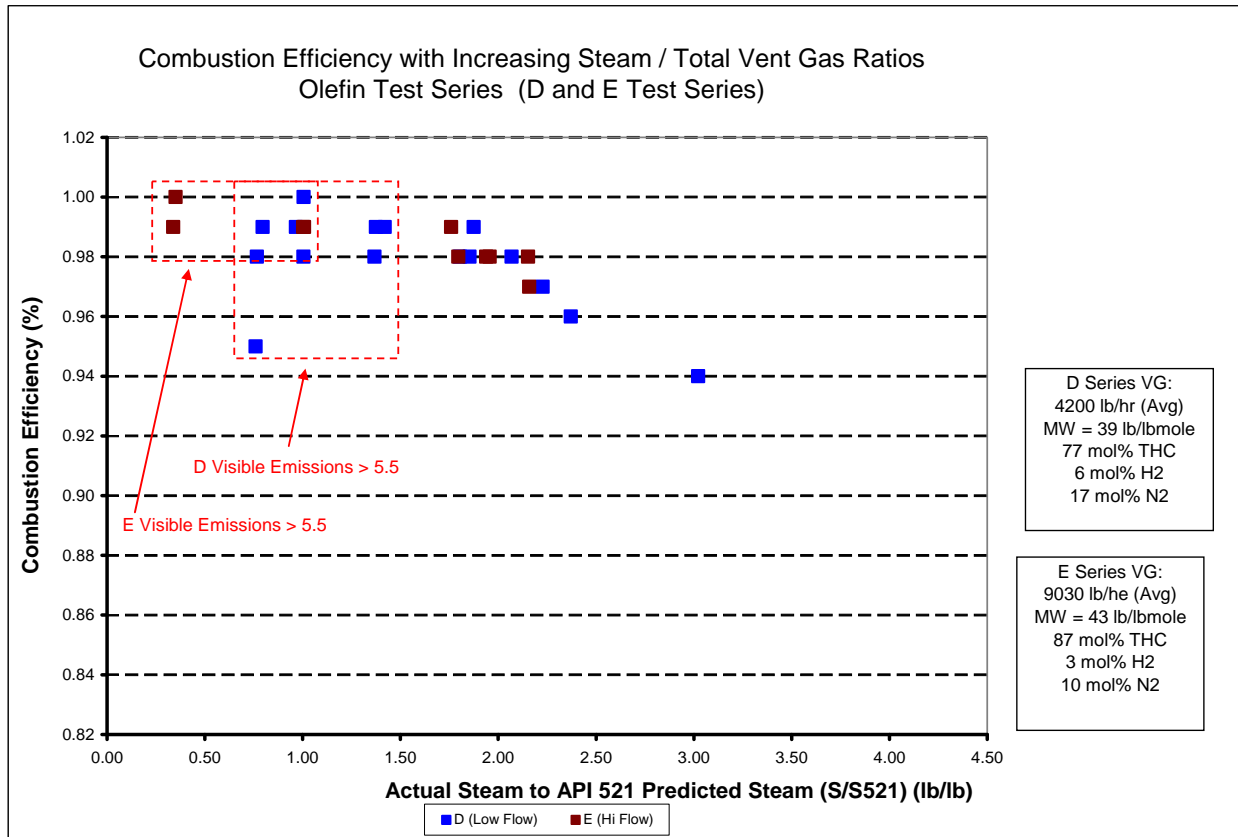


Figure 3.1-9: Olefin Test Series CE vs. S/S521

3.1.2 Observed Impacts of Hydrogen

Conditions F and G were intended to evaluate whether the hydrogen content of the vent gas had an effect on combustion efficiency. With both Test Series F and G, an issue with the sampling technique was identified upon review of the infrared video recordings from the PFTIR aiming camera. Tests conducted on two particular days of the test series, September 23 and 24, experienced wind conditions out of the north-northeast, which pushed the flame plume direction directly away from the PFTIR field of view. During these days, the PFTIR was not able to sample the plume cross-section, but was only able to sample the boundary layer surrounding the flame perimeter closest to the PFTIR instrument's line of sight.

The boundary layer of the flame perimeter may or may not be consistent with the results observed from a plume cross-section. There is not enough information to conclusively make an assertion either way. However, it could be theorized that, although the absolute values of combustion efficiency may potentially not be the same, the trend behavior of the flame boundary layer and plume cross-section may directionally track together.

3.1.2.1 Test Series F – Increasing Hydrogen Content

For Test Series F, the influence of increasing hydrogen content was tested as shown in Figure 3.1-10. For this condition, steam rates were held relatively constant at minimum conditions, with the exception of one run at 81 mol % hydrogen, in which steam rates were increased to a 4.0 S/VG ratio or an 8.0 S/HC ratio. Hydrogen compositions above 30 mol% consistently produce high combustion efficiencies regardless of steam rate.

In a petroleum refinery, there may be relief and/or operational scenarios that would divert highly concentrated hydrogen to a flare. For these cases, hydrogen is not expected to have a negative impact on combustion efficiency, but result in consistently high efficiencies regardless of steam rate. As noted above, all data presented below as well as in Section 5 were impacted by PFTIR view angle with respect to wind direction, therefore are reported for completeness, but should be limited in interpretation to general trend behavior only.

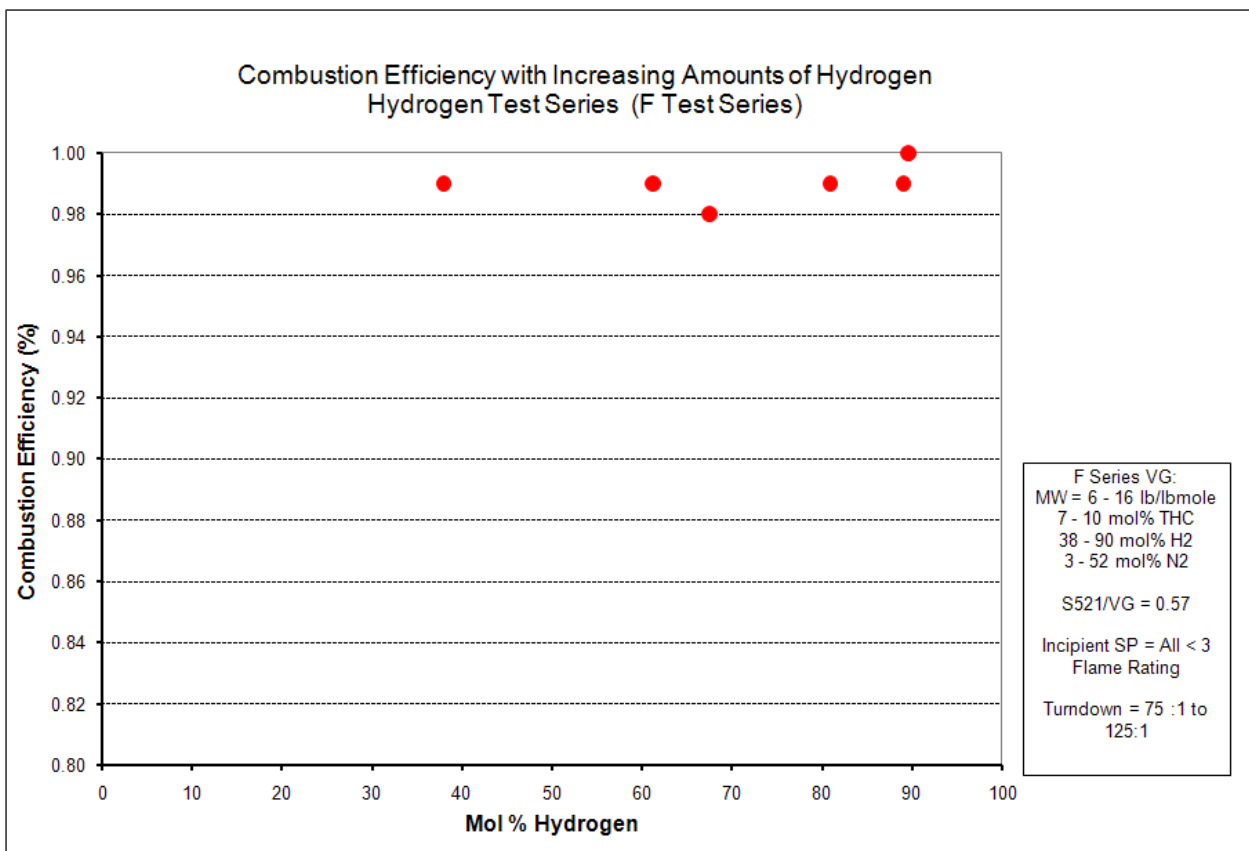


Figure 3.1-10: Combustion Efficiency as Hydrogen Content Increases

3.1.2.2 Test Series G – Increasing Nitrogen Content

Test Series G was designed to test whether hydrogen and nitrogen mixtures that create a vent gas net heating value of less than 300 BTU/scf would achieve high combustion efficiencies. Operating in this manner is not a normal condition for the Texas City main flare and required many operational changes. Sources of refinery fuel gas used to sweep flare headers were turned off and additional nitrogen purge lines were added to the flare. Hydrogen was also added in increments until the net heating value of the vent gas began to change. Combustion efficiency appears to decline as the net heating value of vent gas drops below 300 BTU/scf. As noted above, all data presented below as well as in Section 5 were impacted by PFTIR view angle with respect to wind direction, therefore are reported for completeness, but should be limited in interpretation to general trend behavior only.

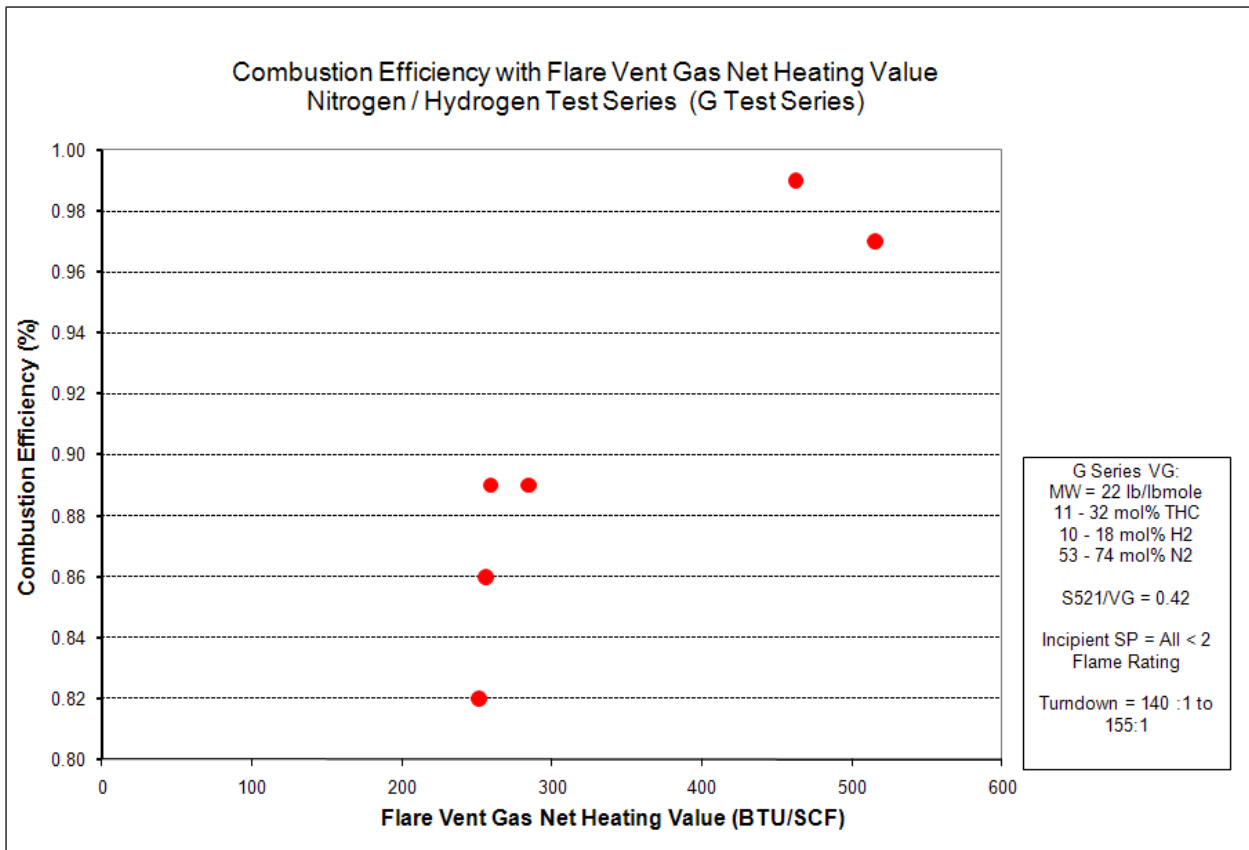


Figure 3.1-11: Combustion Efficiency with Decreasing NHV_{VG}

3.2 Summary and Key Data Trends of Whole Data Set

3.2.1 Composite of All Hydrocarbons Tested

When comparing the combustion efficiency curve of all conditions tested during the Marathon Texas City test program, it is interesting to note that an overall trend emerges as shown in Figure 3.2-1.

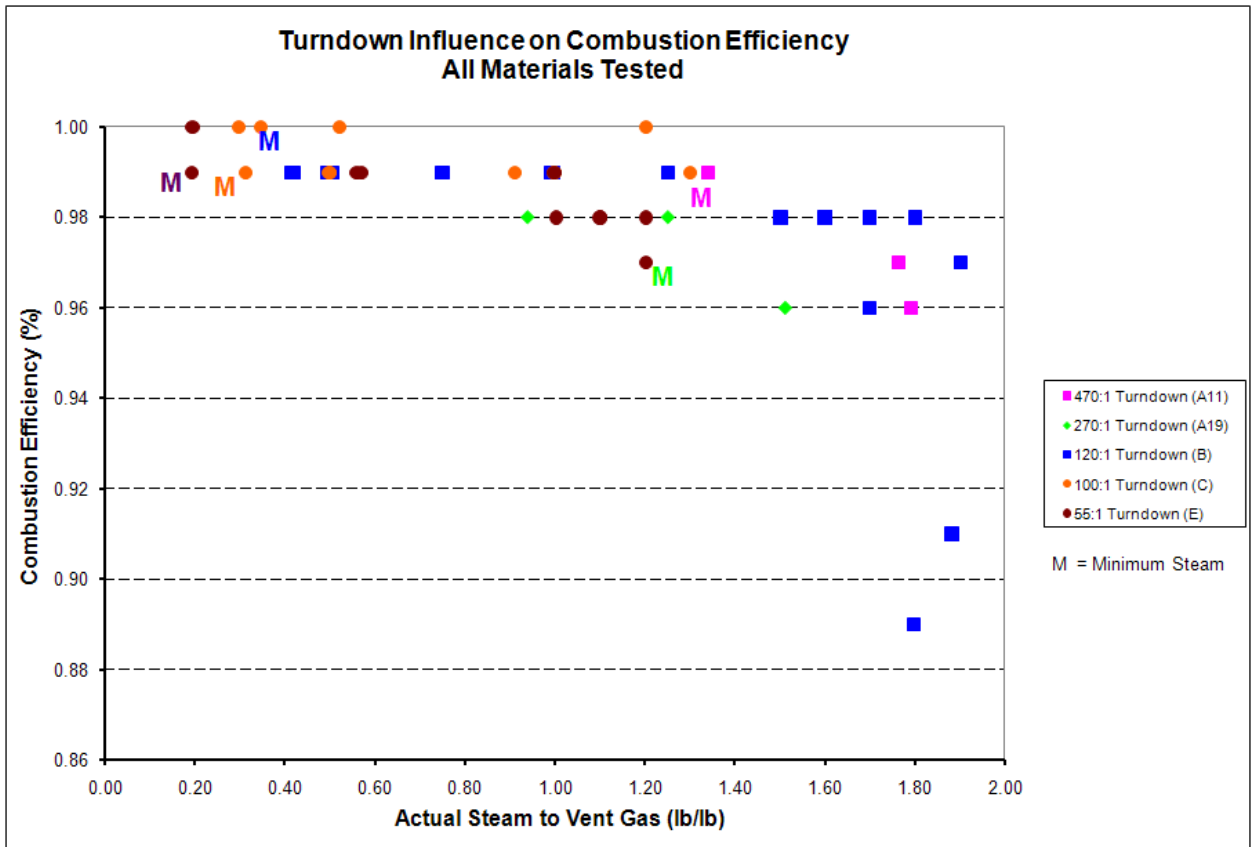


Figure 3.2-1: Combustion Efficiency vs. S/VG Composite of All Materials Tested

For some test conditions, it was not possible to achieve an S/VG ratio less than 1.0 due to the minimum steam requirements at the flare tip. A certain amount of steam is required to be injected into the tip to maintain mechanical integrity and preserve the reliability of the tip. When the flare was being operated at minimum cooling steam only, an “M” denotes the condition on the chart above. Minimum cooling steam rates are set by the manufacturer and are specific for each flare tip design. For the base case Test Series A19 and A11, the minimum steam rates were reached at S/VG ratios of 0.9 and 1.4 lb steam per lb vent gas, respectively.

Performance Test of a Steam-Assisted Elevated Flare Marathon Petroleum Company, Texas City Main Flare

As steam cannot be reduced any further, the only mechanism to reduce the S/VG ratio is to increase the denominator (VG) and flare additional gas. The test program showed that even for base case conditions, the flare can be operated at high combustion efficiencies at minimum steam rates. The operating window under these conditions may be small between the point of visible emissions and the deflection point on combustion efficiency; however, minimum steam rates (or rates slightly above minimum) achieved good combustion and no visible emissions for Marathon's Texas City main flare.

Figure 3.2-2 shows the relationship between combustion efficiency and S/S521 ratio for all components tested.

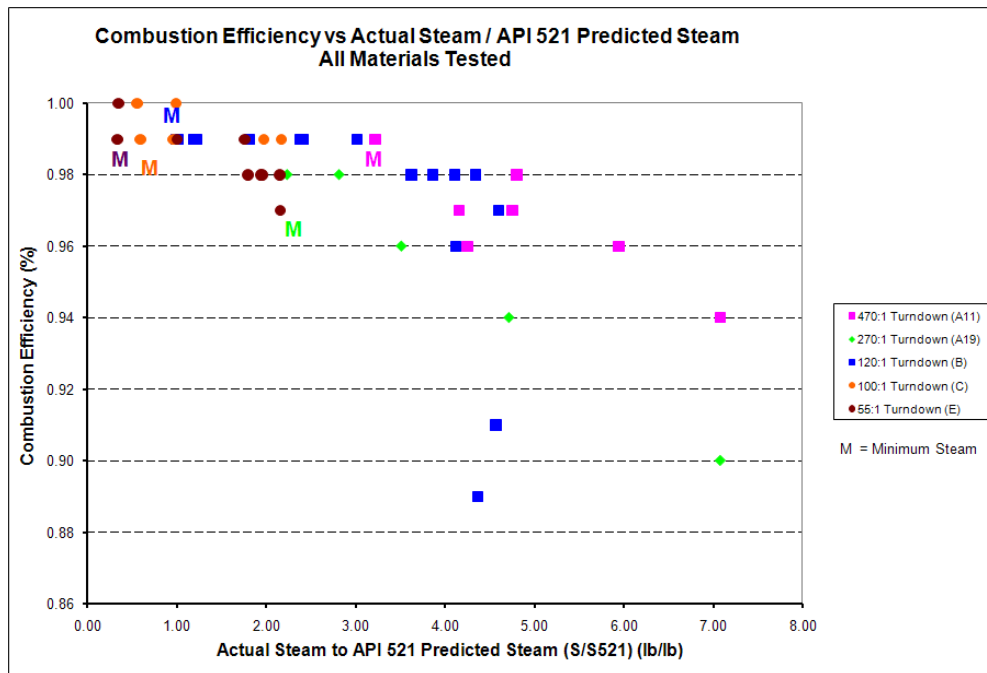


Figure 3.2-2: Combustion Efficiency vs. S/S521 Composite of All Materials Tested

3.2.2 Combustion Zone Gas Net Heating Value

The Combustion Zone Gas (CZG) is located at the mixing zone at the flare tip. It represents the resulting net heating value of the mixture containing all materials under combustion, and is the resultant heat balance of all inputs to the mixing zone and includes the vent gas flow, vent gas net heating value, pilot flow and heating value, as well as the total steam flow. As steam does not have a heat of combustion, its corresponding heat content is zero. CZG is represented in units of BTU/scf. The detailed calculation is presented in Appendix A.1. It has been suggested that net heating value of the mixture can reveal additional information about expected combustion efficiency and may serve as a key performance indicator of flare combustion.

One benefit of the CZG is that it is the only variable that accounts for all components under control of the flare operator. As a result, the CZG can be adjusted based upon more than one independent action. If too low, the CZG can be raised by reducing steam, changing the flare header composition by reducing nitrogen and/or adding a high-heating content hydrocarbon, or increasing total vent gas. No other key performance indicator has this many degrees of freedom under which to operate the flare.

As seen in Figure 3.2-3 below, CZG appears to have a strong correlation to flare combustion efficiency. CZG does not appear to be heavily influenced by material molecular weight or composition. In general, the deflection point of the CZG curve appears to occur just around 225 - 240 BTU/scf.

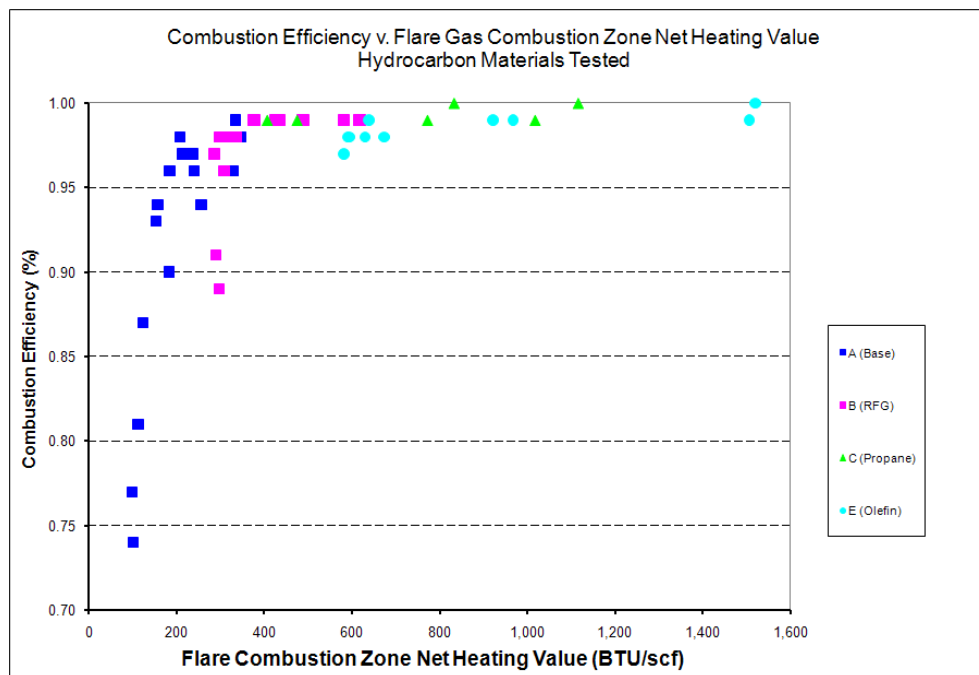


Figure 3.2-3: CZG NHV vs. CE for All Materials Tested

3.2.3 Visible Emissions and Combustion Efficiency

Visible emissions play a key role in environmental compliance for refinery flares. New Source Performance Standards (“NSPS”) and Maximum Achievable Control Technology (“MACT”) standards³ contain time limits for allowable visible emissions or “smoke”, as any five minutes in a two-hour period. As such, the point at which visible emissions begin to form is the primary basis for the lower operating bound.

A visible emissions scale was developed and implemented as part of the test program in order to quantitatively grade the visual flame characteristics. The scale is shown in Table 3.2-1. The incipient smoke point was designated as the number 5 (the center of the scale), and represents the point at which the flare flame displays a “marbly” texture, indicative of small carbon soot particles forming in the flame zone but quickly completing the combustion process. No visible soot particles were present outside of the flame boundary.

Flame ratings above 5 indicate an increasing amount of visible emissions extending beyond the flame boundary observed by increasing amounts of a trailing smoke plume. Flame ratings less than 5 indicate a visible flame decreasing in intensity until it becomes invisible. Ratings of 4 to 2 indicated a visible flame and a rating of 1 indicated a transparent or invisible flame. A flame rating of 0 indicated that the flare was extinguished with steam visually present.

Table 3.2-1: Visual Flame Rating Descriptions

| Flame Rating | Flame Characteristic |
|---------------------|--|
| 0 | Steam plume |
| 1 | Transparent |
| 2 | Mostly transparent, with occasional yellow flame |
| 3 | Mostly yellow flame, with occasional transparency |
| 4 | Yellow to orange flame. |
| 5 | Orange flame with some dark areas in the flame. (Incipient smoke point) |
| 6 | Orange flame with light smoke trail |
| 7 | Clear steam at the flare tip, with an orange flame and a light smoke trail |
| 8 | Orange flame with dark smoke trail leaving the flame |
| 9 | Orange flame with heavy dark smoke trail leaving the flame |
| 10 | Billowing black smoke |

³ Code of Federal Regulations citations - 40 CFR 60.18 and 40 CFR 63.11

Performance Test of a Steam-Assisted Elevated Flare Marathon Petroleum Company, Texas City Main Flare

A flame's visual characteristics appear to have some influence on combustion efficiency. The most important correlation being that efficiency declines rapidly as the flame starts to become transparent, with the exception of high hydrogen-containing vent gas. See Figure 3.2-4.

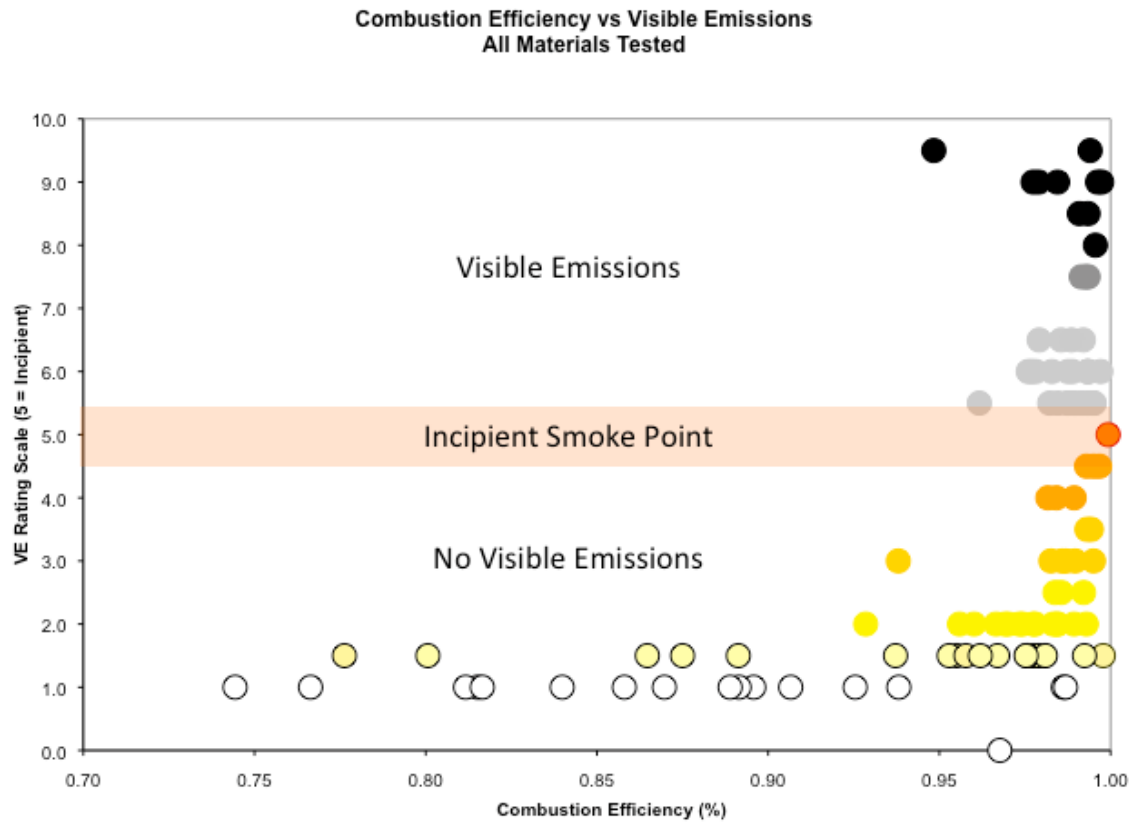


Figure 3.2-4: Combustion Efficiency vs. Visible Emissions Ratings for All Materials Tested

3.2.4 Comparisons to API 521 Table 11

API 521 Table 11 presents design recommendations for steam to hydrocarbon ratios that result in smokeless combustion under relief load scenarios. It has been suggested that Table 11 could also potentially serve as an operating guideline to develop lower operating targets for steam to hydrocarbon ratios during turndown operation of flare systems as well. One of the objectives of this test program was to evaluate whether the ratios in Table 11 could serve as a guide, that is, whether the guidance from design conditions at relief conditions would also apply equally at turndown.

In Figure 3.2-5, the green diamonds represent the point of incipient smoke for the various molecular weights of vent gas tested.

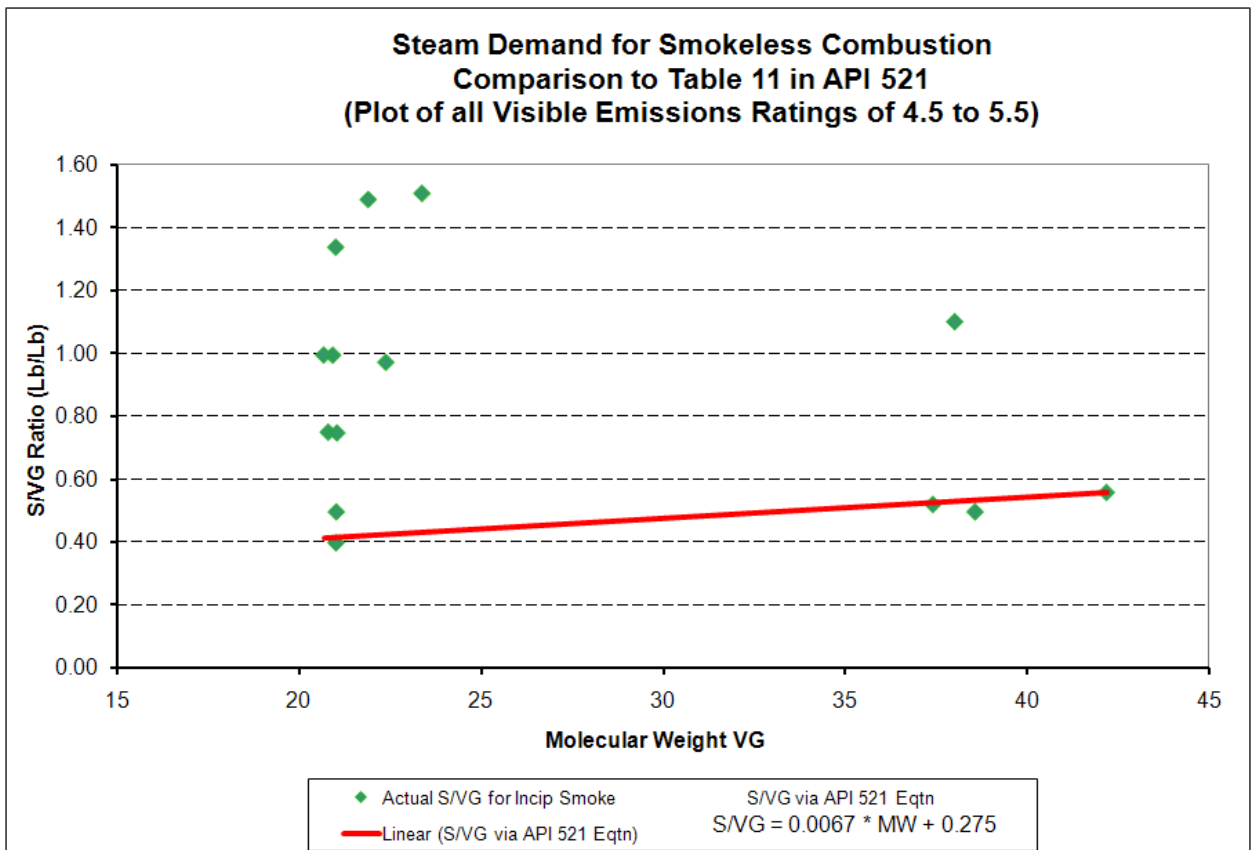


Figure 3.2-5: Incipient Smoke Point vs. API 521 Table 11 Predictions

To the left of the above figure, Test Series A (Base Conditions) and B (Refinery Fuel Gas) are grouped together due to the similarity in molecular weights, ranging from 21 to 23 lb/lbmole, with predictions from API 521 ranging from 0.41 to 0.43 lb steam per lb vent gas.

Performance Test of a Steam-Assisted Elevated Flare Marathon Petroleum Company, Texas City Main Flare

Similarly, Test Series C (Propane) and D and E (Olefin Series) are grouped to the right of the figure having molecular weights between 37 to 42 lb/lbmole.

In all cases, the degree of closeness between the actual steam-to-vent gas achieved versus the value that API 521 predicted (S/S521 approaching 1.0) is directly proportional to the mass load to the flare as shown below in Figure 3.2-6. For Test Series A, the flare was operating at a much lower mass load (i.e. higher turndown factor) than for Test Series C, D, and E. Therefore, the amount of steam needed for smokeless combustion was much higher, as compared to the higher mass loading tests. It is believed this phenomenon is likely due to inadequate mixing at the flare tip, and a certain amount of steam being present but not engaged within flame combustion.

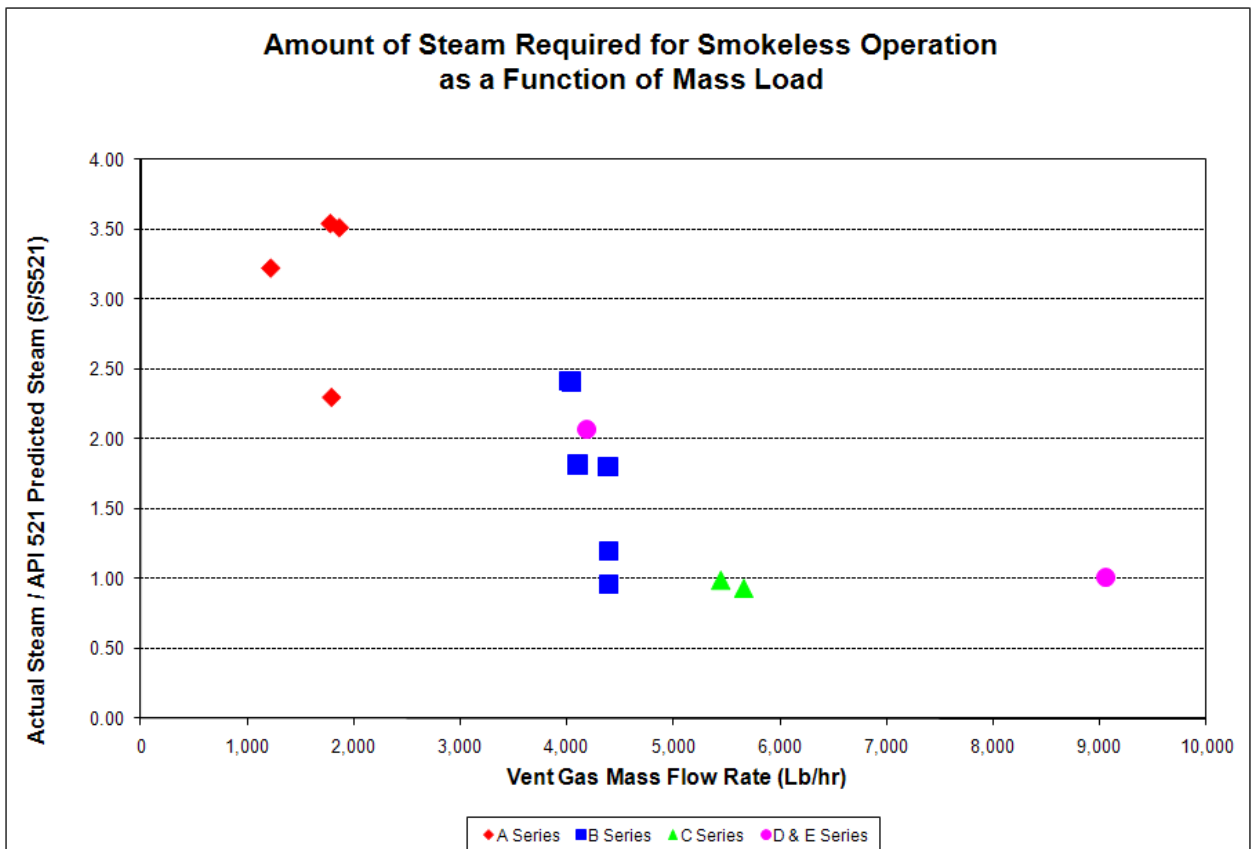


Figure 3.2-6: Incipient Smoke Point Varies with Mass Load

Performance Test of a Steam-Assisted Elevated Flare
Marathon Petroleum Company, Texas City Main Flare

In summary, under high turndown conditions, the amount of steam needed for smokeless combustion was much greater than the value API 521 would have predicted. This could have been influenced by several factors, including:

1. Mixing – lower vent gas rates create less turbulence in the mixing zone making it harder for the motive force generated by steam to get air intimately mixed with the vent gas.
2. Non-contact between steam and vent gas – void areas between vent gas and steam resulting in not only no mixing but no contact between the two materials.
3. Turndown – runs with lower turndown factors (higher vent gas flows) were closer to API 521 predictions than ones at lower vent gas flows.

Table 3.2-2: Runs with Visible Emissions Ratings 4.5 – 5.5

| Test Series | Run |
|-------------|------------------------------|
| A11 | 1-1 |
| A19 | 1-2, 3-1, 3-2 |
| B | 1-3, 2-3, 3-1, 3-3, 4-1, 4-2 |
| C | 2-2, 2-3 |
| D | 5-1 |
| E | 2-3 |

3.3 Factors Influencing Test Results

3.3.1 Mechanical Damage of Flare Tip

During the performance test of the Texas City main flare, mechanical damage was observed in two distinct areas, which are suspected of causing the premature flame extinguishment observed during the performance test. One area was associated with the failure of the shaping steam ring, while the other was a steam leak observed around the muffler area. The most significant of these was the shaping steam ring failure.



Figure 3.3-1: Steam Leak at Shaping Steam Ring

The shaping steam ring is connected to the lower steam ring, and injects a small amount of steam toward the center of the flare tip at an angle determined by the manufacturer. This steam is provided to supply a certain amount of pressure balance, that is, it shapes the flame from a concentric circle whose main function is to keep the hot ball of combustion gases together. The shaping steam is an annular ring, supplied from the lower steam ring at one location.

The shaping steam ring failure caused the shaping pressure to be unbalanced, with one side of the concentric ring starved for steam. As the wind blew towards the area of unbalance, the flame sheared off of the flare tip and was extinguished. It is estimated that approximately 50 to 100 lb/hr of steam was leaking from the shaping steam ring and muffler area during the test, and was not introduced into the flame combustion zone, although it was measured and accounted for in the total steam meter. At higher hydrocarbon mass flow rates (and thus

Performance Test of a Steam-Assisted Elevated Flare Marathon Petroleum Company, Texas City Main Flare

higher steam rates) it is thought that the increased steam from the leak also interfered with the nearby pilot which may have been an additional contributor to premature flame outages.

The shaping steam leak was on the east side of the flare; therefore, winds blowing towards the East / South East quadrant as noted in red in Figure 3.3-2 below exerted pressure towards the area of unbalance. Day to day wind roses for each day of testing are shown in Figure 3.3-7. Winds blew towards the shaping steam leak on 9/15, 9/16, 9/17, and 9/18. At least one series of runs were conducted on the main Test Series for each of these days (A19, A11, B, C, D, and E), therefore it is suspected that the shaping steam leak may have caused premature flare outages for each of the Test Series.

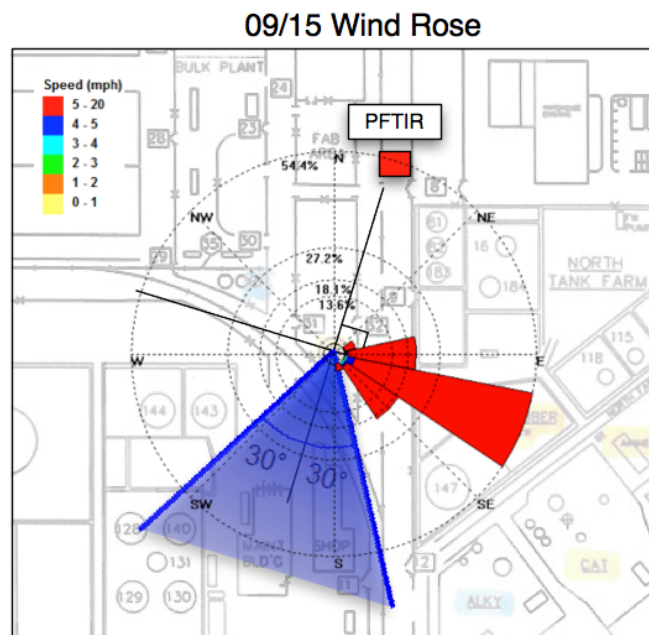


Figure 3.3-2: Wind Direction Impacts to Flare Shaping Steam Leak

It should be noted that as the steam rates were increased during each test series, the flare was being forced into operating at an over-steamed condition near the instability point. This is neither a typical nor a normal operating regime. The requirements of the Clean Air Act 114 Request received by Marathon for this performance test stated that each test progression could only be stopped when the combustion efficiency reached 60% or for other safety considerations. Not only is flame outage a safety concern, but each flame outage is considered to be zero (0%) combustion efficiency.

3.3.2 Wind Effects

During this test program, wind speed and direction were recorded on a minute-by-minute basis from a meteorological station located on-site at the Texas City refinery. These data are shown on the data summary tables in Section 5. The flare height (150 ft.) is much greater than the height of the met station (about 25 ft.) and winds at the flare tip are expected to be higher than those recorded.

Wind speed and direction play an important role in the quality of data collected by the PFTIR method. The alignment of the flare plume with the PFTIR must be optimal to have the best chance of obtaining a representative sample. The best opportunity for the PFTIR to obtain a representative sample of the flare plume is when:

- 1) The flame is buoyant and the plume is rising more or less vertically above the flame, or
- 2) The flame is “bent over” by the wind and the plume is roughly perpendicular to the PFTIR field of view (see Figure 3.3-3)

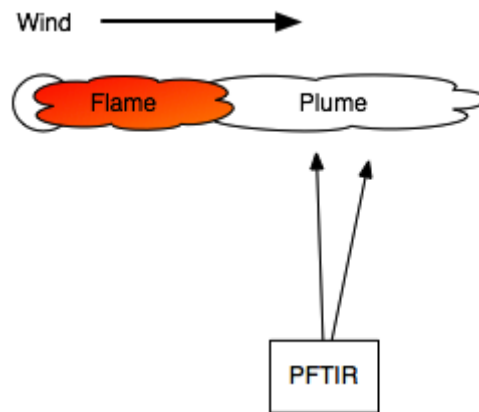


Figure 3.3-3: Example of Good Plume Alignment with PFTIR

The worst alignment occurs when the flame and plume are bent by the wind and blowing directly away from the PFTIR (see Figure 3.3-4). When this occurs, the flare blocks the view of the plume from the PFTIR, making it difficult or impossible to obtain a representative sample (or even any sample) of the plume.

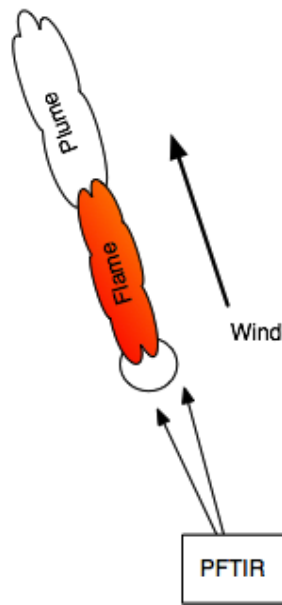


Figure 3.3-4: Example of Poor Plume Alignment with PFTIR

This effect can be seen visually on the PFTIR aiming camera, as shown in Figure 3.3-5. The red square shows the PFTIR field of view. Image (a) shows good plume alignment. In image (b), the flame and plume are bent over and hidden behind the flare. In order to sample any of the plume, the PFTIR must be aimed very close to the flame resulting in invalid data.



Figure 3.3-5: Comparative View from PFTIR Aiming Camera

During the entire test period, wind speed was 5 to 10 mph or more. For most of the test period, the flame was bent by the wind. During the first week of testing, winds were in a favorable direction for testing. However, during the second week, winds shifted to an unfavorable direction and much of the data collected during this time should be considered invalid.

Performance Test of a Steam-Assisted Elevated Flare Marathon Petroleum Company, Texas City Main Flare

A data flagging algorithm was developed to indicate which data points were collected when winds were unfavorable. This algorithm was implemented on the spreadsheets that are included in the electronic submittal for this project.

This algorithm takes both wind speed and direction into account. It first tests wind direction. If wind direction is between 165 and 225 degrees, a data flag is set to FALSE indicating a potentially suspect data point. This range is 30 degrees on either side of the PFTIR viewing axis. This is illustrated in Figure 3.3-6.

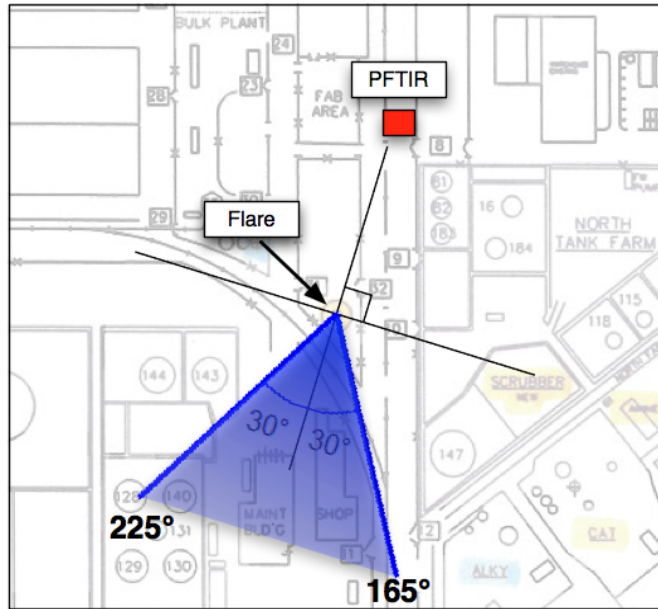


Figure 3.3-6: Wind Flagging Algorithm

A value of 30 degrees was chosen because the data flagged using this value corresponds well to the data flagged during the video review (see Section 3.3.3) as being suspect due to aiming issues. Aiming and wind effects are closely related since it is difficult or impossible to properly aim the PFTIR when winds are blowing within this range.

Next, wind speed was tested. If the wind speed exceeds 5 mph, a second data flag is set to FALSE. A value of 5 mph was used based upon observations of how much wind was required to bend the flame. This value is dependent on flare tip velocity, but 5 mph was a reasonable average for the test period.

If both the wind direction and wind speed flags are set to FALSE, the data point is flagged as being potentially invalid.

Day by day wind roses are shown in Figure 3.3-7.

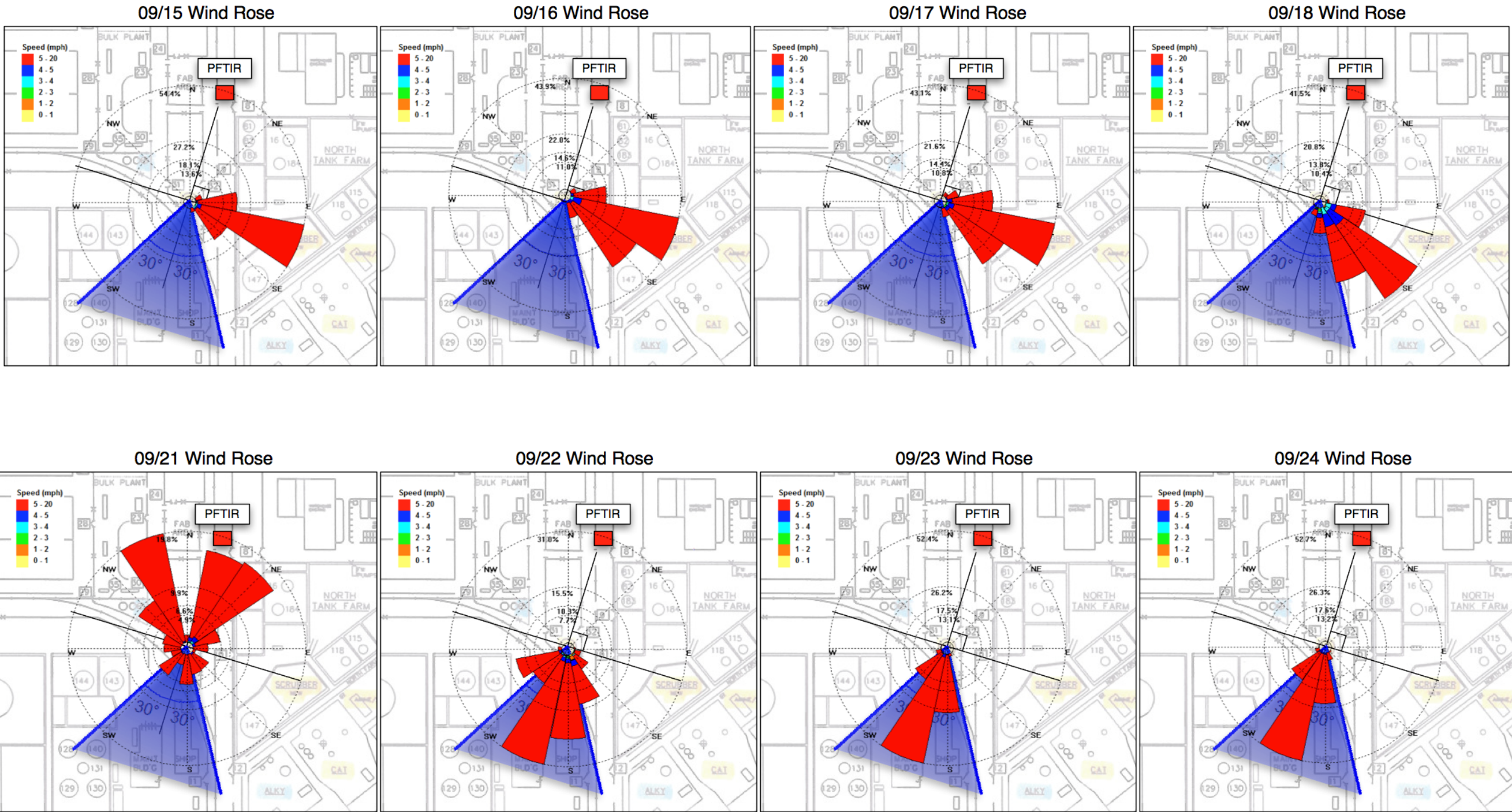


Figure 3.3-7: Day by Day Wind Roses

3.3.3 PFTIR Aiming Issues

Proper aiming of the PFTIR is critical to acquisition of valid data. Ideally, as discussed above, the PFTIR should be aimed near the centerline of the flare plume about one to two flame lengths away from the flame tip. At this distance, it is believed that all thermal destruction reactions have been completed. However, the plume is a moving target. Therefore, in an attempt to maintain the aim of the PFTIR at this optimal sampling point, the instrument must be continually adjusted by the operator. This task becomes increasingly difficult if the wind is continually shifting and it becomes impossible if the wind is blowing the plume directly behind the flare (See Section 3.3.2). Successful aiming is also highly dependent on the skill of the PFTIR operator.

The version of the PFTIR used for the Marathon test program employed two cranks for aiming – one crank was used for tilting the instrument up and down and the other for panning left and right. Continually cranking the instrument proved quite tiring and several operators were used during the test period.

In order to evaluate aiming accuracy for each test run, a panel of four individuals reviewed video from the PFTIR aiming camera for each test run. Each panelist scored aiming accuracy for each run on the following scale.

- 1 – The PFTIR was aimed properly less than 20% of the time.
- 2 – The PFTIR was aimed properly between 20% and 50% of the time.
- 3 – The PFTIR was aimed properly between 50% and 80% of the time.
- 4 – The PFTIR was aimed properly more than 80% of the time.

The scores from each panelist were averaged for an overall test run score. These scores are presented in Section 5.1 Data Summary Tables. In these tables, the test runs are color-coded based on the video score.

It is worth noting that lower video scores correlate well with the days in which the wind was blowing the plume directly away from the PFTIR.

Another aiming issue examined was the impact of aiming distance from the flame tip. As stated above, the aiming objective was to keep the PFTIR aimed at a point one flame length from the tip of the flame. To test the sensitivity of this positioning, a test was conducted with the PFTIR initially aimed at the flame tip then moving in steps away from it. This test was conducted on 09/18 from 12:29 to 12:49 during the Condition D test runs. Images from each test taken from the PFTIR aiming camera are shown in Figure 3.3-8 below. The red square is the PFTIR field of view, that is, the spot on the plume being sampled by the PFTIR.



A - At the flame tip



B - 0.5 flame lengths from the flame tip



C - 1 flame length from the flame tip



D - 2 flame lengths from the flame tip

Figure 3.3-8: Aiming Test: Video Stills from Each Test Point

Performance Test of a Steam-Assisted Elevated Flare Marathon Petroleum Company, Texas City Main Flare

The results of this test are shown in the Figures below. The PFTIR was not able to produce usable data at the flame tip; therefore, data from this position are not included in the analysis below.

Figures 3.3-9 and 3.3-10 show concentration of the plume components at 0.5, 1.0 and 2.0 flame lengths from the flame tip. At two flame lengths, it became difficult for the PFTIR operator to track the plume.

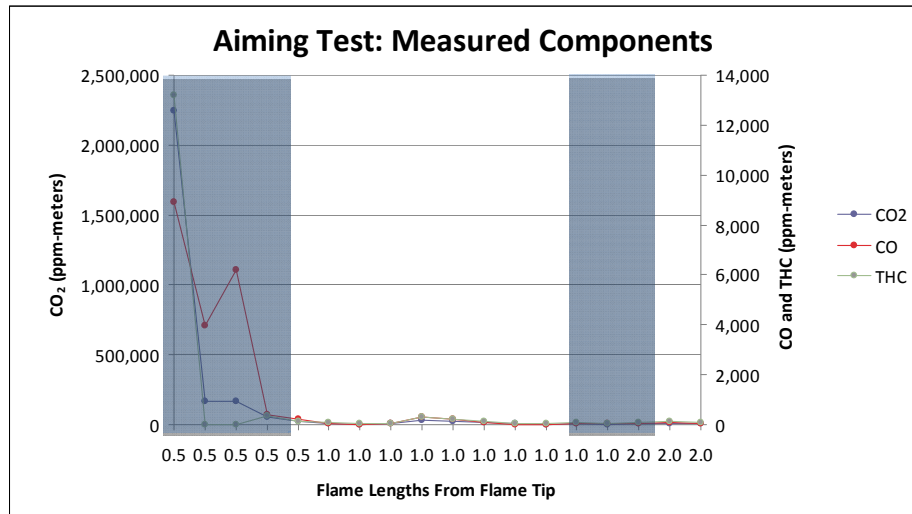


Figure 3.3-9: Aiming Test: Measured Components

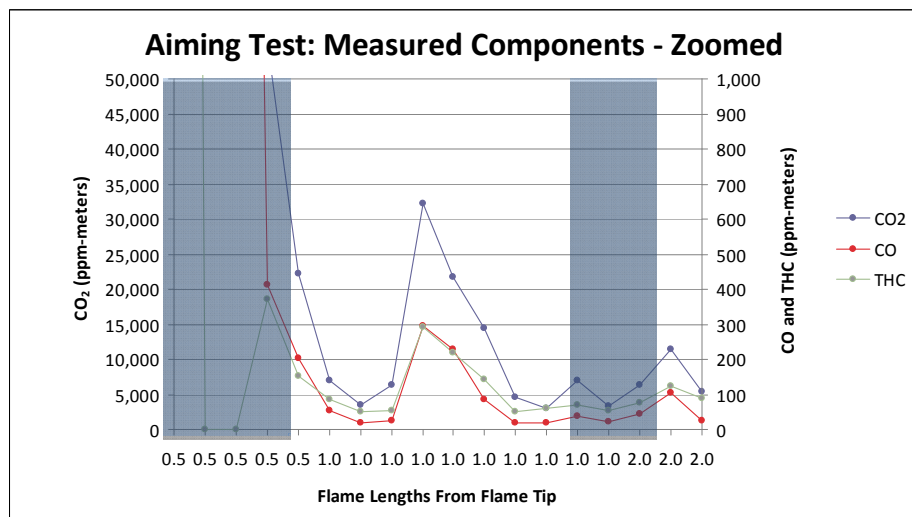


Figure 3.3-10: Aiming Test: Measured Components - Zoomed

Performance Test of a Steam-Assisted Elevated Flare Marathon Petroleum Company, Texas City Main Flare

The data from the 0.5 flame length test indicate that absorbance is too strong at this point and cannot be reliably used to quantify component concentrations. At this point, the absorption features in the spectra are very non-linear in absorbance. At one flame length, the data becomes less extreme and more useful for analysis. One would expect that, as the PFTIR is moved farther from the flame, the component concentrations would decrease due to increasing dilution of the flare plume. It is interesting to note here that when the PFTIR moved from 1 to 2 flame lengths, concentrations remained roughly the same.

Figure 3.3-10 below shows the CO₂ to CO and CO₂ to THC ratios at each distance.

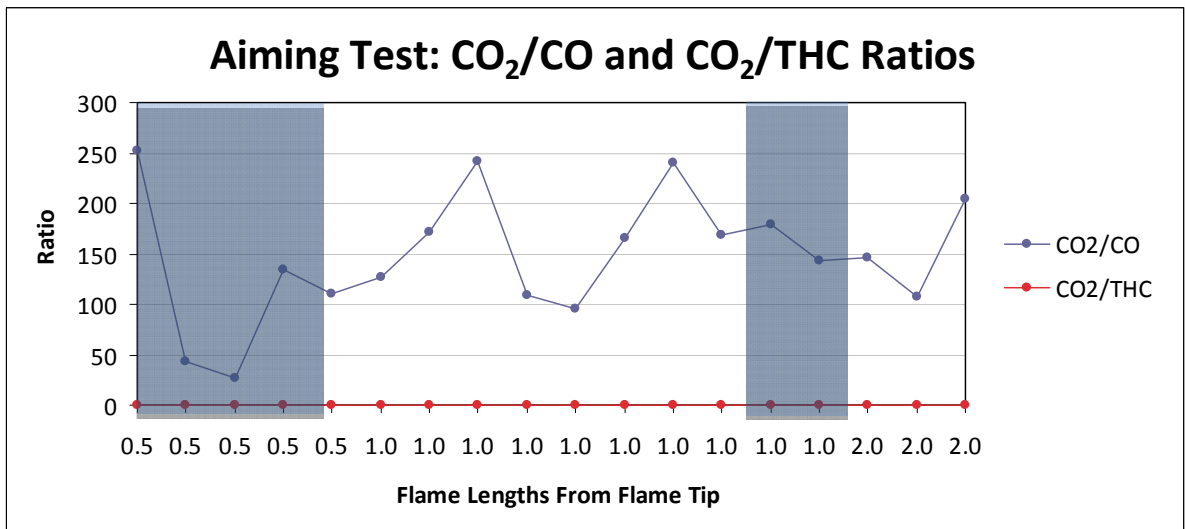


Figure 3.3-11: Aiming Test: CO₂/CO and CO₂/THC Ratios

The significance of component ratios is more fully explained in Section 3.3.4.2 below. However, for the purpose of interpreting this figure, it is important to understand that ideally, even though the absolute concentrations of each component may vary over a wide range, the ratios should be relatively constant given the same flare operating conditions. It can be seen in this figure that the ratios were highly variable. For example, during the one flame length test, the range of the CO₂/CO ratio varied from about 100:1 to about 250:1. This is a much larger range than expected.

Figure 3.3-11 shows the combustion efficiencies at each distance. Figures 3.3-12 through 3.3-15 show flare operating parameters during the aiming test.

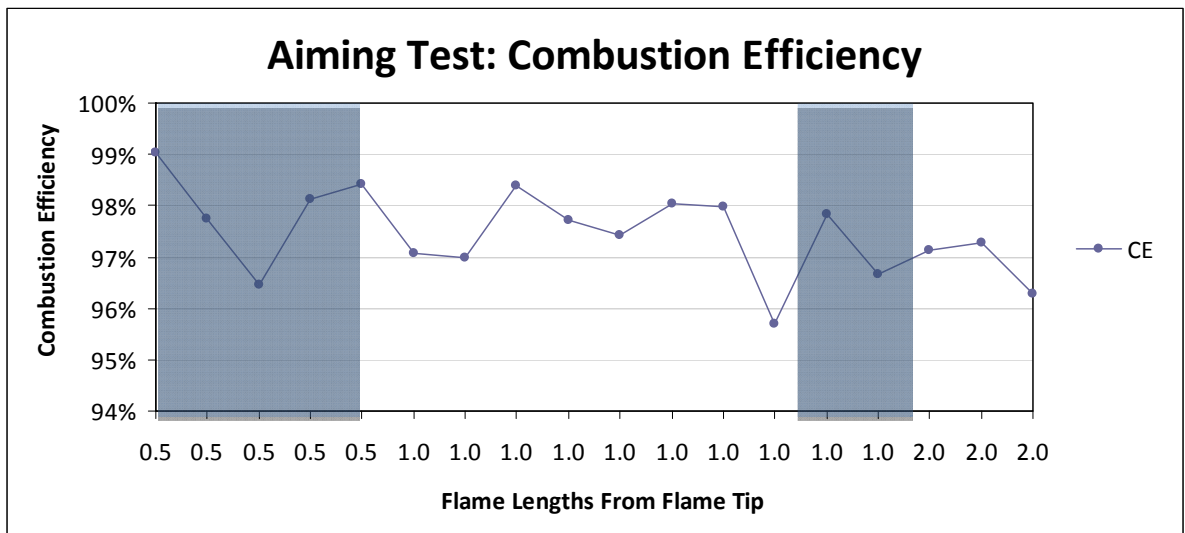


Figure 3.3-12: Aiming Test: Combustion Efficiency

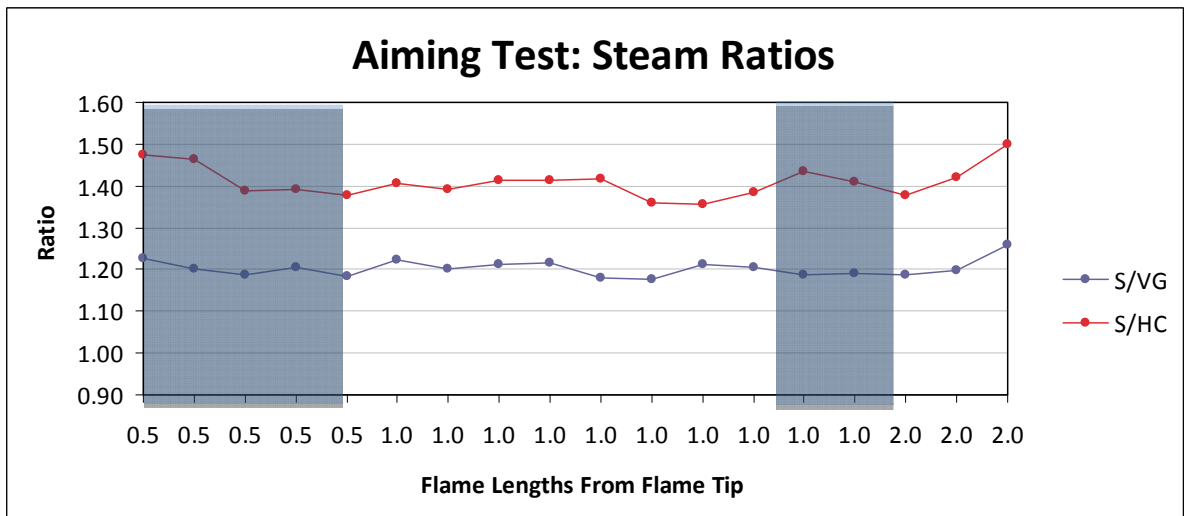


Figure 3.3-13: Aiming Test: Steam Ratios

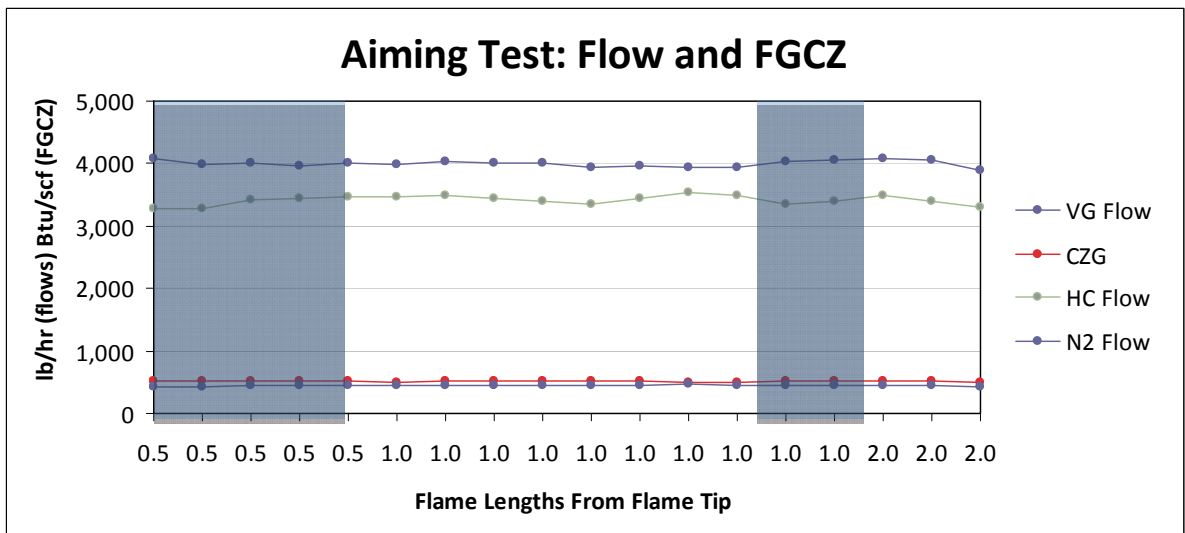


Figure 3.3-14: Aiming Test: Flow and CZG

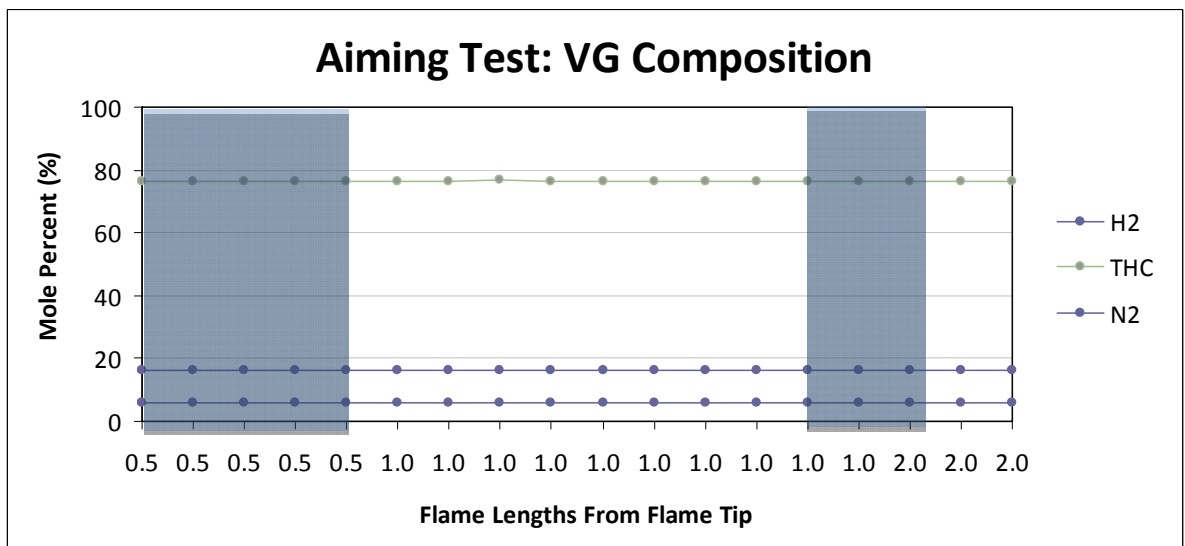


Figure 3.3-15: Aiming Test: VG Composition

3.3.4 Overall Test Variability

When assessing overall data uncertainty for this project, it is important to distinguish uncertainty related to precision (repeatability) issues and uncertainty related to bias (“closeness to truth”) issues. This test program was designed to generate data to evaluate precision of test results. Due to the nature of this open-path technique, definitive assessments of bias are difficult in the field. The “hot-cell” calibration tests described in Section 3.3.4.3 below attempt to define and correct some of the potential biases associated with the PFTIR methodology. However, a definitive assessment of the bias of this technique must be accomplished through a blind validation study. This study has not yet been performed for this method.

3.3.4.1 PFTIR Precision Assessment

This test program was designed to assess data precision in two ways. First, each test condition was to run in triplicate. An estimate of precision could then be made by comparing the results from the three runs (run to run variation). At least one run for each test condition was to be conducted on a different day (day to day variation) in order to take into account longer term variation in meteorological factors, flare operation, and PFTIR operation.

During the test program, some additional tests were added in order to improve data resolution in certain operating areas (e.g. near the flare snuff point). These tests were not conducted in triplicate.

Figure 3.3-16 shows the variability of the data collected for each run in each test condition. The data are presented as box plots. Each box shows the boundaries of the 25th and 75th percentiles and contains, therefore, 50% of the data for that run. The line in the middle of the box indicates the median value of the data. The average is shown by a short black line. The “whiskers” at the top and bottom of the box show the range of the data. The data are shown grouped by replicate (rep) for each test condition. Note that flare operating conditions for each replicate are reproduced as closely as possible.

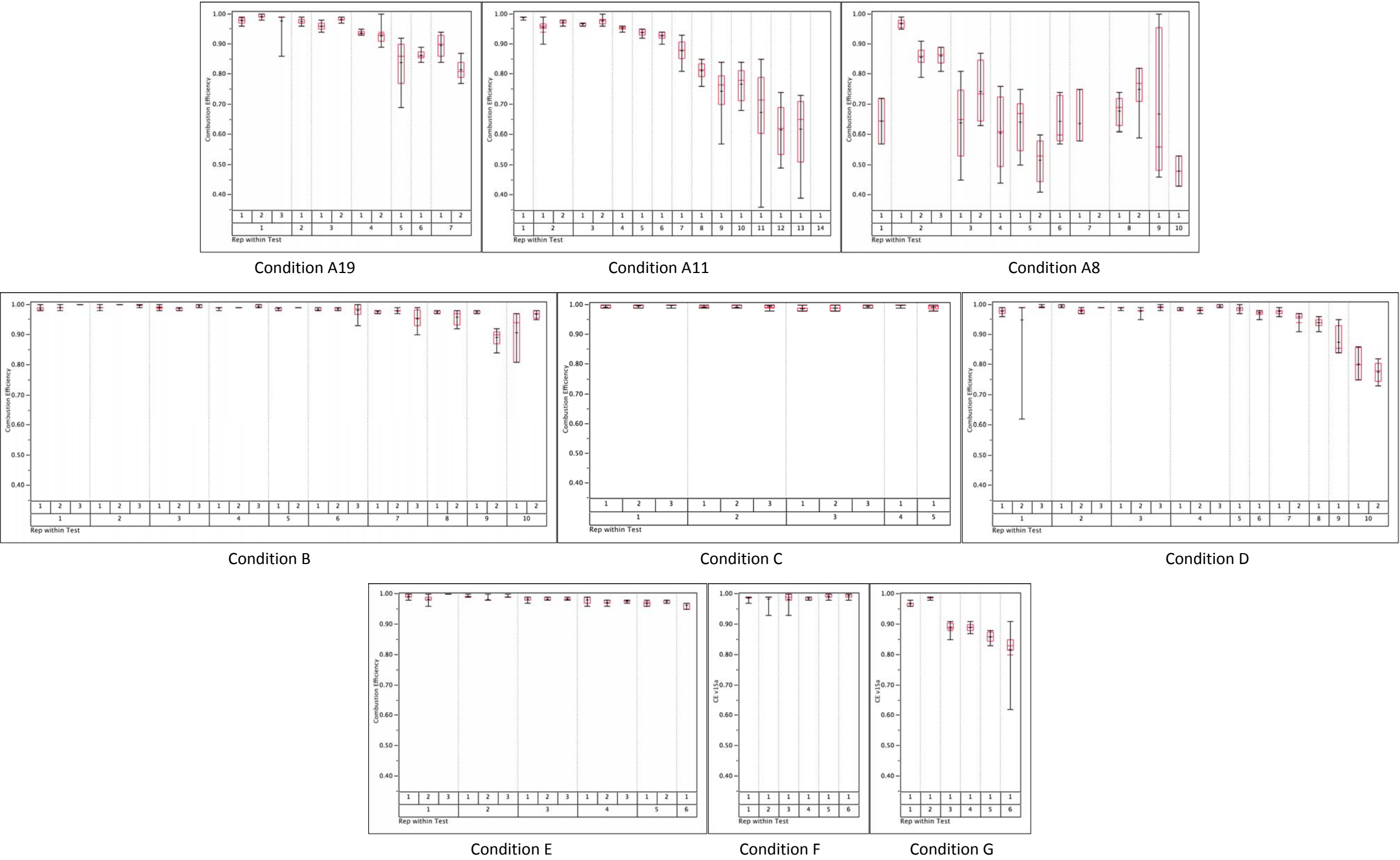


Figure 3.3-16: Run by Run Data Variability Analysis (same scales)

Performance Test of a Steam-Assisted Elevated Flare Marathon Petroleum Company, Texas City Main Flare

In addition to the triplicate runs, a longer term measure of test data variability was conducted. At least once each day (except for the last day of testing on 09/24/09), a test was conducted at the same set of conditions – Condition B with an SVG of 1.00⁴. This series of test runs is referred to as the Long Term Stability (LTS) test. These data show test method repeatability over a range of meteorological conditions and other factors. The results of the LTS test are discussed in more detail in Section 5.11

Figure 3.3-17 shows a summary of the LTS data as box plots. The blue line connects the average (mean) of each test run.

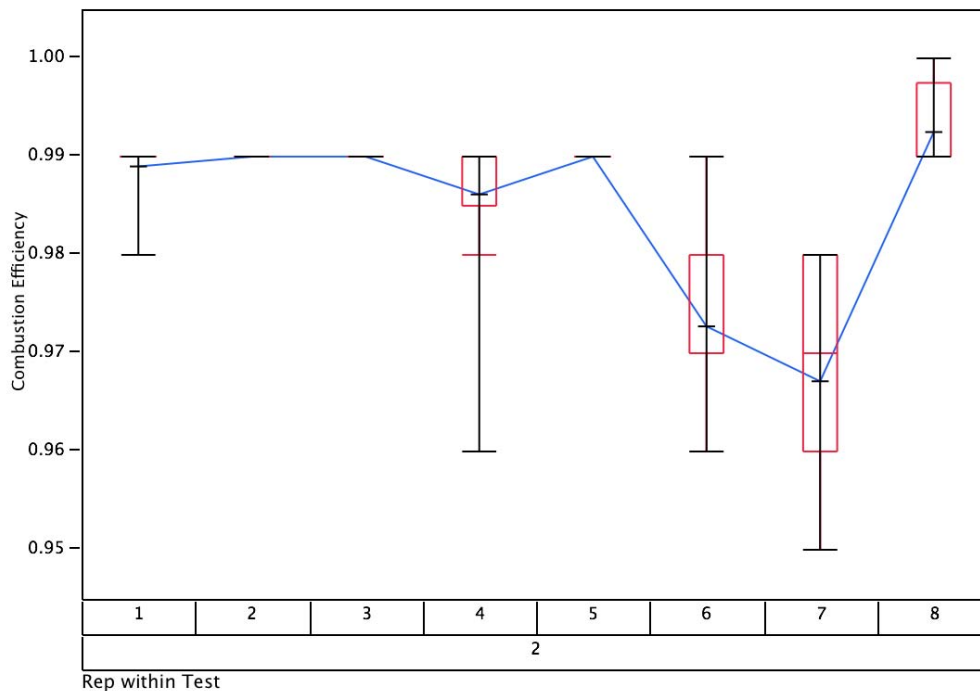


Figure 3.3-17: Long Term Stability Run by Run Variability

Figure 3.3-18 shows a confidence interval determination for the combustion efficiency data from each of the 8 LTS runs. The value for Run 2-8 is shown in red because all of the data points in that run are flagged by the wind speed and direction algorithm. The data below are shown both with and without this run. Also shown is a determination of the upper and lower confidence bounds under three assumptions.

⁴ An initial LTS run was conducted on 09/15 using propane. However, this proved not to be an acceptable condition due to flare smoking and recovery time after the test. This initial test run is not included in any LTS summary data.

Performance Test of a Steam-Assisted Elevated Flare
Marathon Petroleum Company, Texas City Main Flare

| CE Data | | | A | | B | | C | |
|---------|-------|--------|----------|-----------|----------|-----------|---------------|-----------|
| | | | 99% CL | | 95% CL | | 95% CL 3 Runs | |
| | | | All Data | Excl. 2-8 | All Data | Excl. 2-8 | All Data | Excl. 2-8 |
| LTS 2-1 | 98.7% | Avg | 98.5% | 98.4% | 98.5% | 98.4% | 98.5% | 98.4% |
| LTS 2-2 | 99.3% | SD | 0.011 | 0.011 | 0.011 | 0.011 | 0.011 | 0.011 |
| LTS 2-3 | 99.0% | RSD | 1.1% | 1.1% | 1.1% | 1.1% | 1.1% | 1.1% |
| LTS 2-4 | 98.7% | N | 8 | 7 | 8 | 7 | 3 | 3 |
| LTS 2-5 | 99.4% | SE | 0.004 | 0.004 | 0.004 | 0.004 | 0.006 | 0.006 |
| LTS 2-6 | 97.2% | % Prob | 0.99 | 0.99 | 0.95 | 0.95 | 0.95 | 0.95 |
| LTS 2-7 | 96.6% | TINV | 3.50 | 3.71 | 2.36 | 2.45 | 4.30 | 4.30 |
| LTS 2-8 | 99.3% | Factor | 1.3% | 1.5% | 0.9% | 1.0% | 2.6% | 2.7% |
| | | LCL | 97.2% | 96.9% | 97.6% | 97.4% | 95.9% | 95.7% |
| | | AVG | 98.5% | 98.4% | 98.5% | 98.4% | 98.5% | 98.4% |
| | | UCL | 99.8% | 99.9% | 99.4% | 99.4% | 100.0% | 100.0% |

Figure 3.3-18: Confidence Interval Determination from LTS Data

The data in each row are as follows:

- Avg = Average combustion efficiency (CE)
- SD = Sample standard deviation of the CE
- RSD = Relative standard deviation (SD/Avg) of the CE
- N = Number of data points for each data set
- % Prob = The chosen probability level to determine the confidence intervals (99% or 95%)
- TINV = The coverage factor for the confidence interval calculated from the Student's t-distribution
- Factor = The calculated confidence limit based on the criteria above (This is added to and subtracted from the average to arrive at the confidence interval.)
- LCL = The lower confidence limit (Avg – Factor)
- UCL = The upper confidence limit (Avg + Factor)

Assumption A uses a 99% confidence level. Assumption B uses a 95% confidence level. Assumption C uses a 95% confidence level and assumes only three runs are conducted with the data having the same pattern of variation. This assumption is shown since three runs are typical for air emission testing on stacks. Note that the calculated confidence interval is for the average. Individual runs will have a greater variation.

This analysis shows that the measured combustion efficiency under identical process conditions may vary for a flare by about +/- 1.5%.

3.3.4.2 Dilution Assumption

Because the flare plume is continually moving during the test, it is impossible to collect all spectra at exactly the same point in the plume. As the gases in the plume move farther from the combustion zone, they are increasingly diluted by the ambient air. This means that the absolute concentration of the plume components will vary based solely on where in the plume the PFTIR is aimed and collecting data.

Since the calculation of combustion efficiency is based on the ratio of CO₂ to total carbon in the plume (i.e. the sum of CO₂, CO, and THC), it is the ratios of the components that matter rather than their absolute concentration. Therefore, even though absolute concentrations vary at different measurement points due to dilution, the ratios should be the same since, in theory, all plume components are diluted equally at any given sampling point.

The data collected during this test, however, show differing degrees of variation in the CO₂ to CO ratio at different data points collected under the same operating conditions. For example, Figure 3.3-19 shows the ratio variability for the LTS test runs.

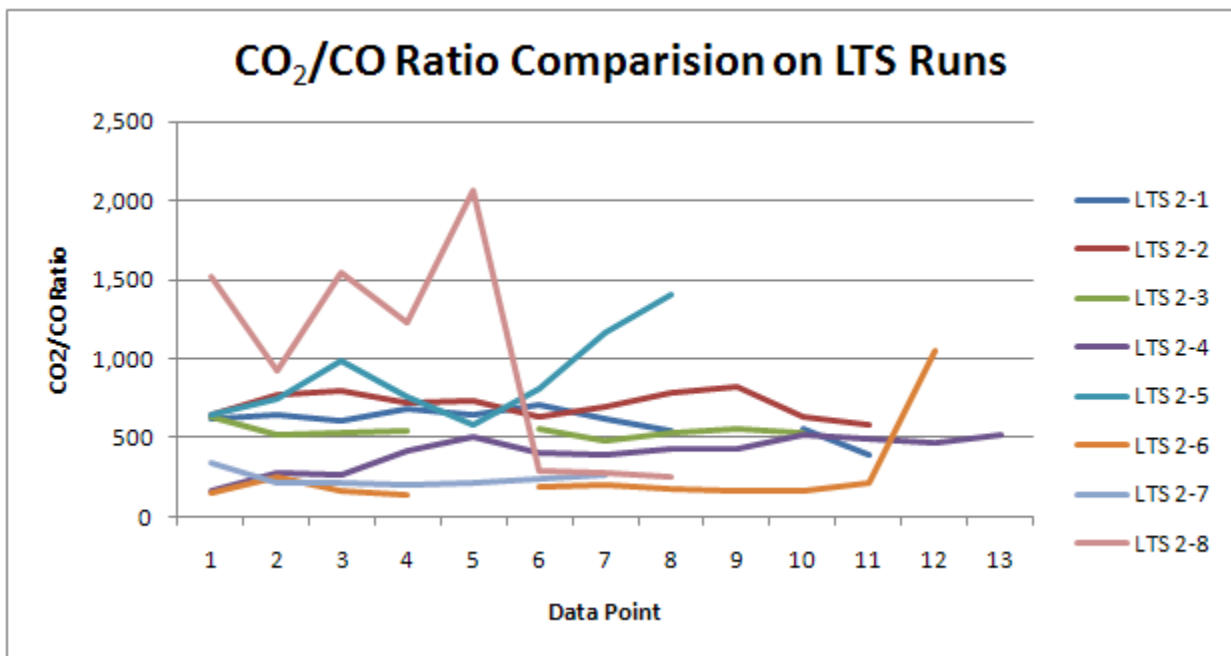


Figure 3.3-19: CO₂/CO Ratio Comparison on LTS Runs

3.3.5 PFTIR Calibration

3.3.5.1 Radiance Calibrations

Radiance calibrations were conducted at least twice each day with a blackbody IR source located at roughly the same distance from the PFTIR as the flare.

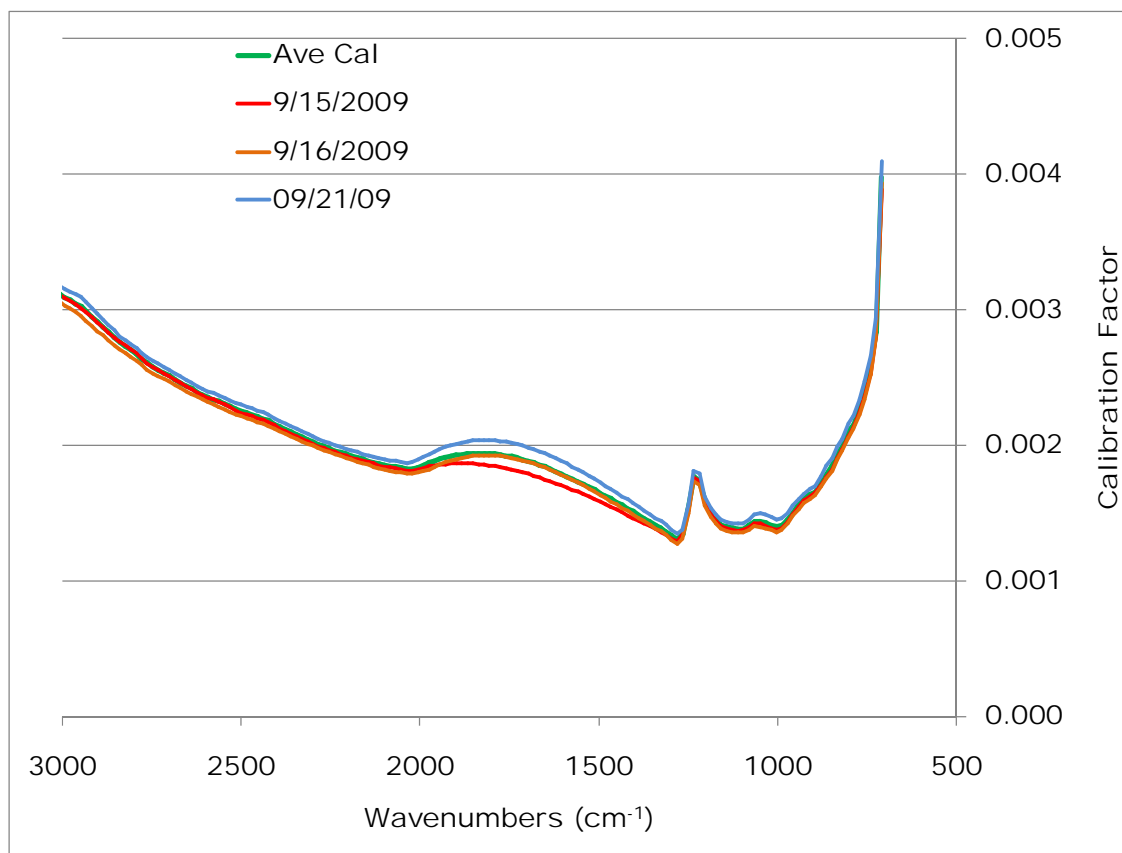


Figure 3.3-20: PFTIR Radiance Calibrations

Calibration factors measured on 09/15, 09/16 and 09/21 and the average calibration factor are shown. The variations between 1500 and 2000 cm^{-1} are due to the background water. Analysis is not done in that region.

3.3.5.2 Hot Cell Calibration

In order to challenge the PFTIR with known concentrations of gas, hot cell calibrations were performed in laboratory setting after the conclusion of the Texas City performance test. In this calibration, a known mixture of CO₂, CO, and methane are metered by mass flow controllers into a heated cell. This cell is placed at the focal point of the collimator used for the radiance and other calibrations and which is located at a distance from the PFTIR. The PFTIR then collects data from the cell and the data is reduced to produce a concentration result. This result is then compared to the known value of the calibration gas concentration. The hot cell calibration was performed at six different concentrations.

From this data, calibration curves were produced as shown in Figures 3.3-21 through 3.3-23 below. The red lines indicate perfect agreement between the known and measured concentrations and are shown to provide an indication of the magnitude of the correction required for each component.

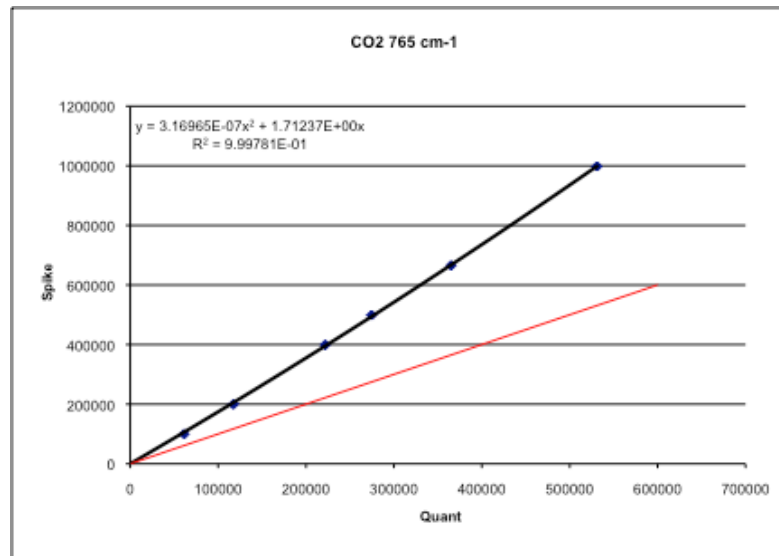


Figure 3.3-21: PFTIR Hot Cell Calibration Curve – CO₂

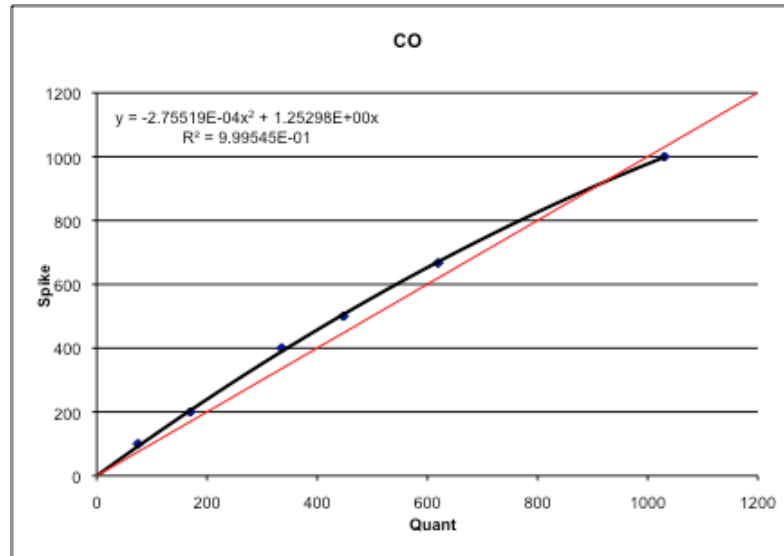


Figure 3.3-22: PFTIR Hot Cell Calibration Curve - CO

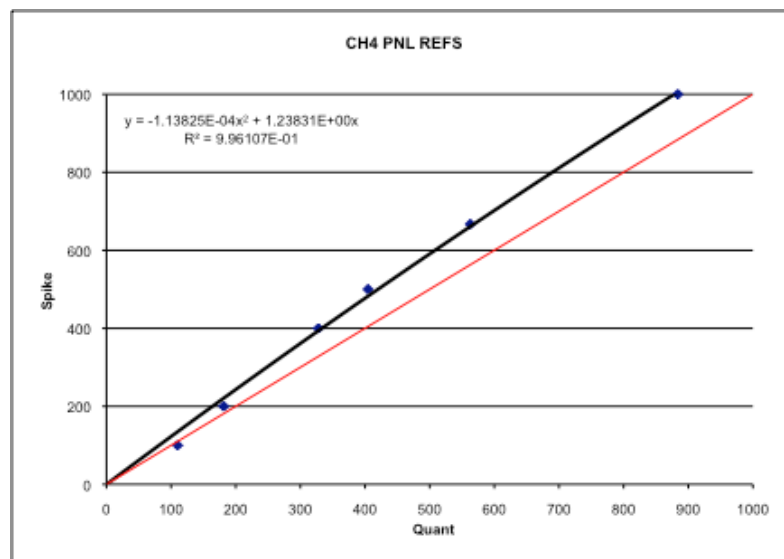


Figure 3.3-23: PFTIR Hot Cell Calibration Curve – Methane

These calibration equations were integrated into the analysis software and applied to the PFTIR raw data to produce the final results.

3.3.6 Methane and Heavy Hydrocarbons

The choice of which regions of the infrared spectrum to use for analysis of a specific compound depends in large part on the sensitivity of the PFTIR detector for a given region. Methane has spectroscopic features at about 3000 and 1360 wavenumbers that can be used for quantification. Because the Mercury-Cadmium-Telluride (MCT) detector used in the PFTIR for this study has low sensitivity in the 3000 wavenumber region, the 1360 wavenumber region was chosen for methane analysis.

The heavier hydrocarbons (C5+) exhibit a large, indistinct feature also at about 3000 wavenumbers. While analysis of the C5+ compounds was attempted in this region, the signal to noise ratio was inadequate for reliable quantification. Unlike methane, however, there are no alternative regions that can be used for C5+ analysis. Therefore, C5+ compounds are not included in the determination of Total Hydrocarbons in this report.

3.3.7 PFTIR Component Errors

In the raw data provided by the PFTIR, an error value is provided for each component measured by the PFTIR. This error value is the residual calculated from fitting the measured spectra to the reference spectra during the Classical Least Squares (CLS) portion of the data analysis procedure. These errors show “goodness of fit” of the measured spectra to the reference spectra.

These errors are not necessarily an indicator of the accuracy of the reported concentration nor are they an indicator of “maximum possible error” for the concentration value and should not be used for that purpose. In fact, these values represent the “minimum error” of the concentration measurement. These errors represent the best that the analysis routine can do in fitting the sample spectra to the reference spectra. The “error” is the residual absorbance left in the quantification region and the analyses routine can only remove interference(s) and fit the reference spectra this well. Other sources of error can add to the total error of the measurement.

As noted in the TCEQ Phase 1 report, “It is possible, particularly with radiance data that this [residual] error could be very small yet a systematic error could still produce a significant effect. This could be the case, for example, if the sky radiance spectrum or the calibration curve used to get plume transmittance from the observed radiance spectrum were incorrect.”

3.3.8 Lack of Integrated Sampling

The carbon dioxide as measured for this study appeared to have a large degree of variability as compared to the other components. This variability is believed to be in part a function of the inhomogeneous nature of the combustion products in the flare plume. Flare flames are well known to produce plumes characterized by a distinctly inhomogeneous distribution of local combustion efficiencies. This inhomogeneity imposes the requirement of careful combustion efficiency integration over the plume both radially and axially to obtain an accurate assessment of emission control performance.

For example, in the US EPA's 1983-86 investigation of the combustion efficiency of industrial flares, the data produced by the extractive-sampling protocols demonstrated that to obtain composite combustion efficiency, i.e. a combustion efficiency that accurately represents a flare's overall emission control performance, requires integration over the flare plume both radially and axially. In order to establish scaling principles in that US EPA investigation, a homologous sequence of flare tips (1½"D, 3"D, 6"D, 12"D) was tested that included four 12"D flare tips of which 3 were of commercial design. Further, extractive sampling methods included the development of special apparatus with a rake appearance that would traverse over the flare plume and produce a composite sample.

When operating flare plumes are tested, the recognition of inhomogeneous distribution of combustion efficiencies is needed to accurately determine the effective composite combustion efficiency of the plume. It must be noted that the PFTIR used in this study is measuring only one small section of the entire plume cross-section with no integration.

3.4 Conclusions

The performance test of the main flare at Marathon's Texas City refinery provided some useful insights to both the operation and performance of a petroleum refinery flare, and also of the PFTIR instrument itself.

Overall Observations

- A flare can be operated with greater than 300 BTU/scf vent gas net heating value and with acceptable exit gas velocities and still be over-steamed.
- Combustion efficiency becomes erratic and generally begins to decline sharply once the flame transitions from a clean, visible flame to one that is invisible. However, not all transparent flames have poor combustion efficiency.
- Combustion efficiency declines with increased steam to hydrocarbon ratios. The same general trends were observed in flare efficiency performance regardless of vent gas composition or turndown factors.
- The PFTIR measures a single point within the plume and not the composite. Variations in chemical composition within the plume itself may influence results.
- The PFTIR reporting units are in concentration x pathlength. This means that the PFTIR cannot be used to determine absolute concentrations or direct emission rates of speciated plume components.
- The PFTIR has not been blind validated; therefore, there is no assessment of bias (i.e. closeness to truth) against established extractive sampling techniques.

3.5 Recommendations for Further Study

Although this test program was robust, several challenges were faced during the course of the program. Marathon's test program was the first opportunity that IMACC used the PFTIR instrument on an operating industrial flare and there were several lessons learned. The areas of improvement identified are as follows:

1. PFTIR site configuration must be well-mapped in accordance with the predominant wind direction observed at the site. Wind directions that cause the flare plume to travel directly away from the PFTIR line of sight must be identified prior to testing, and measurements should not be conducted during periods when the wind is from these directions.

2. A larger field of view may assist the PFTIR instrument in measuring a larger plume cross-section and may help alleviate variability due to plume inhomogeneity.
3. Longer run times may also help address the inhomogeneity issue. Longer run times would allow the PFTIR enough time to navigate around the plume cross-section and not be influenced by flamelets breaking off the flame and passing through the instrument's field of view. However, it is also possible that longer run times would simply reinforce the existing pattern of variability. More study is needed on this topic.

4.0 PFTIR TESTING METHOD AND PROCEDURE

4.1 Description and Principles of Passive FTIR

The instrument used to determine the gas composition of the flare plume is the Passive Fourier Transform Infrared (PFTIR) analyzer. The PFTIR analysis operates on the principle of spectral analysis of thermal radiation emitted by hot gases. Passive means that no “active” infrared light source is used. Instead, the hot gases of the flare are the infrared source. The spectrometer is a receiver only. This approach is possible because the infrared emission spectra of hot gases has the same patterns or “fingerprints” as their absorption spectra does. Consequently, observing a flare with an infrared instrument allows for identification and quantification of species through emission spectroscopy just as with absorption spectroscopy.

For this test program, the PFTIR operation and data analysis was overseen by Dr. Robert Spellicy of Industrial Monitor and Control Corporation (IMACC). The instrument and the analytical software were both developed by IMACC.

The PFTIR was positioned north-northeast of the flare about 180 feet away. Slightly to the east of the flare at approximately the same distance from the PFTIR, a tent containing the PFTIR calibration equipment was set up. See Section 4.2 for a description of the PFTIR siting and plot plan showing the instrument and flare locations.

In order to collect valid data on flare plume composition, the PFTIR must be aimed at the flare plume approximately one flame length from the flame tip. To accomplish this, an IR camera was mounted on the PFTIR body. The IR image of the flare plume was viewed on a monitor by the PFTIR operator. The aiming of the instrument was accomplished by turning two cranks – one for pan and one for tilt. The most important part of the PFTIR operation was its ability to aim at the proper place within the flare plume. The mechanical crank was problematic during the test as it made tracking the plume during periods of wind speed and direction changes very difficult.

Flamelets breaking off the main flame would sometimes cross the instrument’s line of sight, or the instrument would be too close to the flame boundary making resulting data suspect. As a result, a complete review of video collected during the test was conducted and each run

Performance Test of a Steam-Assisted Elevated Flare Marathon Petroleum Company, Texas City Main Flare

was given a Video Review score. Items were identified that will make aiming accuracy better in any future studies conducted with the PFTIR. At the conclusion of the test program, the PFTIR data were analyzed by Dr. Spellicy and the final results provided to Marathon. Details of the data analysis procedures are found in Appendix A.2.

4.2 PFTIR Siting Configuration

Figure 4.2-1 shows the location of the main flare and the PFTIR trailer. Also shown is the location of the two FLIR cameras and one Axis camera located at the project “command center”. A full facility plot plan is shown in Figure 4.2-3 with area below highlighted in red.

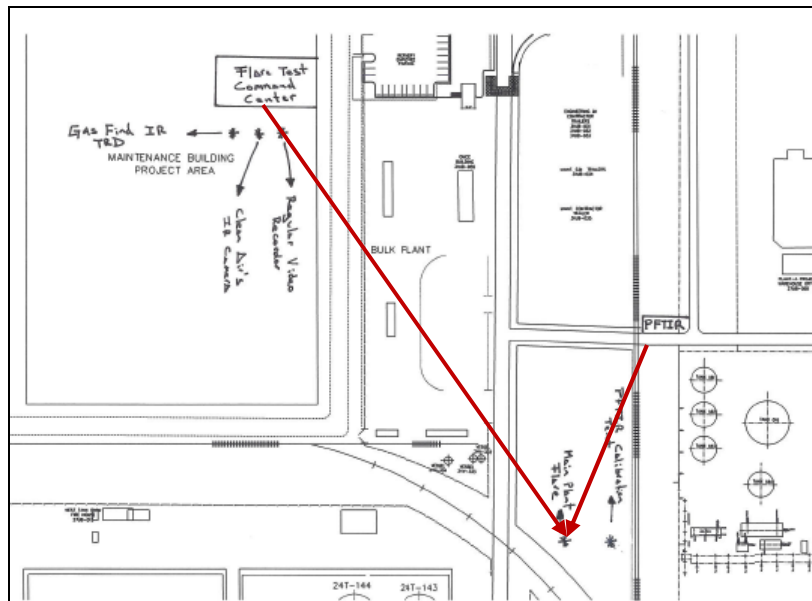


Figure 4.2-1: Location of PFTIR Camera, Flare, and Cameras



Figure 4.2-2: View of Main Flare from PFTIR Location

Performance Test of a Steam-Assisted Elevated Flare
Marathon Petroleum Company, Texas City Main Flare

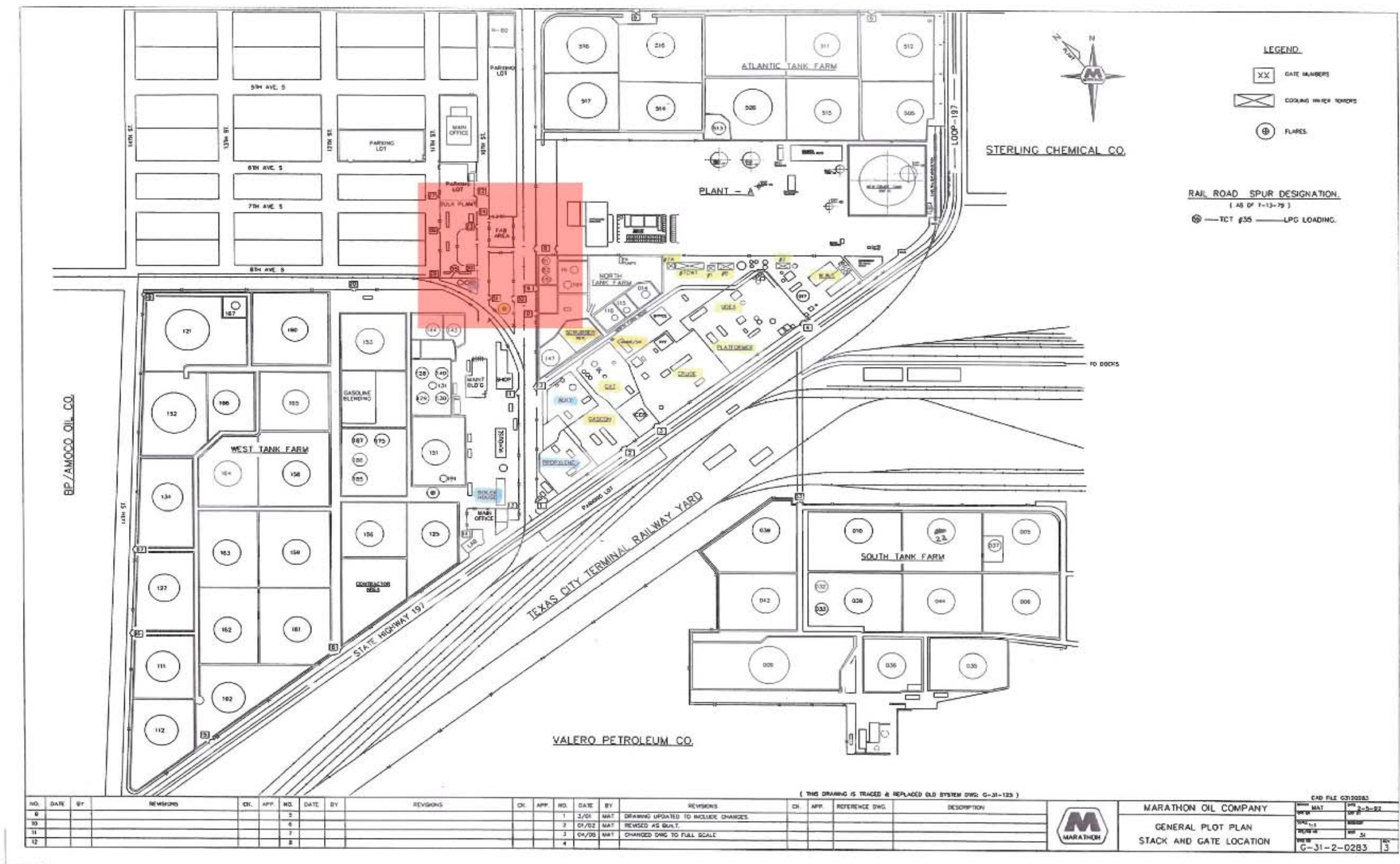


Figure 4.2-3: Marathon Texas City Plot Plan (Area shown in Figure 4.2-1 shown in red)

4.3 Background

To monitor elevated flares, standard “active” IR spectroscopy could be used. However, it is difficult from a practical standpoint to pass a beam of IR light through an elevated flare plume and then capture the transmitted light. Therefore, for this project, a “passive” approach is used that does not require an independent IR light source. Instead, the IR radiation produced by the hot gases of the flare plume is used. With this approach, the spectrometer becomes a passive receiver of IR radiation. This approach is possible because the IR radiation emitted by hot gas, its “radiance spectrum” has the same patterns or “fingerprints” as its absorption spectrum. Spectroscopic techniques developed by Dr. Robert Spellicy, convert this radiance spectrum into an absorption spectrum at which point it can be analyzed with the same techniques used in standard active IR spectroscopy. This technique is referred to as PFTIR.

However, there is one main difference between these two approaches: the radiance spectrum from a hot gas is proportional to the concentration of the gas (as it is in absorption), but it is also affected by gas temperature. In standard absorption FTIR, the temperature of the gas is known and controlled. With PFTIR measurements on a flare plume, the temperature is unknown. Therefore, when conducting PFTIR measurements, the temperature of the flare plume must be determined. Details of how this temperature determination is made are found in Appendix A.2.

Consequently, unlike absorption spectroscopy, the PFTIR signal must be calibrated in absolute units of radiance. This requires that the instrument be calibrated utilizing an IR source of known spectral radiance. This calibration is accomplished with a commercial black body calibrator. This calibrator produces a known radiance IR distribution as predicted by the Planck function. Details of this calibration are found in Appendix A.2.

Calibrations were performed each day at the beginning and end of testing. Calibration results are found in Appendix A.2.

4.4 PFTIR Operation

The PFTIR instrument was located north-northeast of the flare about 180 feet away. It was housed in and operated from a trailer.

Performance Test of a Steam-Assisted Elevated Flare
Marathon Petroleum Company, Texas City Main Flare



Figure 4.4-1: PFTIR Trailer

Another view of the PFTIR instrument taken during the TCEQ Pilot Study is shown in Figure 4.4-2.

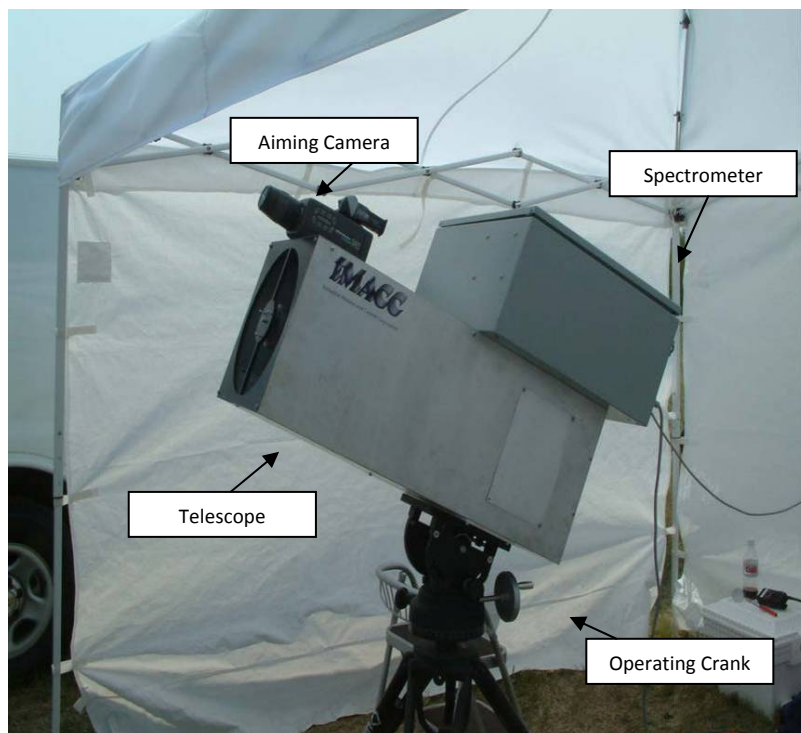


Figure 4.4-2: The PFTIR Instrument

Figure 4.4-3 shows a schematic of the PFTIR set-up.

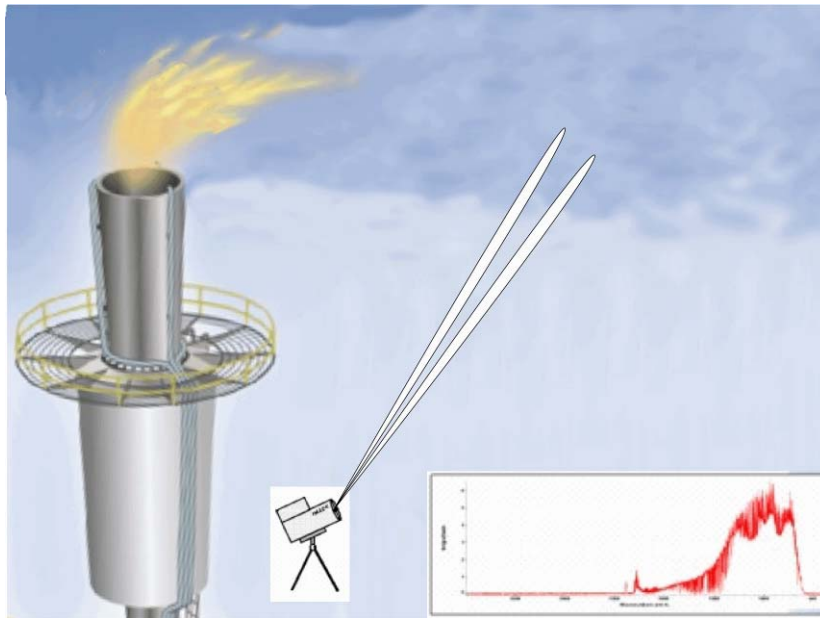


Figure 4.4-3: Schematic of PFTIR set-up

Calibration of the equipment was performed twice each day. Calibration was completed in the morning prior to commencement of testing and again at the end of the day after testing was completed in order to validate the data collected that particular day. Results of these daily calibrations are found in Appendix A.2

The calibration of this equipment required three different calibration sources: a cold source, IR source and a black body source. A more detailed description of the calibration procedure is found in Appendix A.2. Calibration sources were located under a tent on the ground adjacent to the base of the flare. The location was chosen so the distance between the PFTIR and the calibration equipment was approximately the same as the ground distance between the PFTIR and the flare.

After calibration was completed, the equipment was ready to start testing. A sky background was taken to be used in later analysis to subtract background radiance. A new sky background would be taken as sky conditions changed during the testing. In PFTIR testing, it is important to adjust collected spectra with representative sky backgrounds.

Performance Test of a Steam-Assisted Elevated Flare Marathon Petroleum Company, Texas City Main Flare

While the tests were being performed, the team identified several factors that influenced the data collection. The equipment mounting made it difficult to move the instrument. The movement was managed by two manual cranks (pan and tilt), on a commercial azimuth-elevation mount. The movements of the mount were not as smooth or sensitive as would be ideal. This made it difficult to follow the plume with the equipment during periods of changing winds. There was also an issue with stability. The weight of the equipment caused it to bounce around for a few seconds before stabilizing. These have been addressed after the test by re-engineering the azimuth and elevation mounts and by controlling them with a joystick.

During the second day of testing, a failure occurred that was caused by the PFTIR instrument being pointed at such a severe angle over such long periods of time that the interferometer bearing started to foul. The bearing housing had to be disassembled and cleaned. This has also been addressed by modifying the assembly of the FTIR to allow for re-alignment of the FTIR relative to the elevation angle so this problem should not recur.

Another factor influencing the data was the determination of the correct location to aim the PFTIR in order to capture the most representative data. For the majority of the test, the team agreed to focus one flame length away from the tip of the visible flame. Targeting was accomplished by using a thermal IR camera mounted on the front of the PFTIR. The image from this camera was output to a video monitor in the test trailer. However, occasionally it was very difficult to find a suitable aiming location because the flame or the plume would blend with the sky background or be obscured by the flare structure depending on the weather conditions.

The wind direction played a major role in the measurements. At certain times, particularly over the last three days of testing, the wind would cause the plume to be hidden behind the flare from the viewing angle of the PFTIR. That particular scenario made it virtually impossible to collect a representative sample. Relocating the trailer with its equipment was not an easy option because of location, power and calibration time constraints.

For the most part, testing was performed when the wind direction was at right angles to the field of view of the PFTIR trailer. This aspect angle allowed the PFTIR to measure a representative cross-section of the plume. However, there were several days in which the wind direction impacted the view-angle and representativeness of the plume cross-section was suspect. The constant maneuvering of the instrument to stay targeted one flare length away from the tip of the visible flame was a concern. This may have been resolved for future tests with the joystick control of the PFTIR field of view.

4.5 PFTIR Data Reduction

Once collected, the raw PFTIR data must be processed to yield the individual flare component concentrations. This data processing was performed by Dr. Robert Spellicy from IMACC. Data were compiled at approximately one minute intervals. Each one minute data point consists of approximately 40 individual measurements averaged into a single spectrum.

As shown in Figure 4.5-1, the total radiance measured by the PFTIR consists of:

1. The background radiance altered by its transmission through the flare plume and the atmosphere between the plume and the PFTIR instrument.
2. The flare radiance altered by its transmission through the atmosphere between the plume and the PFTIR instrument.
3. The atmospheric radiance of the air between the flare plume and the PFTIR instrument.
4. The radiance from the PFTIR instrument itself.

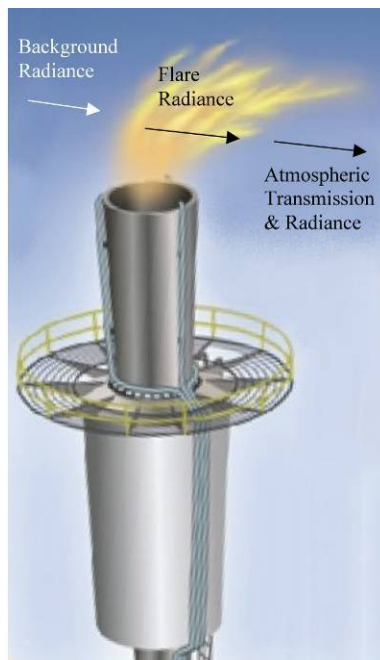


Figure 4.5-1: Contributions to Total Radiance

Performance Test of a Steam-Assisted Elevated Flare Marathon Petroleum Company, Texas City Main Flare

For this test program, everything except the flare transmission is considered interference. In equation form, the measured plume radiance can be represented by:

$$N_{total} = N_{bkg} * \tau_{flr} * \tau_{atm} + N_{flr} * \tau_{atm} + N_{atm} + N_f) \quad \text{Equation 1}$$

Where:

N_{total} = total radiance (radiance observed by the PFTIR)

N_{bkg} = background sky radiance

τ_{flr} = flare transmissivity

τ_{atm} = atmospheric transmissivity

N_{flr} = flare plume radiance

N_{atm} = atmospheric radiance

N_f = radiance of the FTIR instrument itself

In the broadest sense, the data analysis procedure has four major components:

1. Convert the raw interferogram to a single-beam spectrum using a Fourier Transform process,
2. Isolate the flare transmissivity from the other interferences listed above,
3. Convert the isolated flare transmissivity spectrum to an absorbance spectrum so it can be further analyzed with standard spectroscopic techniques,
4. Determine the concentrations of individual components of the flare plume from the absorbance spectrum.

Each of these steps is discussed briefly below. A more detailed treatment is found in Appendix A.2.

Step 1 – Convert the raw interferogram to a radiance spectrum

The raw data from the PFTIR are in the form of an interferogram which is radiance as a function of FTIR scan position. The Fourier Transform (FT) process converts this data into a radiance spectrum which is radiance as a function of wavelength or, in this case, wavenumber. The result is what is referred to as a “single beam” radiance spectrum. These single beam spectra have been supplied on the data hard drives that accompany this report. The FT process is a standard spectroscopic procedure and is not discussed in detail in this report.

Performance Test of a Steam-Assisted Elevated Flare Marathon Petroleum Company, Texas City Main Flare

Step 2 – Isolate the flare transmission spectrum

Once the radiance spectrum has been generated, the flare transmission must be isolated from all the interferants that the PFTIR also “sees”. In order to accomplish this, each term in Equation 1 above must be determined. This is done as follows:

Background radiance (N_{bkg}) – As described in Section 4.1.2, at least once each day, the PFTIR was aimed at an unobstructed part of the sky. Since the background radiance is affected by conditions such as sun position and cloud cover, this procedure was repeated whenever a significant change in background was observed.

Flare transmissivity (τ_{flr}) – This is the value we are looking for and is the result when all competing factors are removed. It actually appears two places: 1) in transmitting the sky background through the flare to the PFTIR and 2) in the radiance term for the flare itself. So the flare transmission must be extracted from the complex mixture of signals received by the PFTIR. This task is accomplished by the IMACC software.

Atmospheric transmissivity (τ_{atm}) – This value is determined by aiming the PFTIR at an IR source and taking the ratio of the value obtained (minus the atmospheric radiance) to a “synthetic background” spectrum. This synthetic background (referred to as I_0) represents the shape of the radiance spectrum that would be generated by the PFTIR in the absence of all gases. For this project the IR source was a SiC source operated at a temperature of 1250 K. This is a standard source used in most active FTIR systems. This source has sufficient signal throughout the infrared to allow for a transmission spectrum to be determined over the range of wavenumbers needed.

Flare plume radiance (N_{flr}) – Plume radiance is $(1 - \text{plume transmission})$ times the Planck function (evaluated at the temperature of the plume). The radiance is what is measured by the PFTIR but it is mixed in with other signals and so must be corrected with respect to this interference.

Atmospheric radiance (N_{atm}) – This value is determined by aiming the PFTIR at very cold source in the calibration telescope located at the same distance from the PFTIR as the flare. Any radiance observed will then be due to the intervening atmosphere plus any radiance from the PFTIR instrument itself. This measured value is referred to as M_n . For this project, the cold source was an aluminum bar immersed in liquid nitrogen.

PFTIR radiance (N_f) – PFTIR radiance is the emissions of the instrument itself. It is measured together with atmospheric radiance and is part of the M_n measurement.

Once these values are known, they are applied to the total radiance spectrum by IMACC proprietary software to isolate the flare transmission spectrum. For a more detailed description of this process, see Appendix A.2.

Step 3 – Convert the transmission spectrum to an absorption spectrum

Once the flare transmission spectrum has been isolated, it must be converted to an absorbance spectrum so that standard spectroscopic techniques can be used for further analysis. Transmission and absorbance are related by the Beer-Lambert law through the following equation.

$$\tau_{plume} = e^{-K(\nu) * c * l}$$

Equation 2

Essentially, absorbance is the negative log of transmission, thus:

$$\text{Absorbance}(\nu) = (0.434)K(\nu) * c * l$$

Equation 3

See Appendix A.2 for further detail. This conversion is a standard spectroscopic procedure.

Step 4 – Determine the concentrations of individual components in the flare plume

Once the absorbance spectrum has been generated, there are several analytical techniques that may be used to estimate individual component concentrations. For this project, a modified Classical Least Squares (CLS) analysis was used. IMACC proprietary software was used for this step of the data analysis. The modifications to standard CLS include algorithms for linearizing the absorbance for each analyte with concentration, corrections for spectral baseline shifts, corrections for any spectral line shifts observed, and algorithms for dynamic reference spectra selection based upon observed concentrations of each compound.

The CLS technique compares measured spectra to combinations reference spectra of known concentration and interfering compounds and matches the absorbance of the data and the references to determine gas concentration. This process is performed for all components present to account for all spectral features present.

After fitting, CLS also determines the difference or residual between the measured and scaled references. The fitting process minimizes the residuals in each analysis region. The software used for this project uses dynamic reference selection to select reference spectra based upon measured gas concentrations. In most cases, this means different reference spectra will be chosen for each analyte in the measured spectrum. This process will be repeated up to four times to optimize all spectra compared to the measured data.

A flow chart of the PFTIR data analysis process is shown in Figure 4.5-2.

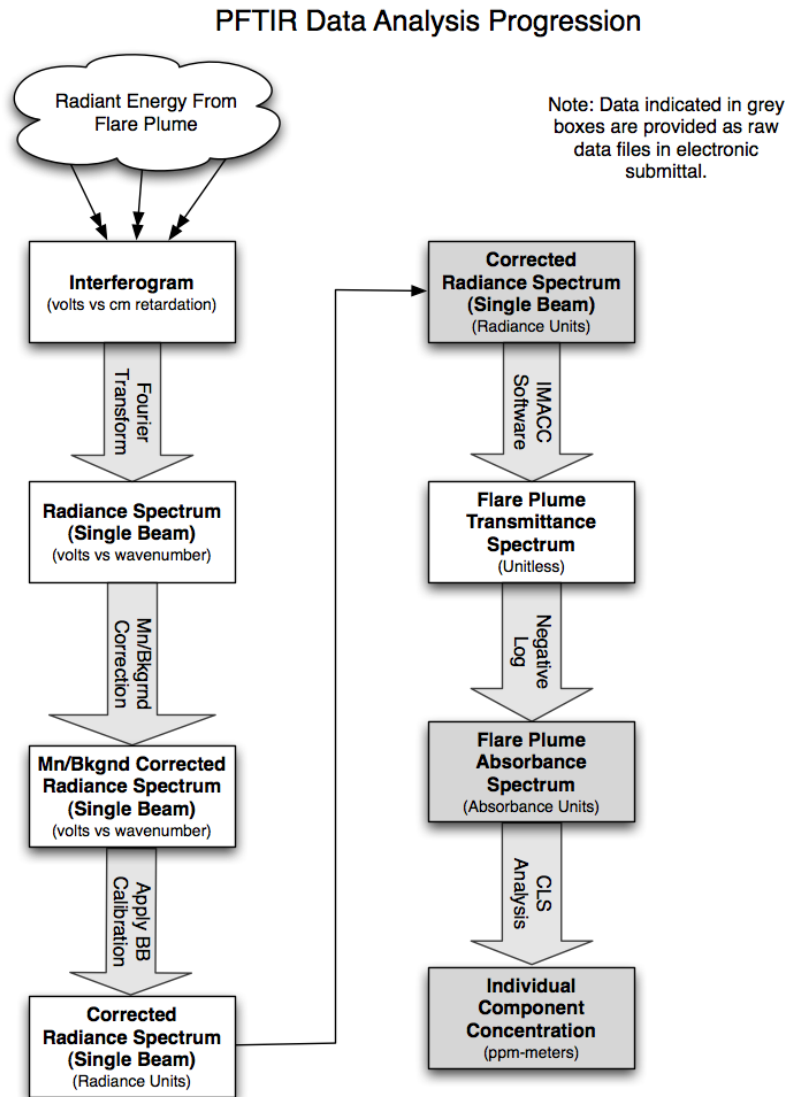


Figure 4.5-2: PFTIR Data Analysis Progression

4.6 Q-Branch Subtraction

If an absorption feature becomes too strong, it will saturate (become totally absorbing) and it is not useful for spectroscopic analysis. During this test program, some of the CO₂ data points at long wavelength exhibited this problem. Rather than discard the spectra as invalid, the analytical process was refined to address this issue, avoiding the spectral regions considered to be invalid. This refinement, referred to here as Q-Branch Subtraction, is described in Appendix A.2.

For some data points, a region of the IR spectrum, called the “Q-Branch”, was opaque in the IR (saturated the detector) and was, therefore, not linear in concentration. The refined analyses routine does not contain the Q branch or any regions for other compounds, which are opaque or otherwise too heavily interfered with by other compounds. This is part of the quality assurance one does after collecting FTIR data.

5.0 DATA TABLES

Due to the large quantity of data collected for this project, three levels of summary are provided. Section 5.1 is the most concise summary providing run averages for a few key parameters at each test condition. Section 5.2 provides more detail on the individual test conditions, shows a larger number of parameters and also provides information on wind effects.

5.1 Data Summary Tables

Tables 5.1-1 through 5.1-10 below present summary data for each test condition. Column headings for these tables are described below:

- Condition:** This is the designation for each test condition described in Section 2.4.
- New Run:** This is the revised run number indicating the test and replicate. For example, Run 3-2 indicates Test 3, Replicate 2. A test is a given S/VG ratio.
- PFTIR Start Date/Time:** The date and time each run began.
- PFTIR Stop Date/Time:** The date and time each run ended.
- Min:** The number of minutes for each run
- S/VG:** Steam to Vent Gas ratio (lb/lb)
- S/HC:** Steam to Hydrocarbon ratio (lb/lb)
- S/S521:** Ratio of actual steam to API 521 recommended steam
- CZG:** Heat content of vent gas in the combustion zone (BTU/scf)
- Smoke:** Smoke rating given to the test according to the scale provided in Table 3.2-1
- CO₂p:** CO₂ as measured by the PFTIR (ppm-meters)
- CO₂m Low:** The low range of CO₂ emissions from the flare as predicted by mass balance. See Section 3.2.3 for further details.
- CO₂m High:** The high range of CO₂ emissions from the flare as predicted by mass balance. See Section 3.2.3 for further details.
- CE:** Combustion Efficiency as calculated with PFTIR data
- Video Score:** A score from a video review panel indicating the degree to which the PFTIR was aimed properly during each run. See Section 4.3.

Performance Test of a Steam-Assisted Elevated Flare
Marathon Petroleum Company, Texas City Main Flare

Note that individual runs are color-coded corresponding to the video review score. Runs scoring between 1.0 and 1.9 (correct aiming <20%) are shaded blue. Runs scoring between 2.0 and 2.9 (correct aiming between 20% and 50%) are shown with blue text.

Performance Test of a Steam-Assisted Elevated Flare
Marathon Petroleum Company, Texas City Main Flare

Table 5.1-1: Condition A19 Test Result Summary

| Condition A19 | | | | | | | | | | | | | | | |
|---------------|---------|---------|-----------------------|----------------------|-----|------|------|--------|------|-------|---------|----------|-----------|-----|-------------|
| Condition | Old Run | New Run | PFTIR Start Date/Time | PFTIR Stop Date/Time | Min | S/VG | S/HC | S/S521 | FGCZ | Smoke | CO2p | CO2m Low | CO2m High | CE | Video Score |
| A19 | 1-1 | 1-1 | 9/15/2009 12:44 | 9/15/2009 13:04 | 20 | 0.94 | 1.73 | 2.23 | 346 | 6.0 | 9,455 | 9,677 | 14,406 | 98% | 3.6 |
| A19 | 1-2 | 1-2 | 9/22/2009 15:05 | 9/22/2009 15:15 | 10 | 0.97 | 1.65 | 2.29 | 360 | 5.5 | 336,831 | 9,620 | 14,325 | 99% | 2.3 |
| A19 | 1-3 | 1-3 | 9/24/2009 9:33 | 9/24/2009 9:43 | 10 | 1.07 | 2.08 | 2.47 | 316 | 6.0 | 31,076 | 9,465 | 14,072 | 98% | 2.0 |
| A19 | 2-1 | 2-1 | 9/15/2009 13:11 | 9/15/2009 13:33 | 22 | 1.25 | 2.06 | 2.81 | 340 | 6.0 | 8,028 | 4,359 | 6,525 | 98% | 3.8 |
| A19 | 3-1 | 3-1 | 9/15/2009 13:37 | 9/15/2009 13:55 | 18 | 1.51 | 2.22 | 3.51 | 331 | 5.5 | 6,914 | 9,789 | 14,555 | 96% | 4.0 |
| A19 | 2-2 | 3-2 | 9/22/2009 15:19 | 9/22/2009 15:29 | 10 | 1.49 | 2.24 | 3.54 | 318 | 5.5 | 31,645 | 9,508 | 14,138 | 98% | 2.3 |
| A19 | 4-1 | 4-1 | 9/15/2009 13:58 | 9/15/2009 14:08 | 10 | 2.01 | 3.16 | 4.71 | 257 | 1.5 | 4,679 | 9,648 | 13,924 | 94% | 3.0 |
| A19 | 3-2 | 4-2 | 9/22/2009 15:40 | 9/22/2009 15:49 | 9 | 2.01 | 2.87 | 4.72 | 268 | 2.0 | 227,849 | 9,891 | 14,656 | 93% | 2.0 |
| A19 | 5-2 | 5-1 | 9/22/2009 17:19 | 9/22/2009 17:29 | 10 | 2.51 | 3.20 | 6.08 | 252 | 1.0 | 8,859 | 9,588 | 14,209 | 84% | 2.0 |
| A19 | 6-2 | 6-1 | 9/22/2009 17:31 | 9/22/2009 17:36 | 5 | 2.69 | 3.62 | 6.48 | 227 | 1.5 | 9,044 | 9,574 | 14,160 | 86% | 2.3 |
| A19 | 5-1 | 7-1 | 9/15/2009 14:12 | 9/15/2009 14:22 | 10 | 3.00 | 4.85 | 7.08 | 183 | 1.0 | 5,391 | 9,464 | 13,924 | 90% | 3.5 |
| A19 | 7-2 | 7-2 | 9/22/2009 17:37 | 9/22/2009 17:43 | 6 | 2.98 | 4.12 | 7.10 | 204 | 1.0 | 6,363 | 9,559 | 14,105 | 82% | 2.3 |

Table 5.1-2: Condition A11 Test Result Summary

| Condition A11 | | | | | | | | | | | | | | | |
|---------------|---------|---------|-----------------------|----------------------|-----|------|-------|--------|------|-------|-------|----------|-----------|-----|-------------|
| Condition | Old Run | New Run | PFTIR Start Date/Time | PFTIR Stop Date/Time | Min | S/VG | S/HC | S/S521 | FGCZ | Smoke | CO2p | CO2m Low | CO2m High | CE | Video Score |
| A11 | 1-2 | 1-1 | 9/17/2009 9:09 | 9/17/2009 9:20 | 11 | 1.34 | 1.99 | 3.22 | 336 | 5.5 | 8,925 | 7,846 | 11,715 | 99% | 4.0 |
| A11 | 1-1 | 2-1 | 9/15/2009 16:11 | 9/15/2009 16:27 | 16 | 1.79 | 3.31 | 4.25 | 240 | 2.0 | 3,193 | 7,896 | 11,711 | 96% | 4.0 |
| A11 | 2-1 | 2-2 | 9/15/2009 16:30 | 9/15/2009 16:41 | 11 | 1.76 | 3.34 | 4.16 | 237 | 2.0 | 5,889 | 7,901 | 11,715 | 97% | 3.8 |
| A11 | 3-1 | 3-1 | 9/15/2009 16:50 | 9/15/2009 17:09 | 19 | 2.01 | 3.95 | 4.75 | 213 | 2.0 | 8,448 | 7,861 | 11,625 | 97% | 3.3 |
| A11 | 5-2 | 3-2 | 9/17/2009 10:35 | 9/17/2009 10:45 | 10 | 2.04 | 3.95 | 4.80 | 209 | 1.5 | 6,902 | 7,854 | 11,615 | 98% | 3.5 |
| A11 | 3-2 | 4-1 | 9/17/2009 9:54 | 9/17/2009 10:02 | 8 | 2.50 | 4.55 | 5.94 | 185 | 1.5 | 5,206 | 7,856 | 11,591 | 96% | 3.8 |
| A11 | 7-2 | 5-1 | 9/17/2009 11:09 | 9/17/2009 11:19 | 10 | 2.99 | 5.64 | 7.08 | 157 | 1.0 | 3,865 | 7,768 | 11,408 | 94% | 3.3 |
| A11 | 2-2 | 6-1 | 9/17/2009 9:30 | 9/17/2009 9:40 | 10 | 3.52 | 5.82 | 8.43 | 154 | 1.0 | 4,420 | 7,685 | 11,287 | 93% | 4.0 |
| A11 | 6-2 | 7-1 | 9/17/2009 10:54 | 9/17/2009 11:04 | 10 | 4.01 | 7.70 | 9.48 | 125 | 1.0 | 3,367 | 7,584 | 11,056 | 87% | 3.3 |
| A11 | 4-2 | 8-1 | 9/17/2009 10:15 | 9/17/2009 10:26 | 11 | 4.50 | 8.46 | 10.64 | 113 | 1.0 | 3,255 | 7,615 | 11,060 | 81% | 3.3 |
| A11 | 8-2 | 9-1 | 9/17/2009 11:24 | 9/17/2009 11:34 | 10 | 5.00 | 9.50 | 11.78 | 102 | 1.0 | 1,986 | 7,505 | 10,869 | 74% | 3.6 |
| A11 | 9-2 | 10-1 | 9/17/2009 11:37 | 9/17/2009 11:48 | 11 | 5.26 | 10.04 | 12.41 | 99 | 1.0 | 2,008 | 7,487 | 10,824 | 77% | 3.5 |
| A11 | 10-2 | 11-1 | 9/17/2009 11:51 | 9/17/2009 12:01 | 10 | 5.51 | 10.96 | 12.98 | 95 | 1.0 | 1,541 | 7,479 | 10,770 | 68% | 3.5 |
| A11 | 11-2 | 11-2 | 9/17/2009 12:11 | 9/17/2009 12:14 | 3 | 5.32 | 10.12 | 12.75 | 96 | 1.0 | 1,254 | 7,503 | 10,827 | 66% | 3.5 |
| A11 | 12-2 | 12-1 | 9/17/2009 12:40 | 9/17/2009 12:51 | 11 | 5.76 | 10.82 | 13.65 | 96 | 1.0 | 1,064 | 7,357 | 10,608 | 62% | 3.4 |
| A11 | 13-2 | 13-1 | 9/17/2009 12:53 | 9/17/2009 13:03 | 10 | 6.01 | 11.85 | 14.15 | 90 | 1.0 | 901 | 7,118 | 11,715 | 62% | 4.0 |
| A11 | 14-2 | 14-1 | 9/17/2009 13:08 | 9/17/2009 13:18 | 10 | 6.96 | 13.48 | 16.34 | 79 | 1.0 | 0 | 7,289 | 10,428 | 0% | 3.5 |

Table 5.1-3: Condition A8 Test Result Summary

| Condition A8 | | | | | | | | | | | | | | | |
|--------------|---------|---------|-----------------------|----------------------|-----|------|-------|--------|--------|-------|---------|----------|-----------|-----|-------------|
| Condition | Old Run | New Run | PFTIR Start Date/Time | PFTIR Stop Date/Time | Min | S/VG | S/HC | S/S521 | FGCZ | Smoke | CO2p | CO2m Low | CO2m High | CE | Video Score |
| A8 | 1-4 | 1-1 | 9/22/2009 12:46 | 9/22/2009 12:57 | 11 | 1.83 | 3.55 | 4.26 | 220 | 1.0 | 1,112 | 8,215 | 12,156 | 65% | 2.5 |
| A8 | 1-3 | 2-1 | 9/22/2009 8:54 | 9/22/2009 9:04 | 10 | 2.18 | 4.48 | 5.05 | 196 | 1.5 | 24,465 | 8,295 | 12,223 | 97% | 2.5 |
| A8 | 1-5 | 2-2 | 9/24/2009 8:38 | 9/24/2009 8:48 | 10 | 2.19 | 4.78 | 5.06 | 177.75 | 1.0 | 4,715 | 7,998 | 11,777 | 86% | 1.5 |
| A8 | 2-5 | 2-3 | 9/24/2009 8:49 | 9/24/2009 8:59 | 10 | 2.18 | 4.74 | 5.02 | 181 | 1.0 | 5,930 | 7,995 | 11,777 | 86% | 2.0 |
| A8 | 2-3 | 3-1 | 9/22/2009 9:16 | 9/22/2009 9:26 | 10 | 3.00 | 6.41 | 6.95 | 159 | 1.0 | 3,827 | 8,035 | 11,757 | 64% | 2.6 |
| A8 | 2-4 | 3-2 | 9/22/2009 13:08 | 9/22/2009 13:21 | 13 | 3.01 | 6.23 | 6.94 | 152 | 1.0 | 5,842 | 8,015 | 11,735 | 74% | 2.3 |
| A8 | 3-3 | 4-1 | 9/22/2009 9:50 | 9/22/2009 10:00 | 10 | 3.57 | 6.99 | 8.26 | 140 | 1.0 | 2,685 | 8,066 | 11,789 | 60% | 2.3 |
| A8 | 4-3 | 5-1 | 9/22/2009 10:07 | 9/22/2009 10:17 | 10 | 3.99 | 7.94 | 9.24 | 129 | 1.0 | 2,603 | 7,942 | 11,556 | 64% | 2.8 |
| A8 | 3-4 | 5-2 | 9/22/2009 13:25 | 9/22/2009 13:35 | 10 | 4.00 | 8.29 | 9.25 | 118.03 | 1.0 | 1,353 | 7,907 | 11,468 | 52% | 1.6 |
| A8 | 5-3 | 6-1 | 9/22/2009 10:24 | 9/22/2009 10:34 | 10 | 4.50 | 8.58 | 10.41 | 117 | 1.0 | 3,569 | 7,956 | 11,576 | 64% | 2.9 |
| A8 | 6-3 | 7-1 | 9/22/2009 10:37 | 9/22/2009 10:46 | 9 | 4.89 | 9.46 | 11.27 | 108 | 1.0 | 2,249 | 7,802 | 11,263 | 64% | 2.3 |
| A8 | 4-4 | 7-2 | 9/22/2009 13:40 | 9/22/2009 13:50 | 10 | 4.90 | 10.16 | 11.42 | 102.95 | 1.0 | 0 | 7,740 | 11,164 | 0% | 1.4 |
| A8 | 5-4 | 8-1 | 9/22/2009 13:52 | 9/22/2009 14:02 | 10 | 5.06 | 9.94 | 11.81 | 98.42 | 1.0 | 2,333 | 7,826 | 11,293 | 68% | 1.8 |
| A8 | 6-4 | 8-2 | 9/22/2009 14:06 | 9/22/2009 14:16 | 10 | 5.03 | 9.87 | 11.74 | 97.66 | 1.0 | 5,658 | 7,787 | 11,245 | 75% | 1.8 |
| A8 | 7-4 | 9-1 | 9/22/2009 14:22 | 9/22/2009 14:32 | 10 | 5.47 | 11.63 | 12.70 | 89.84 | 1.0 | 508,784 | 7,593 | 10,907 | 67% | 1.3 |
| A8 | 8-4 | 10-1 | 9/22/2009 14:33 | 9/22/2009 14:37 | 4 | 5.68 | 12.16 | 13.05 | 86.30 | 1.0 | 955 | 7,779 | 11,146 | 48% | 1.0 |

Performance Test of a Steam-Assisted Elevated Flare
Marathon Petroleum Company, Texas City Main Flare

Table 5.1-4: Condition B Test Result Summary

| Condition B | | | | | | | | | | | | | | | |
|-------------|---------|---------|-----------------------|----------------------|-----|------|------|--------|--------|-------|-----------|----------|-----------|------|-------------|
| Condition | Old Run | New Run | PFTIR Start Date/Time | PFTIR Stop Date/Time | Min | S/VG | S/H | S/S521 | FGCZ | Smoke | CO2p | CO2m Low | CO2m High | CE | Video Score |
| B | 1-1 | 1-1 | 9/16/2009 10:56 | 9/16/2009 11:10 | 14 | 0.42 | 0.56 | 1.02 | 614.40 | 6.5 | 11,957 | 8,028 | 12,059 | 99% | 3.8 |
| B | 1-2 | 1-2 | 9/16/2009 13:23 | 9/16/2009 13:34 | 11 | 0.41 | 0.55 | 1.00 | 619.31 | 6.5 | 10,576 | 8,062 | 12,110 | 99% | 3.7 |
| B | 1-3 | 1-3 | 9/23/2009 10:10 | 9/23/2009 10:20 | 10 | 0.40 | 0.53 | 0.96 | 641.30 | 5.0 | 1,329,918 | 8,098 | 12,165 | 100% | 2.1 |
| B | 2-1 | 2-1 | 9/16/2009 11:16 | 9/16/2009 11:27 | 11 | 0.50 | 0.66 | 1.19 | 582.33 | 6.5 | 18,676 | 8,014 | 12,034 | 99% | 3.8 |
| B | 2-2 | 2-2 | 9/16/2009 13:51 | 9/16/2009 14:01 | 10 | 0.50 | 0.67 | 1.22 | 580.28 | 6.0 | 22,418 | 8,032 | 12,059 | 99% | 3.7 |
| B | 2-3 | 2-3 | 9/23/2009 10:23 | 9/23/2009 10:33 | 10 | 0.50 | 0.65 | 1.20 | 594.78 | 4.5 | 467,749 | 8,086 | 12,140 | 100% | 1.9 |
| B | 3-1 | 3-1 | 9/16/2009 11:32 | 9/16/2009 11:48 | 16 | 0.75 | 1.01 | 1.82 | 490.12 | 5.5 | 37,935 | 7,986 | 11,973 | 99% | 4.0 |
| B | 3-2 | 3-2 | 9/16/2009 14:06 | 9/16/2009 14:16 | 10 | 0.75 | 1.00 | 1.82 | 486.89 | 6.0 | 15,816 | 7,979 | 11,962 | 99% | 3.7 |
| B | 3-3 | 3-3 | 9/23/2009 10:35 | 9/23/2009 10:45 | 10 | 0.75 | 0.98 | 1.80 | 501.01 | 4.5 | 697,040 | 8,064 | 12,090 | 100% | 1.9 |
| B | 4-1 | 4-1 | 9/16/2009 11:55 | 9/16/2009 12:05 | 10 | 1.00 | 1.31 | 2.41 | 431.22 | 5.5 | 33,946 | 8,047 | 12,047 | 99% | 4.0 |
| B | 4-2 | 4-2 | 9/16/2009 14:19 | 9/16/2009 14:29 | 10 | 1.00 | 1.34 | 2.41 | 423.38 | 4.5 | 16,608 | 8,017 | 12,000 | 99% | 3.7 |
| B | 4-3 | 4-3 | 9/23/2009 10:48 | 9/23/2009 10:58 | 10 | 0.99 | 1.29 | 2.38 | 436.29 | 3.5 | 1,536,867 | 8,035 | 12,030 | 99% | 2.4 |
| B | 5-1 | 5-1 | 9/16/2009 12:08 | 9/16/2009 12:18 | 10 | 1.25 | 1.64 | 3.02 | 379.69 | 3.0 | 33,645 | 7,984 | 11,936 | 99% | 4.0 |
| B | 5-2 | 5-2 | 9/16/2009 14:31 | 9/16/2009 14:41 | 10 | 1.25 | 1.65 | 3.02 | 374.59 | 3.0 | 18,940 | 8,008 | 11,970 | 99% | 4.0 |
| B | 6-1 | 6-1 | 9/16/2009 12:22 | 9/16/2009 12:32 | 10 | 1.50 | 2.00 | 3.62 | 336.45 | 2.0 | 31,647 | 7,949 | 11,865 | 98% | 4.0 |
| B | 6-2 | 6-2 | 9/16/2009 14:43 | 9/16/2009 14:54 | 11 | 1.50 | 1.99 | 3.63 | 335.57 | 2.0 | 10,519 | 7,984 | 11,917 | 98% | 4.0 |
| B | 5-3 | 6-3 | 9/23/2009 11:05 | 9/23/2009 11:15 | 10 | 1.50 | 1.96 | 3.61 | 342.07 | 1.5 | 515,324 | 8,010 | 11,958 | 98% | 1.5 |
| B | 7-1 | 7-1 | 9/16/2009 12:35 | 9/16/2009 12:46 | 11 | 1.60 | 2.13 | 3.86 | 322.91 | 1.5 | 13,874 | 7,948 | 11,857 | 98% | 4.0 |
| B | 7-2 | 7-2 | 9/16/2009 14:56 | 9/16/2009 15:23 | 27 | 1.60 | 2.13 | 3.87 | 321.45 | 1.5 | 6,923 | 7,972 | 11,892 | 98% | 3.2 |
| B | 6-3 | 7-3 | 9/23/2009 11:17 | 9/23/2009 11:27 | 10 | 1.60 | 2.10 | 3.85 | 329.11 | 1.5 | 389,900 | 7,986 | 11,914 | 95% | 1.9 |
| B | 8-1 | 8-1 | 9/16/2009 12:48 | 9/16/2009 12:58 | 10 | 1.70 | 2.25 | 4.11 | 310.64 | 1.5 | 18,294 | 7,950 | 11,854 | 98% | 4.0 |
| B | 8-2 | 8-2 | 9/16/2009 15:26 | 9/16/2009 15:38 | 12 | 1.70 | 2.27 | 4.12 | 308.97 | 1.5 | 19,453 | 7,967 | 11,878 | 96% | 3.7 |
| B | 9-1 | 9-1 | 9/16/2009 13:01 | 9/16/2009 13:11 | 10 | 1.80 | 2.41 | 4.34 | 299.27 | 1.5 | 23,780 | 7,931 | 11,818 | 98% | 4.0 |
| B | 9-2 | 9-2 | 9/16/2009 15:40 | 9/16/2009 15:50 | 10 | 1.80 | 2.39 | 4.36 | 297.38 | 1.5 | 10,506 | 7,945 | 11,839 | 98% | 3.7 |
| B | 10-1 | 10-1 | 9/16/2009 13:12 | 9/16/2009 13:15 | 3 | 1.88 | 2.50 | 4.57 | 290.46 | 1.0 | 6,242 | 7,925 | 11,803 | 91% | 2.5 |
| B | 10-2 | 10-2 | 9/16/2009 15:53 | 9/16/2009 16:03 | 10 | 1.90 | 2.53 | 4.60 | 286.41 | 1.5 | 16,697 | 7,922 | 11,798 | 97% | 4.0 |

Table 5.1-5: Condition C Test Result Summary

| Condition C | | | | | | | | | | | | | | | |
|-------------|---------|---------|-----------------------|----------------------|-----|------|------|--------|--------|-------|-----------|----------|-----------|------|-------------|
| Condition | Old Run | New Run | PFTIR Start Date/Time | PFTIR Stop Date/Time | Min | S/VG | S/H | S/S521 | FGCZ | Smoke | CO2p | CO2m Low | CO2m High | CE | Video Score |
| C | 3-1 | 1-1 | 9/17/2009 15:03 | 9/17/2009 15:13 | 10 | 0.31 | 0.38 | 0.60 | 1,016 | 7.5 | 41,111 | 8,844 | 13,282 | 99% | 3.8 |
| C | 4-2 | 1-2 | 9/17/2009 17:05 | 9/17/2009 17:15 | 10 | 0.30 | 0.34 | 0.56 | 1,115 | 8.0 | 79,052 | 8,912 | 13,386 | 100% | 4.0 |
| C | 1-3 | 1-3 | 9/23/2009 13:47 | 9/23/2009 13:57 | 10 | 0.35 | 0.44 | 0.67 | 935.89 | 6.0 | 525,301 | 8,860 | 13,300 | 100% | 1.5 |
| C | 2-1 | 2-1 | 9/17/2009 14:48 | 9/17/2009 14:58 | 10 | 0.50 | 0.64 | 0.96 | 772 | 7.5 | 90,829 | 8,784 | 13,174 | 99% | 3.3 |
| C | 3-2 | 2-2 | 9/17/2009 16:50 | 9/17/2009 17:00 | 10 | 0.50 | 0.57 | 0.93 | 881 | 5.5 | 836,679 | 8,902 | 13,357 | 99% | 4.0 |
| C | 2-3 | 2-3 | 9/23/2009 14:07 | 9/23/2009 14:17 | 10 | 0.52 | 0.62 | 0.99 | 832.19 | 5.5 | 0 | 8,790 | 13,187 | 100% | 1.5 |
| C | 1-1 | 3-1 | 9/17/2009 14:28 | 9/17/2009 14:42 | 14 | 1.00 | 1.38 | 1.97 | 475 | 4.0 | 2,830 | 8,746 | 13,073 | 99% | 3.8 |
| C | 2-2 | 3-2 | 9/17/2009 16:29 | 9/17/2009 16:39 | 10 | 0.91 | 1.45 | 2.17 | 407 | 2.5 | 74,661 | 8,860 | 13,257 | 99% | 3.8 |
| C | 3-3 | 3-3 | 9/23/2009 14:23 | 9/23/2009 14:33 | 10 | 1.00 | 1.12 | 1.90 | 584.87 | 3.5 | 913,387 | 8,840 | 13,229 | 99% | 1.6 |
| C | 4-3 | 4-1 | 9/23/2009 14:39 | 9/23/2009 14:49 | 10 | 1.20 | 1.37 | 2.27 | 516.62 | 1.5 | 2,252,510 | 8,818 | 13,180 | 100% | 1.5 |
| C | 6-3 | 5-1 | 9/23/2009 14:54 | 9/23/2009 15:04 | 10 | 1.30 | 1.46 | 2.46 | 489.10 | 1.5 | 2,523,063 | 8,855 | 13,228 | 99% | 1.8 |

Table 5.1-6: Condition D Test Result Summary

| Condition D | | | | | | | | | | | | | | | |
|-------------|---------|---------|-----------------------|----------------------|-----|------|------|--------|-------|-------|-----------|----------|-----------|------|-------------|
| Condition | Old Run | New Run | PFTIR Start Date/Time | PFTIR Stop Date/Time | Min | S/VG | S/H | S/S521 | FGCZ | Smoke | CO2p | CO2m Low | CO2m High | CE | Video Score |
| D | 1-1 | 1-1 | 9/18/2009 10:30 | 9/18/2009 10:40 | 10 | 0.42 | 0.48 | 0.77 | 993 | 9.0 | 352,610 | 9,140 | 13,715 | 98% | 3.8 |
| D | 1-2 | 1-2 | 9/18/2009 16:44 | 9/18/2009 16:54 | 10 | 0.41 | 0.46 | 0.76 | 1,035 | 9.5 | 27,256 | 9,113 | 13,676 | 95% | 3.8 |
| D | 1-3 | 1-3 | 9/21/2009 13:06 | 9/21/2009 13:17 | 11 | 0.42 | 0.48 | 0.80 | 1,031 | 8.5 | 6,744 | 9,080 | 13,626 | 99% | 3.0 |
| D | 2-1 | 2-1 | 9/18/2009 10:52 | 9/18/2009 11:03 | 11 | 0.55 | 0.64 | 1.01 | 858 | 9.0 | 1,107,795 | 9,139 | 13,702 | 100% | 3.5 |
| D | 2-2 | 2-2 | 9/18/2009 17:08 | 9/18/2009 17:18 | 10 | 0.54 | 0.64 | 1.00 | 856 | 9.0 | 15,248 | 9,134 | 13,695 | 98% | 4.0 |
| D | 2-3 | 2-3 | 9/21/2009 13:22 | 9/21/2009 13:32 | 10 | 0.51 | 0.58 | 0.97 | 898 | 8.5 | 25,948 | 9,167 | 13,748 | 99% | 3.3 |
| D | 3-1 | 3-1 | 9/18/2009 11:07 | 9/18/2009 11:17 | 10 | 0.75 | 0.87 | 1.38 | 712 | 6.0 | 17,647 | 9,105 | 13,637 | 99% | 3.3 |
| D | 3-2 | 3-2 | 9/18/2009 17:24 | 9/18/2009 17:34 | 10 | 0.74 | 0.85 | 1.37 | 716 | 6.5 | 14,484 | 9,192 | 13,766 | 98% | 4.0 |
| D | 3-3 | 3-3 | 9/21/2009 13:37 | 9/21/2009 13:47 | 10 | 0.75 | 0.86 | 1.42 | 727 | 7.5 | 163,340 | 9,085 | 13,607 | 99% | 3.5 |
| D | 4-1 | 4-1 | 9/18/2009 11:23 | 9/18/2009 11:34 | 11 | 1.00 | 1.16 | 1.85 | 585 | 4.0 | 44,351 | 9,116 | 13,634 | 98% | 3.8 |
| D | 4-2 | 4-2 | 9/18/2009 17:41 | 9/18/2009 17:51 | 10 | 1.00 | 1.19 | 1.80 | 590 | 4.0 | 16,238 | 9,091 | 13,596 | 98% | 3.4 |
| D | 4-3 | 4-3 | 9/21/2009 13:54 | 9/21/2009 14:04 | 10 | 0.99 | 1.11 | 1.87 | 612 | 6.0 | 797,199 | 9,126 | 13,652 | 99% | 3.5 |
| D | 5-3 | 5-1 | 9/21/2009 14:09 | 9/21/2009 14:19 | 10 | 1.10 | 1.25 | 2.07 | 567 | 5.5 | 86,603 | 9,117 | 13,630 | 98% | 3.3 |
| D | 6-1 | 6-1 | 9/18/2009 12:13 | 9/18/2009 12:23 | 10 | 1.20 | 1.39 | 2.23 | 514 | 2.0 | 31,169 | 9,090 | 13,580 | 97% | 3.3 |
| D | 7-1 | 7-1 | 9/18/2009 12:53 | 9/18/2009 13:16 | 23 | 1.30 | 1.52 | 2.41 | 483 | 2.0 | 150,948 | 9,063 | 13,532 | 98% | 2.3 |
| D | 5-2 | 7-2 | 9/18/2009 17:59 | 9/18/2009 18:09 | 10 | 1.30 | 1.54 | 2.37 | 494 | 2.0 | 15,696 | 9,085 | 13,563 | 96% | 4.0 |
| D | 6-3 | 8-1 | 9/21/2009 14:39 | 9/21/2009 14:49 | 10 | 1.60 | 1.79 | 3.02 | 433 | 3.0 | 15,222 | 9,063 | 13,514 | 94% | 4.0 |
| D | 7-3 | 9-1 | 9/21/2009 14:56 | 9/21/2009 15:07 | 11 | 1.80 | 2.01 | 3.41 | 394 | 1.5 | 6,229 | 9,031 | 13,455 | 87% | 2.9 |
| D | 8-3 | 10-1 | 9/21/2009 15:10 | 9/21/2009 15:15 | 5 | 2.01 | 2.29 | 3.83 | 361 | 1.5 | 2,329 | 9,016 | 13,411 | 80% | 3.5 |
| D | 9-3 | 10-2 | 9/21/2009 15:22 | 9/21/2009 15:30 | 8 | 2.00 | 2.27 | 3.81 | 360 | 1.5 | 1,052 | 9,002 | 13,397 | 78% | 3.8 |

Performance Test of a Steam-Assisted Elevated Flare
Marathon Petroleum Company, Texas City Main Flare

Table 5.1-7: Condition E Test Result Summary

| Condition E | | | | | | | | | | | | | | | |
|-------------|---------|---------|-----------------------|----------------------|-----|------|------|--------|-------|-------|---------|----------|-----------|------|-------------|
| Conditon | Old Run | New Run | PFTIR Start Date/Time | PFTIR Stop Date/Time | Min | S/VG | S/HC | S/S521 | FGCZ | Smoke | CO2p | CO2m Low | CO2m High | CE | Video Score |
| E | 1-1 | 1-1 | 9/18/2009 14:44 | 9/18/2009 14:54 | 10 | 0.19 | 0.20 | 0.34 | 1,506 | 9.5 | 479,315 | 9,312 | 13,986 | 99% | 4.0 |
| E | 1-2 | 1-2 | 9/21/2009 10:35 | 9/21/2009 10:45 | 10 | 0.17 | 0.18 | 0.31 | 1,581 | 9.0 | 6,704 | 9,345 | 14,036 | 98% | 1.5 |
| E | 1-3 | 1-3 | 9/21/2009 16:38 | 9/21/2009 16:48 | 10 | 0.19 | 0.20 | 0.35 | 1,520 | 9.0 | 6,747 | 9,307 | 13,979 | 100% | 3.0 |
| E | 2-1 | 2-1 | 9/18/2009 15:07 | 9/18/2009 15:17 | 10 | 0.57 | 0.61 | 1.00 | 921 | 6.0 | 39,546 | 9,244 | 13,858 | 99% | 3.8 |
| E | 2-2 | 2-2 | 9/21/2009 11:12 | 9/21/2009 11:22 | 10 | 0.56 | 0.57 | 1.00 | 968 | 6.0 | 7,255 | 9,253 | 13,873 | 98% | 1.5 |
| E | 2-3 | 2-3 | 9/21/2009 16:59 | 9/21/2009 17:09 | 10 | 0.56 | 0.57 | 1.01 | 968 | 5.5 | 7,418 | 9,231 | 13,842 | 99% | 3.3 |
| E | 3-1 | 3-1 | 9/18/2009 15:25 | 9/18/2009 15:36 | 11 | 1.00 | 1.05 | 1.76 | 639 | 2.5 | 33,938 | 9,203 | 13,768 | 99% | 3.8 |
| E | 3-2 | 3-2 | 9/21/2009 11:26 | 9/21/2009 11:36 | 10 | 1.00 | 1.01 | 1.79 | 668 | 2.5 | 10,181 | 9,221 | 13,796 | 98% | 2.3 |
| E | 3-3 | 3-3 | 9/21/2009 17:15 | 9/21/2009 17:25 | 10 | 1.00 | 1.00 | 1.80 | 673 | 3.0 | 20,139 | 9,209 | 13,779 | 98% | 3.0 |
| E | 4-1 | 4-1 | 9/18/2009 15:45 | 9/18/2009 15:56 | 11 | 1.10 | 1.16 | 1.94 | 594 | 1.5 | 25,265 | 9,211 | 13,771 | 98% | 3.8 |
| E | 4-2 | 4-2 | 9/21/2009 11:39 | 9/21/2009 11:49 | 10 | 1.10 | 1.10 | 1.97 | 627 | 2.0 | 8,697 | 9,218 | 13,787 | 97% | 2.3 |
| E | 4-3 | 4-3 | 9/21/2009 17:28 | 9/21/2009 17:38 | 10 | 1.10 | 1.11 | 1.96 | 630 | 2.0 | 11,770 | 9,201 | 13,761 | 98% | 3.0 |
| E | 6-2 | 5-1 | 9/21/2009 11:57 | 9/21/2009 12:07 | 10 | 1.20 | 1.22 | 2.16 | 582 | 0.0 | 7,317 | 9,203 | 13,755 | 97% | 3.3 |
| E | 5-3 | 5-2 | 9/21/2009 17:40 | 9/21/2009 17:50 | 10 | 1.20 | 1.22 | 2.15 | 590 | 1.5 | 9,833 | 9,159 | 13,691 | 98% | 3.3 |
| E | 6-3 | 6-1 | 9/21/2009 17:52 | 9/21/2009 18:02 | 10 | 1.30 | 1.32 | 2.33 | 554 | 1.5 | 7,386 | 9,172 | 13,703 | 96% | 2.9 |

Table 5.1-8: Condition F Test Result Summary

| Condition F | | | | | | | | | | | | | | | |
|-------------|---------|---------|-----------------------|----------------------|-----|------|------|--------|------|-------|-----------|----------|-----------|------|-------------|
| Conditon | Old Run | New Run | PFTIR Start Date/Time | PFTIR Stop Date/Time | Min | S/VG | S/HC | S/S521 | FGCZ | Smoke | CO2p | CO2m Low | CO2m High | CE | Video Score |
| F | 1-1 | 1-1 | 9/24/2009 15:43 | 9/24/2009 15:53 | 10 | 0.45 | 2.21 | 1.19 | 209 | 2.0 | 17,542 | 6,001 | 8,928 | 99% | 1.3 |
| F | 2-1 | 2-1 | 9/24/2009 16:10 | 9/24/2009 16:20 | 10 | 0.45 | 1.65 | 1.30 | 262 | 3.0 | 24,271 | 4,576 | 6,876 | 99% | 1.0 |
| F | 3-1 | 3-1 | 9/24/2009 16:30 | 9/24/2009 16:37 | 7 | 0.45 | 1.31 | 1.35 | 285 | 2.0 | 1,737,650 | 4,290 | 6,459 | 98% | 1.3 |
| F | 1-2 | 4-1 | 9/24/2009 16:53 | 9/24/2009 17:03 | 10 | 4.01 | 8.37 | 12.64 | 162 | 1.0 | 28,533 | 3,781 | 5,632 | 99% | 1.5 |
| F | 2-2 | 5-1 | 9/24/2009 17:13 | 9/24/2009 17:23 | 10 | 1.00 | 2.00 | 3.20 | 305 | 2.0 | 1,282,118 | 3,747 | 5,658 | 99% | 1.0 |
| F | 3-2 | 6-1 | 9/24/2009 17:26 | 9/24/2009 17:36 | 10 | 0.44 | 0.87 | 1.39 | 353 | 3.0 | 947,735 | 3,706 | 5,608 | 100% | 1.3 |

Table 5.1-9: Condition G Test Result Summary

| Condition G | | | | | | | | | | | | | | | |
|-------------|---------|---------|-----------------------|----------------------|-----|------|------|--------|------|-------|---------|----------|-----------|-----|-------------|
| Conditon | Old Run | New Run | PFTIR Start Date/Time | PFTIR Stop Date/Time | Min | S/VG | S/HC | S/S521 | FGCZ | Smoke | CO2p | CO2m Low | CO2m High | CE | Video Score |
| G | 1-1 | 1-1 | 9/24/2009 10:46 | 9/24/2009 10:58 | 24 | 0.56 | 1.52 | 1.29 | 300 | 2.0 | 37,120 | 7,964 | 11,867 | 97% | 1.4 |
| G | 2-1 | 2-1 | 9/24/2009 12:34 | 9/24/2009 12:44 | 10 | 0.54 | 1.59 | 1.29 | 283 | 1.0 | 106,006 | 7,638 | 11,383 | 99% | 1.4 |
| G | 3-1 | 3-1 | 9/24/2009 13:50 | 9/24/2009 14:00 | 10 | 0.56 | 2.88 | 1.32 | 170 | 1.0 | 9,515 | 7,377 | 10,888 | 89% | 1.6 |
| G | 4-1 | 4-1 | 9/24/2009 14:44 | 9/24/2009 14:54 | 10 | 0.52 | 2.92 | 1.21 | 160 | 1.0 | 10,375 | 7,438 | 10,959 | 89% | 1.6 |
| G | 5-1 | 5-1 | 9/24/2009 14:59 | 9/24/2009 15:09 | 10 | 0.60 | 3.46 | 1.42 | 149 | 1.0 | 8,734 | 7,387 | 10,863 | 86% | 1.9 |
| G | 6-1 | 6-1 | 9/24/2009 15:12 | 9/24/2009 15:22 | 10 | 0.70 | 4.09 | 1.65 | 137 | 1.0 | 8,748 | 7,369 | 10,810 | 82% | 1.6 |

Table 5.1-10: LTS Test Result Summary

| Long Term Stabiliy Test | | | | | | | | | | | | | | | |
|-------------------------|---------|---------|-----------------------|----------------------|-----|------|------|--------|--------|-------|-----------|----------|-----------|-----|-------------|
| Conditon | Old Run | New Run | PFTIR Start Date/Time | PFTIR Stop Date/Time | Min | S/VG | S/HC | S/S521 | FGCZ | Smoke | CO2p | CO2m Low | CO2m High | CE | Video Score |
| LTS | 1-1 | 1-1 | 9/15/2009 8:56 | 9/15/2009 9:20 | 24 | 0.83 | 1.14 | 1.58 | 541.12 | 6.0 | 17,106 | | | 99% | 3.3 |
| LTS | 2-1 | 2-1 | 9/16/2009 11:55 | 9/16/2009 12:05 | 10 | 1.00 | 1.31 | 2.41 | 431.61 | 5.5 | 37,973 | | | 99% | 4.0 |
| LTS | 2-2 | 2-2 | 9/16/2009 14:19 | 9/16/2009 14:29 | 10 | 1.00 | 1.34 | 2.42 | 422.94 | 4.5 | 16,019 | | | 99% | 3.8 |
| LTS | 2-3 | 2-3 | 9/16/2009 17:01 | 9/16/2009 17:12 | 11 | 1.00 | 1.33 | 2.42 | 425.47 | 4.0 | 17,600 | | | 99% | 3.8 |
| LTS | 2-4 | 2-4 | 9/17/2009 8:38 | 9/16/2009 8:50 | 12 | 1.01 | 1.98 | 2.44 | 320.86 | 4.0 | 11,336 | | | 99% | 3.8 |
| LTS | 2-5 | 2-5 | 9/18/2009 8:54 | 9/18/2009 9:05 | 11 | 1.00 | 1.31 | 2.43 | 427.59 | 3.0 | 13,587 | | | 99% | 4.0 |
| LTS | 2-6 | 2-6 | 9/21/2009 8:46 | 9/21/2009 8:57 | 11 | 1.00 | 1.36 | 2.45 | 413.94 | 3.0 | 8,896 | | | 97% | 4.0 |
| LTS | 2-7 | 2-7 | 9/22/2009 17:04 | 9/22/2009 17:10 | 6 | 1.01 | 1.25 | 2.44 | 457.66 | 4.0 | 17,311 | | | 97% | 2.0 |
| LTS | 2-8 | 2-8 | 9/23/2009 10:48 | 9/23/2009 10:58 | 10 | 0.99 | 1.29 | 2.38 | 436.12 | 3.5 | 1,671,635 | | | 99% | 2.4 |

5.2 Test Condition A19

The purpose of the Condition A tests is to simulate plant normal base load -- this is the typical flow condition for the flare and represents day-to-day operation. Actual testing for this condition was conducted at three vent gas mass flow rates: 1,900 lb/hr, 1,100 lb/hr, and 800 lb/hr. This section addresses testing conducted at 1,900 lb/hr. This condition (along with Condition A11) represents typical historic vent gas flow rates.

5.2.1 Process Conditions

The values of several key flare operating parameters are shown in Figures 5.2-1 and 5.2-2 below.

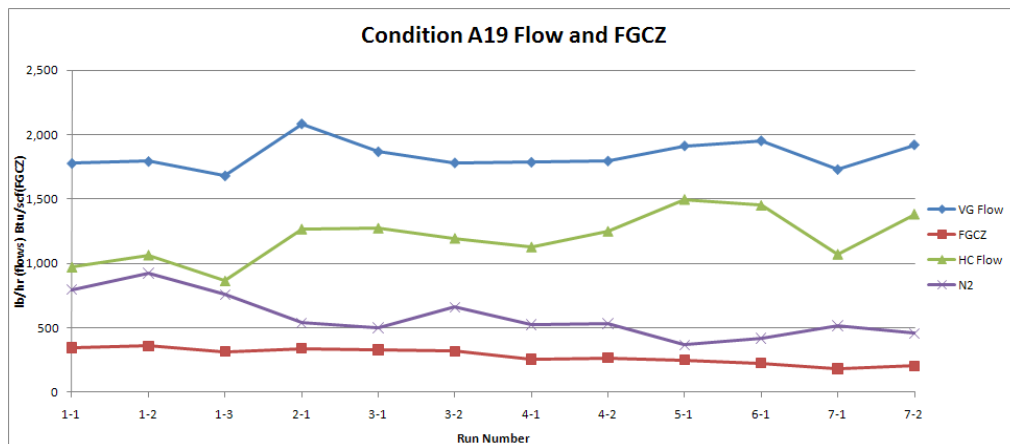


Figure 5.2-1: Condition A19 Flow and CZG Heat Content

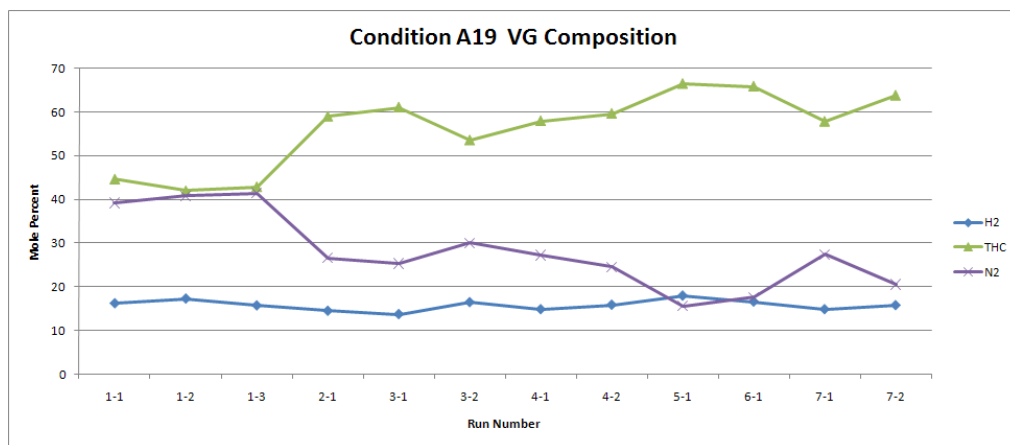


Figure 5.2-2: Condition A19 Vent Gas Composition

5.2.2 Steam Ratios

The Steam to Vent Gas (S/VG) and Steam to Hydrocarbon (S/HC) ratios corresponding to each test condition are shown in Table 5.2-1. Values are rounded to the nearest 0.5.

Table 5.2-1: Condition A19 Steam Ratios

| Test | S/VG | S/HC |
|------|------|------|
| 1 | 1.00 | 1.80 |
| 2 | 1.25 | 2.05 |
| 3 | 1.50 | 2.25 |
| 4 | 2.00 | 3.00 |
| 5 | 2.50 | 3.20 |
| 6 | 2.70 | 3.60 |
| 7 | 3.00 | 4.50 |

5.2.3 Wind Conditions

The direction and speed of the wind can have a significant impact on the quality of data collected by the PFTIR. See Section 3.3.2 for a further discussion of wind effects. Figure 5.2-3 shows wind direction and speed during this Test Condition. The area within the blue 60 deg angle triggers the wind flagging algorithm as described in Section 3.3.2.

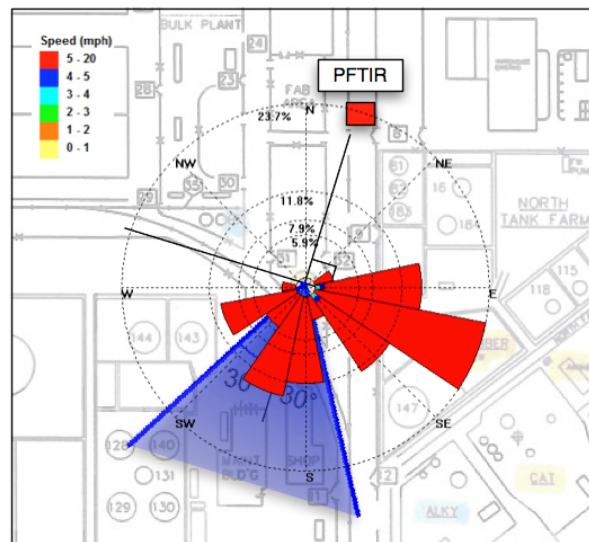


Figure 5.2-3: Condition A19. Wind Speed and Direction during Test

Performance Test of a Steam-Assisted Elevated Flare
Marathon Petroleum Company, Texas City Main Flare

5.2.4 Results

| Run ID | | | | Measured | | Calculated | | | | Vent Gas | | | | | | | | Steam | | | Ratios | | | | | Wind | Vent Gas Composition | | | | |
|-----------|---------|---------|-----|----------|-------|------------|-------|------|------|--------------------|-------|---------|---------|--------------------|----------|----------|-------------|----------|------------|------------|---------------|-------------|-------------|--------------|--------------|--------|----------------------|-------|-------|-------|-------------------|
| Condition | New Run | Old Run | | CO2 | CO | CO2/CO | THCw | CE | DRE | Vent Gas Flow Rate | | N2 Flow | HC Flow | Flare Tip Velocity | MWvg | MWhc | Vent Gas HV | FGCZ NHV | Steam Flow | Steam Temp | API 521 Steam | Actual S/VG | Actual S/HC | API 521 S/VG | API 521 S/HC | S/S521 | Wind Speed | THC | H2 | N2 | Visible Emissions |
| | | | | ppm-m | ppm-m | | ppm-m | % | % | SCFH | lb/hr | lb/hr | lb/hr | ft/s | lb/lbmol | lb/lbmol | Btu/scf | Btu/scf | lb/hr | °F | lb/hr | lb/lb | lb/lb | lb/lb | lb/lb | lb/lb | mph | mol% | mol% | mol % | |
| A19 | 1-1 | 1-1 | Avg | 9,455 | 24 | 407 | 182 | 0.98 | 0.98 | 28,857 | 1,778 | 796 | 971 | 2.72 | 22 | 29 | 746 | 346 | 1,668 | 413 | 758 | 0.94 | 1.73 | 0.42 | 0.47 | 2.23 | 9 | 44.61 | 16.20 | 39 | 6.0 |
| A19 | 1-2 | 1-2 | Avg | 336,831 | 1,158 | 503 | 2,169 | 0.99 | 0.99 | 30,063 | 1,793 | 924 | 1,065 | 2.83 | 22 | 33 | 793 | 360 | 1,756 | 413 | 767 | 0.97 | 1.65 | 0.43 | 0.49 | 2.29 | 10 | 41.94 | 17.28 | 41 | 5.5 |
| A19 | 1-3 | 1-3 | Avg | 31,076 | 632 | 515 | 281 | 0.98 | 0.99 | 26,152 | 1,683 | 758 | 864 | 2.46 | 23 | 30 | 747 | 316 | 1,796 | 413 | 728 | 1.07 | 2.08 | 0.43 | 0.47 | 2.47 | 10 | 43 | 16 | 41 | 6.0 |
| A19 | 2-1 | 2-1 | Avg | 8,028 | 27 | 316 | 165 | 0.98 | 0.98 | 29,641 | 2,081 | 540 | 1,268 | 2.79 | 25 | 28 | 920 | 340 | 2,576 | 413 | 915 | 1.25 | 2.06 | 0.44 | 0.46 | 2.81 | 11 | 58.94 | 14.46 | 27 | 6.0 |
| A19 | 3-1 | 3-1 | Avg | 6,914 | 33 | 250 | 203 | 0.96 | 0.97 | 28,710 | 1,867 | 500 | 1,275 | 2.70 | 23 | 28 | 972 | 331 | 2,811 | 413 | 808 | 1.51 | 2.22 | 0.43 | 0.46 | 3.51 | 9 | 61.02 | 13.69 | 25 | 5.5 |
| A19 | 3-2 | 2-2 | Avg | 31,645 | 93 | 332 | 422 | 0.98 | 0.99 | 30,234 | 1,782 | 661 | 1,196 | 2.85 | 22 | 29 | 889 | 318 | 2,661 | 413 | 754 | 1.49 | 2.24 | 0.42 | 0.47 | 3.54 | 8 | 53.52 | 16.45 | 30 | 5.5 |
| A19 | 4-1 | 4-1 | Avg | 4,679 | 32 | 167 | 273 | 0.94 | 0.95 | 28,453 | 1,787 | 526 | 1,128 | 2.68 | 23 | 26 | 897 | 257 | 3,565 | 413 | 762 | 2.01 | 3.16 | 0.43 | 0.45 | 4.71 | 9 | 57.93 | 14.84 | 27 | 1.5 |
| A19 | 4-2 | 3-2 | Avg | 227,849 | 185 | 2,534 | 1,386 | 0.93 | 0.99 | 28,966 | 1,796 | 534 | 1,250 | 2.73 | 22 | 28 | 929 | 268 | 3,588 | 413 | 756 | 2.01 | 2.87 | 0.43 | 0.46 | 4.72 | 12 | 59.59 | 15.85 | 25 | 2.0 |
| A19 | 5-1 | 5-2 | Avg | 8,859 | 94 | 85 | 1,019 | 0.84 | 0.90 | 34,134 | 1,912 | 367 | 1,499 | 3.22 | 21 | 26 | 974 | 252 | 4,799 | 413 | 790 | 2.51 | 3.20 | 0.41 | 0.45 | 6.08 | 12 | 66.39 | 17.97 | 16 | 1.0 |
| A19 | 6-1 | 6-2 | Avg | 9,044 | 101 | 89 | 1,258 | 0.86 | 0.88 | 34,513 | 1,951 | 418 | 1,452 | 3.25 | 21 | 25 | 930 | 227 | 5,255 | 413 | 813 | 2.69 | 3.62 | 0.42 | 0.44 | 6.48 | 10 | 65.81 | 16.59 | 18 | 1.5 |
| A19 | 7-1 | 5-1 | Avg | 5,391 | 60 | 93 | 556 | 0.90 | 0.91 | 27,641 | 1,731 | 516 | 1,072 | 2.60 | 22 | 26 | 858 | 183 | 5,197 | 413 | 730 | 3.00 | 4.85 | 0.42 | 0.45 | 7.08 | 9 | 57.78 | 14.83 | 27 | 1.0 |
| A19 | 7-2 | 7-2 | Avg | 6,363 | 75 | 85 | 1,356 | 0.82 | 0.83 | 33,711 | 1,921 | 458 | 1,384 | 3.18 | 21 | 25 | 905 | 204 | 5,706 | 413 | 799 | 2.98 | 4.12 | 0.42 | 0.44 | 7.10 | 8 | 63.73 | 15.76 | 21 | 1.0 |

5.3 Test Condition A11

The purpose of the Condition A tests is to simulate plant normal base load -- this is the typical flow condition for the flare and represents day-to-day operation. Actual testing for this condition was conducted at three vent gas mass flow rates: 1,900 lb/hr, 1,100 lb/hr and 800 lb/hr. This section addresses testing conducted at 1,100 lb/hr. This condition (along with Condition A19) represents typical historic vent gas flow rates.

5.3.1 Process Conditions

The values of several key flare operating parameters are shown in Figures 5.3-1 and 5.3-2 below. The data presented are the run averages.

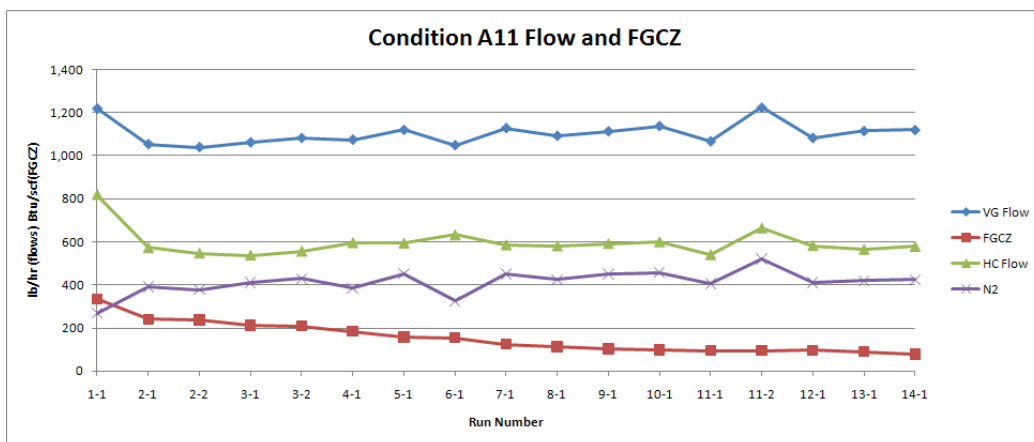


Figure 5.3-1: Condition A11 Flow and CZG Heat Content

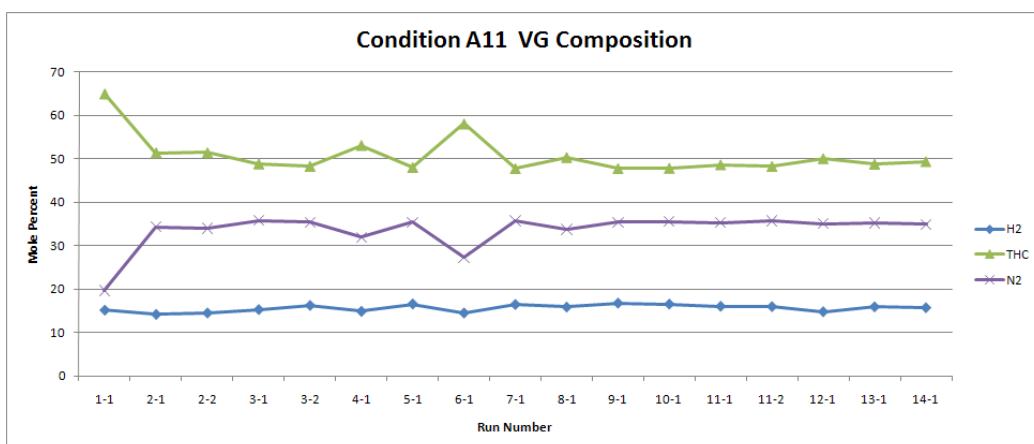


Figure 5.3-2: Condition A11 Vent Gas Composition

5.3.2 Steam Ratios

The Steam to Vent Gas (S/VG) and Steam to Hydrocarbon (S/HC) ratios corresponding to each test condition are shown in Table 5.3-1. Values are rounded to the nearest 0.5.

Table 5.3-1: Condition A11 Steam Ratios

| Test | S/VG | S/HC |
|------|------|-------|
| 1 | 1.35 | 2.00 |
| 2 | 1.80 | 3.35 |
| 3 | 2.00 | 3.95 |
| 4 | 2.50 | 4.55 |
| 5 | 3.00 | 5.65 |
| 6 | 3.50 | 5.80 |
| 7 | 4.00 | 7.70 |
| 8 | 4.50 | 8.45 |
| 9 | 5.00 | 9.50 |
| 10 | 5.25 | 10.05 |
| 11 | 5.40 | 10.55 |
| 12 | 5.75 | 10.80 |
| 13 | 6.00 | 11.85 |
| 14 | 6.95 | 13.50 |

5.3.3 Wind Conditions

The direction and speed of the wind can have a significant impact on the quality of data collected by the PFTIR. See Section 3.3.2 for a further discussion of wind effects.

Figure 5.3-3 shows wind direction and speed during this Test Condition. The area within the blue 60 deg angle triggers the wind flagging algorithm as described in Section 3.3.2.

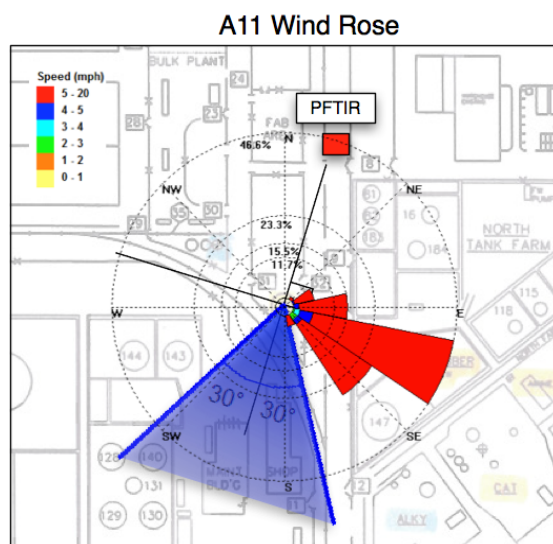


Figure 5.3-3: Condition A11. Wind Speed and Direction during Test

Performance Test of a Steam-Assisted Elevated Flare
Marathon Petroleum Company, Texas City Main Flare

5.3.4 Results

| Run ID | | | | Measured | | Calculated | | | | Vent Gas | | | | | | | | Steam | | | Ratios | | | | | | Wind | Vent Gas Composition | | | |
|-----------|---------|---------|-----|----------|-------|------------|-------|------|------|--------------------|-------|---------|---------|--------------------|----------|----------|-------------|----------|------------|------------|---------------|-------------|-------------|--------------|--------------|--------|------------|----------------------|-------|-------|-------------------|
| Condition | New Run | Old Run | | CO2 | CO | CO2/CO | THCw | CE | DRE | Vent Gas Flow Rate | | N2 Flow | HC Flow | Flare Tip Velocity | MWvg | MWhc | Vent Gas HV | FGCZ NHV | Steam Flow | Steam Temp | API 521 Steam | Actual S/VG | Actual S/HC | API 521 S/VG | API 521 S/HC | S/S521 | Wind Speed | THC | H2 | N2 | Visible Emissions |
| | | | | ppm-m | ppm-m | | ppm-m | % | % | SCFH | lb/hr | lb/hr | lb/hr | ft/s | lb/lbmol | lb/lbmol | Btu/scf | Btu/scf | lb/hr | °F | lb/hr | lb/lb | lb/lb | lb/lb | lb/lb | lb/lb | mph | mol% | mol% | mol % | |
| A11 | 1-1 | 1-2 | Avg | 8,925 | 26 | 343 | 87 | 0.99 | 0.99 | 21,255 | 1,220 | 270 | 821 | 2.00 | 21 | 23 | 852 | 336 | 1,632 | 413 | 506 | 1.34 | 1.99 | 0.42 | 0.43 | 3.22 | 10 | 65.10 | 15.18 | 20 | 5.5 |
| A11 | 2-1 | 1-1 | Avg | 3,193 | 18 | 200 | 119 | 0.96 | 0.96 | 16,835 | 1,053 | 392 | 573 | 1.59 | 22 | 26 | 751 | 240 | 1,885 | 413 | 447 | 1.79 | 3.31 | 0.42 | 0.45 | 4.25 | 8 | 51.43 | 14.21 | 34 | 2.0 |
| A11 | 2-2 | 2-1 | Avg | 5,889 | 28 | 217 | 127 | 0.97 | 0.98 | 16,423 | 1,039 | 378 | 548 | 1.55 | 22 | 25 | 735 | 237 | 1,825 | 413 | 440 | 1.76 | 3.34 | 0.42 | 0.44 | 4.16 | 10 | 51.44 | 14.54 | 34 | 2.0 |
| A11 | 3-1 | 3-1 | Avg | 8,448 | 51 | 166 | 245 | 0.97 | 0.97 | 16,571 | 1,062 | 411 | 538 | 1.56 | 22 | 26 | 720 | 213 | 2,121 | 413 | 453 | 2.01 | 3.95 | 0.42 | 0.45 | 4.75 | 7 | 48.86 | 15.31 | 36 | 2.0 |
| A11 | 3-2 | 5-2 | Avg | 6,902 | 32 | 219 | 183 | 0.98 | 0.97 | 17,116 | 1,082 | 429 | 556 | 1.61 | 22 | 26 | 720 | 209 | 2,193 | 413 | 460 | 2.04 | 3.95 | 0.42 | 0.45 | 4.80 | 8 | 48.31 | 16.26 | 35 | 1.5 |
| A11 | 4-1 | 3-2 | Avg | 5,206 | 40 | 137 | 205 | 0.96 | 0.96 | 17,635 | 1,074 | 384 | 596 | 1.66 | 22 | 25 | 737 | 185 | 2,707 | 413 | 452 | 2.50 | 4.55 | 0.42 | 0.44 | 5.94 | 9 | 53.15 | 14.91 | 32 | 1.5 |
| A11 | 5-1 | 7-2 | Avg | 3,865 | 28 | 145 | 227 | 0.94 | 0.94 | 18,058 | 1,120 | 453 | 594 | 1.70 | 22 | 26 | 727 | 157 | 3,344 | 413 | 476 | 2.99 | 5.64 | 0.42 | 0.45 | 7.08 | 6 | 48.02 | 16.59 | 35 | 1.0 |
| A11 | 6-1 | 2-2 | Avg | 4,420 | 45 | 101 | 307 | 0.93 | 0.94 | 17,757 | 1,048 | 325 | 633 | 1.67 | 21 | 24 | 780 | 154 | 3,678 | 413 | 434 | 3.52 | 5.82 | 0.42 | 0.43 | 8.43 | 7 | 58.12 | 14.54 | 27 | 1.0 |
| A11 | 7-1 | 6-2 | Avg | 3,367 | 39 | 86 | 433 | 0.87 | 0.89 | 17,974 | 1,129 | 452 | 586 | 1.69 | 22 | 26 | 726 | 125 | 4,498 | 413 | 480 | 4.01 | 7.70 | 0.42 | 0.45 | 9.48 | 7 | 47.75 | 16.47 | 36 | 1.0 |
| A11 | 8-1 | 4-2 | Avg | 3,255 | 773 | 76 | 4,358 | 0.81 | 0.48 | 17,601 | 1,092 | 425 | 580 | 1.66 | 22 | 25 | 721 | 113 | 4,903 | 413 | 459 | 4.50 | 8.46 | 0.42 | 0.44 | 10.64 | 7 | 50.33 | 15.87 | 34 | 1.0 |
| A11 | 9-1 | 8-2 | Avg | 1,986 | 31 | 64 | 603 | 0.74 | 0.77 | 17,995 | 1,113 | 451 | 592 | 1.70 | 22 | 27 | 731 | 102 | 5,613 | 413 | 474 | 5.00 | 9.50 | 0.42 | 0.45 | 11.78 | 6 | 47.79 | 16.76 | 35 | 1.0 |
| A11 | 10-1 | 9-2 | Avg | 2,008 | 28 | 72 | 553 | 0.77 | 0.79 | 18,213 | 1,138 | 457 | 600 | 1.72 | 22 | 27 | 731 | 99 | 6,002 | 413 | 482 | 5.26 | 10.04 | 0.42 | 0.45 | 12.41 | 4 | 47.82 | 16.56 | 36 | 1.0 |
| A11 | 11-1 | 10-2 | Avg | 1,541 | 26 | 59 | 598 | 0.68 | 0.72 | 16,272 | 1,066 | 407 | 540 | 1.53 | 22 | 26 | 731 | 95 | 5,904 | 413 | 453 | 5.51 | 10.96 | 0.42 | 0.45 | 12.98 | 7 | 48.62 | 16.06 | 35 | 1.0 |
| A11 | 11-2 | 11-2 | Avg | 1,254 | 18 | 75 | 545 | 0.66 | 0.70 | 20,434 | 1,224 | 521 | 664 | 1.93 | 22 | 26 | 714 | 96 | 6,560 | 413 | 524 | 5.32 | 10.12 | 0.42 | 0.45 | 12.75 | 6 | 48.27 | 15.98 | 36 | 1.0 |
| A11 | 12-1 | 12-2 | Avg | 1,064 | 22 | 42 | 534 | 0.62 | 0.67 | 17,047 | 1,082 | 411 | 582 | 1.61 | 22 | 26 | 767 | 96 | 6,287 | 413 | 459 | 5.76 | 10.82 | 0.42 | 0.45 | 13.65 | 6 | 50.07 | 14.83 | 35 | 1.0 |
| A11 | 13-1 | 13-2 | Avg | 901 | 13 | 62 | 475 | 0.62 | 0.66 | 17,458 | 1,115 | 420 | 565 | 1.64 | 22 | 26 | 744 | 90 | 6,681 | 413 | 471 | 6.01 | 11.85 | 0.42 | 0.45 | 14.15 | 8 | 48.80 | 15.94 | 35 | 1.0 |
| A11 | 14-1 | 14-2 | Avg | 0 | 11 | 0 | 538 | 0.00 | 0.02 | 17,295 | 1,119 | 425 | 578 | 1.63 | 22 | 26 | 742 | 79 | 7,774 | 413 | 474 | 6.96 | 13.48 | 0.42 | 0.45 | 16.34 | 8 | 49.37 | 15.73 | 35 | 1.0 |

5.4 Test Condition A8

A8 was achieved by minimizing normal refinery fuel gas sweep flow for the sole purpose of achieving low heating value conditions suitable for Test G. Analysis of this region is not representative of normal operating conditions of the Texas City main flare. Data are presented here for informational purposes only. In addition, the test data for this condition were compromised by adverse wind conditions. Therefore, data from this test condition is not considered valid and reliable conclusions regarding combustion efficiency cannot be made.

5.4.1 Process Conditions

The values of several key flare operating parameters are shown in Figures 5.4-1 and 5.4-2 below.

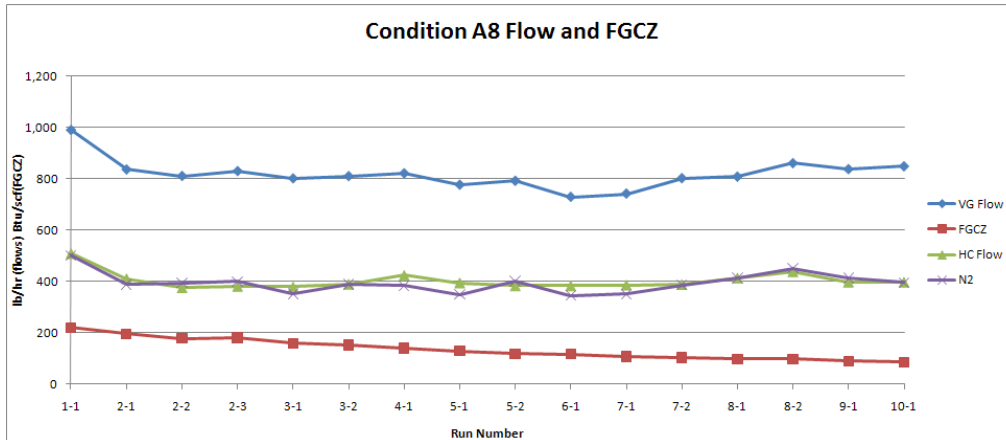


Figure 5.4-1: Condition A8 Flow and CZG Heat Content

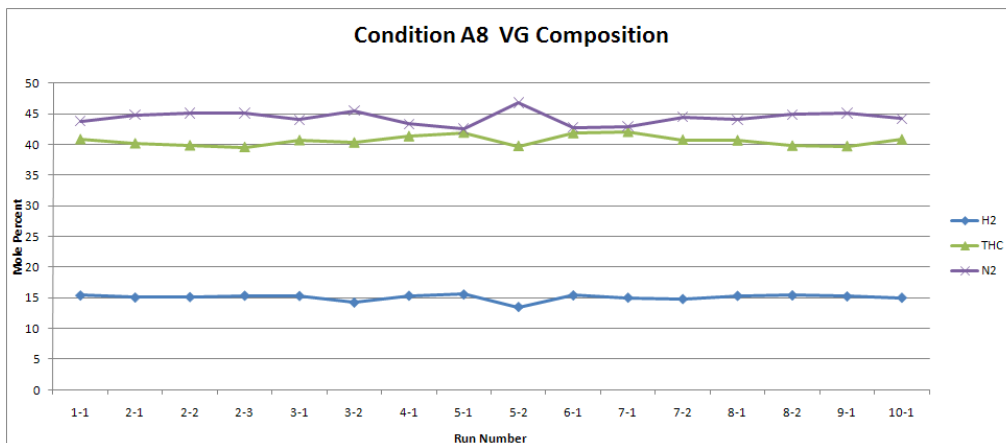


Figure 5.4-2: Condition A8 Vent Gas Composition

5.4.2 Steam Ratios

The Steam to Vent Gas (S/VG) and Steam to Hydrocarbon (S/HC) ratios corresponding to each test condition are shown in Table 5.4-1. Values are rounded to the nearest 0.5.

Table 5.4-1: Condition A8 Steam Ratios

| Test | S/VG | S/HC |
|------|------|-------|
| 1 | 1.85 | 3.55 |
| 2 | 2.20 | 4.65 |
| 3 | 3.00 | 6.30 |
| 4 | 3.55 | 7.00 |
| 5 | 4.00 | 8.10 |
| 6 | 4.50 | 8.60 |
| 7 | 4.90 | 9.80 |
| 8 | 5.05 | 9.90 |
| 9 | 5.45 | 11.65 |
| 10 | 5.70 | 12.15 |

5.4.3 Wind Conditions

The direction and speed of the wind can have a significant impact on the quality of data collected by the PFTIR. See Section 3.3.2 for a further discussion of wind effects.

Figure 5.4-3 shows wind direction and speed during this Test Condition. The area within the blue 60 deg angle triggers the wind flagging algorithm as described in Section 3.3.2.

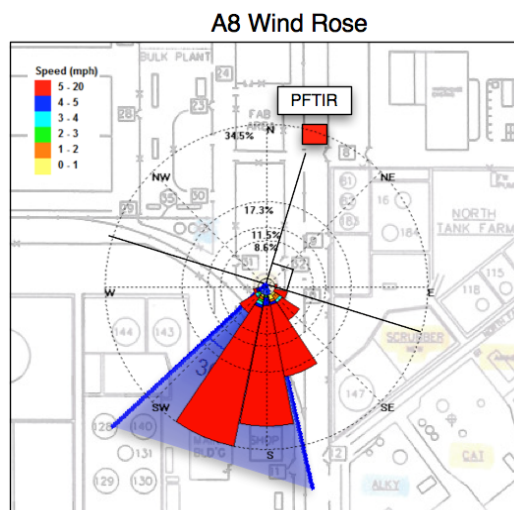


Figure 5.4-3: Condition A8. Wind Speed and Direction During Test

Performance Test of a Steam-Assisted Elevated Flare
Marathon Petroleum Company, Texas City Main Flare

5.4.4 Results

| Run ID | | | | Measured | | | Calculated | | | Vent Gas | | | | | | | | Steam | | | Ratios | | | | | Wind | Vent Gas Composition | | | | |
|-----------|---------|---------|-----|----------|-------|--------|------------|------|------|--------------------|-------|---------|---------|--------------------|----------|----------|-------------|----------|------------|------------|---------------|-------------|-------------|--------------|--------------|--------|----------------------|-------|-------|-------|-------------------|
| Condition | New Run | Old Run | | CO2 | CO | CO2/CO | THCw | CE | DRE | Vent Gas Flow Rate | | N2 Flow | HC Flow | Flare Tip Velocity | MWvg | MWhc | Vent Gas HV | FGCZ NHV | Steam Flow | Steam Temp | API 521 Steam | Actual S/VG | Actual S/HC | API 521 S/VG | API 521 S/HC | S/S521 | Wind Speed | THC | H2 | N2 | Visible Emissions |
| | | | | ppm-m | ppm-m | | ppm-m | % | % | SCFH | lb/hr | lb/hr | lb/hr | ft/s | lb/lbmol | lb/lbmol | Btu/scf | Btu/scf | lb/hr | °F | lb/hr | lb/lb | lb/lb | lb/lb | lb/lb | lb/lb | mph | mol% | mol% | mol % | |
| A8 | 1-1 | 1-4 | Avg | 1,112 | 20 | 37 | 395 | 0.65 | 0.74 | 15,407 | 991 | 502 | 509 | 1.45 | 23 | 31 | 730 | 220 | 1,803 | 413 | 428 | 1.83 | 3.55 | 0.43 | 0.48 | 4.26 | 11 | 40.82 | 15.39 | 44 | 1.0 |
| A8 | 2-1 | 1-3 | Avg | 24,465 | 113 | 243 | 612 | 0.97 | 0.98 | 12,025 | 836 | 388 | 411 | 1.13 | 24 | 33 | 747 | 196 | 1,834 | 413 | 367 | 2.18 | 4.48 | 0.43 | 0.50 | 5.05 | 6 | 40.13 | 15.05 | 45 | 1.5 |
| A8 | 2-2 | 1-5 | Avg | 4,715 | 46 | 106 | 694 | 0.86 | 0.87 | 12,181 | 810 | 395 | 375 | 1.12 | 24 | 30 | 680 | 178 | 1,788 | 413 | 357 | 2.19 | 4.78 | 0.43 | 0.48 | 5.06 | 10 | 39.81 | 15.12 | 45 | 1.0 |
| A8 | 2-3 | 2-5 | Avg | 5,930 | 58 | 102 | 839 | 0.86 | 0.88 | 12,352 | 829 | 400 | 381 | 1.16 | 24 | 30 | 682 | 181 | 1,792 | 413 | 360 | 2.18 | 4.74 | 0.43 | 0.48 | 5.02 | 11 | 39.54 | 15.35 | 45 | 1.0 |
| A8 | 3-1 | 2-3 | Avg | 3,827 | 65 | 56 | 1,614 | 0.64 | 0.71 | 10,994 | 801 | 352 | 379 | 1.04 | 24 | 33 | 768 | 159 | 2,410 | 413 | 348 | 3.00 | 6.41 | 0.43 | 0.49 | 6.95 | 2 | 40.66 | 15.31 | 44 | 1.0 |
| A8 | 3-2 | 2-4 | Avg | 5,842 | 55 | 41 | 846 | 0.74 | 0.87 | 11,756 | 809 | 388 | 389 | 1.11 | 24 | 32 | 733 | 152 | 2,415 | 413 | 350 | 3.01 | 6.23 | 0.43 | 0.49 | 6.94 | 8 | 40.29 | 14.21 | 46 | 1.0 |
| A8 | 4-1 | 3-3 | Avg | 2,685 | 52 | 42 | 1,178 | 0.60 | 0.70 | 12,100 | 821 | 383 | 424 | 1.14 | 24 | 33 | 778 | 140 | 2,944 | 413 | 355 | 3.57 | 6.99 | 0.43 | 0.49 | 8.26 | 7 | 41.32 | 15.34 | 43 | 1.0 |
| A8 | 5-1 | 4-3 | Avg | 2,603 | 75 | 31 | 1,036 | 0.64 | 0.72 | 11,185 | 776 | 350 | 394 | 1.05 | 23 | 32 | 785 | 129 | 3,109 | 413 | 338 | 3.99 | 7.94 | 0.43 | 0.49 | 9.24 | 9 | 41.92 | 15.56 | 43 | 1.0 |
| A8 | 5-2 | 3-4 | Avg | 1,353 | 47 | 30 | 952 | 0.52 | 0.60 | 11,829 | 791 | 401 | 383 | 1.11 | 23 | 31 | 713 | 118 | 3,163 | 413 | 342 | 4.00 | 8.29 | 0.43 | 0.49 | 9.25 | 7 | 39.72 | 13.47 | 47 | 1.0 |
| A8 | 6-1 | 5-3 | Avg | 3,569 | 73 | 32 | 1,091 | 0.64 | 0.77 | 10,950 | 728 | 345 | 383 | 1.03 | 23 | 32 | 777 | 117 | 3,245 | 413 | 318 | 4.50 | 8.58 | 0.43 | 0.49 | 10.41 | 12 | 41.81 | 15.41 | 43 | 1.0 |
| A8 | 7-1 | 6-3 | Avg | 2,249 | 53 | 24 | 650 | 0.64 | 0.78 | 11,152 | 741 | 351 | 386 | 1.05 | 23 | 32 | 772 | 108 | 3,627 | 413 | 321 | 4.89 | 9.46 | 0.43 | 0.49 | 11.27 | 10 | 42.03 | 15.02 | 43 | 1.0 |
| A8 | 7-2 | 4-4 | Avg | 0 | 20 | 0 | 796 | 0 | 0 | 11,768 | 801 | 386 | 388 | 1.11 | 23 | 31 | 733 | 103 | 3,926 | 413 | 344 | 4.90 | 10.16 | 0.43 | 0.48 | 11.42 | 7 | 40.74 | 14.79 | 44 | 1.0 |
| A8 | 8-1 | 5-4 | Avg | 2,333 | 44 | 37 | 768 | 0.68 | 0.76 | 12,703 | 807 | 414 | 414 | 1.20 | 23 | 31 | 720 | 98 | 4,098 | 413 | 347 | 5.06 | 9.94 | 0.43 | 0.48 | 11.81 | 7 | 40.64 | 15.32 | 44 | 1.0 |
| A8 | 8-2 | 6-4 | Avg | 5,658 | 85 | 52 | 1,231 | 0.75 | 0.82 | 13,693 | 860 | 451 | 438 | 1.29 | 23 | 31 | 707 | 98 | 4,301 | 413 | 367 | 5.03 | 9.87 | 0.43 | 0.48 | 11.74 | 7 | 39.75 | 15.41 | 45 | 1.0 |
| A8 | 9-1 | 7-4 | Avg | 508,784 | 28 | 97 | 877 | 0.67 | 1.00 | 12,423 | 837 | 414 | 398 | 1.17 | 23 | 31 | 718 | 90 | 4,609 | 413 | 364 | 5.47 | 11.63 | 0.43 | 0.48 | 12.70 | 12 | 39.68 | 15.24 | 45 | 1.0 |
| A8 | 10-1 | 8-4 | Avg | 955 | 18 | 37 | 621 | 0.48 | 0.61 | 11,949 | 848 | 396 | 397 | 1.13 | 24 | 31 | 721 | 86 | 4,822 | 413 | 369 | 5.68 | 12.16 | 0.44 | 0.49 | 13.05 | 10 | 40.79 | 15.01 | 44 | 1.0 |

5.5 Test Condition B

To demonstrate flare performance with a higher flow rate of hydrocarbons by adding gas (refinery fuel gas) that has a low S/VG ratio for smokeless operation.

5.5.1 Process Conditions

The values of several key flare operating parameters are shown in Figures 5.5-1 and 5.5-2 below.

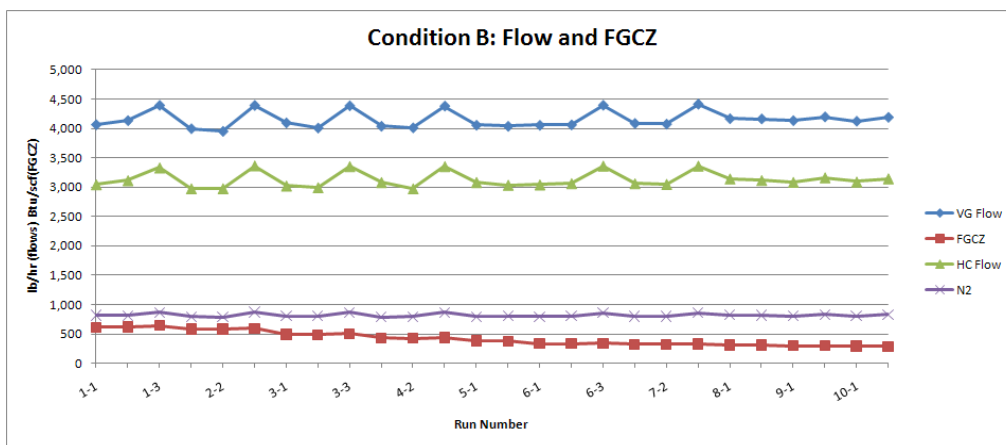


Figure 5.5-1: Condition B Flow and CZG Heat Content

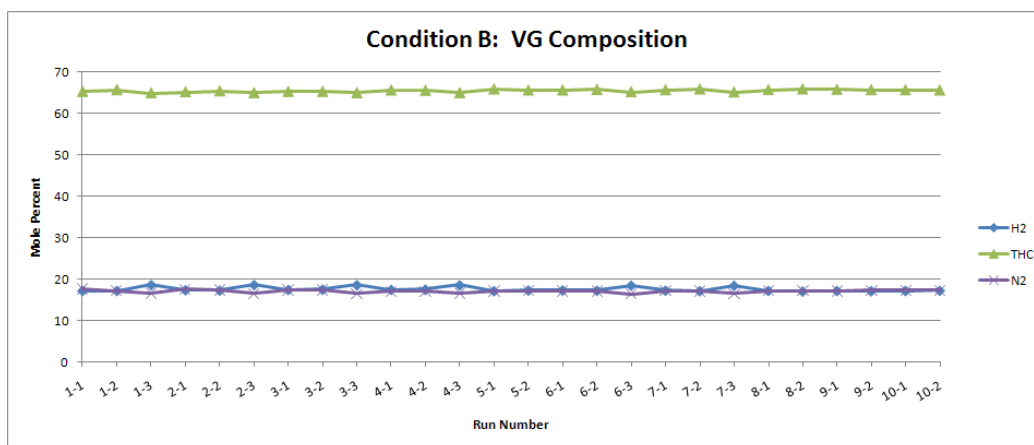


Figure 5.5-2: Condition B Vent Gas Composition

5.5.2 Steam Ratios

The Steam to Vent Gas (S/VG) and Steam to Hydrocarbon (S/HC) ratios corresponding to each test condition are shown in Table 5.5-1. Values are rounded to the nearest 0.5.

Table 5.5-1: Condition B Steam Ratios

| Test | S/VG | S/HC |
|------|------|------|
| 1 | 0.40 | 0.55 |
| 2 | 0.50 | 0.65 |
| 3 | 0.75 | 1.00 |
| 4 | 1.00 | 1.30 |
| 5 | 1.25 | 1.65 |
| 6 | 1.50 | 2.00 |
| 7 | 1.60 | 2.10 |
| 8 | 1.70 | 2.25 |
| 9 | 1.80 | 2.40 |
| 10 | 1.90 | 2.50 |

5.5.3 Wind Conditions

The direction and speed of the wind can have a significant impact on the quality of data collected by the PFTIR. See Section 3.3.2 for a further discussion of wind effects.

Figure 5.5-3 shows wind direction and speed during this Test Condition. The area within the blue 60 deg angle triggers the wind flagging algorithm as described in Section 3.3.2.

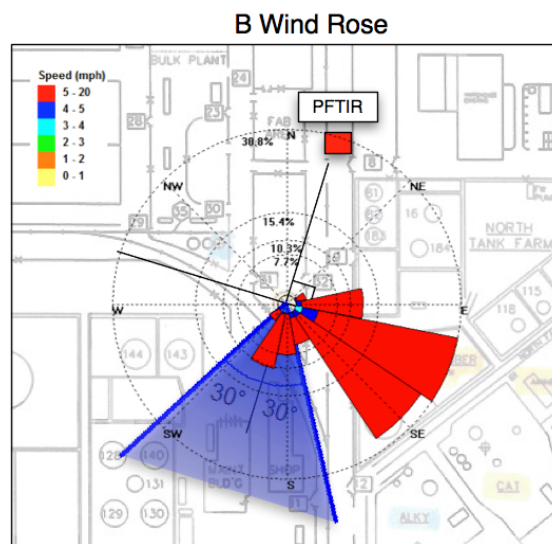


Figure 5.5-3: Condition B. Wind Speed and Direction During Test

Performance Test of a Steam-Assisted Elevated Flare
Marathon Petroleum Company, Texas City Main Flare

5.5.4 Results

| Run ID | | | | Measured | | Calculated | | | | Vent Gas | | | | | | | | Steam | | Ratios | | | | | Wind | Vent Gas Composition | | | | | |
|-----------|---------|---------|-----|-----------|-------|------------|-------|------|------|--------------------|-------|---------|---------|--------------------|----------|----------|-------------|----------|------------|------------|---------------|-------------|-------------|--------------|--------------|----------------------|------------|------|------|-------|-------------------|
| Condition | New Run | Old Run | | CO2 | CO | CO2/CO | THCw | CE | DRE | Vent Gas Flow Rate | | N2 Flow | HC Flow | Flare Tip Velocity | MWvg | MWhc | Vent Gas HV | FGCZ NHV | Steam Flow | Steam Temp | API 521 Steam | Actual S/VG | Actual S/HC | API 521 S/VG | API 521 S/HC | S/S521 | Wind Speed | THC | H2 | N2 | Visible Emissions |
| | | | | ppm-m | ppm-m | | ppm-m | % | % | SCFH | lb/hr | lb/hr | lb/hr | ft/s | lb/lbmol | lb/lbmol | Btu/scf | Btu/scf | lb/hr | °F | lb/hr | lb/lb | lb/lb | lb/lb | lb/lb | lb/lb | mph | mol% | mol% | mol % | |
| B | 1-1 | 1-1 | Avg | 11,957 | 10 | 1,217 | 149 | 0.99 | 0.99 | 74,030 | 4,067 | 819 | 3,047 | 6.97 | 21 | 24 | 909 | 614 | 1,706 | 413 | 1,684 | 0.42 | 0.56 | 0.41 | 0.44 | 1.02 | 8 | 65 | 17 | 18 | 6.5 |
| B | 1-2 | 1-2 | Avg | 10,576 | 8 | 1,420 | 73 | 0.99 | 0.99 | 74,960 | 4,136 | 811 | 3,117 | 7.06 | 21 | 24 | 914 | 619 | 1,717 | 413 | 1,709 | 0.41 | 0.55 | 0.41 | 0.44 | 1.00 | 8 | 66 | 17 | 17 | 6.5 |
| B | 1-3 | 1-3 | Avg | 1,329,918 | 87 | 13,049 | 333 | 1.00 | 1.00 | 78,085 | 4,393 | 866 | 3,330 | 7.36 | 21 | 25 | 939 | 641 | 1,754 | 413 | 1,827 | 0.40 | 0.53 | 0.42 | 0.45 | 0.96 | 9 | 65 | 19 | 17 | 5.0 |
| B | 2-1 | 2-1 | Avg | 18,676 | 18 | 1,107 | 182 | 0.99 | 0.99 | 72,273 | 3,999 | 793 | 2,979 | 6.81 | 21 | 24 | 911 | 582 | 1,973 | 413 | 1,655 | 0.50 | 0.66 | 0.41 | 0.44 | 1.19 | 7 | 65 | 17 | 18 | 6.5 |
| B | 2-2 | 2-2 | Avg | 22,418 | 27 | 935 | 138 | 0.99 | 0.99 | 72,138 | 3,955 | 788 | 2,982 | 6.80 | 20 | 24 | 911 | 580 | 1,992 | 413 | 1,624 | 0.50 | 0.67 | 0.41 | 0.44 | 1.22 | 7 | 65 | 17 | 17 | 6.0 |
| B | 2-3 | 2-3 | Avg | 467,749 | 95 | 2,590 | 383 | 1.00 | 1.00 | 78,899 | 4,391 | 873 | 3,365 | 7.43 | 21 | 25 | 939 | 595 | 2,187 | 413 | 1,825 | 0.50 | 0.65 | 0.42 | 0.44 | 1.20 | 9 | 65 | 19 | 16 | 4.5 |
| B | 3-1 | 3-1 | Avg | 37,935 | 36 | 1,066 | 214 | 0.99 | 0.99 | 73,321 | 4,098 | 804 | 3,027 | 6.91 | 21 | 24 | 912 | 490 | 3,068 | 413 | 1,698 | 0.75 | 1.01 | 0.41 | 0.44 | 1.82 | 8 | 65 | 17 | 17 | 5.5 |
| B | 3-2 | 3-2 | Avg | 15,816 | 19 | 840 | 145 | 0.99 | 0.99 | 73,531 | 4,010 | 808 | 2,998 | 6.93 | 20 | 24 | 901 | 487 | 3,011 | 413 | 1,656 | 0.75 | 1.00 | 0.41 | 0.44 | 1.82 | 7 | 65 | 18 | 17 | 6.0 |
| B | 3-3 | 3-3 | Avg | 697,040 | 726 | 814 | 960 | 1.00 | 1.00 | 78,576 | 4,385 | 867 | 3,353 | 7.40 | 21 | 25 | 939 | 501 | 3,295 | 413 | 1,825 | 0.75 | 0.98 | 0.42 | 0.45 | 1.80 | 9 | 65 | 19 | 17 | 4.5 |
| B | 4-1 | 4-1 | Avg | 33,946 | 54 | 628 | 354 | 0.99 | 0.99 | 72,756 | 4,040 | 788 | 3,086 | 6.85 | 21 | 25 | 931 | 431 | 4,047 | 413 | 1,687 | 1.00 | 1.31 | 0.42 | 0.44 | 2.41 | 10 | 66 | 17 | 17 | 5.5 |
| B | 4-2 | 4-2 | Avg | 16,608 | 24 | 725 | 98 | 0.99 | 0.99 | 72,229 | 4,015 | 792 | 2,980 | 6.81 | 21 | 24 | 905 | 423 | 3,999 | 413 | 1,664 | 1.00 | 1.34 | 0.41 | 0.44 | 2.41 | 7 | 65 | 18 | 17 | 4.5 |
| B | 4-3 | 4-3 | Avg | 1,536,867 | 1,221 | 1,121 | 6,818 | 0.99 | 1.00 | 78,661 | 4,380 | 867 | 3,354 | 7.41 | 21 | 25 | 939 | 436 | 4,342 | 413 | 1,824 | 0.99 | 1.29 | 0.42 | 0.44 | 2.38 | 8 | 65 | 19 | 17 | 3.5 |
| B | 5-1 | 5-1 | Avg | 33,645 | 79 | 421 | 346 | 0.99 | 0.99 | 73,592 | 4,058 | 796 | 3,086 | 6.93 | 21 | 25 | 924 | 380 | 5,072 | 413 | 1,675 | 1.25 | 1.64 | 0.41 | 0.44 | 3.02 | 7 | 66 | 17 | 17 | 3.0 |
| B | 5-2 | 5-2 | Avg | 18,940 | 41 | 446 | 148 | 0.99 | 0.99 | 73,372 | 4,039 | 803 | 3,039 | 6.91 | 21 | 24 | 908 | 375 | 5,026 | 413 | 1,672 | 1.25 | 1.65 | 0.41 | 0.44 | 3.02 | 6 | 66 | 17 | 17 | 3.0 |
| B | 6-1 | 6-1 | Avg | 31,647 | 108 | 295 | 394 | 0.98 | 0.99 | 73,347 | 4,056 | 795 | 3,045 | 6.91 | 21 | 24 | 914 | 336 | 6,078 | 413 | 1,675 | 1.50 | 2.00 | 0.41 | 0.44 | 3.62 | 7 | 66 | 17 | 17 | 2.0 |
| B | 6-2 | 6-2 | Avg | 10,519 | 36 | 297 | 127 | 0.98 | 0.99 | 73,818 | 4,063 | 805 | 3,068 | 6.95 | 21 | 24 | 911 | 336 | 6,102 | 413 | 1,681 | 1.50 | 1.99 | 0.41 | 0.44 | 3.63 | 6 | 66 | 17 | 17 | 2.0 |
| B | 6-3 | 5-3 | Avg | 515,324 | 753 | 551 | 3,243 | 0.98 | 0.99 | 78,654 | 4,394 | 863 | 3,362 | 7.41 | 21 | 25 | 939 | 342 | 6,592 | 413 | 1,828 | 1.50 | 1.96 | 0.42 | 0.44 | 3.61 | 9 | 65 | 18 | 16 | 1.5 |
| B | 7-1 | 7-1 | Avg | 13,874 | 52 | 269 | 256 | 0.98 | 0.98 | 73,738 | 4,088 | 801 | 3,065 | 6.95 | 21 | 24 | 914 | 323 | 6,529 | 413 | 1,686 | 1.60 | 2.13 | 0.41 | 0.44 | 3.86 | 9 | 66 | 17 | 17 | 1.5 |
| B | 7-2 | 7-2 | Avg | 6,923 | 31 | 234 | 120 | 0.98 | 0.98 | 73,651 | 4,076 | 802 | 3,055 | 6.94 | 21 | 24 | 909 | 321 | 6,522 | 413 | 1,681 | 1.60 | 2.13 | 0.41 | 0.44 | 3.87 | 8 | 66 | 17 | 17 | 1.5 |
| B | 7-3 | 6-3 | Avg | 389,900 | 932 | 280 | 7,498 | 0.95 | 0.98 | 78,737 | 4,413 | 862 | 3,361 | 7.42 | 21 | 25 | 939 | 329 | 7,046 | 413 | 1,833 | 1.60 | 2.10 | 0.42 | 0.44 | 3.85 | 8 | 65 | 18 | 16 | 1.5 |
| B | 8-1 | 8-1 | Avg | 18,294 | 78 | 238 | 378 | 0.98 | 0.98 | 75,583 | 4,168 | 821 | 3,146 | 7.12 | 21 | 24 | 914 | 311 | 7,073 | 413 | 1,721 | 1.70 | 2.25 | 0.41 | 0.44 | 4.11 | 6 | 66 | 17 | 17 | 1.5 |
| B | 8-2 | 8-2 | Avg | 19,453 | 100 | 181 | 511 | 0.96 | 0.97 | 75,163 | 4,164 | 816 | 3,119 | 7.08 | 21 | 24 | 909 | 309 | 7,078 | 413 | 1,725 | 1.70 | 2.27 | 0.41 | 0.44 | 4.12 | 8 | 66 | 17 | 17 | 1.5 |
| B | 9-1 | 9-1 | Avg | 23,780 | 115 | 202 | 437 | 0.98 | 0.98 | 74,171 | 4,136 | 806 | 3,088 | 6.99 | 21 | 24 | 916 | 299 | 7,440 | 413 | 1,711 | 1.80 | 2.41 | 0.41 | 0.44 | 4.34 | 7 | 66 | 17 | 17 | 1.5 |
| B | 9-2 | 9-2 | Avg | 10,506 | 125 | 92 | 1,114 | 0.89 | 0.91 | 76,448 | 4,198 | 833 | 3,167 | 7.20 | 21 | 24 | 909 | 297 | 7,558 | 413 | 1,733 | 1.80 | 2.39 | 0.41 | 0.44 | 4.36 | 10 | 66 | 17 | 17 | 1.5 |
| B | 10-1 | 10-1 | Avg | 6,242 | 48 | 131 | 411 | 0.91 | 0.94 | 74,443 | 4,125 | 809 | 3,095 | 7.01 | 21 | 24 | 914 | 290 | 7,739 | 413 | 1,695 | 1.88 | 2.50 | 0.41 | 0.44 | 4.57 | 8 | 66 | 17 | 17 | 1.0 |
| B | 10-2 | 10-2 | Avg | 16,697 | 93 | 177 | 427 | 0.97 | 0.98 | 76,139 | 4,190 | 830 | 3,148 | 7.17 | 21 | 24 | 909 | 286 | 7,961 | 413 | 1,733 | 1.90 | 2.53 | 0.41 | 0.44 | 4.60 | 6 | 66 | 17 | 17 | 1.5 |

5.6 Test Condition C

The purpose of the Condition C tests is to demonstrate flare performance at flow rates similar to Test B, with addition of a saturated gas (propane) that would require a higher S/VG ratio for smokeless operation than the gas added in Condition B. Propane is also one of the materials most frequently used in independent-pilot scale test studies.

5.6.1 Process Conditions

The values of several key flare operating parameters are shown in Figures 5.6-1 and 5.6-2 below.

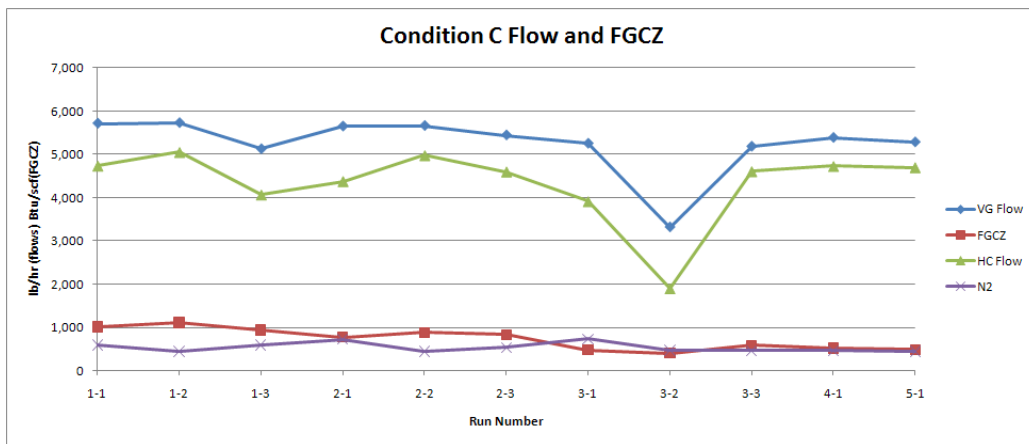


Figure 5.6-1: Condition C Flow and CGZ Heat Content

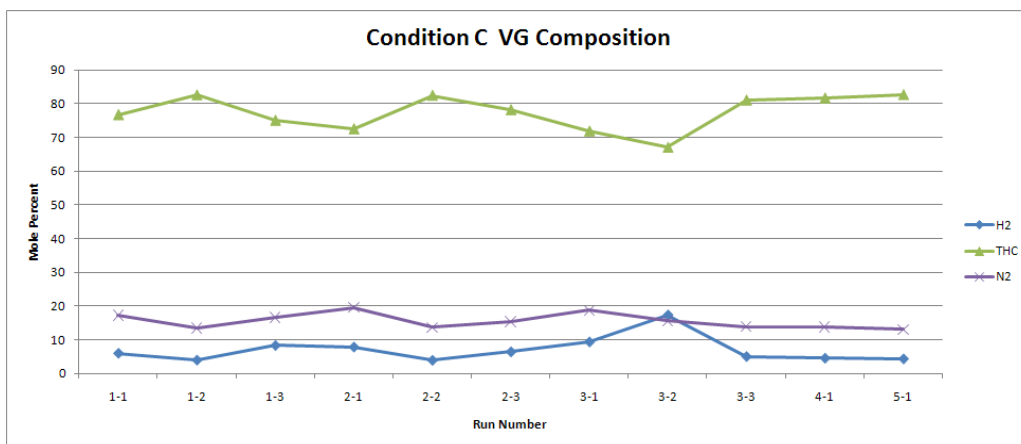


Figure 5.6-2: Condition C Vent Gas Composition

5.6.2 Steam Ratios

The Steam to Vent Gas (S/VG) and Steam to Hydrocarbon (S/HC) ratios corresponding to each test condition are shown in Table 5.6-1. Values are rounded to the nearest 0.5.

Table 5.6-1: Condition C Steam Ratios

| Test | S/VG | S/HC |
|------|------|------|
| 1 | 0.30 | 0.40 |
| 2 | 0.50 | 0.60 |
| 3 | 0.95 | 1.30 |
| 4 | 1.20 | 1.35 |
| 5 | 1.30 | 1.45 |

5.6.3 Wind Conditions

The direction and speed of the wind can have a significant impact on the quality of data collected by the PFTIR. See Section 3.3.2 for a further discussion of wind effects.

Figure 5.6-3 shows wind direction and speed during this Test Condition. The area within the blue 60 deg angle triggers the wind flagging algorithm as described in Section 3.3.2.

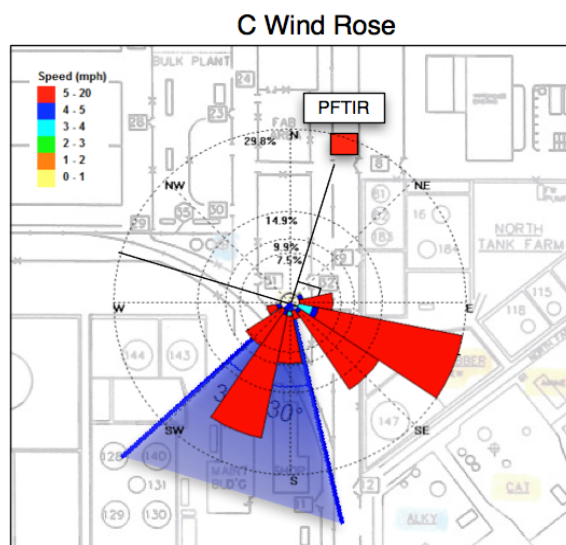


Figure 5.6-3: Condition C. Wind Speed and Direction during Test

Performance Test of a Steam-Assisted Elevated Flare
Marathon Petroleum Company, Texas City Main Flare

5.6.4 Results

| Run ID | | | | Measured | | Calculated | | | | Vent Gas | | | | | | | | Steam | | | Ratios | | | | | Wind | Vent Gas Composition | | | | |
|-----------|---------|---------|-----|-----------|-------|------------|--------|------|------|--------------------|-------|---------|---------|--------------------|----------|----------|-------------|----------|------------|------------|---------------|-------------|-------------|--------------|--------------|--------|----------------------|------|------|-------|-------------------|
| Condition | New Run | Old Run | | CO2 | CO | CO2/CO | THCw | CE | DRE | Vent Gas Flow Rate | | N2 Flow | HC Flow | Flare Tip Velocity | MWvg | MWhc | Vent Gas HV | FGCZ NHV | Steam Flow | Steam Temp | API 521 Steam | Actual S/VG | Actual S/HC | API 521 S/VG | API 521 S/HC | S/S521 | Wind Speed | THC | H2 | N2 | Visible Emissions |
| | | | | ppm-m | ppm-m | | ppm-m | % | % | SCFH | lb/hr | lb/hr | lb/hr | ft/s | lb/lbmol | lb/lbmol | Btu/scf | Btu/scf | lb/hr | °F | lb/hr | lb/lb | lb/lb | lb/lb | lb/lb | lb/lb | mph | mol% | mol% | mol % | |
| C | 1-1 | 3-1 | Avg | 41,111 | 67 | 735 | 203 | 0.99 | 1.00 | 57,409 | 5,710 | 591 | 4,736 | 5.41 | 37 | 41 | 1,678 | 1,016 | 1,786 | 413 | 3,001 | 0.31 | 0.38 | 0.53 | 0.55 | 0.60 | 9 | 77 | 6 | 17 | 7.5 |
| C | 1-2 | 4-2 | Avg | 79,052 | 76 | 956 | 265 | 1.00 | 1.00 | 55,810 | 5,723 | 446 | 5,053 | 5.26 | 39 | 42 | 1,824 | 1,115 | 1,699 | 413 | 3,058 | 0.30 | 0.34 | 0.53 | 0.56 | 0.56 | 7 | 83 | 4 | 13 | 8.0 |
| C | 1-3 | 1-3 | Avg | 525,301 | 71 | 6,923 | 415 | 1.00 | 1.00 | 52,200 | 5,122 | 593 | 4,067 | 4.92 | 36 | 40 | 1,588 | 936 | 1,777 | 413 | 2,634 | 0.35 | 0.44 | 0.52 | 0.54 | 0.67 | 7 | 75 | 8 | 17 | 6.0 |
| C | 2-1 | 2-1 | Avg | 90,829 | 34 | 743 | 180 | 0.99 | 1.00 | 57,730 | 5,644 | 726 | 4,380 | 5.44 | 36 | 40 | 1,552 | 772 | 2,821 | 413 | 2,937 | 0.50 | 0.64 | 0.52 | 0.55 | 0.96 | 9 | 73 | 8 | 20 | 7.5 |
| C | 2-2 | 3-2 | Avg | 74,661 | 139 | 552 | 214 | 0.99 | 1.00 | 55,067 | 5,657 | 445 | 4,980 | 5.19 | 39 | 42 | 1,820 | 881 | 2,818 | 413 | 3,023 | 0.50 | 0.57 | 0.53 | 0.56 | 0.93 | 9 | 82 | 4 | 14 | 5.5 |
| C | 2-3 | 2-3 | Avg | 836,679 | 959 | 2,330 | 2,956 | 1.00 | 1.00 | 54,530 | 5,441 | 540 | 4,602 | 5.14 | 37 | 42 | 1,732 | 832 | 2,836 | 413 | 2,849 | 0.52 | 0.62 | 0.53 | 0.55 | 0.99 | 8 | 78 | 6 | 15 | 5.5 |
| C | 3-1 | 1-1 | Avg | 12,942 | 44 | 346 | 90 | 0.99 | 0.99 | 57,843 | 5,247 | 733 | 3,913 | 5.45 | 34 | 36 | 1,379 | 475 | 5,259 | 413 | 2,661 | 1.00 | 1.38 | 0.50 | 0.52 | 1.97 | 8 | 72 | 9 | 19 | 4.0 |
| C | 3-2 | 2-2 | Avg | 2,830 | 8 | 619 | 18 | 0.99 | 0.99 | 46,186 | 3,319 | 473 | 1,893 | 4.35 | 27 | 24 | 903 | 407 | 2,638 | 413 | 1,582 | 0.91 | 1.45 | 0.45 | 0.43 | 2.17 | 6 | 67 | 17 | 16 | 2.5 |
| C | 3-3 | 3-3 | Avg | 913,387 | 2,385 | 580 | 3,616 | 0.99 | 1.00 | 51,981 | 5,178 | 466 | 4,609 | 4.90 | 38 | 42 | 1,800 | 585 | 5,172 | 413 | 2,727 | 1.00 | 1.12 | 0.53 | 0.56 | 1.90 | 10 | 81 | 5 | 14 | 3.5 |
| C | 4-1 | 4-3 | Avg | 2,252,510 | 1,426 | 1,793 | 3,763 | 1.00 | 1.00 | 52,916 | 5,382 | 462 | 4,728 | 4.99 | 38 | 42 | 1,816 | 517 | 6,453 | 413 | 2,838 | 1.20 | 1.37 | 0.53 | 0.56 | 2.27 | 8 | 82 | 5 | 14 | 1.5 |
| C | 5-1 | 6-3 | Avg | 2,523,063 | 6,463 | 752 | 13,227 | 0.99 | 0.99 | 51,904 | 5,279 | 444 | 4,701 | 4.89 | 38 | 42 | 1,829 | 489 | 6,877 | 413 | 2,797 | 1.30 | 1.46 | 0.53 | 0.56 | 2.46 | 8 | 83 | 4 | 13 | 1.5 |

5.7 Test Condition D

The purpose of the Condition D test is similar to Condition C but adds unsaturates (olefins) to demonstrate performance at an even higher S/VG ratio needed for smokeless operation.

5.7.1 Process Conditions

The values of several key flare operating parameters are shown in Figures 5.7-1 and 5.7-2 below.

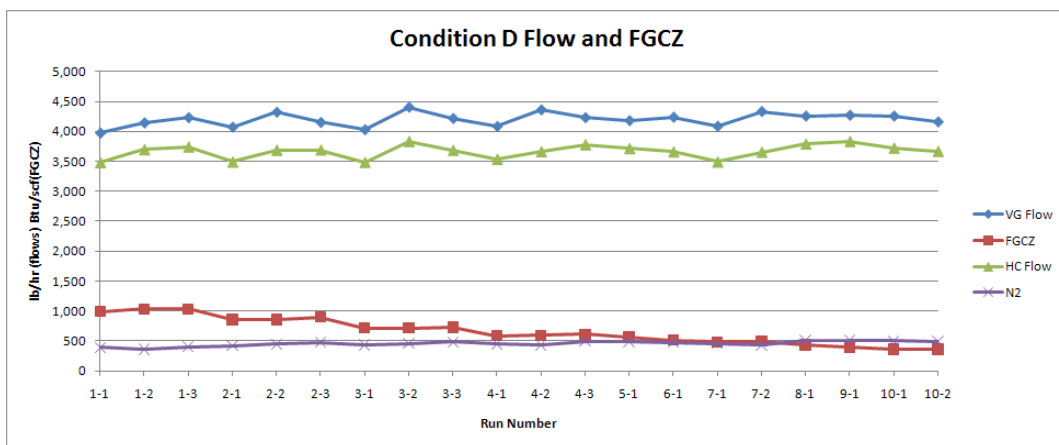


Figure 5.7-1: Condition D Flow and CZG Heat Content

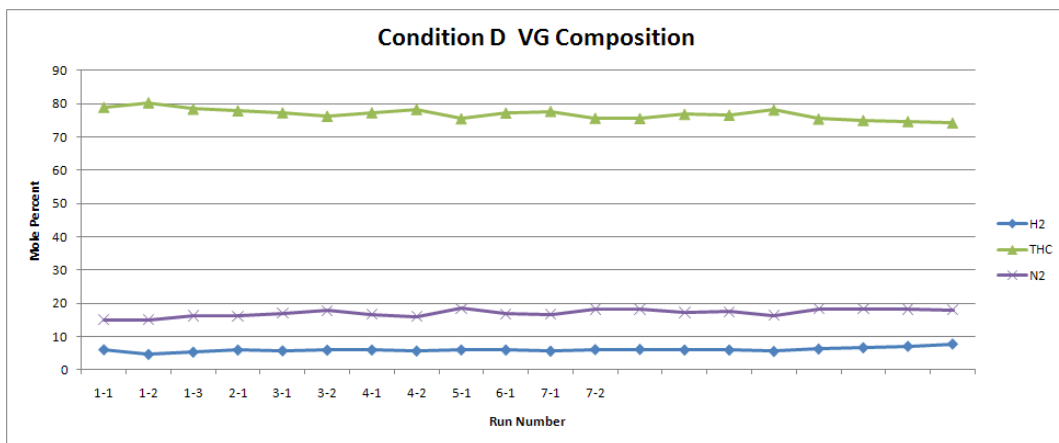


Figure 5.7-2: Condition D Vent Gas Composition

5.7.2 Steam Ratios

The Steam to Vent Gas (S/VG) and Steam to Hydrocarbon (S/HC) ratios corresponding to each test condition are shown in Table 5.7-1. Values are rounded to the nearest 0.5.

Table 5.7-1: Condition D Steam Ratios

| Test | S/VG | S/HC |
|------|------|------|
| 1 | 0.40 | 0.45 |
| 2 | 0.55 | 0.60 |
| 3 | 0.75 | 0.85 |
| 4 | 1.00 | 1.15 |
| 5 | 1.10 | 1.25 |
| 6 | 1.20 | 1.40 |
| 7 | 1.30 | 1.55 |
| 8 | 1.60 | 1.80 |
| 9 | 1.80 | 2.00 |
| 10 | 2.00 | 2.30 |

5.7.3 Wind Conditions

The direction and speed of the wind can have a significant impact on the quality of data collected by the PFTIR. See Section 3.3.2 for a further discussion of wind effects.

Figure 5.7-3 shows wind direction and speed during this Test Condition. The area within the blue 60 deg angle triggers the wind flagging algorithm as described in Section 3.3.2.

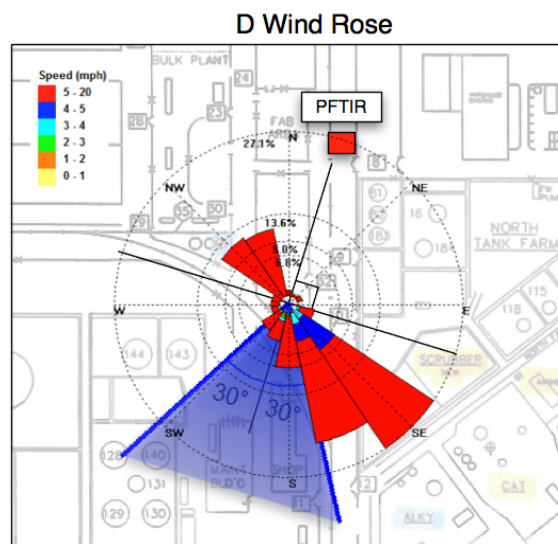


Figure 5.7-3: Condition D. Wind Speed and Direction during Test

Performance Test of a Steam-Assisted Elevated Flare
Marathon Petroleum Company, Texas City Main Flare

5.7.4 Results

| Run ID | | | | Measured | | Calculated | | | | Vent Gas | | | | | | | | Steam | | | Ratios | | | | | Wind | Vent Gas Composition | | | | |
|-----------|---------|---------|-----|-----------|-------|------------|-------|------|------|--------------------|-------|---------|---------|--------------------|----------|----------|-------------|----------|------------|------------|---------------|-------------|-------------|--------------|--------------|--------|----------------------|------|------|-------|-------------------|
| Condition | New Run | Old Run | | CO2 | CO | CO2/CO | THCw | CE | DRE | Vent Gas Flow Rate | | N2 Flow | HC Flow | Flare Tip Velocity | MWvg | MWhc | Vent Gas HV | FGCZ NHV | Steam Flow | Steam Temp | API 521 Steam | Actual S/VG | Actual S/HC | API 521 S/VG | API 521 S/HC | S/S521 | Wind Speed | THC | H2 | N2 | Visible Emissions |
| | | | | ppm-m | ppm-m | | ppm-m | % | % | SCFH | lb/hr | lb/hr | lb/hr | ft/s | lb/lbmol | lb/lbmol | Btu/scf | Btu/scf | lb/hr | °F | lb/hr | lb/lb | lb/lb | lb/lb | lb/lb | lb/lb | mph | mol% | mol% | mol % | |
| D | 1-1 | 1-1 | Avg | 352,610 | 5,023 | 72 | 2,872 | 0.98 | 0.99 | 36,914 | 3,979 | 388 | 3,481 | 3.48 | 40 | 46 | 1,929 | 993 | 1,672 | 413 | 2,175 | 0.42 | 0.48 | 0.55 | 0.58 | 0.77 | 7 | 79 | 6 | 15 | 9.0 |
| D | 1-2 | 1-2 | Avg | 27,256 | 757 | 237 | 3,605 | 0.95 | 0.89 | 38,153 | 4,146 | 357 | 3,696 | 3.59 | 40 | 47 | 1,989 | 1,035 | 1,715 | 413 | 2,256 | 0.41 | 0.46 | 0.54 | 0.59 | 0.76 | 7 | 80 | 5 | 15 | 9.5 |
| D | 1-3 | 1-3 | Avg | 6,744 | 25 | 317 | 32 | 0.99 | 1.00 | 39,587 | 4,231 | 404 | 3,739 | 3.73 | 38 | 47 | 1,954 | 1,031 | 1,789 | 413 | 2,244 | 0.42 | 0.48 | 0.53 | 0.59 | 0.80 | 11 | 78 | 5 | 16 | 8.5 |
| D | 2-1 | 2-1 | Avg | 1,107,795 | 134 | 307 | 144 | 1.00 | 1.00 | 37,408 | 4,074 | 423 | 3,493 | 3.52 | 40 | 46 | 1,910 | 858 | 2,237 | 413 | 2,207 | 0.55 | 0.64 | 0.54 | 0.59 | 1.01 | 9 | 78 | 6 | 16 | 9.0 |
| D | 2-2 | 2-2 | Avg | 15,248 | 113 | 170 | 210 | 0.98 | 0.99 | 39,744 | 4,319 | 444 | 3,686 | 3.74 | 40 | 46 | 1,895 | 856 | 2,348 | 413 | 2,350 | 0.54 | 0.64 | 0.54 | 0.59 | 1.00 | 9 | 77 | 6 | 17 | 9.0 |
| D | 2-3 | 2-3 | Avg | 25,948 | 125 | 219 | 118 | 0.99 | 1.00 | 40,116 | 4,152 | 473 | 3,688 | 3.78 | 38 | 47 | 1,881 | 898 | 2,151 | 413 | 2,216 | 0.51 | 0.58 | 0.53 | 0.59 | 0.97 | 10 | 76 | 6 | 18 | 8.5 |
| D | 3-1 | 3-1 | Avg | 17,647 | 82 | 234 | 121 | 0.99 | 0.99 | 37,613 | 4,034 | 436 | 3,487 | 3.54 | 40 | 46 | 1,900 | 712 | 3,022 | 413 | 2,202 | 0.75 | 0.87 | 0.54 | 0.59 | 1.38 | 6 | 77 | 6 | 17 | 6.0 |
| D | 3-2 | 3-2 | Avg | 14,484 | 46 | 384 | 224 | 0.98 | 0.98 | 40,561 | 4,399 | 459 | 3,830 | 3.82 | 41 | 47 | 1,912 | 716 | 3,274 | 413 | 2,400 | 0.74 | 0.85 | 0.55 | 0.59 | 1.37 | 7 | 78 | 6 | 16 | 6.5 |
| D | 3-3 | 3-3 | Avg | 163,340 | 1,166 | 171 | 349 | 0.99 | 1.00 | 40,298 | 4,217 | 483 | 3,684 | 3.80 | 38 | 47 | 1,884 | 727 | 3,178 | 413 | 2,233 | 0.75 | 0.86 | 0.53 | 0.59 | 1.42 | 8 | 76 | 6 | 18 | 7.5 |
| D | 4-1 | 4-1 | Avg | 44,351 | 250 | 178 | 306 | 0.98 | 0.99 | 38,286 | 4,087 | 453 | 3,538 | 3.61 | 40 | 46 | 1,885 | 585 | 4,101 | 413 | 2,232 | 1.00 | 1.16 | 0.54 | 0.58 | 1.85 | 5 | 77 | 6 | 17 | 4.0 |
| D | 4-2 | 4-2 | Avg | 16,238 | 36 | 451 | 231 | 0.98 | 0.99 | 38,902 | 4,357 | 433 | 3,661 | 3.67 | 41 | 47 | 1,926 | 590 | 4,354 | 413 | 2,405 | 1.00 | 1.19 | 0.55 | 0.59 | 1.80 | 5 | 78 | 6 | 17 | 4.0 |
| D | 4-3 | 4-3 | Avg | 797,199 | 3,990 | 187 | 2,573 | 0.99 | 1.00 | 40,998 | 4,230 | 496 | 3,777 | 3.86 | 38 | 47 | 1,889 | 612 | 4,185 | 413 | 2,244 | 0.99 | 1.11 | 0.53 | 0.59 | 1.87 | 10 | 76 | 6 | 18 | 6.0 |
| D | 5-1 | 5-3 | Avg | 86,603 | 577 | 170 | 215 | 0.98 | 1.00 | 40,357 | 4,182 | 491 | 3,714 | 3.80 | 38 | 47 | 1,887 | 567 | 4,622 | 413 | 2,216 | 1.10 | 1.25 | 0.53 | 0.59 | 2.07 | 11 | 76 | 6 | 18 | 5.5 |
| D | 6-1 | 6-1 | Avg | 31,169 | 290 | 125 | 509 | 0.97 | 0.98 | 39,910 | 4,237 | 476 | 3,660 | 3.76 | 40 | 46 | 1,872 | 514 | 5,084 | 413 | 2,289 | 1.20 | 1.39 | 0.54 | 0.58 | 2.23 | 6 | 77 | 6 | 17 | 2.0 |
| D | 7-1 | 7-1 | Avg | 150,948 | 1,477 | 127 | 1,213 | 0.98 | 0.99 | 38,259 | 4,090 | 458 | 3,492 | 3.60 | 40 | 46 | 1,863 | 483 | 5,309 | 413 | 2,207 | 1.30 | 1.52 | 0.54 | 0.58 | 2.41 | 5 | 77 | 6 | 17 | 2.0 |
| D | 7-2 | 5-2 | Avg | 15,696 | 122 | 131 | 476 | 0.96 | 0.97 | 38,306 | 4,330 | 425 | 3,652 | 3.61 | 41 | 47 | 1,948 | 494 | 5,620 | 413 | 2,369 | 1.30 | 1.54 | 0.55 | 0.59 | 2.37 | 6 | 78 | 6 | 16 | 2.0 |
| D | 8-1 | 6-3 | Avg | 15,222 | 213 | 72 | 700 | 0.94 | 0.96 | 41,247 | 4,255 | 504 | 3,786 | 3.89 | 38 | 47 | 1,882 | 433 | 6,789 | 413 | 2,252 | 1.60 | 1.79 | 0.53 | 0.59 | 3.02 | 11 | 75 | 6 | 18 | 3.0 |
| D | 9-1 | 7-3 | Avg | 6,229 | 55 | 55 | 302 | 0.87 | 0.95 | 42,006 | 4,270 | 515 | 3,828 | 3.96 | 38 | 47 | 1,873 | 394 | 7,695 | 413 | 2,244 | 1.80 | 2.01 | 0.53 | 0.59 | 3.41 | 11 | 75 | 7 | 18 | 1.5 |
| D | 10-1 | 8-3 | Avg | 2,329 | 50 | 45 | 465 | 0.80 | 0.84 | 41,028 | 4,256 | 501 | 3,720 | 3.87 | 38 | 47 | 1,860 | 361 | 8,503 | 413 | 2,227 | 2.01 | 2.29 | 0.53 | 0.59 | 3.83 | 12 | 75 | 7 | 18 | 1.5 |
| D | 10-2 | 9-3 | Avg | 1,052 | 23 | 41 | 238 | 0.78 | 0.82 | 40,648 | 4,161 | 495 | 3,669 | 3.83 | 38 | 47 | 1,857 | 360 | 8,305 | 413 | 2,185 | 2.00 | 2.27 | 0.53 | 0.59 | 3.81 | 8 | 74 | 8 | 18 | 1.5 |

5.8 Test Condition E

The purpose of the Condition E test is the same as Test D, but with a higher flow rate (and thus higher unsaturate mass flow) to see flare performance at higher flows for the unsaturate condition

5.8.1 Process Conditions

The values of several key flare operating parameters are shown in Figures 5.8-1 and 5.8-2 below.

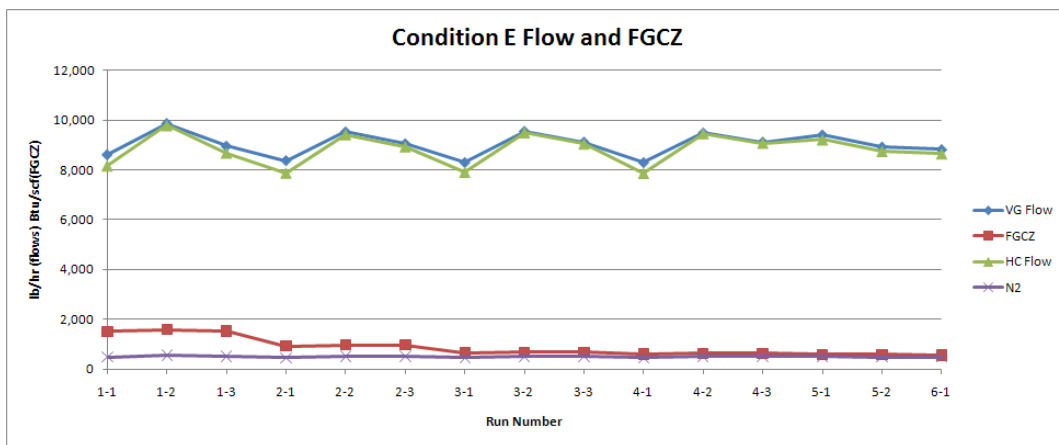


Figure 5.8-1: Condition E Flow and CZG Heat Content

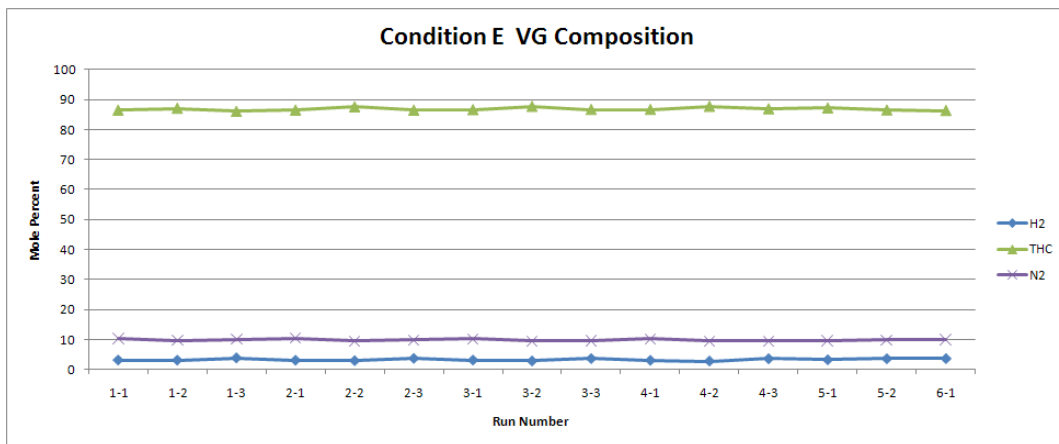


Figure 5.8-2: Condition E Vent Gas Composition

5.8.2 Steam Ratios

The Steam to Vent Gas (S/VG) and Steam to Hydrocarbon (S/HC) ratios corresponding to each test condition are shown in Table 5.8-1. Values are rounded to the nearest 0.5.

Table 5.8-1: Condition E Steam Ratios

| Test | S/VG | S/HC |
|------|------|------|
| 1 | 0.20 | 0.20 |
| 2 | 0.55 | 0.60 |
| 3 | 1.00 | 1.00 |
| 4 | 1.10 | 1.10 |
| 5 | 1.20 | 1.20 |
| 6 | 1.30 | 1.30 |

5.8.3 Wind Conditions

The direction and speed of the wind can have a significant impact on the quality of data collected by the PFTIR. See Section 3.3.2 for a further discussion of wind effects.

Figure 5.8-3 shows wind direction and speed during this Test Condition. The area within the blue 60 deg angle triggers the wind flagging algorithm as described in Section 3.3.2.

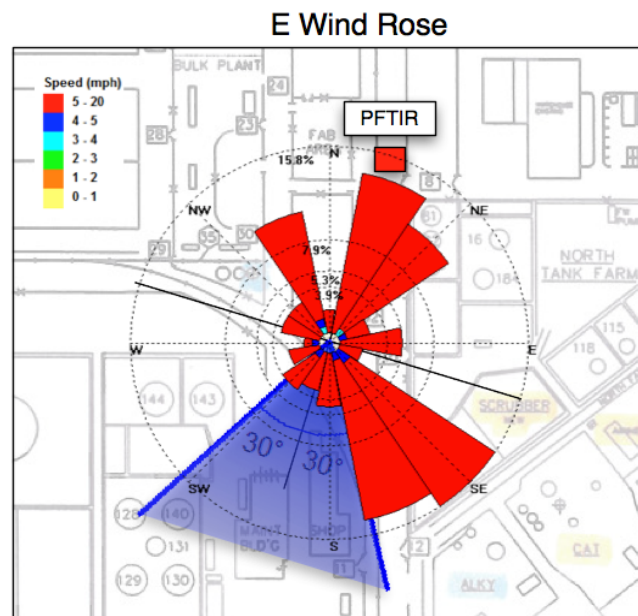


Figure 5.8-3: Condition E. Wind Speed and Direction during Test

Performance Test of a Steam-Assisted Elevated Flare
Marathon Petroleum Company, Texas City Main Flare

5.8.4 Results

| Run ID | | | | Measured | | Calculated | | | | Vent Gas | | | | | | | | Steam | | | Ratios | | | | | Wind | Vent Gas Composition | | | | |
|-----------|---------|---------|-----|----------|-------|------------|-------|------|------|--------------------|-------|---------|---------|--------------------|----------|----------|-------------|----------|------------|------------|---------------|-------------|-------------|--------------|--------------|--------|----------------------|------|------|-------|-------------------|
| Condition | New Run | Old Run | | CO2 | CO | CO2/CO | THCw | CE | DRE | Vent Gas Flow Rate | | N2 Flow | HC Flow | Flare Tip Velocity | MWvg | MWhc | Vent Gas HV | FGCZ NHV | Steam Flow | Steam Temp | API 521 Steam | Actual S/VG | Actual S/HC | API 521 S/VG | API 521 S/HC | S/S521 | Wind Speed | THC | H2 | N2 | Visible Emissions |
| | | | | ppm-m | ppm-m | | ppm-m | % | % | SCFH | lb/hr | lb/hr | lb/hr | ft/s | lb/lbmol | lb/lbmol | Btu/scf | Btu/scf | lb/hr | °F | lb/hr | lb/lb | lb/lb | lb/lb | lb/lb | lb/lb | mph | mol% | mol% | mol % | |
| E | 1-1 | 1-1 | Avg | 479,315 | 2,133 | 216 | 2,613 | 0.99 | 0.99 | 74,650 | 8,612 | 480 | 8,171 | 7.03 | 44 | 49 | 2,218 | 1,506 | 1,660 | 413 | 4,926 | 0.19 | 0.20 | 0.57 | 0.60 | 0.34 | 8 | 86 | 3 | 10 | 9.5 |
| E | 1-2 | 1-2 | Avg | 6,704 | 11 | 627 | 103 | 0.98 | 0.98 | 88,874 | 9,867 | 550 | 9,794 | 8.37 | 42 | 49 | 2,227 | 1,581 | 1,714 | 413 | 5,529 | 0.17 | 0.18 | 0.56 | 0.60 | 0.31 | 7 | 87 | 3 | 10 | 9.0 |
| E | 1-3 | 1-3 | Avg | 6,747 | 17 | 394 | 0 | 1.00 | 1.00 | 79,802 | 8,955 | 515 | 8,683 | 7.52 | 42 | 49 | 2,209 | 1,520 | 1,738 | 413 | 4,966 | 0.19 | 0.20 | 0.56 | 0.60 | 0.35 | 9 | 86 | 4 | 10 | 9.0 |
| E | 2-1 | 2-1 | Avg | 39,546 | 46 | 942 | 198 | 0.99 | 1.00 | 72,648 | 8,376 | 457 | 7,878 | 6.84 | 44 | 48 | 2,198 | 921 | 4,791 | 413 | 4,767 | 0.57 | 0.61 | 0.57 | 0.60 | 1.00 | 9 | 86 | 3 | 10 | 6.0 |
| E | 2-2 | 2-2 | Avg | 7,255 | 7 | 1,194 | 119 | 0.98 | 0.98 | 85,769 | 9,526 | 507 | 9,428 | 8.08 | 42 | 48 | 2,229 | 968 | 5,340 | 413 | 5,300 | 0.56 | 0.57 | 0.56 | 0.60 | 1.00 | 6 | 88 | 3 | 10 | 6.0 |
| E | 2-3 | 2-3 | Avg | 7,418 | 14 | 575 | 35 | 0.99 | 1.00 | 81,447 | 9,052 | 509 | 8,939 | 7.67 | 42 | 49 | 2,241 | 968 | 5,085 | 413 | 5,055 | 0.56 | 0.57 | 0.56 | 0.60 | 1.01 | 8 | 86 | 4 | 10 | 5.5 |
| E | 3-1 | 3-1 | Avg | 33,938 | 125 | 282 | 337 | 0.99 | 0.99 | 73,275 | 8,299 | 457 | 7,914 | 6.90 | 44 | 48 | 2,187 | 639 | 8,326 | 413 | 4,720 | 1.00 | 1.05 | 0.57 | 0.60 | 1.76 | 7 | 87 | 3 | 10 | 2.5 |
| E | 3-2 | 3-2 | Avg | 10,181 | 29 | 348 | 126 | 0.98 | 0.99 | 86,529 | 9,552 | 509 | 9,508 | 8.15 | 42 | 48 | 2,224 | 668 | 9,573 | 413 | 5,329 | 1.00 | 1.01 | 0.56 | 0.60 | 1.79 | 7 | 88 | 3 | 9 | 2.5 |
| E | 3-3 | 3-3 | Avg | 20,139 | 97 | 223 | 264 | 0.98 | 0.99 | 82,170 | 9,120 | 510 | 9,055 | 7.74 | 42 | 49 | 2,247 | 673 | 9,099 | 413 | 5,076 | 1.00 | 1.00 | 0.56 | 0.60 | 1.80 | 8 | 87 | 4 | 10 | 3.0 |
| E | 4-1 | 4-1 | Avg | 25,265 | 96 | 265 | 329 | 0.98 | 0.99 | 72,979 | 8,299 | 455 | 7,864 | 6.88 | 44 | 48 | 2,176 | 594 | 9,145 | 413 | 4,709 | 1.10 | 1.16 | 0.57 | 0.60 | 1.94 | 10 | 87 | 3 | 10 | 1.5 |
| E | 4-2 | 4-2 | Avg | 8,697 | 45 | 206 | 187 | 0.97 | 0.98 | 86,272 | 9,487 | 507 | 9,468 | 8.13 | 42 | 48 | 2,220 | 627 | 10,382 | 413 | 5,266 | 1.10 | 1.10 | 0.56 | 0.60 | 1.97 | 7 | 88 | 3 | 9 | 2.0 |
| E | 4-3 | 4-3 | Avg | 11,770 | 57 | 206 | 207 | 0.98 | 0.98 | 82,076 | 9,121 | 504 | 9,081 | 7.73 | 42 | 49 | 2,256 | 630 | 10,053 | 413 | 5,097 | 1.10 | 1.11 | 0.56 | 0.60 | 1.96 | 8 | 87 | 4 | 9 | 2.0 |
| E | 5-1 | 6-2 | Avg | 7,317 | 36 | 207 | 202 | 0.97 | 0.97 | 84,628 | 9,403 | 504 | 9,221 | 7.97 | 42 | 48 | 2,206 | 582 | 11,275 | 413 | 5,225 | 1.20 | 1.22 | 0.56 | 0.60 | 2.16 | 8 | 87 | 3 | 10 | 0.0 |
| E | 5-2 | 5-3 | Avg | 9,833 | 57 | 172 | 190 | 0.98 | 0.98 | 79,530 | 8,921 | 488 | 8,750 | 7.49 | 42 | 49 | 2,251 | 590 | 10,717 | 413 | 4,985 | 1.20 | 1.22 | 0.56 | 0.60 | 2.15 | 9 | 86 | 4 | 10 | 1.5 |
| E | 6-1 | 6-3 | Avg | 7,386 | 51 | 143 | 223 | 0.96 | 0.97 | 78,820 | 8,817 | 487 | 8,654 | 7.43 | 42 | 49 | 2,239 | 554 | 11,444 | 413 | 4,910 | 1.30 | 1.32 | 0.56 | 0.60 | 2.33 | 9 | 86 | 4 | 10 | 1.5 |

5.9 Test Condition F

The purpose of the Condition F test is to demonstrate performance when operating at higher levels of hydrogen than typically found in the base load. Hydrogen (H_2) has been shown to have exceptional combustion characteristics, but it has a low volumetric heat content (275 BTU/scf). Note that the base load may contain nominal amounts of hydrogen from 10 to 30% mole weight.

Note that this test condition differs from others because the objective was not to determine how S/VG affects combustion efficiency, but rather how H_2 affects flare performance. Therefore, during the first part of this test series, H_2 levels were increased while holding S/VG constant. In the latter part of the test, a higher S/VG was used.

Also note that virtually all of the data from this test condition are compromised due to adverse wind conditions on the day of testing. See Figure 5.9-3 below for a wind rose showing wind speed and direction on this day. Due to these adverse conditions, this data is considered invalid and is not used to draw conclusions regarding flare performance under the tested conditions.

5.9.1 Process Conditions

The values of several key flare operating parameters are shown in Figures 5.9-1 and 5.9-2 below.

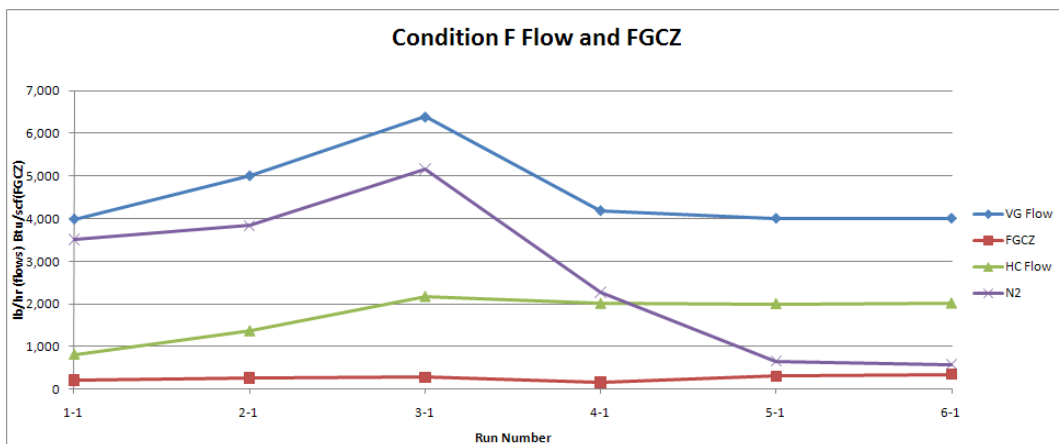


Figure 5.9-1: Condition F Flow and CZG Heat Content

Performance Test of a Steam-Assisted Elevated Flare
Marathon Petroleum Company, Texas City Main Flare

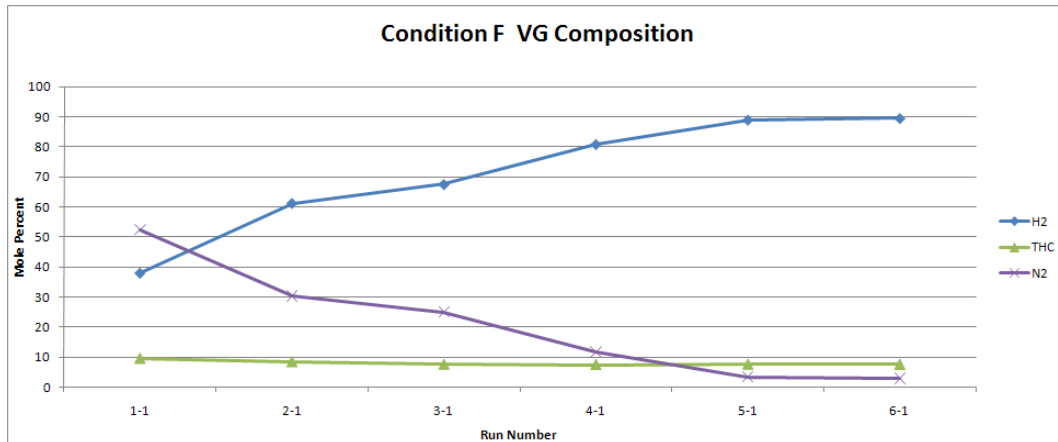


Figure 5.9-2: Condition F Vent Gas Composition

5.9.2 Steam Ratios

The Steam to Vent Gas (S/VG) and Steam to Hydrocarbon (S/HC) ratios corresponding to each test condition are shown in Table 5.9-1. Values are rounded to the nearest 0.5.

Table 5.9-1: Condition F Steam Ratios

| Test | S/VG | S/HC |
|------|------|------|
| 1 | 0.45 | 2.20 |
| 2 | 0.45 | 1.65 |
| 3 | 0.45 | 1.30 |
| 4 | 4.00 | 8.35 |
| 5 | 1.00 | 2.00 |
| 6 | 0.45 | 0.85 |

Performance Test of a Steam-Assisted Elevated Flare
Marathon Petroleum Company, Texas City Main Flare

5.9.4 Results

| Run ID | | | Measured | | Calculated | | | | Vent Gas | | | | | | | | Steam | | | Ratios | | | | | Wind | Vent Gas Composition | | | | | |
|-----------|---------|---------|----------|-----------|------------|--------|--------|------|--------------------|---------|---------|---------|--------------------|-------|----------|-------------|----------|------------|------------|---------------|-------------|-------------|--------------|--------------|--------|----------------------|------|------|-------|-------------------|-----|
| | | | | | | | | | Vent Gas Flow Rate | | N2 Flow | HC Flow | Flare Tip Velocity | MWvg | MWhc | Vent Gas HV | FGCZ NHV | Steam Flow | Steam Temp | API 521 Steam | Actual S/VG | Actual S/HC | API 521 S/VG | API 521 S/HC | S/S521 | Wind Speed | THC | H2 | N2 | Visible Emissions | |
| Condition | New Run | Old Run | | CO2 | CO | CO2/CO | THCw | CE | DRE | SCFH | lb/hr | lb/hr | lb/hr | ft/s | lb/lbmol | lb/lbmol | Btu/scf | Btu/scf | lb/hr | °F | lb/hr | lb/lb | lb/lb | lb/lb | lb/lb | mph | mol% | mol% | mol % | | |
| F | 1-1 | 1-1 | Avg | 17,542 | 12 | 1,420 | 156 | 0.99 | 0.99 | 92,911 | 3,982 | 3,512 | 818 | 8.75 | 16 | 36 | 292 | 209 | 1,810 | 413 | 1,527 | 0.45 | 2.21 | 0.38 | 0.51 | 1.19 | 7 | 10 | 38 | 52 | 2.0 |
| F | 2-1 | 2-1 | Avg | 24,271 | 15 | 1,195 | 174 | 0.99 | 0.99 | 173,597 | 5,006 | 3,840 | 1,370 | 16.36 | 11 | 36 | 334 | 262 | 2,256 | 413 | 1,744 | 0.45 | 1.65 | 0.35 | 0.52 | 1.30 | 7 | 8 | 61 | 30 | 3.0 |
| F | 3-1 | 3-1 | Avg | 1,737,650 | 6,243 | 347 | 29,389 | 0.98 | 0.98 | 287,269 | 6,390 | 5,162 | 2,170 | 27.07 | 9 | 39 | 345 | 285 | 2,833 | 413 | 2,102 | 0.45 | 1.31 | 0.33 | 0.53 | 1.35 | 9 | 8 | 68 | 25 | 2.0 |
| F | 4-1 | 1-2 | Avg | 28,533 | 91 | 281 | 231 | 0.99 | 0.99 | 265,508 | 4,181 | 2,276 | 2,008 | 25.02 | 6 | 39 | 383 | 162 | 16,802 | 413 | 1,326 | 4.01 | 8.37 | 0.32 | 0.54 | 12.64 | 8 | 7 | 81 | 12 | 1.0 |
| F | 5-1 | 2-2 | Avg | 1,282,118 | 1,620 | 631 | 8,098 | 0.99 | 0.99 | 263,538 | 4,001 | 656 | 2,003 | 24.83 | 6 | 39 | 403 | 305 | 4,010 | 413 | 1,253 | 1.00 | 2.00 | 0.31 | 0.53 | 3.20 | 10 | 8 | 89 | 3 | 2.0 |
| F | 6-1 | 3-2 | Avg | 947,735 | 2,383 | 580 | 2,723 | 1.00 | 1.00 | 266,986 | 4,002 | 578 | 2,016 | 25.15 | 6 | 39 | 402 | 353 | 1,752 | 413 | 1,259 | 0.44 | 0.87 | 0.31 | 0.53 | 1.39 | 9 | 8 | 90 | 3 | 3.0 |

5.10 Test Condition G

The purpose of the Condition G test is to demonstrate performance with additional inert material (i.e. nitrogen) combined with hydrogen in the base load. The objective was to seek an overall vent gas heat content of less than 300 BTU/scf or less than 200 BTU/scf in flare combustion zone. In addition to the inert testing, this test provides data point demonstrating the effect of hydrogen on a low BTU gas.

Note that virtually all of the data from this test condition are compromised due to adverse wind conditions on the day of testing. See section 5.10-3 below for a wind rose showing wind speed and direction on this day. Due to these adverse conditions, this data is considered invalid and is not used to draw conclusions regarding flare performance under the tested conditions.

5.10.1 Process Conditions

The values of several key flare operating parameters are shown in Figures 5.10-1 and 5.10-2 below.

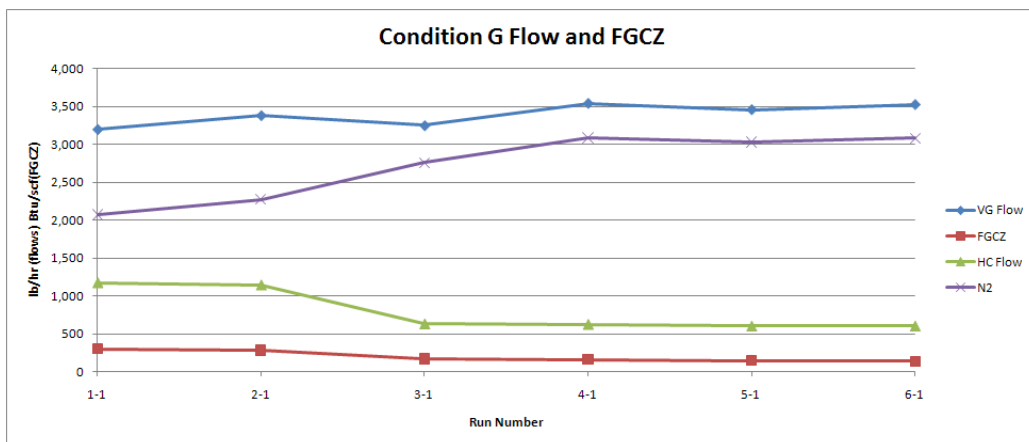


Figure 5.10-1: Condition G Flow and CZG Heat Content

Performance Test of a Steam-Assisted Elevated Flare
Marathon Petroleum Company, Texas City Main Flare

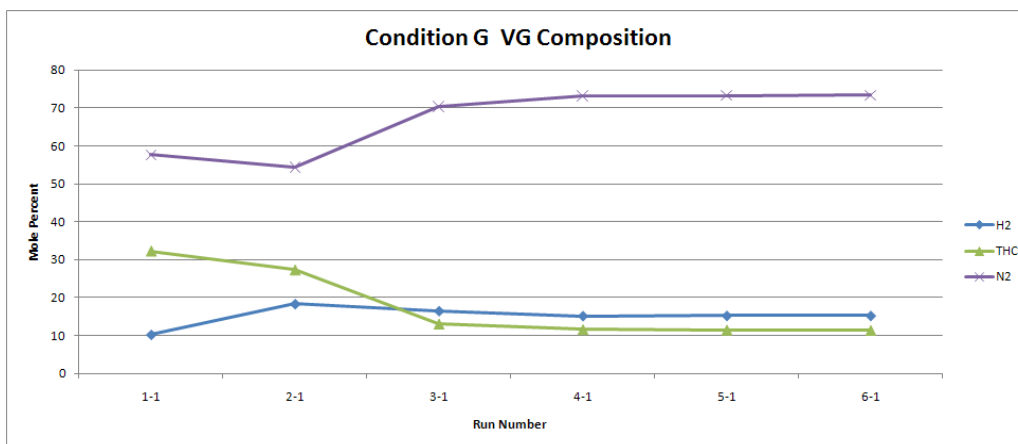


Figure 5.10-2: Condition G Vent Gas Composition

5.10.2 Steam Ratios

The Steam to Vent Gas (S/VG) and Steam to Hydrocarbon (S/HC) ratios corresponding to each test condition are shown in Table 5.10-1. Values are rounded to the nearest 0.5.

Table 5.10-1: Condition G Steam Ratios

| Test | S/VG | S/HC |
|------|------|------|
| 1 | 0.55 | 1.50 |
| 2 | 0.55 | 1.60 |
| 3 | 0.55 | 2.90 |
| 4 | 0.50 | 2.90 |
| 5 | 0.60 | 3.45 |
| 6 | 0.70 | 4.10 |

5.10.3 *Wind Conditions*

The direction and speed of the wind can have a significant impact on the quality of data collected by the PFTIR. See Section 3.3.2 for a further discussion of wind effects.

Figure 5.10-3 shows wind direction and speed during this Test Condition. The area within the blue 60 deg angle triggers the wind flagging algorithm as described in Section 3.3.2.

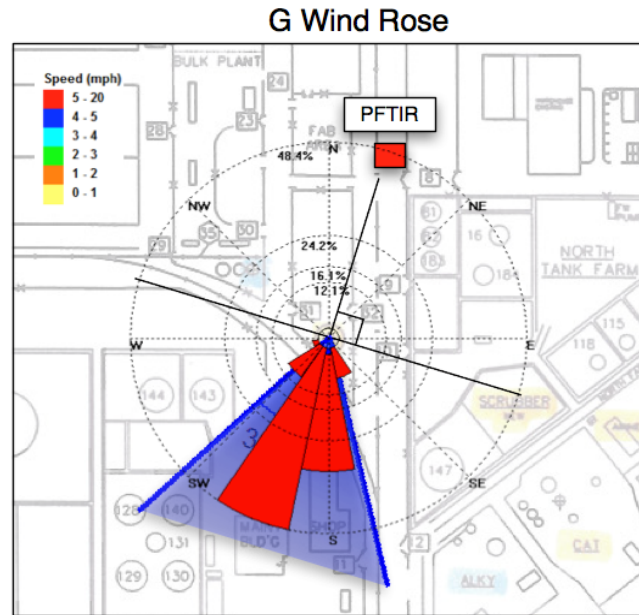


Figure 5.10-3: Condition G. Wind Speed and Direction during Test

Performance Test of a Steam-Assisted Elevated Flare
Marathon Petroleum Company, Texas City Main Flare

5.10.4 Results

| Run ID | | | | Measured | | Calculated | | | | Vent Gas | | | | | | | | Steam | | | Ratios | | | | | Wind | Vent Gas Composition | | | | |
|-----------|---------|---------|-----|----------|-------|------------|-------|------|------|--------------------|-------|---------|---------|--------------------|----------|----------|-------------|----------|------------|------------|---------------|-------------|-------------|--------------|--------------|--------|----------------------|------|------|-------|-------------------|
| Condition | New Run | Old Run | | CO2 | CO | CO2/CO | THCw | CE | DRE | Vent Gas Flow Rate | | N2 Flow | HC Flow | Flare Tip Velocity | MWvg | MWhc | Vent Gas HV | FGCZ NHV | Steam Flow | Steam Temp | API 521 Steam | Actual S/VG | Actual S/HC | API 521 S/VG | API 521 S/HC | S/S521 | Wind Speed | THC | H2 | N2 | Visible Emissions |
| | | | | ppm-m | ppm-m | | ppm-m | % | % | SCFH | lb/hr | lb/hr | lb/hr | ft/s | lb/lbmol | lb/lbmol | Btu/scf | Btu/scf | lb/hr | °F | lb/hr | lb/lb | lb/lb | lb/lb | lb/lb | lb/lb | mph | mol% | mol% | mol % | |
| G | 1-1 | 1-1 | Avg | 37,120 | 198 | 186 | 955 | 0.97 | 0.98 | 51,083 | 3,202 | 2,075 | 1,178 | 4.81 | 23 | 28 | 515 | 300 | 1,787 | 413 | 1,383 | 0.56 | 1.52 | 0.43 | 0.46 | 1.29 | 10 | 32 | 10 | 58 | 2.0 |
| G | 2-1 | 2-1 | Avg | 106,006 | 324 | 305 | 838 | 0.99 | 0.99 | 58,415 | 3,382 | 2,276 | 1,148 | 5.50 | 22 | 28 | 462 | 283 | 1,825 | 413 | 1,419 | 0.54 | 1.59 | 0.42 | 0.46 | 1.29 | 10 | 27 | 18 | 54 | 1.0 |
| G | 3-1 | 3-1 | Avg | 9,515 | 117 | 86 | 983 | 0.89 | 0.91 | 55,227 | 3,252 | 2,759 | 631 | 5.20 | 22 | 34 | 284 | 170 | 1,819 | 413 | 1,376 | 0.56 | 2.88 | 0.42 | 0.50 | 1.32 | 10 | 13 | 17 | 70 | 1.0 |
| G | 4-1 | 4-1 | Avg | 10,375 | 133 | 83 | 1,090 | 0.89 | 0.91 | 59,676 | 3,540 | 3,090 | 626 | 5.62 | 22 | 35 | 259 | 160 | 1,826 | 413 | 1,504 | 0.52 | 2.92 | 0.42 | 0.51 | 1.21 | 8 | 12 | 15 | 73 | 1.0 |
| G | 5-1 | 5-1 | Avg | 8,734 | 120 | 73 | 1,261 | 0.86 | 0.88 | 58,467 | 3,460 | 3,031 | 603 | 5.51 | 22 | 35 | 256 | 149 | 2,082 | 413 | 1,470 | 0.60 | 3.46 | 0.42 | 0.51 | 1.42 | 8 | 11 | 15 | 73 | 1.0 |
| G | 6-1 | 6-1 | Avg | 8,748 | 126 | 68 | 1,678 | 0.82 | 0.84 | 59,404 | 3,526 | 3,084 | 604 | 5.60 | 22 | 34 | 251 | 137 | 2,469 | 413 | 1,496 | 0.70 | 4.09 | 0.42 | 0.51 | 1.65 | 9 | 11 | 15 | 73 | 1.0 |

5.11 Long Term Stability Test

The purpose of the Long Term Stability (LTS) test is to obtain an indication of the repeatability of the PFTIR measurement system. This test differs from the other tests conducted under this project in that the objective of the LTS was to reproduce process conditions as accurately as possible for each test run. Therefore, the run-to-run variation in test results is an indication of the instrument repeatability.

The initial test condition chosen for the LTS runs was Condition C at an SV/G of 1.00. However, after one test run, it was decided that this condition was not suitable for the LTS series because 1) the flare was smoking at this condition, and 2) the flare recovery time was very long (1 to 2 hours) before another test condition could be run. Data from this first LTS run are included in the Appendix but is not included in the data analysis in this Section.

The LTS test conditions were changed to Condition B at an S/VG of 1.00. This condition proved satisfactory, especially since Condition B provided the most stable flare operation of any test condition.

5.11.1 Process Conditions

The values of several key flare operating parameters are shown in Figures 5.11-1 and 5.11-2 below.

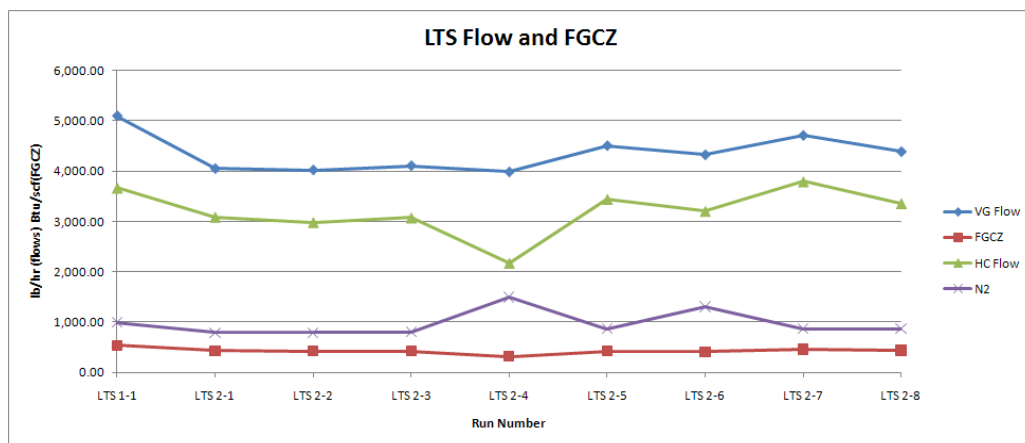


Figure 5.11-1: Long Term Stability Flow and CZG Heat Content

Performance Test of a Steam-Assisted Elevated Flare
Marathon Petroleum Company, Texas City Main Flare

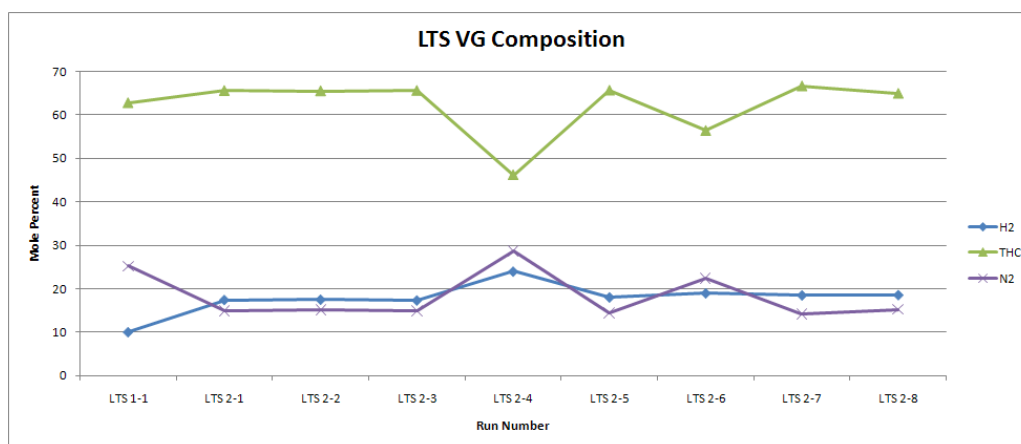


Figure 5.11-2: Long Term Stability Vent Gas Composition

5.11.2 Steam Ratios

The Steam to Vent Gas (S/VG) and Steam to Hydrocarbon (S/HC) ratios corresponding to each test condition are shown in Table 5.11-1. Values are rounded to the nearest 0.5.

Table 5.11-1: Long Term Stability Steam Ratios

| Test | S/VG | S/HC |
|------|------|------|
| 1 | 1.00 | 1.30 |
| 2 | 1.00 | 1.35 |
| 3 | 1.00 | 1.35 |
| 4 | 1.00 | 2.00 |
| 5 | 1.00 | 1.30 |
| 6 | 1.00 | 1.35 |
| 7 | 1.00 | 1.25 |
| 8 | 1.00 | 1.30 |

5.11.3 Wind Conditions

The direction and speed of the wind can have a significant impact on the quality of data collected by the PFTIR. See Section 3.3.2 for a further discussion of wind effects.

Figure 5.11-3 shows wind direction and speed during this Test Condition. The area within the blue 60 deg angle triggers the wind flagging algorithm as described in Section 3.3.2.

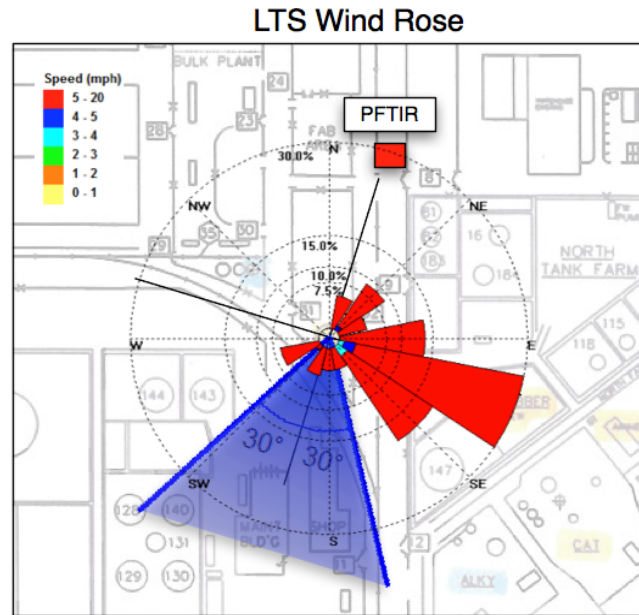


Figure 5.11-3: Long Term Stability. Wind Speed and Direction during Test

Performance Test of a Steam-Assisted Elevated Flare
Marathon Petroleum Company, Texas City Main Flare

5.11.4 Results

| Run ID | | | | Measured | | Calculated | | | | Vent Gas | | | | | | | | Steam | | | Ratios | | | | | Wind | Vent Gas Composition | | | | |
|-----------|---------|---------|-----|-----------|-------|------------|-------|------|------|--------------------|-------|---------|---------|--------------------|----------|----------|-------------|----------|------------|------------|---------------|-------------|-------------|--------------|--------------|--------|----------------------|------|------|-------|-------------------|
| Condition | New Run | Old Run | | CO2 | CO | CO2/CO | THCw | CE | DRE | Vent Gas Flow Rate | | N2 Flow | HC Flow | Flare Tip Velocity | MWvg | MWhc | Vent Gas HV | FGCZ NHV | Steam Flow | Steam Temp | API 521 Steam | Actual S/VG | Actual S/HC | API 521 S/VG | API 521 S/HC | S/S521 | Wind Speed | THC | H2 | N2 | Visible Emissions |
| | | | | ppm-m | ppm-m | | ppm-m | % | % | SCFH | lb/hr | lb/hr | lb/hr | ft/s | lb/lbmol | lb/lbmol | Btu/scf | Btu/scf | lb/hr | °F | lb/hr | lb/lb | lb/lb | lb/lb | lb/lb | lb/lb | mph | mol% | mol% | mol % | |
| B | LTS 2-1 | 1.00 | Avg | 37,973 | 68 | 604 | 399 | 0.99 | 0.99 | 72,898 | 4,049 | 789 | 3,091 | 6.87 | 21 | 25 | 932 | 432 | 4,057 | 413 | 1,690 | 1.00 | 1.31 | 0.42 | 0.44 | 2.41 | 10 | 66 | 17 | 15 | 5.5 |
| B | LTS 2-2 | 1.00 | Avg | 16,019 | 23 | 712 | 95 | 0.99 | 0.99 | 72,325 | 4,021 | 793 | 2,985 | 6.81 | 21 | 24 | 906 | 423 | 4,013 | 413 | 1,666 | 1.00 | 1.34 | 0.41 | 0.44 | 2.42 | 7 | 65 | 17 | 15 | 4.5 |
| B | LTS 2-3 | 1.00 | Avg | 17,600 | 32 | 542 | 159 | 0.99 | 0.99 | 74,130 | 4,106 | 802 | 3,075 | 6.98 | 21 | 24 | 910 | 425 | 4,101 | 413 | 1,695 | 1.00 | 1.33 | 0.41 | 0.44 | 2.42 | 9 | 66 | 17 | 15 | 4.0 |
| B | LTS 2-4 | 1.00 | Avg | 11,336 | 29 | 406 | 99 | 0.99 | 0.99 | 71,925 | 3,982 | 1,499 | 2,176 | 6.78 | 21 | 25 | 693 | 321 | 4,016 | 413 | 1,654 | 1.01 | 1.98 | 0.41 | 0.44 | 2.44 | 8 | 46 | 24 | 29 | 4.0 |
| B | LTS 2-5 | 1.00 | Avg | 13,587 | 17 | 890 | 67 | 0.99 | 1.00 | 83,041 | 4,504 | 870 | 3,443 | 7.82 | 21 | 24 | 916 | 428 | 4,515 | 413 | 1,862 | 1.00 | 1.31 | 0.41 | 0.44 | 2.43 | 5 | 66 | 18 | 14 | 3.0 |
| B | LTS 2-6 | 1.00 | Avg | 8,896 | 44 | 261 | 196 | 0.97 | 0.98 | 80,228 | 4,322 | 1,307 | 3,206 | 7.56 | 20 | 27 | 880 | 414 | 4,343 | 413 | 1,780 | 1.00 | 1.36 | 0.41 | 0.46 | 2.45 | 6 | 56 | 19 | 22 | 3.0 |
| B | LTS 2-7 | 1.00 | Avg | 17,311 | 77 | 245 | 468 | 0.97 | 0.97 | 84,209 | 4,707 | 868 | 3,794 | 7.93 | 21 | 26 | 992 | 458 | 4,753 | 413 | 1,938 | 1.01 | 1.25 | 0.42 | 0.45 | 2.44 | 12 | 67 | 18 | 14 | 4.0 |
| B | LTS 2-8 | 1.00 | Avg | 1,671,635 | 2,356 | 1,013 | 8,509 | 0.99 | 0.99 | 78,799 | 4,384 | 869 | 3,360 | 7.42 | 21 | 25 | 939 | 436 | 4,349 | 413 | 1,826 | 0.99 | 1.29 | 0.42 | 0.44 | 2.38 | 9 | 65 | 19 | 15 | 3.5 |

6.0 APPENDIX

A.1 Calculations

A.2 PFTIR Calibration and Operation

A.3 VOC Emission Calculations

A.4 Personnel Involved with Flare Performance Test

Appendix A.1

Calculations

The following calculations are used this report.

1. Mass Flow - Hydrocarbons

The flare vent gas GC measures the following hydrocarbons on a 10-minute cycle.

| <i>i</i> | Measured Component | MW | Range | GC Units |
|----------|--------------------|-------|---------|----------|
| 1 | Methane | 16.04 | 0 - 100 | Mole % |
| 2 | Ethane | 30.07 | 0 - 100 | Mole % |
| 3 | Ethylene | 28.06 | 0 - 100 | Mole % |
| 4 | Acetylene | 26.04 | 0 - 100 | Mole % |
| 5 | Propane | 44.10 | 0 - 100 | Mole % |
| 6 | Propylene | 42.08 | 0 - 100 | Mole % |
| 7 | Iso-Butane | 58.12 | 0 - 100 | Mole % |
| 8 | Normal Butane | 58.12 | 0 - 100 | Mole % |
| 9 | i-Butene, Butene-1 | 56.11 | 0 - 100 | Mole % |
| 10 | Trans-Butene-2 | 56.11 | 0 - 100 | Mole % |
| 11 | Cis-Butene-2 | 56.11 | 0 - 100 | Mole % |
| 12 | 1,3 Butadiene | 54.09 | 0 - 100 | Mole % |
| 13 | Pentane-Plus (C5+) | 72.15 | 0 - 100 | Mole % |

Table A.1-1. List of hydrocarbons measured by Gas Chromatograph

The hydrocarbon mass flow rate is determined as follows:

$$Q_{HC} = \sum_{i=1}^{13} \left(\frac{MW_i \times HC_{mol_i}}{386} \right) \times Q_{FM} \quad \text{Eq. A.1-1}$$

Where:

Q_{HC} = Total hydrocarbon flow (lb/hr)

MW_i = Molecular weight of each compound (i) from Table A.1-1 above

Q_{FM} = Vent gas flow from ultrasonic monitor (scf/hr)

HC_{moli} = lb-mole of each compound (i) as a percentage of total mole% of vent gas from GC

386 = Molar volume of an ideal gas at 68 °F and 1 atm (scf/lb-mole)

2. Hydrocarbon Molecular Weight

$$MW_{hc} = \sum_{i=1}^{13} MW_i \times \left(\frac{HCmol_i}{HCmol_{total}} \right) \quad \text{Eq. A.1-2}$$

Where:

MW_{hc} = Molecular weight of the hydrocarbon fraction of the vent gas (lb/lb-mole)

MW_i = Molecular weight of each compound (i) from Table A.1-1 above

$HCmol_i$ = lb-mole of each compound (i) as a percentage of total mole% of vent gas from GC

$HCmol_{total}$ = lb-mole of total hydrocarbon fraction of the vent gas

3. Net Heating Value

The Net Heating Value of the Vent Gas is calculated from the GC data at the conclusion of each analytical cycle (~10 minutes). The Net Heating Value is the Lower Heating Value or LHV defined as:

“Lower Heating Value” or “LHV” shall mean the theoretical total quantity of heat liberated by the complete combustion of a unit volume or weight of a fuel initially at 25° Centigrade and 760 mmHg, assuming that the produced water is vaporized and all combustion products remain at, or are returned to, 25° Centigrade; however, the standard for determining the volume corresponding to one mole is 20° Centigrade.

The Net Heating Value of the Flare Combustion Zone Gas is determined as follows:

Performance Test of a Steam-Assisted Elevated Flare
Marathon Petroleum Company, Texas City Main Flare

$$NHV_{FCZG} = \frac{[(VG)(NHV_{VG})(386 / MW_{VG})] + [(PG)(NHV_{PG})(386 / MW_{PG})]}{[(VG)(386 / MW_{VG}) + (PG)(386 / MW_{PG}) + (S)(386 / 18)]} \quad \text{Eq. A.1-3}$$

Where:

| Parameter | Description (Unit) | Source |
|----------------|---|--|
| $NHV_{FCZG} =$ | Flare Combustion Zone Gas net heating value (BTU/scf) | Result |
| $VG =$ | Vent Gas mass flow rate (lb/hr) | From ultrasonic flare gas flow monitor |
| $NHV_{VG} =$ | Vent Gas Net Heating Value (BTU/scf) | From GC |
| $MW_{VG} =$ | Vent Gas molecular weight (lb/lb-mole) | From ultrasonic flow monitor |
| $PG =$ | Pilot Gas mass flow rate (lb/hr) | Constant = 6 |
| $NHV_{PG} =$ | Pilot Gas net heating value (BTU/scf) | Constant = 898 |
| $MW_{PG} =$ | Pilot Gas molecular weight (lb/lb-mole) | Constant = 18.5 |
| $S =$ | Actual total steam mass flow rate (lb/hr) | From ultrasonic steam flow monitor |
| $386 =$ | Constant (scf/lb-mole @ 68 °F and 1 atm) | Ideal Gas Law |

4. Steam Ratios

Five steam ratios are included in this report. They are calculated as described below.

a) Actual Total Steam to API 521 Total Steam Ratio (S/S_{521})

The Actual Total Steam to API 521 Total Steam Ratio is calculated as follows:

$$\frac{S}{S_{521}} \quad \text{Eq. A.1-4}$$

Where:

S = Actual Total Steam Mass Rate (lb/hr)

S_{521} = API 521 Total Steam Mass Rate (lb/hr)

The Actual Total Steam Mass Rate is calculated as:

$$S = FR_{ATS} \times (18 / 386)$$

Where:

S = Actual Total Steam Mass Rate (lb/hr)

FR_{ATS} = Steam Volumetric Flow Rate (scf/hr) from the ultrasonic flow monitor

18 = MW of water (lb/lb-mole)

386 = Constant (scf/lb-mole @ 68 °F and 1 atm)

The API 521 Total Steam Mass Rate is calculated as:

$$S_{521} = [0.0067 \times MW_{VG} + 0.275] \times VG \quad \text{Eq. A.1-5}$$

Where:

S_{521} = API 521 Total Steam Mass Rate (lb/hr)

MW_{VG} = Vent Gas molecular weight (lb/lb-mole) from ultrasonic flow monitor

VG = Vent Gas mass flow rate (lb/hr) from ultrasonic flow monitor

Performance Test of a Steam-Assisted Elevated Flare
Marathon Petroleum Company, Texas City Main Flare

Note: The equation is derived from a regression on the compound-specific steam-to-gas-ratios (pounds of steam to pounds of gas) set forth in Table 11 of the American Petroleum Institute's *Recommended Practice 521* (Fifth Edition, May 2007)

b) Actual Total Steam to Vent Gas Ratio (S/VG)

The Actual Total Steam to Vent Gas Ratio is calculated as follows:

$$\frac{S}{VG} \quad \text{Eq. A.1-6}$$

Where:

S = Actual Total Steam Mass Rate (lb/hr) calculated above

VG = Vent Gas Mass Rate (lb/hr) as measured by the ultrasonic flow monitor.
Direct measurement - no external calculation required.

c) Actual Total Steam to Hydrocarbon Ratio (S/HC)

The Actual Total Steam to Vent Gas Ratio is calculated as follows:

$$\frac{S}{HC} \quad \text{Eq. A.1-7}$$

Where:

S = Actual Total Steam Mass Rate (lb/hr) calculated above

HC = Hydrocarbon Mass Flow Rate (lb/hr) as calculated above.

d) API 521 Total Steam to Vent Gas Ratio (S₅₂₁/VG)

The API 521 Total Steam to Vent Gas Ratio is calculated as follows:

$$\frac{S_{521}}{VG} \quad \text{Eq. A.1-8}$$

Where:

S₅₂₁ = API 521 Total Steam Mass Rate (lb/hr) as calculated above

VG = Vent Gas Mass Rate (lb/hr) as measured by the ultrasonic flow monitor.
Direct measurement - no external calculation required.

e) API 521 Total Steam to Hydrocarbon Ratio (S521/HC)

The API 521 Total Steam to Hydrocarbon Ratio is calculated as follows:

$$\frac{S_{521}}{HC} \quad \text{Eq. A.1-9}$$

Where:

S_{521} = API 521 Total Steam Mass Rate (lb/hr) as calculated above

HC = Hydrocarbon Mass Flow Rate (lb/hr) as calculated above.

5. Total Hydrocarbons

Two hydrocarbon calculations are used in this report – weighted and unweighted. Each is shown below.

a) Total Hydrocarbons (unweighted)

$$THC = C_{CH_4} + C_{C_2H_4} + C_{C_3H_6} + C_{But} + C_{13But} + C_{HC} \quad \text{Eq. A.1-10}$$

Where:

THC = Total Hydrocarbon concentration (ppm-meters)

C_{CH_4} = Concentration of methane (ppm-meters)

$C_{C_2H_4}$ = Concentration of ethylene (ppm-meters)

$C_{C_3H_6}$ = Concentration of propylene (ppm-meters)

C_{But} = Concentration of butane (ppm-meters)

C_{13But} = Concentration of 1,3 Butadiene (ppm-meters)

C_{HC} = Concentration of all C5+ hydrocarbons (ppm-meters)

b) Total Hydrocarbons (weighted)

$$THC_w = C_{CH_4} + (C_{C_2H_4} \times 2) + (C_{C_3H_6} \times 3) + (C_{But} \times 4) + (C_{13But} \times 4) + (C_{HC} \times 5) \quad \text{Eq. A.1-11}$$

Where:

THC_w = Total Hydrocarbon weighted concentration (ppm-meters)

C_{xxx} = Concentration of individual hydrocarbons as in above equation

2, 3, ... = Number of carbon atoms in each molecule

6. Flare Combustion Efficiency

“Flare Combustion Efficiency” means the actual measured efficiency of converting organic carbon compounds to carbon dioxide as determined by the following equation:

$$CE = \frac{CO_2}{CO_2 + CO + OC}$$

Eq. A.1-12

Where:

CE = Combustion Efficiency

CO_2 = Carbon Dioxide (vol. %) measured by the PFTIR immediately above the Flare Combustion Zone

CO = Carbon Monoxide (vol. %) measured by the PFTIR immediately above the Flare Combustion Zone

OC = Organic Carbon (vol. %) measured by the PFTIR immediately above the Flare Combustion Zone, counting each carbon molecule separately where the concentration of each individual compound is multiplied by the number of carbon atoms it contains before summing (e.g. 0.1 volume percent ethane shall count as 0.2 volume percent OC because ethane has two carbon atoms).

7. Flare Destruction Efficiency

“Flare Destruction Efficiency” means the actual measured efficiency of converting organic carbon compounds to carbon dioxide and carbon monoxide as determined by the following equation:

$$DE = \frac{CO_2 + CO}{CO_2 + CO + OC}$$

Eq. A.1-13

Performance Test of a Steam-Assisted Elevated Flare
Marathon Petroleum Company, Texas City Main Flare

Where:

DE = Destruction Efficiency

CO₂ = Carbon Dioxide (vol. %) measured by the PFTIR immediately above the Flare Combustion Zone

CO = Carbon Monoxide (vol. %) measured by the PFTIR immediately above the Flare Combustion Zone

OC = Organic Carbon (vol. %) measured by the PFTIR immediately above the Flare Combustion Zone, counting each carbon molecule separately where the concentration of each individual compound is multiplied by the number of carbon atoms it contains before summing (e.g. 0.1 volume percent ethane shall count as 0.2 volume percent OC because ethane has two carbon atoms).

Appendix A.2

PFTIR Calibration and Operation

A.2-1 PFTIR Analytical Method and Procedure

Gases have highly variable absorption with wavelength. It is this variation that produces the absorption patterns that allow for their identification in the infrared. If the transmission of a gas is given by $\tau(\nu, T)$ then $[1 - \tau(\nu, T)]$ is the amount of absorption. The radiation the gas emits at temperature T is then given by:

$$N(\nu, T) = [1 - \tau(\nu, T)] * N_{bb}(\nu, T) \quad (1)$$

For flare measurements, it is this signal that is being detected from the hot gases above the combustion zone.

However, there are also other contributions to the signal an analyzer “sees.” As shown in Figure A.2-1, the background (typically the sky) has some emission, also defined by equation (2) that when transmitted through the plume and the intervening atmosphere is seen by the analyzer. The plume emissions transmitted through this same atmospheric path provides the signal of interest. The intervening atmosphere itself has some emission as does the FTIR instrument itself. These are also seen by the analyzer.

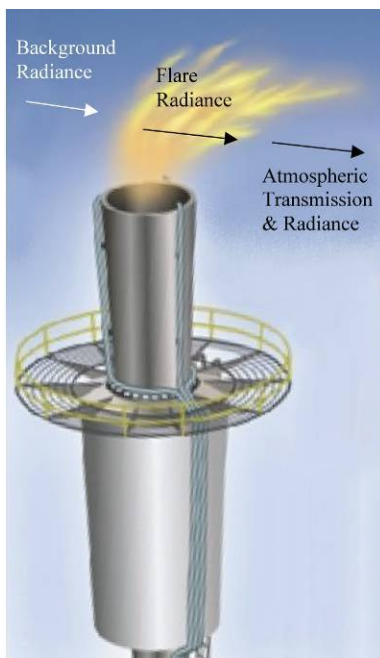


Figure A.2-1: Contributions to the measured flare radiance that must be accounted for.

Performance Test of a Steam-Assisted Elevated Flare Marathon Petroleum Company, Texas City Main Flare

The total radiant signal received then consists of:

$$N_{total} = N_{bkg} * \tau_{flr} * \tau_{atm} + N_{flr} * \tau_{atm} + N_{atm} + N_f \quad (2)$$

In Equation (3), the arguments v,T have been dropped for clarity and the individual terms are:

N_{total} = total radiance

N_{bkg} = background sky radiance

τ_{flr} = flare transmissivity

τ_{atm} = atmospheric transmissivity

N_{flr} = flare radiance

N_{atm} = atmospheric radiance

N_f = radiance of the FTIR instrument itself

The actual measurements performed by the PFTIR consist of the following:

M_{flr} = The measured plume radiance given by equation (2)

M_b = The measured background radiance taken by moving the PFTIR off the flare to monitor the sky background. This is given by

$$M_b = N_{bkg} * \tau_{atm} + N_{atm} + N_f$$

M_n = A measurement made looking at the calibration source (see below) with a cold (liquid nitrogen) emitter in place of the normal (black body)

M_{bb} = A measurement made looking at the calibration source with a commercial black body emitter in the source

τ_{atm} = Measured atmospheric path transmission

A.2-2 From Radiance to Transmission Spectra

Based on these measurements Equation (3) can be rearranged to give the plume transmission as:

$$\tau_{flr} = \frac{C * (M_{flr} - M_n) - N_{BB}^{flr} * \tau_{atm}}{C * (M_b - M_n) - N_{BB}^{flr} * \tau_{atm}} \quad (3)$$

In this equation, the superscript on the Planck function radiance (N_{BB}) denotes that this is the Planck function computed at the temperature of the flare. C is a calibration measurement made with a black body calibration source.

Atmospheric transmission τ_{atm} is also measured using the calibration source. In this case the black body is replaced by a standard infrared source and the measurement is made at a path length roughly equal to that of the slant-path from the PFTIR to the flare.

Performance Test of a Steam-Assisted Elevated Flare Marathon Petroleum Company, Texas City Main Flare

Atmospheric transmission is then given by:

$$\tau_{atm} = \frac{M_{IR} - M_n}{I_0} \quad (4)$$

M_{IR} is the measured signal from the calibration source using the IR source and M_n is the measured cold source as defined earlier. The only term not defined is I_0 . This is the so-called synthetic background. It is frequently used in open-path FTIR measurements to convert a measured spectrum to transmission. It represents the shape of the spectrum that the PFTIR would measure if no gases were present. It can be synthesized from the $(M_{IR} - M_n)$ measurement by doing a mathematical fit to points in the spectrum known to be free of molecular absorptions. An example is given in Figure A.2-2. In this Figure, the bottom plot is the measured spectrum (here a relatively clean spectrum done in the laboratory), the middle plot the points chosen for fitting, and the top plot the mathematical fit to the chosen points. The top plot is the I_0 spectrum.

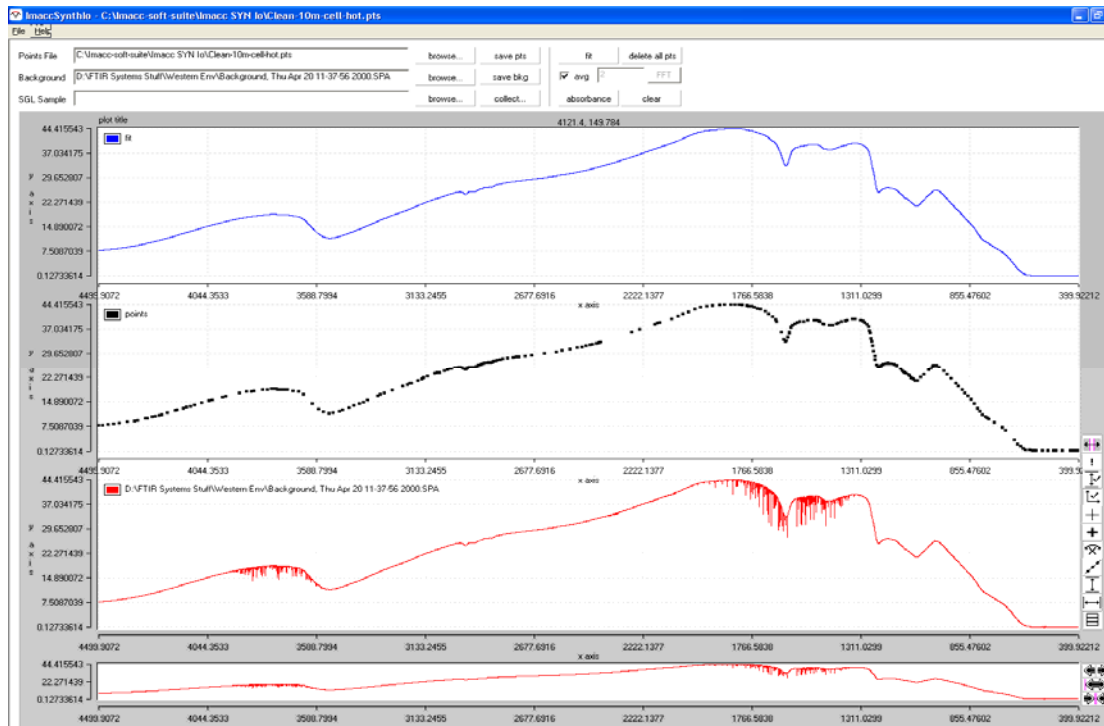


Figure A.2-2 Development of Synthetic Spectrum

A.2-3 Determination of Flare Temperature

With Equations (4) and (5), Equation (3) then contains only measured or computed terms. However, to compute the Planck function at the temperature of the flare

$$N_{BB}^{flr} \quad (5)$$

Performance Test of a Steam-Assisted Elevated Flare Marathon Petroleum Company, Texas City Main Flare

the flare gas temperature must be known. Fortunately, this can be measured using features in the PFTIR data itself. One convenient feature is the CO band near 2150 cm^{-1} . Figure A.2-3 shows this band at two different temperatures. The upper plot is at ambient temperature (300 K) and the bottom plot is at 550 K. The effect of increasing temperature is to expand the band shifting the peak position away from band center while increasing the strength of the weaker lines farther from band center. This is a sensitive function of temperature, so the shape of the band essentially measures temperature.

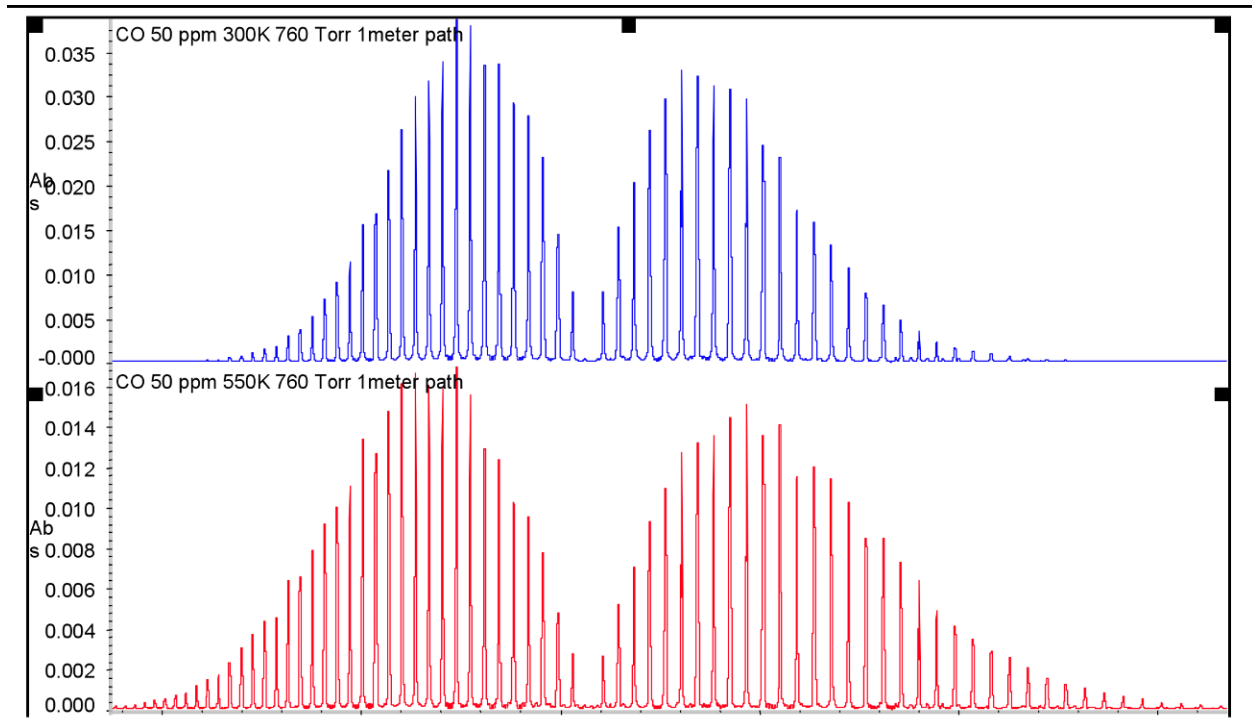


Figure A.2-3. Structure of the Fundamental CO Band at 300K (top) and 550K (bottom)
Showing Alteration of Band Shape with Temperature

The CO lines arise (in emission) from a transition of the molecule from a higher vibration/rotation state to a lower one. The transitions are dictated by quantum mechanics. However, the intensities of the individual lines are strongly influenced by the number of molecules in the initial state available to make the transition. This “population” of the initial states is dictated by the Boltzmann distribution which is given by:

$$N_{J''} = N_0 \frac{2J''+1}{Q} \exp\left[\frac{-E''}{kT}\right] \quad (6)$$

Here $N_{J''}$ is the number of molecules in the initial rotational state defined by the rotational quantum number J'' . N_0 is the total number of molecules available, E'' the energy of the initial state, k Boltzmann’s constant, T the absolute temperature, and Q a “partition sum.” The partition sum is just the sum of the exponential term over all possible energy levels. If the log of the

Performance Test of a Steam-Assisted Elevated Flare Marathon Petroleum Company, Texas City Main Flare

measured intensity of the CO lines is plotted against the initial state energy, the plot is linear and its slope is proportional to

$$\frac{hc}{kT} \quad (7)$$

Where h is Planck's constant and c the speed of light.

Temperature can therefore be determined by measuring the slope of the plot. An example of this process is shown in Figure B-5. In this case the temperature was 225° C and the group of lines to the left in Figure B-4 was used. These are defined as the R-branch lines of the CO band.

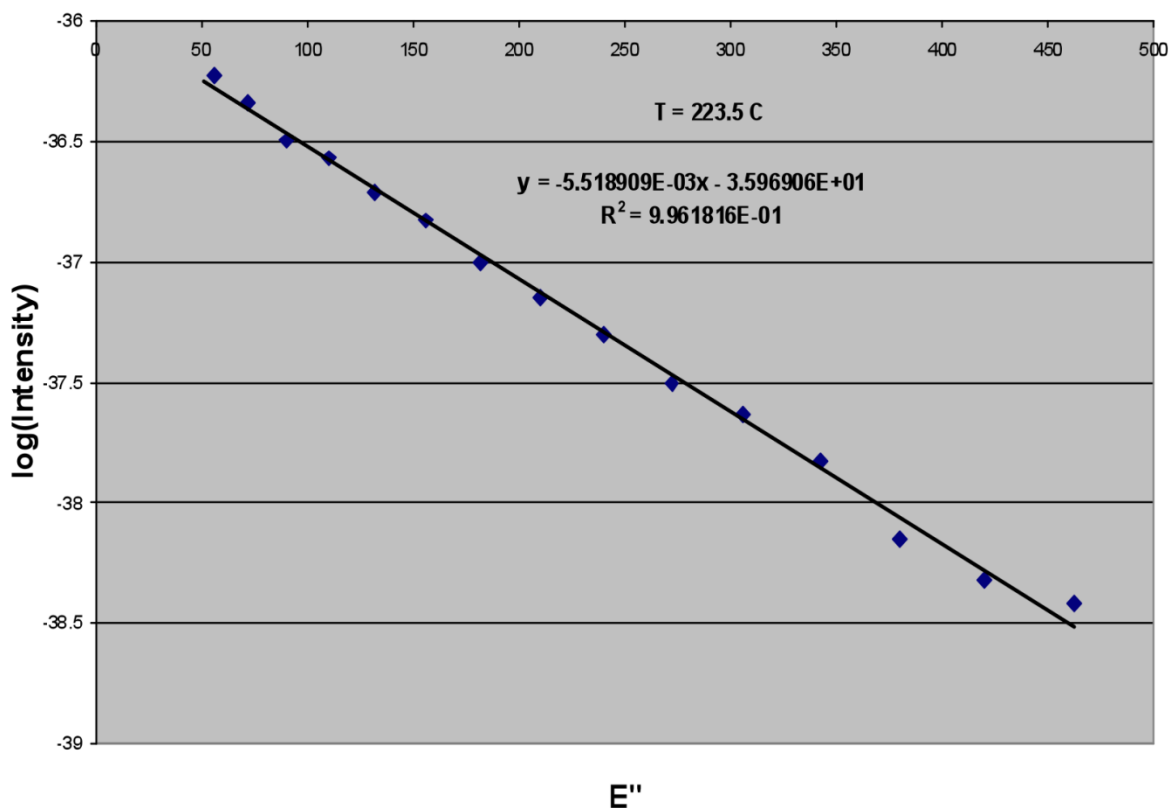


Figure A.2-4 Plot of the log of the measured intensity of the CO lines vs. initial state energy

Given temperature, all terms in Equation 3 can be determined. Equation 3 represents the transmission spectrum, just as would be observed if an active FTIR were used and an IR beam propagated through the plume. As a result, the same algorithms used in normal spectroscopy can be used to analyze this transmission spectrum.

A.2-4 From Transmission to Absorption Spectra

As in normal absorption spectroscopy, the transmission is exponential in gas concentration. That is transmission is given by:

$$\tau_{plume} = e^{-K(v)*c*l} \quad (8)$$

Where $K(v)$ is the absorption coefficient for the spectral line, c the gas concentration, and l the path length in the gas. Effectively $K(v)$ is the reference standard in the FTIR for the gas being monitored. Taking the negative log of this equation gives what is called Absorbance. For historical reasons, log base 10 is used and thus gives:

$$\text{Absorbance}(v) = (0.434)K(v) * c * l \quad (9)$$

where the constant 0.434 is the log base 10 of e . Absorbance is linear in concentration times path length and the absorbance spectrum is analyzed using standard Classical Least Squares (CLS) procedures to get the individual gas concentrations in the spectrum.

A.2-5 Determination of Component Concentrations with Classical Least Squares Analysis

In most real measurement scenarios, there are several gases present. The job of Classical least squares is to analyze a measured spectrum and determine the concentration of all gases that have features in the spectrum. To make the job as easy as possible, the full spectrum is divided into analysis regions. These regions are chosen to have strong features of the gases of interest and to have as few as possible other gas features present. Because of the complexity of infrared spectra, it is not possible to find regions with only one compound present. There are always other compounds absorbing in the same region and these become interferences in the analysis. CLS then tries to match the measured spectrum using a combination of reference spectra each of which is scaled in concentration to make the match as good as possible. In mathematical form this is:

$$S_i = \sum_j R_j C_j \quad (10)$$

The i in this equation is the data point number which simply counts all the data points (or wavenumber points) in the analysis region. The j sums over all the compounds present in the region. Because there will be hundreds of points (i) in any analysis region and only a small number of compounds (j) the best way to make the right side of this equation match the left side is to perform a least squares fitting. This is the same process that is done in fitting a curve to data points in a plot. The least squares process essentially makes the difference given by

$$\Delta_i = S_i - \sum_j R_j C_j \quad (11)$$

as small as possible. In reality, this is done by minimizing the sum of the square differences or

$$\sum_i \Delta_i^2 = \text{minimum} \quad (12)$$

To minimize equation (12) its derivative is taken and this derivative is set to zero (the condition for a minimum). In the process of doing this, two new sums appear. These are defined as:

$$X_{jk} = \sum_i [R_{ij} R_{ik}] \quad (13)$$

and

$$Y_k = \sum_i [S_i R_{ik}] \quad (14)$$

In terms of these two sums the minimizing of equation (12) comes down to solving the equation:

$$\sum_j C_j X_{jk} = Y_k \quad (15)$$

This can be put in matrix form as:

$$C \cdot X = Y \quad (16)$$

The formal solution to this is to multiply both sides by the inverse matrix of X giving the gas concentration matrix as:

$$C = X^{-1} \cdot Y \quad (17)$$

If this is put back in the form of sums it is:

$$\sum_k Z_{jk} Y_k = C_j \quad (18)$$

The determination of gas concentrations therefore reduces to forming the sums in equations 13 and 14, generating the inverse of the X matrix and substituting in equation 18 to compute the concentrations.

One bonus in solving by least squares is that the errors associated with the fitting can be determined. These are essentially the differences of equation 11. However, generally one reports the standard deviation or RMS difference. This is defined by:

$$\sigma_j = \sqrt{\frac{\sum_i d_i^2}{[N-NJ]}} \quad (19)$$

Here N is the total number of data points in the region and NJ the number of concentrations being solved for. By substituting in the definition of Δ and rearranging terms, it can be shown that this can be expressed as:

$$\sigma_j = \left\{ \frac{\sum_i d_i^2}{[N-NJ]} \left[\sum_i S_i^2 - \sum_i S_i \sum_k C_k R_{ik} \right] \right\} \quad (20)$$

All terms in this equation are as defined previously and Z_{jj} is the j,j diagonal element of the Z matrix which is the inverse of the X matrix. What is normally reported in CLS routines is $2 \cdot \sigma$ or the 95% confidence interval.

Performance Test of a Steam-Assisted Elevated Flare Marathon Petroleum Company, Texas City Main Flare

To compute combustion efficiency, the concentrations of CO, CO₂, and total hydrocarbon (THC) are used to compute:

$$Eff = \frac{[CO_2]}{[CO_2] + [CO] + [THC] + [soot]} \quad (21)$$

The remaining term, [soot], is the concentration of any soot present. If it is present at any significant concentration, it will be seen in the IR spectra as an attenuation of the signal with characteristic spectral shapes driven by particle size distribution. It is not believed that soot will be a significant issue in most well run flares but if it is present procedures can be developed to treat it.

A.2-6 Additional Detail on Determination of Flare Plume Temperature

As stated above, transmission is given by:

$$T(\nu) = e^{-\kappa(\nu) \cdot C \cdot L} \quad (22)$$

Absorbance is defined as the log of transmittance. For historical reasons, this is log base 10 so absorbance is:

$$-\log_{10}[T(\nu)] = (0.434) * \kappa(\nu) * C * L \quad (23)$$

$\kappa(\nu)$ is the absorption coefficient. It consists of the line strength and a “form factor” that is dependent on the broadening mechanism for the conditions of the measurement. At pressures near atmospheric, the broadening is pressure broadening so the line shape is given by the Lorentz function. This makes $\kappa(\nu)$ equal to:

$$\kappa(\nu) = \frac{S \gamma}{\pi[(\nu - \nu_0)^2 + \gamma^2]} \quad (24)$$

The peak of the absorption coefficient is then given by $\nu = \nu_0$, or:

$$\kappa(\nu)^{pk} = \frac{S}{\pi \gamma} \quad (25)$$

But the line strength is given by:

$$S = \frac{8\pi^2 \nu}{3hc} \frac{e^{-E''/kT}}{Q} [1 - e^{-hc\nu/kT}] |\langle \Psi'' | \mu(r) | \Psi' \rangle|^2 \quad (26)$$

The first exponential term is the Boltzman distribution. The second term is the spontaneous emission term and the final expression the quantum mechanical transition moment for the

transition. Because the variation in the transition moment across the band is small, the important term is the Boltzman distribution. The Boltzman distribution says that the line strength will vary as the initial state energy E'' ratioed to Q . Where Q is the sum of all the possible energy levels (E'') for the molecule. Because S will vary as:

$$e^{-E''/kT} \quad (27)$$

so will $\kappa(\nu)^{P_R}$. For molecules like CO the initial state energy E'' is given by:

$$E'' = B_v J(J+1) \quad (28)$$

Where B_v is the rotational constant for vibrational state v and J is the quantum number for rotational state J . Given these definitions:

$$\kappa(\nu_0)^{P_R} = \frac{e^{-\frac{B_v J(J+1)hc}{kT}}}{Z} \quad (29)$$

Where h is Planck's constant and c is the speed of light. Therefore the absorbance which is the log of this gives:

$$-\log[\kappa(\nu_0)^{P_R}] = \frac{B_v J(J+1)hc}{kT} \quad (30)$$

This means that a plot of the peak absorbance of the lines times their half width against $B_v J(J+1)$ will be linear and the slope will be:

$$\frac{hc}{kT} \quad (31)$$

This is, therefore, a measurement of the temperature.

A.2-7 Additional Detail on Q-Branch Subtraction

If an absorption becomes too strong, it will saturate (become totally absorbing), and it is not useful for spectroscopic analysis. During this test program, some of the CO₂ data points at long wavelength exhibited this problem. Rather than discard the spectra as invalid, an alternative analysis was applied, avoiding the spectral regions considered to be invalid. This alternative analysis, referred to here as Q-branch Subtraction, is described below. All minute-by-minute CO₂ data points have the Q-branch subtracted.

In the case of CO₂, the analytical region used is from 725 cm⁻¹ to 765 cm⁻¹. This band has P, Q and R branches structures as shown in Figure A.2-5. The Q-branch, as is typical, is narrow and

very intense compared to the P and R branches. This is because the Q-branch consists of many overlapped lines each adding to the absorption intensity.

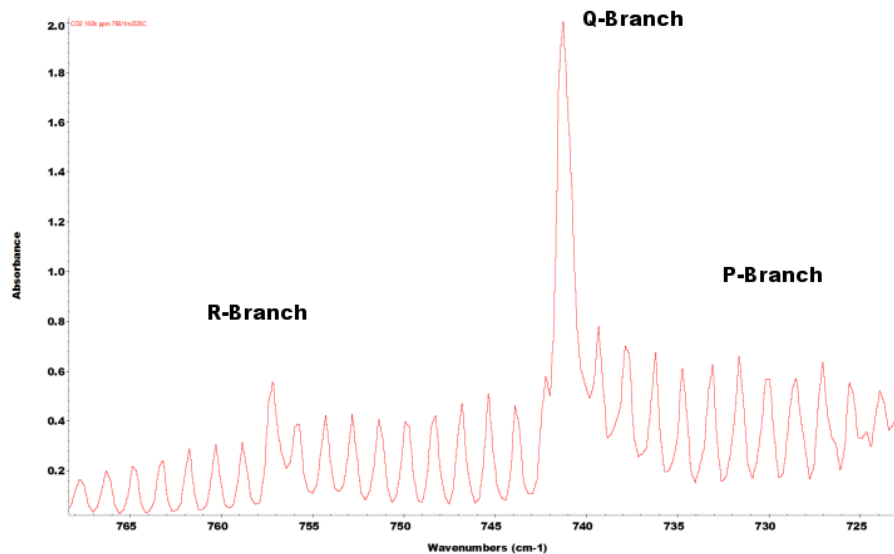


Figure A.2-5: CO₂ Band at 725 to 765 cm⁻¹ Showing P, Q, and R, Branches

If absorption features are not too strong (absorbance < 1.0 absorbance units-AU) they tend to be linear in absorbance. As they get stronger, the center of the lines become opaque (absorbance > 1.0 AU) and become very non linear. The only growth possible for an opaque line is in the wings which will grow more as the square root of concentration (i.e. the line just gets broader in total absorption). An example of this is shown in Figures A.2-6 and A.2-7. Figure A.2-6 shows the transmission of a very strong CO₂ band with the Q-branch becoming totally absorbing (opaque). In absorbance units the same spectrum appears as in Figure A.2-7. The opaque Q-branch has absorbance ~2.0 AU.

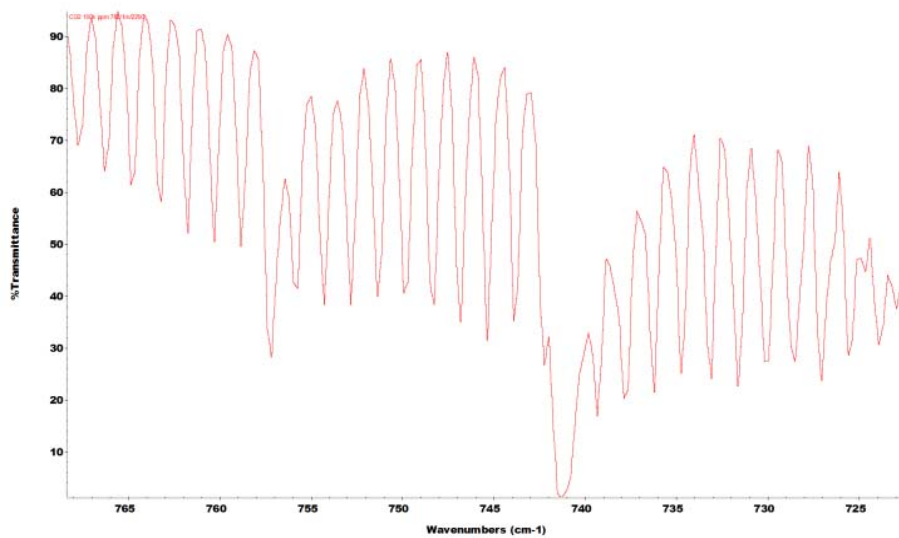


Figure A.2-6: CO₂ Band at 725 cm⁻¹ to 765 cm⁻¹ Showing Q-branch Totally Absorbing near 741 cm⁻¹

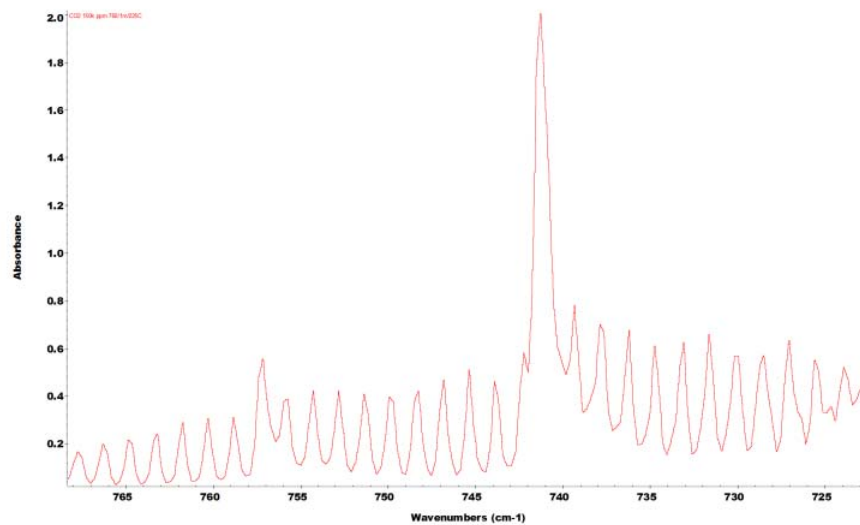


Figure A.2-7: CO₂ Band of Figure A.2-6 Converted to Absorbance
(The Q-branch has absorbance ~ 2.0)

When absorbance gets too strong, the analysis will be compromised because of the slow variation of absorbance with concentration. To optimize the analysis method, opaque regions must be avoided. For the CO₂ band above, this means eliminating the Q-branch from the analysis when it gets too strong. An example of this is shown in Figure A.2-8. Here, the band is divided into two windows (as shown in white) excluding the Q-branch from analysis, shown in grey. This division of analysis windows allows the reliable quantification of much higher concentrations of CO₂ than would be otherwise possible.

Performance Test of a Steam-Assisted Elevated Flare Marathon Petroleum Company, Texas City Main Flare

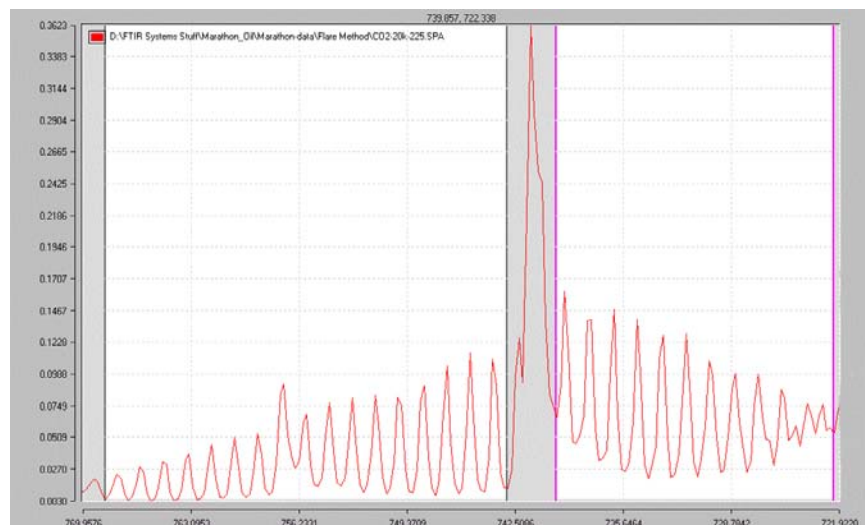


Figure A.2-8: Analysis Region for CO₂ Showing Sub-windows (in white) eliminating the Q-branch from the Analysis

Appendix A.3

VOC Emission Calculations

The CAA 114 request received by Marathon Petroleum Company required that the emissions from flares be estimated as a result of this performance test. The emissions rate and destruction removal efficiency of non-methane, non-ethane organics are required to be submitted, along with speciated compounds in terms of ppmvd, pounds per hour (lb/hr) and tons per year (ton/yr).

The Passive FTIR cannot be used to determine absolute concentrations in the flare plume. The resulting output is in terms of concentration x pathlength, and the pathlength remains an unknown. In fact, due to wind speed, direction, and other external factors, the pathlength was constantly in motion, likely changing from run average to run average for any given test series. Therefore, the PFTIR data cannot be used to determine the absolute concentration or emissions rate of speciated compounds.

Marathon has prepared the following estimates of non-methane, non-ethane total VOCs in the using the following estimating technique.

$$Q_{VOC} = VG - VG(x_{Ethane} + x_{Methane} + x_{Hydrogen} + x_{Nitrogen})$$

Where,

Q_{voc} = Flow Rate of VOC compounds (lb/hr)

VG = Total vent gas flow (lb/hr)

x_i = mass fraction of component as measured by the gas chromatograph present on flare header.

$$E_{VOC} = Q_{VOC} \times (1 - DRE)$$

Where,

E_{voc} = Emissions rate of VOC compounds (lb/hr)

DRE = Destruction Removal Efficiency calculated using PFTIR data.

Performance Test of a Steam-Assisted Elevated Flare
Marathon Petroleum Company, Texas City Main Flare

| Condition/Run | | | Process Data | | | | | | | | | | | Emissions | |
|---------------|---------|-----|--------------|------|--------------------|-------|---------|---------|--------|-------------|----------------------|----------------|---------------------------------|---------------------|---------------------|
| | | | Efficiency | | Vent Gas | | | | | Ratio | Vent Gas Composition | | | Emissions | |
| Condition | New Run | | CE | DRE | Vent Gas Flow Rate | | N2 Flow | HC Flow | MWvg | Actual S/VG | Non-VOC Components | VOC Components | Total VOC in Vent Gas Mass Flow | Total VOC Emissions | Total VOC Emissions |
| | | | | | SCFH | #/hr | #/hr | #/hr | #/#mol | | wt% | wt% | lb/hr | lb/hr | TPY |
| A19 | 1-1 | Avg | 0.98 | 0.98 | 28,857 | 1,778 | 796 | 971 | 22.45 | 0.94 | 0.64 | 0.36 | 640 | 13 | 56 |
| A19 | 1-2 | Avg | 0.99 | 0.99 | 30,063 | 1,793 | 924 | 1,065 | 22.39 | 0.97 | 0.60 | 0.40 | 712 | 7 | 31 |
| A19 | 1-3 | Avg | 0.98 | 0.99 | 26,152 | 1,683 | 758 | 864 | 23.26 | 1.07 | 0.64 | 0.36 | 599 | 6 | 26 |
| A19 | 2-1 | Avg | 0.98 | 0.98 | 29,641 | 2,081 | 540 | 1,268 | 25.06 | 1.25 | 0.57 | 0.43 | 891 | 18 | 78 |
| A19 | 3-1 | Avg | 0.96 | 0.97 | 28,710 | 1,867 | 500 | 1,275 | 23.38 | 1.51 | 0.57 | 0.43 | 808 | 24 | 106 |
| A19 | 3-2 | Avg | 0.98 | 0.99 | 30,234 | 1,782 | 661 | 1,196 | 21.90 | 1.49 | 0.61 | 0.39 | 698 | 7 | 31 |
| A19 | 4-1 | Avg | 0.94 | 0.94 | 28,453 | 1,787 | 526 | 1,128 | 22.67 | 2.01 | 0.63 | 0.37 | 666 | 40 | 175 |
| A19 | 4-2 | Avg | 0.93 | 0.94 | 28,966 | 1,796 | 534 | 1,250 | 22.41 | 2.01 | 0.59 | 0.41 | 742 | 45 | 195 |
| A19 | 5-1 | Avg | 0.84 | 0.85 | 34,134 | 1,912 | 367 | 1,499 | 20.70 | 2.51 | 0.62 | 0.38 | 730 | 109 | 480 |
| A19 | 6-1 | Avg | 0.86 | 0.87 | 34,513 | 1,951 | 418 | 1,452 | 20.90 | 2.69 | 0.65 | 0.35 | 682 | 89 | 388 |
| A19 | 7-1 | Avg | 0.90 | 0.91 | 27,641 | 1,731 | 516 | 1,072 | 22.31 | 3.00 | 0.64 | 0.36 | 617 | 56 | 243 |
| A19 | 7-2 | Avg | 0.82 | 0.82 | 33,711 | 1,921 | 458 | 1,384 | 21.08 | 2.98 | 0.65 | 0.35 | 671 | 121 | 529 |
| A11 | 1-1 | Avg | 0.99 | 0.99 | 21,255 | 1,220 | 270 | 821 | 21.01 | 1.34 | 0.71 | 0.29 | 356 | 4 | 16 |
| A11 | 2-1 | Avg | 0.96 | 0.96 | 16,835 | 1,053 | 392 | 573 | 21.83 | 1.79 | 0.69 | 0.31 | 331 | 13 | 58 |
| A11 | 2-2 | Avg | 0.97 | 0.98 | 16,423 | 1,039 | 378 | 548 | 21.96 | 1.76 | 0.70 | 0.30 | 313 | 6 | 27 |
| A11 | 3-1 | Avg | 0.97 | 0.97 | 16,571 | 1,062 | 411 | 538 | 21.94 | 2.01 | 0.70 | 0.30 | 323 | 10 | 42 |
| A11 | 3-2 | Avg | 0.98 | 0.98 | 17,116 | 1,082 | 429 | 556 | 22.14 | 2.04 | 0.69 | 0.31 | 331 | 7 | 29 |
| A11 | 4-1 | Avg | 0.96 | 0.96 | 17,635 | 1,074 | 384 | 596 | 21.74 | 2.50 | 0.71 | 0.29 | 316 | 13 | 55 |
| A11 | 5-1 | Avg | 0.94 | 0.94 | 18,058 | 1,120 | 453 | 594 | 22.28 | 2.99 | 0.68 | 0.32 | 354 | 21 | 93 |
| A11 | 6-1 | Avg | 0.93 | 0.93 | 17,757 | 1,048 | 325 | 633 | 21.22 | 3.52 | 0.71 | 0.29 | 302 | 21 | 93 |
| A11 | 7-1 | Avg | 0.87 | 0.88 | 17,974 | 1,129 | 452 | 586 | 22.23 | 4.01 | 0.69 | 0.31 | 353 | 42 | 186 |
| A11 | 8-1 | Avg | 0.81 | 0.82 | 17,601 | 1,092 | 425 | 580 | 22.02 | 4.50 | 0.70 | 0.30 | 326 | 59 | 257 |
| A11 | 9-1 | Avg | 0.74 | 0.76 | 17,995 | 1,113 | 451 | 592 | 22.30 | 5.00 | 0.68 | 0.32 | 355 | 85 | 373 |
| A11 | 10-1 | Avg | 0.77 | 0.78 | 18,213 | 1,138 | 457 | 600 | 22.28 | 5.26 | 0.68 | 0.32 | 364 | 80 | 351 |
| A11 | 11-1 | Avg | 0.68 | 0.69 | 16,272 | 1,066 | 407 | 540 | 22.24 | 5.51 | 0.68 | 0.32 | 339 | 105 | 460 |
| A11 | 11-2 | Avg | 0.66 | 0.67 | 20,434 | 1,224 | 521 | 664 | 21.95 | 5.32 | 0.69 | 0.31 | 374 | 123 | 540 |
| A11 | 12-1 | Avg | 0.62 | 0.69 | 17,047 | 1,082 | 411 | 582 | 22.05 | 5.76 | 0.68 | 0.32 | 349 | 108 | 473 |
| A11 | 13-1 | Avg | 0.62 | 0.63 | 17,458 | 1,115 | 420 | 565 | 22.34 | 6.01 | 0.70 | 0.30 | 335 | 124 | 542 |
| A11 | 14-1 | Avg | 0.00 | 0.00 | 17,295 | 1,119 | 425 | 578 | 22.33 | 6.96 | 0.68 | 0.32 | 353 | 353 | 1546 |

Performance Test of a Steam-Assisted Elevated Flare
Marathon Petroleum Company, Texas City Main Flare

| Condition/Run | | | | Process Data | | | | | | | | | | Emissions | |
|---------------|---------|-----|------------|--------------|--------------------|-------|---------|---------|--------|-------------|----------------------|----------------|---------------------------------|---------------------|---------------------|
| | | | Efficiency | | Vent Gas | | | | | Ratio | Vent Gas Composition | | | Emissions | |
| Condition | New Run | | CE | DRE | Vent Gas Flow Rate | | N2 Flow | HC Flow | MWvg | Actual S/VG | Non-VOC Components | VOC Components | Total VOC in Vent Gas Mass Flow | Total VOC Emissions | Total VOC Emissions |
| | | | | | SCFH | #/hr | #/hr | #/hr | #/#mol | | wt% | wt% | lb/hr | lb/hr | TPY |
| B | 1-1 | Avg | 0.99 | 0.99 | 74,030 | 4,067 | 819 | 3,047 | 20.66 | 0.42 | 0.65 | 0.35 | 1424 | 14 | 62 |
| B | 1-2 | Avg | 0.99 | 0.99 | 74,960 | 4,136 | 811 | 3,117 | 20.74 | 0.41 | 0.64 | 0.36 | 1471 | 15 | 64 |
| B | 1-3 | Avg | 1.00 | 1.00 | 78,085 | 4,393 | 866 | 3,330 | 21.02 | 0.40 | 0.63 | 0.37 | 1625 | 0 | 0 |
| B | 2-1 | Avg | 0.99 | 0.99 | 72,273 | 3,999 | 793 | 2,979 | 20.71 | 0.50 | 0.65 | 0.35 | 1409 | 14 | 62 |
| B | 2-2 | Avg | 0.99 | 0.99 | 72,138 | 3,955 | 788 | 2,982 | 20.48 | 0.50 | 0.65 | 0.35 | 1390 | 14 | 61 |
| B | 2-3 | Avg | 1.00 | 1.00 | 78,899 | 4,391 | 873 | 3,365 | 21.02 | 0.50 | 0.63 | 0.37 | 1623 | 0 | 0 |
| B | 3-1 | Avg | 0.99 | 0.99 | 73,321 | 4,098 | 804 | 3,027 | 20.80 | 0.75 | 0.65 | 0.35 | 1444 | 14 | 63 |
| B | 3-2 | Avg | 0.99 | 0.99 | 73,531 | 4,010 | 808 | 2,998 | 20.48 | 0.75 | 0.66 | 0.34 | 1362 | 14 | 60 |
| B | 3-3 | Avg | 1.00 | 1.00 | 78,576 | 4,385 | 867 | 3,353 | 21.04 | 0.75 | 0.63 | 0.37 | 1626 | 0 | 0 |
| B | 4-1 | Avg | 0.99 | 0.99 | 72,756 | 4,040 | 788 | 3,086 | 20.93 | 1.00 | 0.63 | 0.37 | 1506 | 15 | 66 |
| B | 4-2 | Avg | 0.99 | 0.99 | 72,229 | 4,015 | 792 | 2,980 | 20.68 | 1.00 | 0.65 | 0.35 | 1397 | 14 | 61 |
| B | 4-3 | Avg | 0.99 | 0.99 | 78,661 | 4,380 | 867 | 3,354 | 21.03 | 0.99 | 0.63 | 0.37 | 1622 | 16 | 71 |
| B | 5-1 | Avg | 0.99 | 0.99 | 73,592 | 4,058 | 796 | 3,086 | 20.73 | 1.25 | 0.64 | 0.36 | 1465 | 15 | 64 |
| B | 5-2 | Avg | 0.99 | 0.99 | 73,372 | 4,039 | 803 | 3,039 | 20.69 | 1.25 | 0.65 | 0.35 | 1420 | 14 | 62 |
| B | 6-1 | Avg | 0.98 | 0.99 | 73,347 | 4,056 | 795 | 3,045 | 20.73 | 1.50 | 0.65 | 0.35 | 1438 | 14 | 63 |
| B | 6-2 | Avg | 0.98 | 0.99 | 73,818 | 4,063 | 805 | 3,068 | 20.65 | 1.50 | 0.65 | 0.35 | 1436 | 14 | 63 |
| B | 6-3 | Avg | 0.98 | 0.98 | 78,654 | 4,394 | 863 | 3,362 | 21.02 | 1.50 | 0.63 | 0.37 | 1628 | 33 | 143 |
| B | 7-1 | Avg | 0.98 | 0.98 | 73,738 | 4,088 | 801 | 3,065 | 20.74 | 1.60 | 0.64 | 0.36 | 1452 | 29 | 127 |
| B | 7-2 | Avg | 0.98 | 0.98 | 73,651 | 4,076 | 802 | 3,055 | 20.65 | 1.60 | 0.65 | 0.35 | 1430 | 29 | 125 |
| B | 7-3 | Avg | 0.95 | 0.96 | 78,737 | 4,413 | 862 | 3,361 | 20.99 | 1.60 | 0.63 | 0.37 | 1635 | 65 | 286 |
| B | 8-1 | Avg | 0.98 | 0.98 | 75,583 | 4,168 | 821 | 3,146 | 20.71 | 1.70 | 0.64 | 0.36 | 1483 | 30 | 130 |
| B | 8-2 | Avg | 0.96 | 0.96 | 75,163 | 4,164 | 816 | 3,119 | 20.64 | 1.70 | 0.65 | 0.35 | 1461 | 58 | 256 |
| B | 9-1 | Avg | 0.98 | 0.98 | 74,171 | 4,136 | 806 | 3,088 | 20.71 | 1.80 | 0.64 | 0.36 | 1470 | 29 | 129 |
| B | 9-2 | Avg | 0.89 | 0.90 | 76,448 | 4,198 | 833 | 3,167 | 20.64 | 1.80 | 0.65 | 0.35 | 1472 | 147 | 645 |
| B | 10-1 | Avg | 0.91 | 0.92 | 74,443 | 4,125 | 809 | 3,095 | 20.70 | 1.88 | 0.64 | 0.36 | 1466 | 117 | 514 |
| B | 10-2 | Avg | 0.97 | 0.97 | 76,139 | 4,190 | 830 | 3,148 | 20.67 | 1.90 | 0.65 | 0.35 | 1469 | 44 | 193 |
| C | 1-1 | Avg | 0.99 | 0.99 | 57,409 | 5,710 | 591 | 4,736 | 37.47 | 0.31 | 0.15 | 0.85 | 4835 | 48 | 212 |
| C | 1-2 | Avg | 1.00 | 1.00 | 55,810 | 5,723 | 446 | 5,053 | 38.58 | 0.30 | 0.11 | 0.89 | 5102 | 0 | 0 |
| C | 1-3 | Avg | 1.00 | 1.00 | 52,200 | 5,122 | 593 | 4,067 | 36.16 | 0.35 | 0.20 | 0.80 | 4081 | 0 | 0 |
| C | 2-1 | Avg | 0.99 | 0.99 | 57,730 | 5,644 | 726 | 4,380 | 36.47 | 0.50 | 0.20 | 0.80 | 4507 | 45 | 197 |
| C | 2-2 | Avg | 0.99 | 1.00 | 55,067 | 5,657 | 445 | 4,980 | 38.58 | 0.50 | 0.11 | 0.89 | 5039 | 0 | 0 |
| C | 2-3 | Avg | 1.00 | 1.00 | 54,530 | 5,441 | 540 | 4,602 | 37.42 | 0.52 | 0.15 | 0.85 | 4620 | 0 | 0 |
| C | 3-1 | Avg | 0.99 | 0.99 | 57,843 | 5,247 | 733 | 3,913 | 34.21 | 1.00 | 0.29 | 0.71 | 3742 | 37 | 164 |
| C | 3-2 | Avg | 0.99 | 0.99 | 46,186 | 3,319 | 473 | 1,893 | 26.63 | 0.91 | 0.67 | 0.33 | 1079 | 11 | 47 |
| C | 3-3 | Avg | 0.99 | 1.00 | 51,981 | 5,178 | 466 | 4,609 | 37.54 | 1.00 | 0.13 | 0.87 | 4522 | 0 | 0 |
| C | 4-1 | Avg | 1.00 | 1.00 | 52,916 | 5,382 | 462 | 4,728 | 37.86 | 1.20 | 0.12 | 0.88 | 4728 | 0 | 0 |
| C | 5-1 | Avg | 0.99 | 0.99 | 51,904 | 5,279 | 444 | 4,701 | 37.97 | 1.30 | 0.12 | 0.88 | 4663 | 47 | 204 |

Performance Test of a Steam-Assisted Elevated Flare
Marathon Petroleum Company, Texas City Main Flare

| Condition/Run | | | | | Process Data | | | | | | | | | Emissions | |
|---------------|---------|-----|------------|------|--------------------|---------|---------|-------|-------------|--------------------|----------------------|---------------------------------|---------------------|---------------------|------|
| | | | Efficiency | | Vent Gas | | | | | Ratio | Vent Gas Composition | | | Emissions | |
| Condition | New Run | | CE | DRE | Vent Gas Flow Rate | N2 Flow | HC Flow | MWvg | Actual S/VG | Non-VOC Components | VOC Component s | Total VOC in Vent Gas Mass Flow | Total VOC Emissions | Total VOC Emissions | |
| | | | | | SCFH | #/hr | #/hr | #/hr | #/#mol | | wt% | wt% | lb/hr | lb/hr | TPY |
| D | 1-1 | Avg | 0.98 | 1.00 | 36,914 | 3,979 | 388 | 3,481 | 40.44 | 0.42 | 0.14 | 0.86 | 3426 | 0 | 0 |
| D | 1-2 | Avg | 0.95 | 0.96 | 38,153 | 4,146 | 357 | 3,696 | 40.12 | 0.41 | 0.12 | 0.88 | 3654 | 146 | 640 |
| D | 1-3 | Avg | 0.99 | 1.00 | 39,587 | 4,231 | 404 | 3,739 | 38.10 | 0.42 | 0.13 | 0.87 | 3669 | 0 | 0 |
| D | 2-1 | Avg | 1.00 | 1.00 | 37,408 | 4,074 | 423 | 3,493 | 40.25 | 0.55 | 0.15 | 0.85 | 3484 | 0 | 0 |
| D | 2-2 | Avg | 0.98 | 0.98 | 39,744 | 4,319 | 444 | 3,686 | 40.23 | 0.54 | 0.14 | 0.86 | 3711 | 74 | 325 |
| D | 2-3 | Avg | 0.99 | 1.00 | 40,116 | 4,152 | 473 | 3,688 | 38.10 | 0.51 | 0.15 | 0.85 | 3537 | 0 | 0 |
| D | 3-1 | Avg | 0.99 | 0.99 | 37,613 | 4,034 | 436 | 3,487 | 40.15 | 0.75 | 0.15 | 0.85 | 3439 | 34 | 151 |
| D | 3-2 | Avg | 0.98 | 0.98 | 40,561 | 4,399 | 459 | 3,830 | 40.52 | 0.74 | 0.14 | 0.86 | 3789 | 76 | 332 |
| D | 3-3 | Avg | 0.99 | 1.00 | 40,298 | 4,217 | 483 | 3,684 | 38.12 | 0.75 | 0.15 | 0.85 | 3582 | 0 | 0 |
| D | 4-1 | Avg | 0.98 | 0.99 | 38,286 | 4,087 | 453 | 3,538 | 39.98 | 1.00 | 0.15 | 0.85 | 3475 | 35 | 152 |
| D | 4-2 | Avg | 0.98 | 0.98 | 38,902 | 4,357 | 433 | 3,661 | 40.90 | 1.00 | 0.14 | 0.86 | 3756 | 75 | 329 |
| D | 4-3 | Avg | 0.99 | 1.00 | 40,998 | 4,230 | 496 | 3,777 | 38.06 | 0.99 | 0.15 | 0.85 | 3597 | 0 | 0 |
| D | 5-1 | Avg | 0.98 | 0.99 | 40,357 | 4,182 | 491 | 3,714 | 38.02 | 1.10 | 0.15 | 0.85 | 3552 | 36 | 156 |
| D | 6-1 | Avg | 0.97 | 0.98 | 39,910 | 4,237 | 476 | 3,660 | 39.70 | 1.20 | 0.15 | 0.85 | 3597 | 72 | 315 |
| D | 7-1 | Avg | 0.98 | 0.99 | 38,259 | 4,090 | 458 | 3,492 | 39.80 | 1.30 | 0.15 | 0.85 | 3470 | 35 | 152 |
| D | 7-2 | Avg | 0.96 | 0.97 | 38,306 | 4,330 | 425 | 3,652 | 41.00 | 1.30 | 0.14 | 0.86 | 3742 | 112 | 492 |
| D | 8-1 | Avg | 0.94 | 0.95 | 41,247 | 4,255 | 504 | 3,786 | 37.92 | 1.60 | 0.15 | 0.85 | 3611 | 181 | 791 |
| D | 9-1 | Avg | 0.87 | 0.89 | 42,006 | 4,270 | 515 | 3,828 | 37.65 | 1.80 | 0.15 | 0.85 | 3617 | 398 | 1743 |
| D | 10-1 | Avg | 0.80 | 0.82 | 41,028 | 4,256 | 501 | 3,720 | 37.57 | 2.01 | 0.15 | 0.85 | 3601 | 648 | 2839 |
| D | 10-2 | Avg | 0.78 | 0.80 | 40,648 | 4,161 | 495 | 3,669 | 37.58 | 2.00 | 0.15 | 0.85 | 3521 | 704 | 3084 |
| E | 1-1 | Avg | 0.99 | 1.00 | 74,650 | 8,612 | 480 | 8,171 | 44.13 | 0.19 | 0.07 | 0.93 | 7987 | 0 | 0 |
| E | 1-2 | Avg | 0.98 | 0.99 | 88,874 | 9,867 | 550 | 9,794 | 42.24 | 0.17 | 0.07 | 0.93 | 9169 | 92 | 402 |
| E | 1-3 | Avg | 1.00 | 1.00 | 79,802 | 8,955 | 515 | 8,683 | 41.96 | 0.19 | 0.07 | 0.93 | 8295 | 0 | 0 |
| E | 2-1 | Avg | 0.99 | 0.99 | 72,648 | 8,376 | 457 | 7,878 | 43.66 | 0.57 | 0.07 | 0.93 | 7770 | 78 | 340 |
| E | 2-2 | Avg | 0.98 | 0.98 | 85,769 | 9,526 | 507 | 9,428 | 41.88 | 0.56 | 0.07 | 0.93 | 8877 | 178 | 778 |
| E | 2-3 | Avg | 0.99 | 1.00 | 81,447 | 9,052 | 509 | 8,939 | 42.19 | 0.56 | 0.07 | 0.93 | 8409 | 0 | 0 |
| E | 3-1 | Avg | 0.99 | 0.99 | 73,275 | 8,299 | 457 | 7,914 | 43.53 | 1.00 | 0.07 | 0.93 | 7699 | 77 | 337 |
| E | 3-2 | Avg | 0.98 | 0.99 | 86,529 | 9,552 | 509 | 9,508 | 41.91 | 1.00 | 0.07 | 0.93 | 8906 | 89 | 390 |
| E | 3-3 | Avg | 0.98 | 0.99 | 82,170 | 9,120 | 510 | 9,055 | 42.23 | 1.00 | 0.07 | 0.93 | 8478 | 85 | 371 |
| E | 4-1 | Avg | 0.98 | 0.98 | 72,979 | 8,299 | 455 | 7,864 | 43.56 | 1.10 | 0.07 | 0.93 | 7698 | 154 | 674 |
| E | 4-2 | Avg | 0.97 | 0.98 | 86,272 | 9,487 | 507 | 9,468 | 41.84 | 1.10 | 0.07 | 0.93 | 8843 | 177 | 775 |
| E | 4-3 | Avg | 0.98 | 0.98 | 82,076 | 9,121 | 504 | 9,081 | 42.22 | 1.10 | 0.07 | 0.93 | 8487 | 170 | 743 |
| E | 5-1 | Avg | 0.97 | 0.97 | 84,628 | 9,403 | 504 | 9,221 | 41.97 | 1.20 | 0.07 | 0.93 | 8752 | 263 | 1150 |
| E | 5-2 | Avg | 0.98 | 0.98 | 79,530 | 8,921 | 488 | 8,750 | 42.22 | 1.20 | 0.07 | 0.93 | 8296 | 166 | 727 |
| E | 6-1 | Avg | 0.96 | 0.97 | 78,820 | 8,817 | 487 | 8,654 | 42.24 | 1.30 | 0.07 | 0.93 | 8195 | 246 | 1077 |

Performance Test of a Steam-Assisted Elevated Flare
Marathon Petroleum Company, Texas City Main Flare

| Condition/Run | | | | | Process Data | | | | | | | | | Emissions | | |
|---------------|---------|-----|------------|------|---------------|-------|-------|-------|-------------|------------|----------------------|-------------------|---------------------|---------------------|-------|-----|
| Condition | New Run | | Efficiency | | Vent Gas | | | | | Ratio | Vent Gas Composition | | | Emissions | | |
| | | | CE | DRE | Vent Gas Flow | N2 | HC | MWvg | Actual S/VG | Non-VOC | VOC | Total VOC in Vent | Total VOC Emissions | Total VOC Emissions | | |
| | | | | | Rate | Flow | Flow | | | Components | Component | Gas Mass Flow | | | lb/hr | TPY |
| | | | | | SCFH | #/hr | #/hr | #/hr | #/=mol | | wt% | wt% | lb/hr | | | |
| F | 1-1 | Avg | 0.99 | 0.99 | 92,911 | 3,982 | 3,512 | 818 | 16.16 | 0.45 | 0.85 | 0.15 | 595 | 6 | 26 | |
| F | 2-1 | Avg | 0.99 | 0.99 | 173,597 | 5,006 | 3,840 | 1,370 | 11.07 | 0.45 | 0.81 | 0.19 | 965 | 10 | 42 | |
| F | 3-1 | Avg | 0.98 | 0.98 | 287,269 | 6,390 | 5,162 | 2,170 | 8.59 | 0.45 | 0.78 | 0.22 | 1408 | 28 | 123 | |
| F | 4-1 | Avg | 0.99 | 0.99 | 265,508 | 4,181 | 2,276 | 2,008 | 6.12 | 4.01 | 0.69 | 0.31 | 1303 | 13 | 57 | |
| F | 5-1 | Avg | 0.99 | 0.99 | 263,538 | 4,001 | 656 | 2,003 | 5.86 | 1.00 | 0.58 | 0.42 | 1683 | 17 | 74 | |
| F | 6-1 | Avg | 1.00 | 1.00 | 266,986 | 4,002 | 578 | 2,016 | 5.82 | 0.44 | 0.57 | 0.43 | 1712 | 0 | 0 | |
| G | 1-1 | Avg | 0.97 | 0.97 | 51,083 | 3,202 | 2,075 | 1,178 | 23.48 | 0.56 | 0.79 | 0.21 | 681 | 20 | 90 | |
| G | 2-1 | Avg | 0.99 | 0.99 | 58,415 | 3,382 | 2,276 | 1,148 | 21.57 | 0.54 | 0.80 | 0.20 | 667 | 7 | 29 | |
| G | 3-1 | Avg | 0.89 | 0.90 | 55,227 | 3,252 | 2,759 | 631 | 22.16 | 0.56 | 0.85 | 0.15 | 478 | 48 | 210 | |
| G | 4-1 | Avg | 0.89 | 0.90 | 59,676 | 3,540 | 3,090 | 626 | 22.24 | 0.52 | 0.86 | 0.14 | 488 | 49 | 214 | |
| G | 5-1 | Avg | 0.86 | 0.87 | 58,467 | 3,460 | 3,031 | 603 | 22.24 | 0.60 | 0.87 | 0.13 | 467 | 61 | 266 | |
| G | 6-1 | Avg | 0.82 | 0.83 | 59,404 | 3,526 | 3,084 | 604 | 22.24 | 0.70 | 0.87 | 0.13 | 468 | 80 | 349 | |

Appendix A.4

Personnel Involved with Flare Performance Test

Alison Moscarillo, Marathon
Ruth Cade, Marathon
Brian Wilt, Marathon
Elizabeth Brackin, Marathon
John Bigham, Marathon
J.P. Mahan, Marathon
Lloyd Criss, Marathon
Richard Gardin, Marathon
Adolfo Yanez Jr., Marathon
Eric Campbell, Clean Air Engineering
Scott Evans, Clean Air Engineering
Jodi Kizzee, Marathon
Harold Scott, Marathon
Alejandro Acuña, Marathon
Katie Rickle, Marathon
Todd Palmer, Marathon
Melissa Seedorf, Marathon
Curtis Laush, IMACC
Melissa Walker, Marathon
Jim Franklin, John Zink
Gary Pope, John Zink
Robert Spellicy, IMACC
Tom Kindervater, Marathon
Scott Fox, John Zink
Lucy Thurston, Marathon
Raul Vela, Marathon
Keegan Mukabana, Marathon
Peter Kaufmann, Clean Air Engineering
Walter Lizard, Marathon
Bill O'Donnell, Marathon
Karen Utley, Marathon
Jerry Isam, Marathon